EFFECT OF COPPER NANOPARTICLES ON RAINBOW TROUT OLFACTION AND RECOVERY

PARASTOO RAZMARA
Master of Science, Isfahan University of Technology, 2014

A thesis submitted
in partial fulfilment of the requirements for the degree of

DOCTOR OF PHILOSOPHY

in

BIOSYSTEMS AND BIODIVERSITY

Department of Biological Sciences
University of Lethbridge
LETHBRIDGE, ALBERTA, CANADA

EFFECT OF COPPER NANOPARTICLES ON RAINBOW TROUT OLFACTION AND RECOVERY

PARASTOO RAZMARA

Date of Defence: April 14, 2021

Dr. G. Pyle Thesis Supervisor	Professor	Ph.D.
Dr. A. Hontela Thesis Examination Committee Member	Professor	Ph.D.
Dr. A. Russell Thesis Examination Committee Member	Associate Professor	Ph.D.
Dr. S. Niyogi External Examiner University of Saskatchewan	Professor	Ph.D.
Dr. M. Bogard Internal External Examiner	Assistant Professor	Ph.D.
Dr. R. Laird Chair, Thesis Examination Committee	Associate Professor	Ph.D.

DEDICATION

This dissertation is dedicated to my beloved parents, Safar and Rouhi, who have been unconditionally supportive and kind.

And, to my husband, Milad, who has encouraged and supported me during challenging moments of the graduate school.

ABSTRACT

Fish depend on olfaction for reproduction and survival. Here, using molecular to behavioural endpoints, we compared the effect of two neurotoxic contaminants, Cu ions (Cu^{2+}) and copper nanoparticles (CuNPs) on rainbow trout olfaction. Exposure to equitoxic concentrations of Cu^{2+} and CuNPs resulted in distinct toxicity patterns over time in rainbow trout olfactory mucosa. During continuous exposure to Cu^{2+}, fish olfactory function was partially recovered. However, the olfactory function of CuNP-exposed fish showed a steady decline over time. Gene-transcript profiles of Cu^{2+}-exposed olfactory mucosa showed neural repair mechanisms were upregulated to recover the olfactory dysfunction. In the CuNP treatment, dysregulation of transcripts that regulate function and reestablishment of damaged olfactory mucosa represented key mechanisms of CuNP-induced olfactory toxicity. Moreover, our findings revealed the CuNP-induced olfactory dysfunction was irreversible after the 7-day recovery period. Collectively, CuNPs and Cu^{2+} exert their effects via separate mechanisms in rainbow trout olfactory mucosa.

ACKNOWLEDGMENTS

Firstly, I would like to thank my wonderful supervisor, Dr. Greg Pyle, for his guidance in development and completion of this complex study; for his time (especially, during the coronavirus pandemic, during which communications were not easy) spent discussing my results, conference dry runs, papers, and the present dissertation; for teaching me how to write scripts in R, for the opportunity to be a guest lecturer and a session chair at conferences; for the opportunity to train and supervise undergraduate students; for allowing me to act independently and for the freedom to investigate the endpoints that I was interested in. His immense knowledge, experience, and continuous support has brough the best out of me and motivated me to achieve my academic goals. Thank you to my supervisory committee, Dr. Alice Hontela and Dr. Tony Russell, for providing their invaluable guidance, insights, and critiques throughout my research. Thank you to my internal examiner, Dr. Matt Bogard, and external examiner, Dr. Som Niyogi, for their comments on my dissertation and their virtual participation in my thesis defence. Thank you to Dr. Rob Laird for assistance with statistical analyses and for chairing my Ph.D. defense.

Many thanks to Dr. Greg Goss and Yueyang Zhang, who have helped me with copper nanoparticles characterization in the University of Alberta. A special thank you to Dr. Caren Helbing, Dr. Patrick Gauthier, Jacob Imbery, and Emily Koide for their assistance with differential gene expression analyses of RNA-seq data. Many thanks to Dr. Steve Wiseman for his invaluable guidance and feedback and for allowing me to use his laboratory equipment and materials. Thank you to Justin Miller for training me to use molecular protocols. Further support in this study came from Douglas Bray and Dr.

Maurice Needham, who trained me on a complicated and time-consuming protocol to prepare samples for transmission electron microscopy. Thank you to Dr. Athanasios Zovoilis and Travis Haight for allowing me to use their supercomputer to analyse my RNA-seq data. Thank you to Justin Sharpe, who collected a part of the behavioural data. Also special thanks to Effat Mohaddes and Alicia Macdonald-Wilson for being excellent laboratory technicians. I would also like to thank you Dr. Ebrahim Lari for his invaluable advice and guidance in my study. Thanks to the University of Lethbridge Aquatic Research Facility, Dr. Shamsuddin Mamun and Holly Shepperd for taking care of experimental fish. Thanks to Sarah Bogart for training me on graphite furnace atomic absorption spectrometry. I would also like to further extend my gratitude to all my colleagues and fellow lab-mates, Dr. Jaimie Klemish, Raegan Plomp, Lauren Zink, Carolyn Simonis, and Nicole Guidony for their helpful discussions, teaching me new English expressions, and support during my Ph.D. study. Many thanks to my source of funding, including the Natural Sciences and Engineering Research Council of Canada (NSERC) Discovery Grant (to Dr. Greg Pyle), University of Lethbridge Dean's Scholarship, University of Lethbridge Tuition Scholarship, and NEXEN fellowship.

I would like to express my gratitude to Laurie Pyle, who has kindly supported me like a family member over the past 5 years and made my life a delightful time in Canada. My appreciation also goes out to my dear husband, Milad Razmara, for his permanent love and support, for keeping things going, for watching my dry runs before conference presentations, for assisting me in my experiments, for always being there, and for having faith in me. Lastly, I would like to thank my family, Safar, Rouhi, Ramina, Pegah, Anita,

Mahsa, Mahnaz, and Mahmoud for their encouragement and emotional support through the Ph.D. study.

TABLE OF CONTENT

LIST OF TABLES

LIST OF FIGURES

LIST OF ABBREVIATIONS

ACIII	Adenylyl Cyclase III
ACTB	Beta Actin
ADAMTS1	A Disintegrin and Metalloproteinase with Thrombospondin Motif 1
AEP	Alberta Environment and Parks
AgNPs	Silver Nanoparticles
ANOVA	Analysis of Variances
AO	Adverse Outcome
AOP	Adverse Outcome Pathway
AP	Action Potential
APC	Adenomatous Polyposis Coli Protein
ARE	Antioxidant Response Element
ARF	Aquatic Research Facility
ATP1A1	Na^+/K^+ ATPase Alpha-1 Subunit
ATP6AP1	V-type Proton ATPase Subunit S1
BAX	Apoptosis Regulator BAX
BLM	Biotic Ligand Model
BLOC1S1	Biogenesis of Lysosome-related Organelles Complex 1 Subunit 1
BP180	Bullous Pemphigoid antigen 2
BP230	Bullous Pemphigoid antigen 1
C-REL	Proto-oncogene c-Rel
CaCC	Calcium-gated Chloride Channel
CaCNB1	Voltage-dependent L-type Calcium Channel Subunit Beta1
CALM	Phosphatidylinositol-binding Clathrin Assembly Protein
CAM	Calmodulin
cAMP	Cyclic Adenosine Monophosphate
CASP	Caspase
CAT	Catalase
CCC	Criterion Continuous Concentration
CCL	C-C Motif Chemokine
CCME	Canadian Council of Ministers of the Environment
CD151	CD151 antigen
CF	Characterization Factor
CLD	Claudin
CMC	Criterion Maximum Concentration
CNG	Cyclic Nucleotide Gated Channel
CNS	Central Nervous System
CTRB1	Transcription of Copper Transporter 1B
Cu^{2+}	Copper Ion
CuNP	Copper Nanoparticle
CuO	Copper Oxide
CX	Connexin

DAG	Diacylglycerol
ddH_2O	Double Distilled Water
DLS	Dynamic Light Scattering
DLVO	Derjaguine-Landaue-Verweye-Overbeek Theory
DNM1	Dynamin 1
DOC	Dissolved Organic Carbon
DOC2B	Double C2-like Domain-containing Protein Beta
DOLT-4	Dogfish Liver Certified Reference Material for Trace Metals
DSC	Desmocollin
DSP	Desmoplakin
ECM	Extracellular Matrix
EDL	Electric Double Layer
EF1a	Elongation Factor 1 Alpha
ENPs	Engineered Nanoparticles
EOG	Electro-olfactography
EPHA4	Ephrin Type-A Receptor 4
EPS15L1	Epidermal Growth Factor Receptor Substrate
ER	Endoplasmic Reticulum
EVPL	Envoplakin
FGFR2	Fibroblast Growth Factor Receptor 2
FINC	Fibronectin
G	G Protein
GATA3	GATA-binding Factor 3
GBC	Globose Basal Cell
GCLC	Glutamate-cysteine Ligase Catalytic Subunit
GFAAS	Graphite Furnace Atomic Absorption Spectrometry
GNB1	Guanine Nucleotide-binding Protein G(I)/G(S)/G(T) subunit beta1
GO	Gene Ontology
GPX7	Glutathione Peroxidase 7
GSH	Glutathione
GSTA	Glutathione S-transferase A
HBC	Horizontal Basal Cell
HDD	Hydrodynamic Diameter
IC20	20% Inhibitory Concentration
IC50	50% Inhibitory Concentration
IKK	Inhibitor of NF- κB Kinase
IL-1β	Interleukin-1 Beta
IP_3	Inositol Triphosphate
IκBα	NF-kappa-B Inhibitor Alpha
JAM	Junctional Adhesion Molecule
JNK	c-Jun N-terminal Kinase
JUN	Transcription Factor AP-1
KCNB1	Potassium Voltage-gated Channel Subfamily B Member 1

KE	Key Event
KRT13	Keratin type I cytoskeletal 13
KRT8	Keratin Type II Cytoskeletal 8
LAMB3	Laminin Subunit Beta 3
LHX2	LIM/homeobox Protein Lhx2
LOEC	Lowest Observed Effect Concentration
MAP1A	Microtubule-associated Protein 1A
MAP1B	Microtubule-associated Protein 1B
MC	Mitral Cell
MDA	Malondialdehyde
MDL	Measured Detection Limit
MEFV	Pyrin
MIE	Molecular Initiating Event
MSLN	Mesothelin-like Protein
MSRA	Mitochondrial Peptide Methionine Sulfoxide Reductase
MT	Metallothionein
MTF1	Metal-responsive Transcription Factor 1
MUC2L	Mucin 2 Like
MUC5AC	Mucin 5 AC
N-CAD	Neural Cadherin
NCAM1	Neural Cell Adhesion Molecule 1
NCBI	National Center for Biotechnology Information
NCKX3	Sodium/Potassium/Calcium Exchanger 3
NCLX	Mitochondria Sodium/Calcium Exchanger
NCX1	Sodium-calcium Exchanger 1
NDUFS1	NADH-ubiquinone Oxidoreductase 75 kDa Subunit
NDUFS8	NADH Dehydrogenase [ubiquinone] Iron-sulfur Protein 8
NF-κB2	NF-kappa-B p100 Subunit
NIK	NF- κB Inducing Kinase
NLRC3	NLR Family CARD Domain Containing 3
NLRP1b	NACHT, LRR and PYD Domains-containing Protein 1b
NLRP3	NACHT, LRR and PYD Domains-containing Protein 3
NMDS	Non-metric Multidimensional Scaling
NOM	Natural Organic Matter
NRF1	Nuclear Factor Erythroid 2-related Factor 1
NT	Neurotransmitter
NTN1	Netrin 1
OB	Olfactory Bulb
OE	Olfactory Epithelium
OEC	Olfactory Ensheathing Cell
OLF472	Olfactory Receptor 472
OMP	Olfactory Marker Protein
OR	Olfactory Receptor

OR10G4	Olfactory Receptor 10G4
OR2AT4	Olfactory Receptor 2AT4
OR2M3	Olfactory Receptor 2M3
OR4C5	Olfactory Receptor Family 4 Subfamily C Member 5
OR52A	Olfactory Receptor 52A
OSN	Olfactory Sensory Neuron
OST	Olfactory Signal Transduction
OTX1	Homeobox Protein OTX1
P120	P120 Catenin
PAR3	Partitioning Defective 3 Homolog
PAX6	Paired Box Protein Pax-6
PBX1	Pre-B-cell Leukemia Transcription Factor 1
PCP	Planar Cell Polarity
PDI	Polydispersity Index
PEC	Predicted Environmental Concentration
PG	Plakoglobin
PKP	Plakophilin
PLC	Phospholipase C
PLEC	Plectin
PLEKHA7	Pleckstrin homology domain containing A7
PM	Particulate Matter
PMCA2	Plasma Membrane Calcium-transporting ATPase 2
QA/QC	Quality Assurance/Quality Control
qPCR	Quantitative Polymerase Chain Reaction
RAB10	Ras-related Protein Rab-10
RAB3	Ras-related Protein Rab-3A
RIN	RNA Integrity Number
ROBO2	Roundabout Homolog 2
ROS	Reactive Oxygen Species
Rv	Response Variable
SCA17A9	Solute Carrier Family 17 Member 9
SCN8A	Sodium Channel Protein Type 8 Subunit Alpha
SD	Standard Deviation
SEM	Standard Error of Mean
SERPINE1	Serpin Family E Member 1
SLRS-6	River Water Certified Reference Material for Trace Metals
SOX2	Transcription Factor SOX-2
SP3	Transcription Factor SP3
SP8	Transcription Factor SP8
SPARC	Secreted Protein Acidic and Cysteine Rich
SV	Synaptic Vesicle
TBARS	Thiobarbituric Acid Reactive Substances
TCA	Taurocholic Acid

TCF7L2	Transcription Factor 7 Like 2
TEM	Transmission Electron Microscopy
TF	Transcription Factor
TIAM1	T-lymphoma Invasion and Metastasis-inducing Protein 1
TNFR	Tumor Necrosis Factor Receptor
TNR5	Tumor Necrosis Factor Receptor Superfamily Member 5
TPCN2	Two Pore Calcium Channel Protein 2
TRIM46	Tripartite Motif-containing Protein 46
vATPase	Vacuole Proton Pump
VGCC	Voltage-gated Calcium Channel
VR	Vomeronasal Receptor
WQC	Water Quality Criteria
WWTP	Wastewater Treatment Plant
ZO	Zonula Occludens
α-CAT	α-Catenin
β-CAT	β-Catenin
β3GNT1	N-acetyllactosaminide Beta-1,3-N-acetylglucosaminyltransferase

CHAPTER 1: Introduction

Nanoparticles and aquatic ecosystems

The production of engineered nanoparticles (ENPs) and their occurrence in the environment is a result of a fast-growing nanotechnology industry. Nanoparticles are defined as particles ranging in size from 1 to 100 nm in at least one dimension. Particles in this size range have a high surface area to volume ratio, which makes them unique in their physicochemical properties compared to their larger counterparts (Vale et al., 2016). Due to possessing exceptional properties, ENPs are applied in myriad fields, including enhanced oil recovery processes (Sun et al., 2017), biofuel production processes (Sekoai et al., 2019), water and wastewater treatment (Qu et al., 2013), drug delivery (Wilczewska et al., 2012), cosmetics (Khezri et al., 2018), and food and agriculture (He et al., 2019). With the rapid and worldwide increase in production and commercialization of ENPs, the incidental release of ENPs to the atmosphere, geosphere, and hydrosphere is anticipated (Courtois et al., 2019; Li et al., 2020; Souza et al., 2021).

Aquatic ecosystems are the final destinations for many of ENPs. Nanoparticles may be released to the environment during any or all stages of their lifecycle — from production to disposal (Bundschuh et al., 2018). The entrance of ENPs to surface waters may occur through soil leaching, atmospheric deposition, effluent discharges, and urban runoff (Scown et al., 2010; Wang et al., 2020). The presence of ENPs in surface waters was confirmed in multiple water samples that were collected from rivers in the Netherlands (Peters et al., 2018). The concentrations of detected ENPs ranged from 0.3 ng/L to 8.1 µg/L (Peters et al., 2018). The concentration of ENPs, which was detected in a major municipal wastewater treatment system in the USA, reached up to 390 µg/L (Choi et al., 2018).

Drinking water sources and tap water have also been contaminated with ENPs (Sousa and Teixeira, 2020). The presence of ENPs in aquatic environments may pose a risk to the health of aquatic and terrestrial biota.

Copper nanoparticles and aquatic ecosystems

Copper nanoparticles (CuNPs) are metal-based ENPs and offer unique optical, catalytic, conductivity, and antimicrobial properties (Purohit et al., 2020; Ramyadevi et al., 2012; Wei et al., 2010; Yu et al., 2011). Copper nanoparticles find potential applications in the treatment of industrial and municipal wastewaters (Dlamini et al., 2019; Noman et al., 2020), oil additives and nanofluids (Choi et al., 2009; Gurav et al., 2014), inkjet-printed electronics (Luechinger et al., 2008; Magdassi et al., 2010), lithium batteries and solar cells (Liu et al., 2018; Shen et al., 2016; Yang et al., 2012), sensors (Athanassiou et al., 2006; Lin et al., 2013), and cancer therapy (Guo et al., 2014; Vaid et al., 2020). Moreover, CuNPs can act as potent microbiocidal agents in dental applications (Fernández-Arias et al., 2020), wound dressings (Villanueva et al., 2016), textiles (Radetić and Marković, 2019), filters (Dankovich and Smith, 2014), paints and antifouling coatings (Abiraman and Balasubramanian, 2017; Bellotti et al., 2015), and agriculture and aquaculture (Chari et al., 2017; Ponmurugan et al., 2016).

The extensive application of CuNPs in industrial and commercial processes increased the likelihood of their presence in the aquatic environments. Release of CuNPs from an antifouling paint leachate into natural waters has been reported (Adeleye et al., 2016). After 180 days, the concentration of Cu released from painted aluminum and wood minibars was 41 and 626 mg/L, respectively (Adeleye et al., 2016). Given that nanocopper

is used in fungicides, herbicides, pesticides, and nano-fertilizers, agricultural runoff is another source of CuNPs which is ultimately released to surface waters (Keller et al., 2017).

In addition to the release of engineered CuNPs to aquatic environment, Cu-containing objects may incidentally release CuNPs. For instance, copper wires have been shown to spontaneously generate CuNPs (Glover et al., 2011). Atmospheric deposition CuNPs into water is also a major source of CuNPs contamination in aquatic environments. A recent study reported that atmospheric particulate matter (PM) of a steel manufacturing facility released several metal NPs, including CuNPs, into water (Souza et al., 2020). The concentration of released Cu from PM was 495 mg/L (Souza et al., 2020). Moreover, naturally produced CuNPs from Cu-containing ores are a source of CuNP contamination in aquatic environments, which has been understudied in last decades. To examine the presence of naturally produced metal-containing nanoparticles in water, several water samples were collected from deep ground water and residential wells located near four major metal deposits in China (Hu and Cao, 2019). The presence of metal-containing NPs, including CuNPs (1.7-9.4 μg/L), was confirmed in samples of both ground water and wells (Hu and Cao, 2019). Water flows can translocate the ore-originated NPs and contaminate an extensive area. These results, for the first time, revealed that CuNPs can have a natural origin in the aquatic environment.

The proportion of discharged CuNPs from wastewater treatment plants (WWTP) to the aquatic environment, however, is relatively low. The predicted concentration of CuNPs in the effluent and biosolids of the San Francisco Bay WWTP is in the range of ng/L (Keller and Lazareva, 2014). Activated sludges, which are used in WWTP, are able to efficiently remove 95% of the CuNPs from municipal wastewaters (Ganesh et al., 2010).

Ganesh et al. (2010) found that CuNPs were aggregated and settled in the sludge. Nevertheless, due to the antimicrobial effects of CuNPs, a number of studies reported that the aggregated CuNPs can change the bacterial composition and purification efficiency of activated sludges (Chen et al., 2014; Zhang et al., 2018). The nitrifying removal capacity of denitrifying granules sludge was reduced by 52% after exposure to 5 mg/L of CuNPs (Cheng et al., 2019). The relative abundances of denitrifying bacteria and the genes related to denitrification were also decreased in the CuNP-exposed sludge (Cheng et al., 2019). The amount of ions released by CuNPs (i.e., dissolution of CuNPs) were increased in a concentration-dependent manner, and the dehydrogenase activity of the sludge was reduced by 99.9% relative to the initial sludge (Cheng et al., 2019). Furthermore, long term exposure of wastewater treatment sludge to 5 mg/L CuNPs reduced the physiological activity and abundance of anammox bacteria (anerobic ammonium oxidation bacteria) (Zhang et al., 2018). Similar to the Chen el al. (2019) study, dissolution of CuNPs was also reported in the CuNP-exposed sludge (Zhang et al., 2018). Given that the dissolved Cu (e.g., Cu^{2+}) cannot be completely removed by WWTP (Ganesh et al., 2010), the effluent discharges of WWTP to natural waters may contain dissolved Cu, which may be more toxic than CuNPs. Another study reported that, following 30 days of exposure to 5 mg/L CuNPs, the nitrogen removal capacity of anammox reactor was nearly eliminated and the abundance of anammox bacteria was reduced from 30% to 18% (Zhang et al., 2017). Nonetheless, 70 days after removing the CuNPs from the activated sludge, the capacity of nitrogen removal in anammox biomass was fully recovered (Zhang et al., 2017). However, in practice, it is not possible to stop the receiving of wastewaters containing CuNPs to recover biological filters.

To our knowledge, no study has reported the actual concentration of CuNPs in surface waters. Nevertheless, a few models have estimated the environmental concentrations of CuNPs in aquatic environments. For instance, based on the results of a predictive model, in a number of receiving waters, the predicted environmental concentrations (PECs) of CuNPs are 60 µg/L (Chio et al., 2012). Another model, which included the predicted CuNPs concentrations of WWTP effluents in their estimates, reported that CuNPs PECs in freshwaters are < 0.01 ng/L (Pu et al., 2016). This model study also predicted that North American subcontinental region, which includes Canada, has the second highest nanocopper characterization factor (CF) after Africa. The CF is an ecotoxicological index that is proposed by USEtox (consensus model that characterizes ecotoxicological impacts of chemicals) (Pu et al., 2016). The CF has a positive correlation with nanocopper bioavailability and persistence in freshwater ecosystems and reflects the potential influence of nanocopper on organisms based the region-specific freshwater characterization (Pu et al., 2016). Considering the adverse effects that CuNPs can induce in the organisms, there is an urgent need to measure the CuNPs in aquatic ecosystems.

Copper as an essential micronutrient or a toxicant?

Copper (Cu) is an essential element for all aerobic organisms through acting as both electron donor and receiver in a number of enzymatic processes (Stern, 2010). Copper deficiency impairs many vital processes in vertebrates, including the development of healthy bones (Lall and Lewis-McCrea, 2007), maturation of oocytes (Riggio et al., 2003), differentiation of neurons (Hatori et al., 2016), and notochord development (Mendelsohn et al., 2006). In addition to the Cu deficiency implications for organisms, Cu overload can induce many adverse effects in cells. Under excessive Cu concentrations, the unbound

ionic Cu (e.g., Cu^{2+}) may induce oxidative stress or change metalloenzyme function by indiscriminately binding to their thiol groups (Letelier et al., 2005; Stern, 2010).

To maintain the Cu concentration within an optimal range, organisms employ different Cu-regulatory mechanisms. Homeostasis of Cu is maintained through regulating intake, distribution, elimination, and detoxification of the excessive Cu. Cellular Cu is regulated through many molecular mechanisms. For instance, metal-responsive transcription factor 1 (MTF1) is a zinc finger protein which plays a crucial role in Cu homeostasis. When the Cu concentration is exceeded, MTF1 promotes the transcription of metallothionein (MT), which is involved in Cu detoxification (Balamurugan and Schaffner, 2006). Under Cu deficiency conditions, however, MTF1 activates the transcription of copper transporter 1B (CTRB1) to increase the uptake of Cu from the surrounding microenvironment (Balamurugan and Schaffner, 2006). Copper chaperons are a novel family of proteins which serve as shuttles delivering Cu to specific targets in cells. As a homeostatic response to any change in cellular Cu, the expression of Cu chaperons can regulate cellular Cu trafficking (Bertinato and L'Abbé, 2004). Nonetheless, when the cellular Cu concentrations exceed the organism's optimal range, homeostatic strategies may malfunction, and cellular toxicity may occur.

Copper nanoparticles versus Cu ions

Copper, specifically Cu^{2+}, can be found naturally in pristine freshwater environments with concentrations of 0.2 to 30 µg/L (Craig et al., 2007). In exploited areas, Cu^{2+} concentrations can be dramatically increased up to >560 µg/L by anthropogenic activities associated with mining, fertilizers, electric equipment, and municipal wastewaters (Atli and Grosell, 2016; Craig et al., 2007). Ionic Cu is the most bioavailable

form of Cu that exerts the highest toxicity in living organisms. Short-term exposure of fish to sublethal Cu^{2+} concentrations had many adverse effects on swimming performance (De Boeck et al., 2006), ion balance and Na^+/K^+-ATPase activity in gills (Suvetha et al., 2010), Na^+ uptake by gills (Grosell and Wood, 2002), antioxidant activity(Jiang et al., 2014), metabolism (Santos et al., 2010), immunity (Geist et al., 2007), learning capacity (Pilehvar et al., 2020), mechanosensory perception (Linbo et al., 2006), chemosensory perception, and olfactory-driven behaviour (Pyle and Mirza, 2007).

In addition to Cu^{2+}, CuNPs and Cu oxide (CuO) NPs have been shown to induce toxicity in a broad range of aquatic organisms, including microalgae (Barreto et al., 2020), duckweeds (Yue et al., 2018), water fleas (Xiao et al., 2018a), barnacles (Yang and Wang, 2019), bivalves (Ray et al., 2020; Scola et al., 2021), and fishes (Malhotra et al., 2020). Nonetheless, it is not entirely clear whether the toxicity of CuNPs is associated with the released Cu^{2+} or the particles themselves. A number of studies reported that the dissolution of CuNPs is the main driver of CuNP toxicity (Song et al., 2015; Zhu et al., 2017). However, the majority of studies reported some differences between the effects induced by CuNPs and Cu^{2+}, which suggests that dissolved ions are not the only contributor to the CuNP-induced toxicity in aquatic organisms (Al-Bairuty et al., 2013; Griffitt et al., 2009; Griffitt et al., 2007; Hua et al., 2014; Tesser et al., 2020; Vicario-Parés et al., 2018; Xiao et al., 2018a; Yang and Wang, 2019).

Factors affecting the toxicity of CuNPs

Nanocopper physicochemical characteristics and ambient fluid properties can dramatically change the dissolution, bioavailability, and toxicity of CuNPs (Peijnenburg et al., 2015). The rate of NPs dissolution can be affected by physicochemical properties of

metal particles. In most cases, there is a relationship between the size of metal NPs and number of released ions. The dissolution rate of smaller NPs is higher than larger ones because the ratio of surface area relative to volume is higher in small particles (Cross et al., 2015; Mortimer et al., 2010). Surface modifications on NPs through the use of capping agents can also alter dissolution behaviour. A chitosan coating of CuNPs reduced the concentration of released ions (Worthington et al., 2013). The shape of metal NPs is another factor that can control the amount of dissolution. For instance, spherical CuO-NPs have greater dissolution rates compared to rod shaped particles (Misra et al., 2012a). In addition, dissolved organic matter (DOM) is able to bind to the dissolved free ions released by metal NPs and consequently decrease the bioavailability and toxicity of dissolved ions (Aiken et al., 2011). In waters with a high content of total organic carbon the dissolution of CuNPs was significantly reduced (Conway et al., 2015). The presence of dissolved organic carbon (DOC) can also decrease the dissolution (i.e., release of dissolved Cu to water) of NPs by either coating the NPs surface or binding to the released ions. Following the 48 h after adding DOC (5-50 mg C/L) to water containing CuNPs, the dissolution of CuNPs was reduced by 3-5 fold (Xiao et al., 2018b). Another factor that modifies metal NP dissolution is pH. In the absence of DOC, lower pH (i.e., 6) has resulted in higher dissolution relative to higher pH (i.e., 9) (Xiao et al., 2018b). The presence of oxygen is important for the dissolution process as no dissolved Cu was released from CuNPs under anoxic conditions (Mulenos et al., 2020). Ionic strength has an indirect effect on metal NPs dissolution behaviour through altering the aggregation of NPs. In general, there is a positive correlation between ionic strength and NPs aggregation. Aggregated particles have smaller

surface area to the volume ratio compared to individual NPs, and, therefore, release fewer ions from their surfaces (Conway et al., 2015; Misra et al., 2012b).

A recent study investigating the fate of Cu-based NPs (Kocide, a nano $Cu(OH)_2$ agricultural fungicide) in a freshwater wetland mesocosm reported that about 60% of Kocide dissolved following the 48 h of being added to the mesocosm (Avellan et al., 2020). Samples collected from mesocosm water indicated that the majority of ion species were first bound to sulfides and second to organic matter (Avellan et al., 2020). Dissolved Cu, which was highly mobile relative to NPs, was able to accumulate in grazer snails and was transferred into deep aquatic sediments (Avellan et al., 2020). These results suggest that released ions from nanocopper has the potential to transfer to different trophic levels.

Bioavailability and toxicity of NPs is also dependent on the aggregation behaviour of NPs in the medium. Fewer aggregated NPs are less bioavailable than non-aggregated NPs for pelagic organisms because Cu aggregated at the micron scale rapidly settles out (Keller et al., 2017). After metal NPs are released to the aquatic environment, they will interact with natural colloidal matter and form heteroaggregates. Natural colloids are defined as materials with a dimension from 1 nm to 1000 nm. Colloids are composed of three components: 1) organic matter such as humic acid and biogenic exudates (e.g. proteins and polysaccharide), 2) inorganic fractions including metal oxides, and 3) biological constituents such as viruses and bacteria (Klaine et al., 2008; Scown et al., 2010). Interaction among the same NPs results in homo-aggregation. Nonetheless, hetero-aggregates are more common in natural environments (Amde et al., 2017). The stability of colloids is determined by Derjaguine-Landaue-Verweye-Overbeek (DLVO) theory (Derjaguin and Landau, 1993; Verwey and Overbeek, 1955). According to DLVO theory,

the interaction of attractive or repulsive forces will determine the aggregation behaviour of colloids. The balance of these opposite forces highly depends on physiochemical properties of ambient fluids and characteristics of metal NPs. The majority of suspended materials in the water have a negative charge which means that while they are attracted to positive ions and induce the repulsive electric double layer (EDL), they can repel other negative colloids. If colloids have enough electrical charge, they can remain stable in suspension and overcome aggregation (Amde et al., 2017; Cross et al., 2015). The interaction of CuO NPs with humic acids and citric acids increased the stability of NPs in the water (Peng et al., 2017).

Toxicity of CuNPs in fish

Routes of NP entry to cells are dependent on the size of NPs, as well as the cell's ability to form adequately sized membrane vesicles to phagocytose large NPs or pinocytose smaller NPs (Pulido-Reyes et al., 2017). Based on the cellular effector mediating vesicle formation, pinocytosis can be subdivided into macro-pinocytosis, clathrin-mediated endocytosis, caveolin-mediated endocytosis, and clathrin/caveolin-independent endocytosis (Pulido-Reyes et al., 2017). Endocytosis pathways are the most common ways for NPs to be taken up by the cells (Handy et al., 2008). Nanoparticles that are smaller than 10 nm may pass directly through the cellular membrane bilayer (Pulido-Reyes et al., 2017). After endocytosis, NPs are converted into early endosomes. Early endosomes act as sorting hubs that deliver their cargo to the endoplasmic reticulum (ER), the Golgi apparatus, or the endosomal recycling pathway (Patel et al., 2019). In the endosomal recycling process, early endosomes undergo some structural alterations and form late endosomes which ultimately fuse to lysosomes (Patel et al., 2019). Most NPs end up in lysosomes which have an acidic

pH (~ 4.5-5.5). Under low pH conditions, metal NPs can be dissolved. Depending on the NPs properties, complete dissolution of metal NPs may take a few weeks to months (Zhu et al., 2013). In some cases, NP overload may disrupt lysosomal enzymes and the activity of proton pumps and lead to the release of undigested NPs to the cytosol (Zhu et al., 2013).

Depending on the routes of exposure, as well as the characteristics and concentration of NPs, and types of cells in contact with the environment, NPs may be taken up by organisms. Accumulation of Cu in CuNP-exposed fish gills suggests that gill epithelial cells may be able to take up CuNPs (Al-Bairuty et al., 2016; Griffitt et al., 2007; Lindh et al., 2019; Shaw et al., 2012). However, in these studies, it was not clear if the accumulated Cu was in the form of CuNPs or Cu ions. Elevated concentration of Cu in the intestine of fish force-fed CuNP-containing food through gastric gavage, suggests that dietary uptake of CuNPs is possible. Copper concentration was also increased in the gut of fish that were exposed to waterborne CuNPs (Shaw et al., 2012). Moreover, Cu accumulated in the liver, kidney, and carcass of CuNP-injected and gavaged rainbow trout (Lindh et al., 2019). Therefore, distribution of CuNPs in internal organs is possible.

Wide ranges of CuNP-induced toxicities have been reported in fish (Malhotra et al., 2020). The exposure of fish to CuNPs has led to gill injury (e.g., edema of gill filaments) (Griffitt et al., 2007), reduced activity of Na^+/K^+-ATPase in gills, intestine, and brain (Shaw et al., 2012), impaired function of ionocytes and disrupted ion homeostasis (Lee et al., 2020), impaired embryonic intestinal development (Zhao et al., 2020b), induced anemia (Tesser et al., 2020), and impaired embryo cardiogenesis and neural development (Xu et al., 2017).

In recent years, a few studies have demonstrated that CuNPs can induce neurotoxic effects in the peripheral nervous system of fish. A 4 h exposure to 50 μg/L CuNPs resulted in a significant reduction in the number of lateral-line neuromasts in zebrafish embryos (McNeil et al., 2014). The CuNP-exposed embryos showed impaired rheotaxis behaviour which did not recover after a 24 h recovery period (McNeil et al., 2014). In another study, 4 h exposure of zebrafish embryos to 100 μg/L impaired the morphological structure of hair cells in neuromast, reduced the number of hair cells, and reduced the calcium influx in survived hair cells by 31% (Yen et al., 2019). When the exposure time extended to 96 h, no hair cells were found in the embryos that were exposed to 100 μg/L of CuNPs, and 10 μg/L of CuNPs was sufficient to reduce the calcium influx and the number of hair cells (Yen et al., 2019). These results demonstrated that fish mechanosensory system, which plays a crucial role in fish survival, is also vulnerable to CuNPs. Exposure to CuNPs (~250 μg/L) during zebrafish embryonic development (0-96 h post fertilization) has resulted in retinal development deficits (Zhao et al., 2020a). The CuNP-exposed zebrafish showed reduced numbers of retinal cells, reduced expressions of retinal-related genes, structural damage in ER and mitochondria, increased unfold protein responses, and retinal cell apoptosis (Zhao et al., 2020a). Despite the importance of the peripheral nervous system in fish reproduction and survival, there are several considerable gaps in our understanding of the effects of CuNPs on fish sensory systems.

Fish olfactory system

Organization of fish olfactory system

Teleost fish have a pair of nasal cavities located on the dorsal anterior side of the head. Through an intranarial nasal septum, each cavity is divided into anterior and posterior

nares which facilitates water inflow and outflow, respectively (Laberge and Hara, 2001). In some fishes such as rainbow trout, an epithelial sheet, the olfactory epithelium (OE), covers a lamellar structure known as the olfactory rosette (Hansen and Zielinski, 2005) (Fig. 1.1). The rosette structure provides an extensive surface area that maximizes contact between olfactory sensory neurons (OSNs) residing in the OE and odorant molecules (Hansen and Zielinski, 2005). There are three classes of OSNs in the OE: ciliated sensory neurons, microvillous sensory neurons, and crypt cells. Ciliated sensory neurons are stimulated by bile salts (e.g., alarm substances in skin), microvillous sensory neurons are responsible for reception of food odorants, and crypt cells receive sex pheromones (Døving, 2007). These bipolar OSNs give rise to a single dendrite composed of several olfactory cilia extending into the mucus layer (Fig. 1.1). The OSNs also have a single axon that transmits olfactory information to the brain. Millions of OSN axons join together and form cranial nerve I (a.k.a., olfactory nerve) (Laberge and Hara, 2001). In vertebrates, the axons of OSNs project directly to the mitral cells in the olfactory bulb (OB), which in turn, send the olfactory inputs to processing centers in the telencephalon via an axon pathway, the olfactory tract.

In addition to OSNs, there are other types of cells residing in the OE (Fig. 1.1). Goblet cells are distributed in the apical domain of OE and provide a protective barrier for epithelial cells by secreting mucus (Bols et al., 2001). Sustentacular cells (a.k.a., supporting cells), and basal stem cells are the other cell classes that are present in the OE. Sustentacular cells play various roles in the OE, including metabolism of toxicants, physical and chemical insulation of OSNs, phagocytosis of dead cells, and regulation of the extracellular ionic environment (Hegg et al., 2009). Basal stem cells are responsible for regeneration of

epithelial cells and have two classes: horizontal basal cells (HBCs) and globose basal cells (GBCs). The HBCs act as a reserve population which can only be activated after extensive injury, whereas GBCs are mitotically active during the organism's life (Choi and Goldstein, 2018). The basal domain of the OE is attached to a basement membrane, the basal lamina, which, together with the OE, forms the olfactory mucosa (Fig. 1.1). In the olfactory rosette, there is another type of specialized cells called olfactory ensheathing cells (OECs). When the axons of OSNs leave the OE toward the OB, OECs sheath the axons and promote axonal projections to the olfactory bulb (Su and He, 2010). Various cell types present in the olfactory mucosa are connected through junctional complexes, such as tight junctions, which facilitate paracellular adhesions and communications (Sarkar and De, 2014; Van Itallie and Anderson, 2014). The well-organized structure of the olfactory mucosa provides an efficient sensory function in fish that is able to detect minute concentrations (i.e., nM) of odorants.

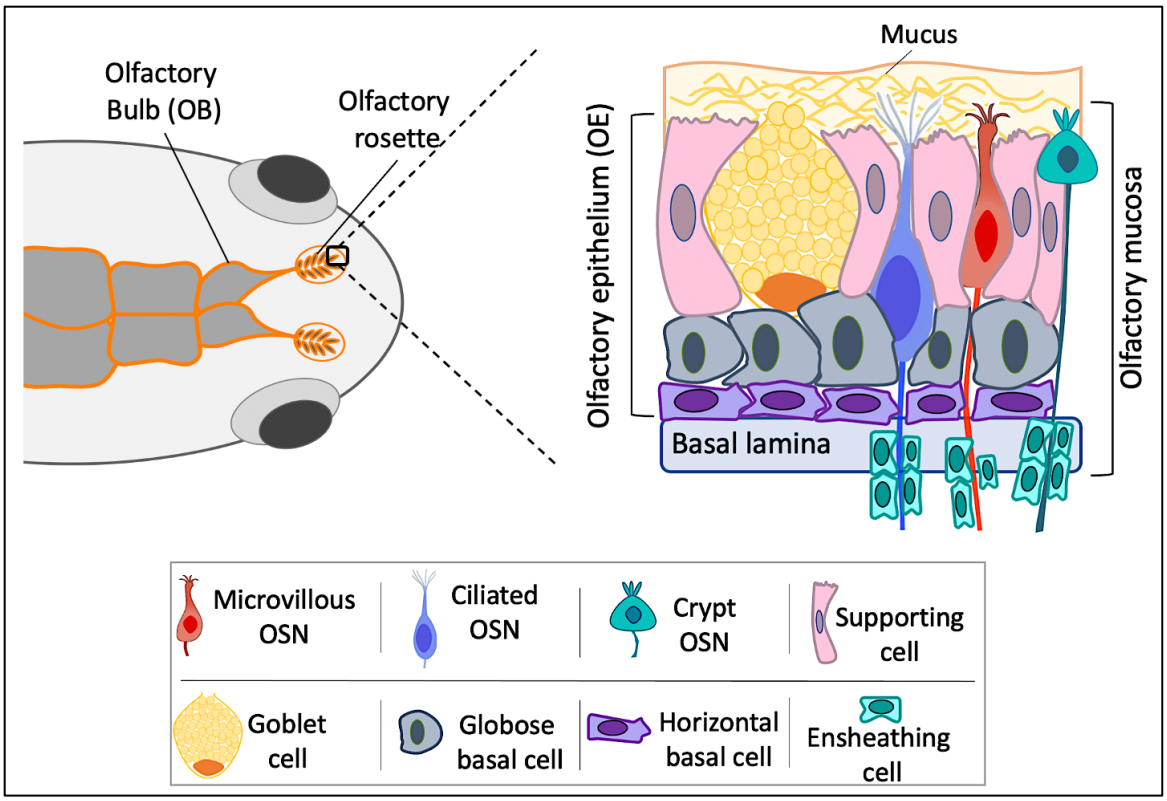

Figure 1.1. Schematic representation of fish olfactory system. Left drawing shows the position of olfactory system in the dorsal anterior side of the head. Right drawing shows the organization of different types of sensory (i.e., olfactory sensory neurons (OSNs)) and non-sensory cells residing in the olfactory mucosa.

Fish olfactory function and Cu^{2+} toxicity

Transduction of olfactory information is mediated through a series of molecular events that ultimately convert the chemical signals of odorant to an electrical signal named receptor potential. There are two pathways that conduct olfactory signal transduction (OST) in fish OSNs: inositol triphosphate (IP_3) and cyclic adenosine monophosphate (cAMP) mechanisms (Miyamoto et al., 1992) (Fig. 1.2). In general, OST begins with the odorant binding to specific odorant receptors on the cilia of OSNs. Stimulation of odorant receptors leads to production of secondary messengers, such as cAMP and IP_3 (Hansen and Zielinski, 2005; Laberge and Hara, 2001) . Cyclic-AMP activates ion channels that permit the influx of Na^+ and Ca^{2+} and depolarize OSNs, and IP_3 stimulates the release of Ca^{2+} from

intracellular storage (e.g., ER) (Fig. 1.2). The increased intracellular Ca^{2+} activates chloride channels which extrude Cl^- and consequently amplify the membrane depolarization. The cAMP-mediated OST pathway mainly operates in ciliated OSNs, whereas the IP_3-mediated OST pathway performs in microvillous OSNs (Hansen et al., 2003). Once the receptor potential has been generated, it propagates to the axon hillock and initiates the generation of an action potential. The generated action potential is directly transmitted to the brain where it is processed and ultimately translated to a specific olfactory-driven behaviour.

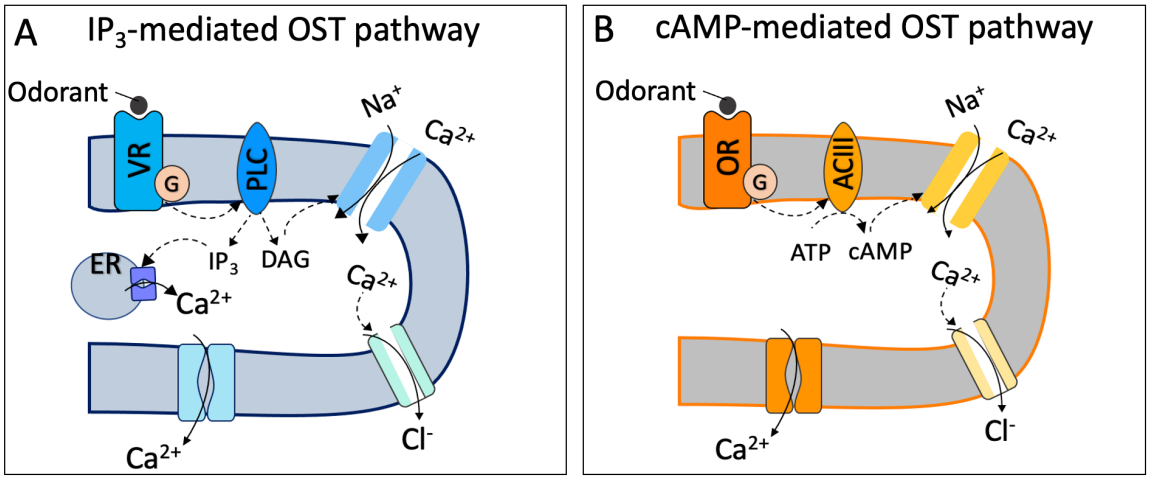

Figure 1.2. Schematic representation of two olfactory signal transduction (OST) pathways in fish. (A) inositol triphosphate (IP3)-mediated OST pathway which operates in microvillous OSNs. (B) cyclic adenosine monophosphate (cAMP)-mediated OST pathway which operates in ciliated OSNs. VR: vomeronasal receptor, PLC: phospholipase C, DAG: diacylglycerol, ER: endoplasmic reticulum, OR: olfactory receptor, ACIII: adenylyl cyclase III. G: G protein.

Perception of olfactory inputs mediates many fundamental activities in fish, including foraging, social interactions, avoiding contaminants, avoiding predation, mating, and homing (Olivares and Schmachtenberg, 2019). Therefore, any impairment in olfactory function can pose a threat to fish survival on the small scale and population loss on the larger scale. Due to the direct connection of OSNs to ambient water, they are exceptionally

exposed to many waterborne contaminants. As consequence of exposure to hazardous substances, OSNs may subject to functional impairment (Tierney et al., 2010).

The Cu^{2+} is a neurotoxicant which induces olfactory dysfunction in fish (Pyle and Mirza, 2007). Various aspects of Cu^{2+}-induced olfactory toxicity have been studied in recent decades (Tierney et al., 2010). Several studies have reported that exposure to Cu^{2+} can impair neurophysiological function (i.e., generation of receptor potential by OSNs) and behavioural responses to food stimuli and bile salts in fishes (Baldwin et al., 2003; Baldwin et al., 2011; Dew et al., 2012; Green et al., 2010; Pyle and Mirza, 2007). Waterborne exposure of fathead minnows to Cu^{2+} (5-50 µg/L) revealed a rapid accumulation of Cu^{2+} in the olfactory rosette which reached a plateau by 3 h (Green et al., 2010). A small increase (15 %) in the Cu accumulation in the OE can lead to an inhibition of olfactory sensitivity by > 50% (Green et al., 2010). A 4 h exposure of rainbow trout to 25 µg/L Cu^{2+} induced cellular necrosis in the OE and reduced the number of OSNs (Hansen et al., 1999). In coho salmon, exposure to 25 µg/L Cu^{2+} for 4 h reduced the protein expression of type III adenylate cyclase which is involved in cAMP production in the OST (Wang et al., 2013b). The number of OSNs was also reduced in the Cu^{2+}-exposed coho salmon (Wang et al., 2013b).

Copper ions have differential effects on ciliated and microvillous OSNs. Exposure to 5 and 10 µg/L Cu^{2+} had significantly reduced the ciliated OSN response to taurocholic acid (a bile salt stimulating ciliated OSNs), whereas microvillous responses to L-alanine (an amino acid-simulating microvillous OSN) were not affected in fathead minnows (Dew et al., 2014). Antipredator responses of fathead minnows to conspecific alarm cue —which stimulates ciliated OSNs—were also impaired by Cu^{2+} (Dew et al., 2014). Another study

demonstrated that the density of ciliated OSNs in zebrafish was more affected relative to the microvillous neurons after a 96 h exposure to 30 µg/L Cu^{2+}. The density of Cu^{2+}-exposed ciliated and microvillous OSNs underwent a 60% and 30% reduction, respectively (Lazzari et al., 2017). Furthermore, a significant loss of ciliated OSNs was reported in larval zebrafish that were exposed to 16 - 635 µg/L Cu^{2+} for 3 h (Ma et al., 2018). The population of microvillous OSNs was not affect by Cu^{2+} (Ma et al., 2018). These results suggest that ciliated OSNs and cAMP-mediated OST pathway are more sensitive to Cu^{2+} toxicity relative to the microvillous OSNs and the IP_3-based OST pathway (Dew et al., 2014; Ma et al., 2018).

Mechanism of Cu^{2+} toxicity and recovery in fish olfactory mucosa

Tilton et al. (2008) suggested that dysregulation of genes involved in ion homeostasis and OST are the underlying mechanisms of fish olfactory impairments measured at neurophysiological and behavioural levels. A 24 h exposure of zebrafish to 6 - 40 µg/L Cu^{2+} downregulated the transcript abundances of genes encoding odorant receptors and ion channels (Tilton et al., 2008). Moreover, dysregulation of miRNAs regulating the expression of genes involved in the OST pathway was reported in Cu^{2+}-exposed zebrafish (Wang et al., 2013a). However, in these molecular studies, no attempt was made to separate the OB from the olfactory rosette when trying to study the Cu^{2+}-induced transcriptional alteration in the zebrafish olfactory system. Using a pool of two tissues makes it difficult to discriminate the molecular events that were only affected in a single tissue—olfactory mucosa. Therefore, further investigation on the transcript profile of isolated olfactory mucosa can be beneficial in our understanding of Cu^{2+}-induced olfactory toxicity in fish.

Toxicity of Cu^{2+} in other tissues is associated with oxidative stress in part (Sanchez et al., 2005; Wang et al., 2015). For instance, exposure to 63.5 µg/L Cu^{2+} for 2 h led to the generation of reactive oxygen species (ROS) and DNA fragmentation (an indicator of apoptosis) in lateral line hair cells of zebrafish larvae (Olivari et al., 2008). Treatment of larvae with antioxidant compounds, such as reduced glutathione (GSH), protected hair cells against Cu^{2+}-induced ROS as no hair cell loss was observed in the GSH-treated larvae (Olivari et al., 2008). Nonetheless, to our knowledge, there is no report of Cu^{2+}-induced oxidative stress in fish olfactory mucosa. It is possible that mechanisms of Cu^{2+} toxicity are tissue-specific, which requires further investigation.

There is a possibility that fish can recover their olfactory function after being exposed to Cu^{2+}. Recovery may occur during continuous exposure conditions at low, ecologically relevant metal concentrations despite the continued presence of Cu^{2+} (Beyers and Farmer, 2001; Dew et al., 2012). Elimination of Cu^{2+} from fish culture water has also resulted in olfactory recovery in fish (Bettini et al., 2006; Sandahl et al., 2006). Nonetheless, the mechanism of fish olfactory recovery is largely unknown. Regeneration of OSNs from basal stem cells is the most probable mechanism of neural repair which requires further exploration.

Effect of CuNPs on fish olfactory system

Despite the importance of olfaction for fish reproduction and survival the toxicity of CuNPs on fish olfactory mucosa has not been well investigated. There is only one study that has evaluated the effect of CuNPs on rainbow trout olfactory system. For the first time, Sovová et al. (2014) reported that a 12 h exposure to 50 µg/L CuNPs can impair the olfactory mediated behavioural responses of fish to alarm substance (skin extract). They

also reported that CuNP induce greater behavioural impairment relative to the 50 µg/L Cu^{2+}. Exposure to CuNPs eliminated all fish responses to alarm substance, such as immediate freeze responses after delivering the odorant (Sovová et al., 2014). These results suggest that CuNP-exposed fish did not perceive the alarm substance. Copper ion-exposed fish exhibited reduced, but not eliminated, responses to the alarm substance (Sovová et al., 2014). Results of scanning electron microscopy demonstrated a pronounced reduction of cilia of sensory and non-sensory epithelial cells in the Cu^{2+} treatment. In contrast, CuNPs had no significant effects on the cilia of epithelial cells (Sovová et al., 2014).

Nevertheless, there are several gaps in our understanding of CuNPs toxicity in fish olfactory mucosa. Many aspects of CuNP-induced olfactory toxicity, including CuNPs uptake and accumulation, functionality of CuNP-exposed ciliated and microvillous OSNs, olfactory-driven behavioral responses to other odorants, effect of CuNPs exposure time on the olfaction, induction of oxidative stress and apoptosis, contribution of dissolved Cu in CuNPs toxicity, and recovery of CuNP-exposed OSNs, needs to be investigated. Moreover, the mechanisms underlying the CuNP-induced olfactory toxicity remained elusive. In this dissertation, we aim to close many of these knowledge gaps.

Rainbow trout and ecotoxicology studies

Rainbow trout is a common fish species used in toxicological research. This species is a suitable model organism for environmental research owing to its global distribution, high sensitivity to environmental contaminants, abundance in freshwater ecosystems, and economic importance (Miller and Hontela, 2011; Ondarza et al., 2012). Different studies have shown that the olfactory system of rainbow trout is sensitive to metals. For example, cadmium can impair olfactory-mediated social behaviour of rainbow trout (Sloman et al.,

2003). Both Copper NPs and Cu^{2+}, caused functional impairments in the rainbow trout olfactory system (Saucier and Astic, 1995; Sovová et al., 2014). Thus, rainbow trout is an ideal species for evaluating the mechanism of CuNPs and Cu^{2+}-induced olfactory toxicity.

Thesis objectives

The goal the PhD project outlined in this thesis is to expand our understanding of CuNPs toxicity in rainbow trout olfactory mucosa. The main thesis objectives are as follows:

1. To investigate the time-dependent effects of CuNPs and Cu^{2+} on the olfactory sensitivity and olfactory-driven behaviors of rainbow trout.

2. To explore the olfactory responses of rainbow trout upon encountering equitoxic concentrations of CuNPs and Cu^{2+}. In this objective, we evaluate if the rainbow trout olfactory system can detect and perceive the presence of CuNPs and Cu^{2+} in the water.

3. To investigate the molecular mechanism underlying CuNP-induced olfactory toxicity.

4. To evaluate the effect of CuNPs and Cu^{2+} on the structure of rainbow trout olfactory mucosa.

5. To ascertain the molecular basis of neural repair mechanisms that were affected by CuNPs and Cu^{2+} in rainbow trout olfactory mucosa.

6. To compare the recovery of rainbow trout olfactory mucosa after being exposed to CuNPs and Cu^{2+}.

In the next chapters (chapter 2-7) we address the above-mentioned objectives.

Thesis outcomes and adverse outcome pathway (AOP)

In the last decade, regulatory environmental risk assessors have faced a number of challenges, including increasing number of chemicals that need to be evaluated while decreasing the use of experimental animals in toxicity experiments (Villeneuve et al., 2014). Therefore, development of strategies that have high predictability and reliability in chemicals assessment is urgent. The concept of AOP was developed to meet this requirement. Adverse outcome pathway is a strategy that links the molecular initiating event (MIE) of a chemical, a series of key events (KEs) occurring at different biological levels, and the consequent adverse outcomes (AOs) (Ankley et al., 2010) (Figure 1.3). The KE is a measurable change in biological state that might lead to biological perturbation and a specific AO (e.g., reduced reproduction and survival). The goal of AOP development is to be a predictive tool by supporting the application of mechanistically based data in risk assessment and regulatory decision making (Ankley et al., 2010; Villeneuve et al., 2014).

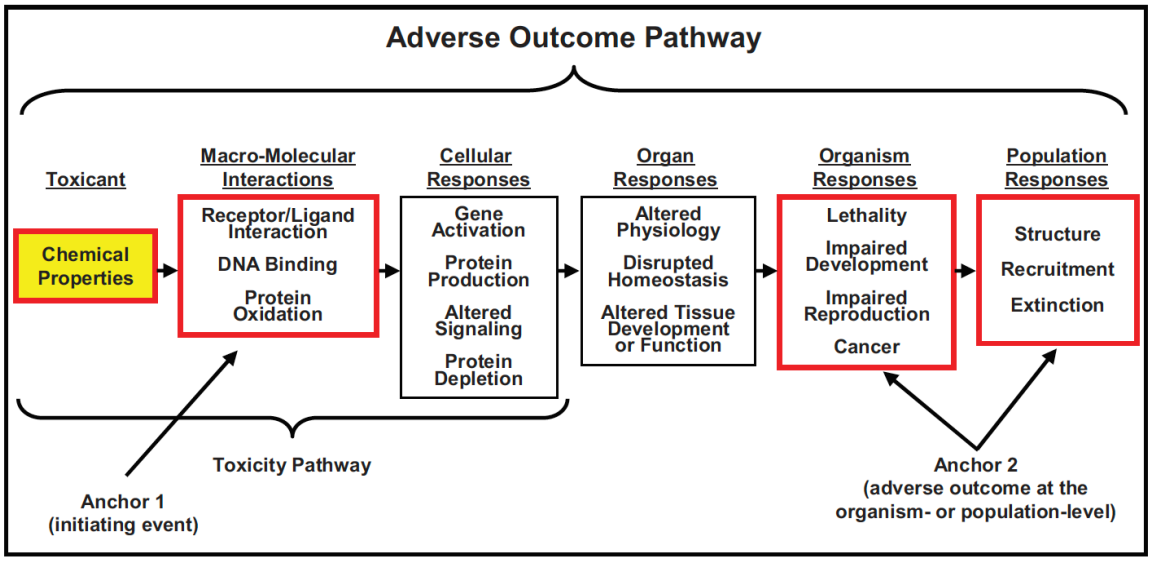

Figure 1.3. The diagram shows key features of adverse outcome pathway. Once a molecular initiating event is triggered by a toxicant, a sequence of key events will be activated toward the final step, an adverse outcome, in the biological cascade (Ankley et al., 2010).

Given that the loss of olfaction can threaten fish survival and reproduction, impairment of fish olfactory system can be a suitable AOP in evaluating the toxicity of aquatic contaminants (Williams and Gallagher, 2013). The outcomes of this dissertation can provide linkage among KEs occurred at the molecular level, neurophysiological level, and behavioural level in the fish olfactory system and facilitate the development of a designated AOP for fish olfactory injury. Considering that AOPs are not chemical-specific, environmental risk assessors can benefit from fish olfactory-based AOP to predict the AO of any environmental contaminant that triggers the MIE in the olfactory mucosal cells.

References

Abiraman T, Balasubramanian S. Synthesis and characterization of large-scale (< 2 nm) chitosan-decorated copper nanoparticles and their application in antifouling coating. Industrial & Engineering Chemistry Research 2017; 56: 1498-1508.

Adeleye AS, Oranu EA, Tao M, Keller AA. Release and detection of nanosized copper from a commercial antifouling paint. Water Research 2016; 102: 374-382.

Aiken GR, Hsu-Kim H, Ryan JN. Influence of dissolved organic matter on the environmental fate of metals, nanoparticles, and colloids. ACS Publications, 2011.

Al-Bairuty GA, Boyle D, Henry TB, Handy RD. Sublethal effects of copper sulphate compared to copper nanoparticles in rainbow trout (*Oncorhynchus mykiss*) at low pH: physiology and metal accumulation. Aquatic Toxicology 2016; 174: 188-198.

Al-Bairuty GA, Shaw BJ, Handy RD, Henry TB. Histopathological effects of waterborne copper nanoparticles and copper sulphate on the organs of rainbow trout (*Oncorhynchus mykiss*). Aquatic Toxicology 2013; 126: 104-115.

Amde M, Liu J-f, Tan Z-Q, Bekana D. Transformation and bioavailability of metal oxide nanoparticles in aquatic and terrestrial environments. A review. Environmental Pollution 2017; 230: 250-267.

Ankley GT, Bennett RS, Erickson RJ, Hoff DJ, Hornung MW, Johnson RD, et al. Adverse outcome pathways: a conceptual framework to support ecotoxicology research and risk assessment. Environmental Toxicology and Chemistry: An International Journal 2010; 29: 730-741.

Athanassiou EK, Grass RN, Stark WJ. Large-scale production of carbon-coated copper nanoparticles for sensor applications. Nanotechnology 2006; 17: 1668.

Atli G, Grosell M. Characterization and response of antioxidant systems in the tissues of the freshwater pond snail (*Lymnaea stagnalis*) during acute copper exposure. Aquatic Toxicology 2016; 176: 38-44.

Avellan A, Simonin M, Anderson SM, Geitner NK, Bossa N, Spielman-Sun E, et al. Differential reactivity of copper-and gold-based nanomaterials controls their seasonal biogeochemical cycling and fate in a freshwater wetland mesocosm. Environmental Science & Technology 2020; 54: 1533-1544.

Balamurugan K, Schaffner W. Copper homeostasis in eukaryotes: teetering on a tightrope. Biochimica et Biophysica Acta (BBA)-Molecular Cell Research 2006; 1763: 737-746.

Baldwin DH, Sandahl JF, Labenia JS, Scholz NL. Sublethal effects of copper on *coho salmon*: impacts on nonoverlapping receptor pathways in the peripheral olfactory nervous system. Environmental Toxicology and Chemistry: An International Journal 2003; 22: 2266-2274.

Baldwin DH, Tatara CP, Scholz NL. Copper-induced olfactory toxicity in salmon and steelhead: extrapolation across species and rearing environments. Aquatic Toxicology 2011; 101: 295-297.

Barreto DM, Tonietto AE, Lombardi AT. Environmental concentrations of copper nanoparticles affect vital functions in Ankistrodesmus densus. Aquatic Toxicology 2020; 231: 105720.

Bellotti N, Romagnoli R, Quintero C, Domínguez-Wong C, Ruiz F, Deyá C. Nanoparticles as antifungal additives for indoor water borne paints. Progress in Organic Coatings 2015; 86: 33-40.

Bertinato J, L'Abbé MR. Maintaining copper homeostasis: regulation of copper-trafficking proteins in response to copper deficiency or overload. The Journal of Nutritional Biochemistry 2004; 15: 316-322.

Bettini S, Ciani F, Franceschini V. Recovery of the olfactory receptor neurons in the African *Tilapia mariae* following exposure to low copper level. Aquatic Toxicology 2006; 76: 321-328.

Beyers DW, Farmer MS. Effects of copper on olfaction of Colorado pikeminnow. Environmental Toxicology and Chemistry: An International Journal 2001; 20: 907-912.

Bols NC, Brubacher JL, Ganassin RC, Lee LE. Ecotoxicology and innate immunity in fish. Developmental & Comparative Immunology 2001; 25: 853-873.

Bundschuh M, Filser J, Lüderwald S, McKee MS, Metreveli G, Schaumann GE, et al. Nanoparticles in the environment: where do we come from, where do we go to? Environmental Sciences Europe 2018; 30: 1-17.

Chari N, Felix L, Davoodbasha M, Ali AS, Nooruddin T. In vitro and in vivo antibiofilm effect of copper nanoparticles against aquaculture pathogens. Biocatalysis and Agricultural Biotechnology 2017; 10: 336-341.

Chen H, Zheng X, Chen Y, Li M, Liu K, Li X. Influence of copper nanoparticles on the physical-chemical properties of activated sludge. PLoS One 2014; 9: e92871.

Cheng Y-F, Zhang Q, Li G-F, Xue Y, Zheng X-P, Cai S, et al. Long-term effects of copper nanoparticles on granule-based denitrification systems: Performance, microbial communities, functional genes and sludge properties. Bioresource Technology 2019; 289: 121707.

Chio C-P, Chen W-Y, Chou W-C, Hsieh N-H, Ling M-P, Liao C-M. Assessing the potential risks to zebrafish posed by environmentally relevant copper and silver nanoparticles. Science of the Total Environment 2012; 420: 111-118.

Choi R, Goldstein BJ. Olfactory epithelium: cells, clinical disorders, and insights from an adult stem cell niche. Laryngoscope Investigative Otolaryngology 2018; 3: 35-42.

Choi S, Johnston M, Wang G-S, Huang C. A seasonal observation on the distribution of engineered nanoparticles in municipal wastewater treatment systems exemplified by TiO2 and ZnO. Science of the Total Environment 2018; 625: 1321-1329.

Choi Y, Lee C, Hwang Y, Park M, Lee J, Choi C, et al. Tribological behavior of copper nanoparticles as additives in oil. Current Applied Physics 2009; 9: e124-e127.

Conway JR, Adeleye AS, Gardea-Torresdey J, Keller AA. Aggregation, dissolution, and transformation of copper nanoparticles in natural waters. Environmental Science & Technology 2015; 49: 2749-2756.

Courtois P, Rorat A, Lemiere S, Guyoneaud R, Attard E, Levard C, et al. Ecotoxicology of silver nanoparticles and their derivatives introduced in soil with or without sewage sludge: A review of effects on microorganisms, plants and animals. Environmental Pollution 2019; 253: 578-598.

Craig PM, Wood CM, McClelland GB. Oxidative stress response and gene expression with acute copper exposure in zebrafish (*Danio rerio*). American Journal of Physiology-Regulatory, Integrative and Comparative Physiology 2007; 293: R1882-R1892.

Cross RK, Tyler C, Galloway TS. Transformations that affect fate, form and bioavailability of inorganic nanoparticles in aquatic sediments. Environmental Chemistry 2015; 12: 627-642.

Dankovich TA, Smith JA. Incorporation of copper nanoparticles into paper for point-of-use water purification. Water Research 2014; 63: 245-251.

De Boeck G, van der Ven K, Hattink J, Blust R. Swimming performance and energy metabolism of rainbow trout, common carp and gibel carp respond differently to sublethal copper exposure. Aquatic Toxicology 2006; 80: 92-100.

Derjaguin B, Landau L. Theory of the stability of strongly charged lyophobic sols and of the adhesion of strongly charged particles in solutions of electrolytes. Progress in Surface Science 1993; 43: 30-59.

Dew WA, Azizishirazi A, Pyle GG. Contaminant-specific targeting of olfactory sensory neuron classes: Connecting neuron class impairment with behavioural deficits. Chemosphere 2014; 112: 519-525.

Dew WA, Wood CM, Pyle GG. Effects of continuous copper exposure and calcium on the olfactory response of fathead minnows. Environmental Science & Technology 2012; 46: 9019-9026.

Dlamini NG, Basson AK, Pullabhotla VSR. Optimization and application of bioflocculant passivated copper nanoparticles in the wastewater treatment. International Journal of Environmental Research and Public Health 2019; 16: 2185.

Døving KB. The functional organization of the fish olfactory system. Progress in Neurobiology 2007; 82: 80-86.

Fernández-Arias M, Boutinguiza M, Del Val J, Covarrubias C, Bastias F, Gómez L, et al. Copper nanoparticles obtained by laser ablation in liquids as bactericidal agent for dental applications. Applied Surface Science 2020; 507: 145032.

Ganesh R, Smeraldi J, Hosseini T, Khatib L, Olson BH, Rosso D. Evaluation of nanocopper removal and toxicity in municipal wastewaters. Environmental Science & Technology 2010; 44: 7808-7813.

Geist J, Werner I, Eder KJ, Leutenegger CM. Comparisons of tissue-specific transcription of stress response genes with whole animal endpoints of adverse effect in striped bass (*Morone saxatilis*) following treatment with copper and esfenvalerate. Aquatic Toxicology 2007; 85: 28-39.

Glover RD, Miller JM, Hutchison JE. Generation of metal nanoparticles from silver and copper objects: nanoparticle dynamics on surfaces and potential sources of nanoparticles in the environment. ACS Nano 2011; 5: 8950-8957.

Green WW, Mirza RS, Wood CM, Pyle GG. Copper binding dynamics and olfactory impairment in fathead minnows (*Pimephales promelas*). Environmental Science & Technology 2010; 44: 1431-1437.

Griffitt RJ, Hyndman K, Denslow ND, Barber DS. Comparison of molecular and histological changes in zebrafish gills exposed to metallic nanoparticles. Toxicological Sciences 2009; 107: 404-415.

Griffitt RJ, Weil R, Hyndman KA, Denslow ND, Powers K, Taylor D, et al. Exposure to copper nanoparticles causes gill injury and acute lethality in zebrafish (*Danio rerio*). Environmental Science & Technology 2007; 41: 8178-8186.

Grosell M, Wood CM. Copper uptake across rainbow trout gills: mechanisms of apical entry. Journal of Experimental Biology 2002; 205: 1179-1188.

Guo L, Yan DD, Yang D, Li Y, Wang X, Zalewski O, et al. Combinatorial photothermal and immuno cancer therapy using chitosan-coated hollow copper sulfide nanoparticles. ACS Nano 2014; 8: 5670-5681.

Gurav P, Naik SS, Ansari K, Srinath S, Kishore KA, Setty YP, et al. Stable colloidal copper nanoparticles for a nanofluid: Production and application. Colloids and Surfaces A: Physicochemical and Engineering Aspects 2014; 441: 589-597.

Handy RD, Henry TB, Scown TM, Johnston BD, Tyler CR. Manufactured nanoparticles: their uptake and effects on fish—a mechanistic analysis. Ecotoxicology 2008; 17: 396-409.

Hansen A, Rolen SH, Anderson K, Morita Y, Caprio J, Finger TE. Correlation between olfactory receptor cell type and function in the channel catfish. Journal of Neuroscience 2003; 23: 9328-9339.

Hansen A, Zielinski BS. Diversity in the olfactory epithelium of bony fishes: development, lamellar arrangement, sensory neuron cell types and transduction components. Journal of Neurocytology 2005; 34: 183-208.

Hansen JA, Rose JD, Jenkins RA, Gerow KG, Bergman HL. Chinook salmon (*Oncorhynchus tshawytscha*) and rainbow trout (*Oncorhynchus mykiss*) exposed to copper: neurophysiological and histological effects on the olfactory system. Environmental Toxicology and Chemistry: An International Journal 1999; 18: 1979-1991.

Hatori Y, Yan Y, Schmidt K, Furukawa E, Hasan NM, Yang N, et al. Neuronal differentiation is associated with a redox-regulated increase of copper flow to the secretory pathway. Nature Communications 2016; 7: 1-12.

He X, Deng H, Hwang H-m. The current application of nanotechnology in food and agriculture. Journal of Food and Drug Analysis 2019; 27: 1-21.

Hegg CC, Irwin M, Lucero MT. Calcium store-mediated signaling in sustentacular cells of the mouse olfactory epithelium. Glia 2009; 57: 634-644.

Hu G, Cao J. Metal-containing nanoparticles derived from concealed metal deposits: An important source of toxic nanoparticles in aquatic environments. Chemosphere 2019; 224: 726-733.

Hua J, Vijver MG, Ahmad F, Richardson MK, Peijnenburg WJ. Toxicity of different-sized copper nano-and submicron particles and their shed copper ions to zebrafish embryos. Environmental Toxicology and Chemistry 2014; 33: 1774-1782.

Jiang W-D, Liu Y, Hu K, Jiang J, Li S-H, Feng L, et al. Copper exposure induces oxidative injury, disturbs the antioxidant system and changes the Nrf2/ARE (CuZnSOD) signaling in the fish brain: protective effects of myo-inositol. Aquatic Toxicology 2014; 155: 301-313.

Keller AA, Adeleye AS, Conway JR, Garner KL, Zhao L, Cherr GN, et al. Comparative environmental fate and toxicity of copper nanomaterials. NanoImpact 2017; 7: 28-40.

Keller AA, Lazareva A. Predicted releases of engineered nanomaterials: from global to regional to local. Environmental Science & Technology Letters 2014; 1: 65-70.

Khezri K, Saeedi M, Dizaj SM. Application of nanoparticles in percutaneous delivery of active ingredients in cosmetic preparations. Biomedicine & Pharmacotherapy 2018; 106: 1499-1505.

Klaine SJ, Alvarez PJ, Batley GE, Fernandes TF, Handy RD, Lyon DY, et al. Nanomaterials in the environment: behavior, fate, bioavailability, and effects. Environmental Toxicology and Chemistry: An International Journal 2008; 27: 1825-1851.

Laberge F, Hara TJ. Neurobiology of fish olfaction: a review. Brain Research Reviews 2001; 36: 46-59.

Lall SP, Lewis-McCrea LM. Role of nutrients in skeletal metabolism and pathology in fish—an overview. Aquaculture 2007; 267: 3-19.

Lazzari M, Bettini S, Milani L, Maurizii MG, Franceschini V. Differential response of olfactory sensory neuron populations to copper ion exposure in zebrafish. Aquatic Toxicology 2017; 183: 54-62.

Lee C-Y, Horng J-L, Liu S-T, Lin L-Y. Exposure to copper nanoparticles impairs ion uptake, and acid and ammonia excretion by ionocytes in zebrafish embryos. Chemosphere 2020; 261: 128051.

Letelier ME, Lepe AM, Faúndez M, Salazar J, Marín R, Aracena P, et al. Possible mechanisms underlying copper-induced damage in biological membranes leading to cellular toxicity. Chemico-Biological Interactions 2005; 151: 71-82.

Li M, Liu W, Slaveykova VI. Effects of mixtures of engineered nanoparticles and metallic pollutants on aquatic organisms. Environments 2020; 7: 27.

Lin K-C, Lin Y-C, Chen S-M. A highly sensitive nonenzymatic glucose sensor based on multi-walled carbon nanotubes decorated with nickel and copper nanoparticles. Electrochimica Acta 2013; 96: 164-172.

Linbo TL, Stehr CM, Incardona JP, Scholz NL. Dissolved copper triggers cell death in the peripheral mechanosensory system of larval fish. Environmental Toxicology and Chemistry: An International Journal 2006; 25: 597-603.

Lindh S, Razmara P, Bogart S, Pyle G. Comparative tissue distribution and depuration characteristics of copper nanoparticles and soluble copper in rainbow trout (*Oncorhynchus mykiss*). Environmental Toxicology and Chemistry 2019; 38: 80-89.

Liu L, Li M, Lyu J, Zhao T, Li T. Facile and green preparation of three-dimensionally nanoporous copper films by low-current electrical field-induced assembly of copper nanoparticles for lithium-ion battery applications. Journal of Materials Engineering and Performance 2018; 27: 4680-4692.

Luechinger NA, Athanassiou EK, Stark WJ. Graphene-stabilized copper nanoparticles as an air-stable substitute for silver and gold in low-cost ink-jet printable electronics. Nanotechnology 2008; 19: 445201.

Ma EY, Heffern K, Cheresh J, Gallagher EP. Differential copper-induced death and regeneration of olfactory sensory neuron populations and neurobehavioral function in larval zebrafish. Neurotoxicology 2018; 69: 141-151.

Magdassi S, Grouchko M, Kamyshny A. Copper nanoparticles for printed electronics: routes towards achieving oxidation stability. Materials 2010; 3: 4626-4638.

Malhotra N, Ger T-R, Uapipatanakul B, Huang J-C, Chen KH-C, Hsiao C-D. Review of copper and copper nanoparticle toxicity in fish. Nanomaterials 2020; 10: 1126.

McNeil PL, Boyle D, Henry TB, Handy RD, Sloman KA. Effects of metal nanoparticles on the lateral line system and behaviour in early life stages of zebrafish (*Danio rerio*). Aquatic Toxicology 2014; 152: 318-323.

Mendelsohn BA, Yin C, Johnson SL, Wilm TP, Solnica-Krezel L, Gitlin JD. Atp7a determines a hierarchy of copper metabolism essential for notochord development. Cell Metabolism 2006; 4: 155-162.

Miller L, Hontela A. Species-specific sensitivity to selenium-induced impairment of cortisol secretion in adrenocortical cells of rainbow trout (Oncorhynchus mykiss) and brook trout (Salvelinus fontinalis). Toxicology and Applied Pharmacology 2011; 253: 137-144.

Misra SK, Dybowska A, Berhanu D, Croteau MNl, Luoma SN, Boccaccini AR, et al. Isotopically modified nanoparticles for enhanced detection in bioaccumulation studies. Environmental Science & Technology 2012a; 46: 1216-1222.

Misra SK, Dybowska A, Berhanu D, Luoma SN, Valsami-Jones E. The complexity of nanoparticle dissolution and its importance in nanotoxicological studies. Science of the Total Environment 2012b; 438: 225-232.

Miyamoto T, Restrepo D, Cragoe EJ, Teeter JH. IP 3-and cAMP-induced responses in isolated olfactory receptor neurons from the channel catfish. The Journal of Membrane Biology 1992; 127: 173-183.

Mortimer M, Kasemets K, Kahru A. Toxicity of ZnO and CuO nanoparticles to ciliated protozoa *Tetrahymena thermophila*. Toxicology 2010; 269: 182-189.

Mulenos MR, Liu J, Lujan H, Guo B, Lichtfouse E, Sharma VK, et al. Copper, silver, and titania nanoparticles do not release ions under anoxic conditions and release only minute ion levels under oxic conditions in water: Evidence for the low toxicity of nanoparticles. Environmental Chemistry Letters 2020: 1-10.

Noman M, Shahid M, Ahmed T, Niazi MBK, Hussain S, Song F, et al. Use of biogenic copper nanoparticles synthesized from a native Escherichia sp. as photocatalysts for azo dye degradation and treatment of textile effluents. Environmental Pollution 2020; 257: 113514.

Olivares J, Schmachtenberg O. An update on anatomy and function of the teleost olfactory system. PeerJ 2019; 7: e7808.

Olivari FA, Hernández PP, Allende ML. Acute copper exposure induces oxidative stress and cell death in lateral line hair cells of zebrafish larvae. Brain Research 2008; 1244: 1-12.

Ondarza PM, Gonzalez M, Fillmann G, Miglioranza KS. Increasing levels of persistent organic pollutants in rainbow trout (*Oncorhynchus mykiss*) following a mega-flooding episode in the Negro River basin, Argentinean Patagonia. Science of the Total Environment 2012; 419: 233-239.

Patel S, Kim J, Herrera M, Mukherjee A, Kabanov AV, Sahay G. Brief update on endocytosis of nanomedicines. Advanced Drug Delivery Reviews 2019; 144: 90-111.

Peijnenburg WJ, Baalousha M, Chen J, Chaudry Q, Von der kammer F, Kuhlbusch TA, et al. A review of the properties and processes determining the fate of engineered nanomaterials in the aquatic environment. Critical Reviews in Environmental Science and Technology 2015; 45: 2084-2134.

Peng C, Shen C, Zheng S, Yang W, Hu H, Liu J, et al. Transformation of CuO nanoparticles in the aquatic environment: influence of pH, electrolytes and natural organic matter. Nanomaterials 2017; 7: 326.

Peters RJ, van Bemmel G, Milani NB, den Hertog GC, Undas AK, van der Lee M, et al. Detection of nanoparticles in Dutch surface waters. Science of the Total Environment 2018; 621: 210-218.

Pilehvar A, Town RM, Blust R. The effect of copper on behaviour, memory, and associative learning ability of zebrafish (*Danio rerio*). Ecotoxicology and Environmental Safety 2020; 188: 109900.

Ponmurugan P, Manjukarunambika K, Elango V, Gnanamangai BM. Antifungal activity of biosynthesised copper nanoparticles evaluated against red root-rot disease in tea plants. Journal of Experimental Nanoscience 2016; 11: 1019-1031.

Pu Y, Tang F, Adam P-M, Laratte B, Ionescu RE. Fate and characterization factors of nanoparticles in seventeen subcontinental freshwaters: a case study on copper nanoparticles. Environmental Science & Technology 2016; 50: 9370-9379.

Pulido-Reyes G, Leganes F, Fernández-Piñas F, Rosal R. Bio-nano interface and environment: A critical review. Environmental Toxicology and Chemistry 2017; 36: 3181-3193.

Purohit P, Samadi A, Bendix PM, Laserna JJ, Oddershede LB. Optical trapping reveals differences in dielectric and optical properties of copper nanoparticles compared to their oxides and ferrites. Scientific Reports 2020; 10: 1-10.

Pyle GG, Mirza RS. Copper-impaired chemosensory function and behavior in aquatic animals. Human and Ecological Risk Assessment 2007; 13: 492-505.

Qu X, Alvarez PJ, Li Q. Applications of nanotechnology in water and wastewater treatment. Water Research 2013; 47: 3931-3946.

Radetić M, Marković D. Nano-finishing of cellulose textile materials with copper and copper oxide nanoparticles. Cellulose 2019; 26: 8971-8991.

Ramyadevi J, Jeyasubramanian K, Marikani A, Rajakumar G, Rahuman AA. Synthesis and antimicrobial activity of copper nanoparticles. Materials Letters 2012; 71: 114-116.

Ray A, Gautam A, Das S, Pal K, Das S, Karmakar P, et al. Effects of copper oxide nanoparticle on gill filtration rate, respiration rate, hemocyte associated immune parameters and oxidative status of an Indian freshwater mussel. Comparative Biochemistry and Physiology Part C: Toxicology & Pharmacology 2020; 237: 108855.

Riggio M, Filosa S, Parisi E, Scudiero R. Changes in zinc, copper and metallothionein contents during oocyte growth and early development of the teleost Danio rerio (zebrafish). Comparative Biochemistry and Physiology Part C: Toxicology & Pharmacology 2003; 135: 191-196.

Sanchez W, Palluel O, Meunier L, Coquery M, Porcher J-M, Ait-Aissa S. Copper-induced oxidative stress in three-spined stickleback: relationship with hepatic metal levels. Environmental Toxicology and Pharmacology 2005; 19: 177-183.

Sandahl JF, Miyasaka G, Koide N, Ueda H. Olfactory inhibition and recovery in chum salmon (*Oncorhynchus keta*) following copper exposure. Canadian Journal of Fisheries and Aquatic Sciences 2006; 63: 1840-1847.

Santos EM, Ball JS, Williams TD, Wu H, Ortega F, Van Aerle R, et al. Identifying health impacts of exposure to copper using transcriptomics and metabolomics in a fish model. Environmental Science & Technology 2010; 44: 820-826.

Sarkar SK, De SK. Functional anatomy of cellular junctions in olfactory neuroepithelium of *Pseudapocryptes lanceolatus* (Bloch and Schneider). 2014.

Saucier D, Astic L. Morpho-functional alterations in the olfactory system of rainbow trout (*Oncorhynchus mykiss*) and possible acclimation in response to long-lasting exposure to low copper levels. Comparative Biochemistry and Physiology Part A: Physiology 1995; 112: 273-284.

Scola S, Blasco J, Campana O. “Nanosize effect” in the metal-handling strategy of the bivalve *Scrobicularia plana* exposed to CuO nanoparticles and copper ions in whole-sediment toxicity tests. Science of The Total Environment 2021; 760: 143886.

Scown T, Van Aerle R, Tyler C. Do engineered nanoparticles pose a significant threat to the aquatic environment? Critical Reviews in Toxicology 2010; 40: 653-670.

Sekoai PT, Ouma CNM, Du Preez SP, Modisha P, Engelbrecht N, Bessarabov DG, et al. Application of nanoparticles in biofuels: An overview. Fuel 2019; 237: 380-397.

Shaw BJ, Al-Bairuty G, Handy RD. Effects of waterborne copper nanoparticles and copper sulphate on rainbow trout,(*Oncorhynchus mykiss*): physiology and accumulation. Aquatic Toxicology 2012; 116: 90-101.

Shen P, Liu Y, Long Y, Shen L, Kang B. High-performance polymer solar cells enabled by copper nanoparticles-induced plasmon resonance enhancement. The Journal of Physical Chemistry C 2016; 120: 8900-8906.

Sloman KA, Scott GR, Diao Z, Rouleau C, Wood CM, McDonald DG. Cadmium affects the social behaviour of rainbow trout, *Oncorhynchus mykiss*. Aquatic Toxicology 2003; 65: 171-185.

Song L, Vijver MG, Peijnenburg WJ, Galloway TS, Tyler CR. A comparative analysis on the in vivo toxicity of copper nanoparticles in three species of freshwater fish. Chemosphere 2015; 139: 181-189.

Sousa VS, Teixeira MR. Metal-based engineered nanoparticles in the drinking water treatment systems: A critical review. Science of The Total Environment 2020; 707: 136077.

Souza IdC, Morozesk M, Mansano AS, Mendes VA, Azevedo VC, Matsumoto ST, et al. Atmospheric particulate matter from an industrial area as a source of metal nanoparticle contamination in aquatic ecosystems. Science of The Total Environment 2020; 753: 141976.

Souza IdC, Morozesk M, Mansano AS, Mendes VA, Azevedo VC, Matsumoto ST, et al. Atmospheric particulate matter from an industrial area as a source of metal nanoparticle contamination in aquatic ecosystems. Science of The Total Environment 2021; 753: 141976.

Sovová T, Boyle D, Sloman KA, Pérez CV, Handy RD. Impaired behavioural response to alarm substance in rainbow trout exposed to copper nanoparticles. Aquatic Toxicology 2014; 152: 195-204.

Stern BR. Essentiality and toxicity in copper health risk assessment: overview, update and regulatory considerations. Journal of Toxicology and Environmental Health, Part A 2010; 73: 114-127.

Su Z, He C. Olfactory ensheathing cells: biology in neural development and regeneration. Progress in Neurobiology 2010; 92: 517-532.

Sun X, Zhang Y, Chen G, Gai Z. Application of nanoparticles in enhanced oil recovery: a critical review of recent progress. Energies 2017; 10: 345.

Suvetha L, Ramesh M, Saravanan M. Influence of cypermethrin toxicity on ionic regulation and gill Na+/K+-ATPase activity of a freshwater teleost fish Cyprinus carpio. Environmental Toxicology and Pharmacology 2010; 29: 44-49.

Tesser ME, de Paula AA, Risso WE, Monteiro RA, Santo Pereira AdE, Fraceto LF, et al. Sublethal effects of waterborne copper and copper nanoparticles on the freshwater Neotropical teleost *Prochilodus lineatus*: A comparative approach. Science of The Total Environment 2020; 704: 135332.

Tierney KB, Baldwin DH, Hara TJ, Ross PS, Scholz NL, Kennedy CJ. Olfactory toxicity in fishes. Aquatic toxicology 2010; 96: 2-26.

Tilton F, Tilton SC, Bammler TK, Beyer R, Farin F, Stapleton PL, et al. Transcriptional biomarkers and mechanisms of copper-induced olfactory injury in zebrafish. Environmental Science & Technology 2008; 42: 9404-9411.

Vaid P, Raizada P, Saini AK, Saini RV. Biogenic silver, gold and copper nanoparticles-A sustainable green chemistry approach for cancer therapy. Sustainable Chemistry and Pharmacy 2020; 16: 100247.

Vale G, Mehennaoui K, Cambier S, Libralato G, Jomini S, Domingos RF. Manufactured nanoparticles in the aquatic environment-biochemical responses on freshwater organisms: a critical overview. Aquatic Toxicology 2016; 170: 162-174.

Van Itallie CM, Anderson JM. Architecture of tight junctions and principles of molecular composition. Seminars in Cell & Developmental Biology. 36. Elsevier, 2014, pp. 157-165.

Verwey E, Overbeek JTG. Theory of the stability of lyophobic colloids. Journal of Colloid Science 1955; 10: 224-225.

Vicario-Parés U, Lacave JM, Reip P, Cajaraville MP, Orbea A. Cellular and molecular responses of adult zebrafish after exposure to CuO nanoparticles or ionic copper. Ecotoxicology 2018; 27: 89-101.

Villanueva ME, Diez AMadR, González JA, Pérez CJ, Orrego M, Piehl L, et al. Antimicrobial activity of starch hydrogel incorporated with copper nanoparticles. ACS Applied Materials & Interfaces 2016; 8: 16280-16288.

Villeneuve DL, Crump D, Garcia-Reyero N, Hecker M, Hutchinson TH, LaLone CA, et al. Adverse outcome pathway (AOP) development I: strategies and principles. Toxicological Sciences 2014; 142: 312-320.

Wang B, Feng L, Jiang W-D, Wu P, Kuang S-Y, Jiang J, et al. Copper-induced tight junction mRNA expression changes, apoptosis and antioxidant responses via NF-κB, TOR and Nrf2 signaling molecules in the gills of fish: preventive role of arginine. Aquatic Toxicology 2015; 158: 125-137.

Wang J, Nabi MM, Mohanty SK, Afrooz AN, Cantando E, Aich N, et al. Detection and quantification of engineered particles in urban runoff. Chemosphere 2020; 248: 126070.

Wang L, Bammler TK, Beyer RP, Gallagher EP. Copper-induced deregulation of microRNA expression in the zebrafish olfactory system. Environmental Science & Technology 2013a; 47: 7466-7474.

Wang L, Espinoza HM, Gallagher EP. Brief exposure to copper induces apoptosis and alters mediators of olfactory signal transduction in coho salmon. Chemosphere 2013b; 93: 2639-2643.

Wei Y, Chen S, Kowalczyk B, Huda S, Gray TP, Grzybowski BA. Synthesis of stable, low-dispersity copper nanoparticles and nanorods and their antifungal and catalytic properties. The Journal of Physical Chemistry C 2010; 114: 15612-15616.

Wilczewska AZ, Niemirowicz K, Markiewicz KH, Car H. Nanoparticles as drug delivery systems. Pharmacological Reports 2012; 64: 1020-1037.

Williams CR, Gallagher EP. Effects of cadmium on olfactory mediated behaviors and molecular biomarkers in coho salmon (*Oncorhynchus kisutch*). Aquatic Toxicology 2013; 140: 295-302.

Worthington KL, Adamcakova-Dodd A, Wongrakpanich A, Mudunkotuwa IA, Mapuskar KA, Joshi VB, et al. Chitosan coating of copper nanoparticles reduces in vitro toxicity and increases inflammation in the lung. Nanotechnology 2013; 24: 395101.

Xiao Y, Peijnenburg WJ, Chen G, Vijver MG. Impact of water chemistry on the particle-specific toxicity of copper nanoparticles to *Daphnia magna*. Science of the Total Environment 2018a; 610: 1329-1335.

Xiao Y, Vijver MG, Peijnenburg WJ. Impact of water chemistry on the behavior and fate of copper nanoparticles. Environmental Pollution 2018b; 234: 684-691.

Xu J, Zhang Q, Li X, Zhan S, Wang L, Chen D. The effects of copper oxide nanoparticles on dorsoventral patterning, convergent extension, and neural and cardiac development of zebrafish. Aquatic Toxicology 2017; 188: 130-137.

Yang L, Wang W-X. Comparative contributions of copper nanoparticles and ions to copper bioaccumulation and toxicity in barnacle larvae. Environmental Pollution 2019; 249: 116-124.

Yang W, Salim J, Li S, Sun C, Chen L, Goodenough JB, et al. Perovskite Sr 0.95 Ce 0.05 CoO 3− δ loaded with copper nanoparticles as a bifunctional catalyst for lithium-air batteries. Journal of Materials Chemistry 2012; 22: 18902-18907.

Yen H-J, Horng J-L, Yu C-H, Fang C-Y, Yeh Y-H, Lin L-Y. Toxic effects of silver and copper nanoparticles on lateral-line hair cells of zebrafish embryos. Aquatic Toxicology 2019; 215: 105273.

Yu W, Xie H, Wang X. Enhanced thermal conductivity of liquid Paraffin based nanofluids containing copper nanoparticles. Journal of Dispersion Science and Technology 2011; 32: 948-951.

Yue L, Zhao J, Yu X, Lv K, Wang Z, Xing B. Interaction of CuO nanoparticles with duckweed (*Lemna minor*. L): Uptake, distribution and ROS production sites. Environmental Pollution 2018; 243: 543-552.

Zhang Z-Z, Cheng Y-F, Wu J, Bai Y-H, Xu J-J, Shi Z-J, et al. Discrepant effects of metal and metal oxide nanoparticles on anammox sludge properties: A comparison between Cu and CuO nanoparticles. Bioresource Technology 2018; 266: 507-515.

Zhang Z-Z, Hu H-Y, Xu J-J, Shi Z-J, Shen Y-Y, Shi M-L, et al. Susceptibility, resistance and resilience of anammox biomass to nanoscale copper stress. Bioresource Technology 2017; 241: 35-43.

Zhao G, Sun H, Zhang T, Liu J-X. Copper induce zebrafish retinal developmental defects via triggering stresses and apoptosis. Cell Communication and Signaling 2020a; 18: 1-14.

Zhao G, Zhang T, Sun H, Liu J-X. Copper nanoparticles induce zebrafish intestinal defects via endoplasmic reticulum and oxidative stress. Metallomics 2020b; 12: 12-22.

Zhu M, Nie G, Meng H, Xia T, Nel A, Zhao Y. Physicochemical properties determine nanomaterial cellular uptake, transport, and fate. Accounts of Chemical Research 2013; 46: 622-631.

Zhu Y, Xu J, Lu T, Zhang M, Ke M, Fu Z, et al. A comparison of the effects of copper nanoparticles and copper sulfate on Phaeodactylum tricornutum physiology and transcription. Environmental Toxicology and Pharmacology 2017; 56: 43-49.

CHAPTER 2: The effect of copper nanoparticles on olfaction in rainbow trout (*Oncorhynchus mykiss*)

My thesis has broadly investigated how exposure to CuNPs induces olfactory toxicity in rainbow trout. The first step in this journey was to determine the contribution of dissolved Cu in the CuNPs toxicity. In this research chapter, we initially determined a concentration of CuNPs and Cu^{2+} that can induce equal olfactory toxicities (i.e., 50% inhibition in the olfactory function). Afterward, we exposed fish to the equitoxic concentrations of Cu contaminants over different exposure periods and compared their effects on the fish neurophysiological and behavioural responses.

This thesis is a manuscript-style thesis which is organized based on the University of Lethbridge thesis submission regulations. Inevitably, there is some repetition of content in the introduction and materials and methods sections of research chapters. A version of this chapter has been published in *Environmental Science: Nano*:

Razmara, P., Lari, E., Mohaddes, E., Zhang, Y., Goss, G., Pyle, G. (2019). The effect of copper nanoparticles on olfaction in rainbow trout (*Oncorhynchus mykiss*). Environmental Science: Nano, 6, 2094–2104.

https://pubs.rsc.org/lv/content/articlelanding/2019/en/c9en00360f/unauth#!divAbstract

Contribution of authors: I designed and performed research, collected and analysed data, and wrote the manuscript. Dr. Lari provided scientific input and training. Effat Mohaddes conducted the water quality analyses and assisted me in fish exposures. Yueyang Zhang provided training on nanoparticles characterization. Dr. Goss provided guidance, scientific input, and access to his laboratory in the University of Alberta. Dr.

Pyle provided guidance, scientific input, supervision, and funding for this research. All authors edited and approved the final manuscript.

2.1. Abstract

Although olfactory toxicity of copper (particularly Cu^{2+}) in fish has drawn considerable research attention, the impact of copper nanoparticles (CuNPs) on the olfactory system is not well characterized. The main objective of this study was to investigate the time-dependent effects of CuNPs and Cu^{2+} on olfactory sensitivity and olfactory-mediated behaviours of rainbow trout (*Oncorhynchus mykiss*). To establish olfactory-impairment thresholds, 24 h inhibitory concentration (IC) curves, induced by CuNPs or Cu^{2+} on ciliated and microvillous olfactory sensory neurons (OSNs) were determined using electro-olfactography (EOG). The results indicated ciliated cells are more sensitive to both CuNPs and Cu^{2+} exposure relative to microvillous OSNs. Thus, the concentration of contaminants that induced 50% inhibition in ciliated OSNs (24 h-IC50; 322 and 7 µg/L for CuNPs and Cu^{2+}, respectively) were selected as equi-toxic concentrations. Fish were exposed to 24 h-IC50 concentrations for 24 h or 96 h, and their olfactory sensitivity was studied using EOG and a behavioural assay. Results of EOG demonstrated a gradual, time-dependent increase in the inhibitory effect of CuNPs, whereas fish under Cu^{2+} exposure displayed a partial recovery at 96 h, as compared to the 24 h time point. Fish behavioural results followed a similar pattern as in neurophysiological experiments. Overall, exposure to CuNPs resulted in a different time-dependent toxicity pattern on the fish olfactory system than Cu^{2+} after exposure at equi-toxic concentrations. Our data suggest that CuNPs and Cu^{2+} affected chemosensory function and behaviour differently in rainbow trout.

2.2. Introduction

In recent decades, the use of engineered metal and metal oxide nanoparticles (NPs) has become more common due to their unique properties relative to larger particles (Schrand et al., 2010). For instance, copper nanoparticles (CuNPs) are used in the manufacture of electronic devices and metallic inks owing to their distinctive conductive, optical and catalytic properties (Li et al., 2014; Tang et al., 2010). They are also used in hygienic clothing and various other applications (e.g. agriculture) (Rai and Ingle, 2012; Shende et al., 2016) for their unique antimicrobial properties(Perelshtein et al., 2009; Ramyadevi et al., 2012; Teli and Sheikh, 2013). Due to the increasing worldwide production and application of CuNPs, aquatic ecosystems will become increasingly contaminated with CuNPs through various input routes, including soil leaching and effluent discharges (Joo and Zhao, 2017).

Increased risk of CuNP exposure and its potential for causing harm to aquatic ecosystems has triggered general concerns related to aquatic organism health. It has been estimated that the concentration of CuNPs in a number of receiving waters is approximately 60 μg/L (Chio et al., 2012). This environmental concentration might lead to adverse outcomes in aquatic organisms. The results of a recent study have demonstrated that the 96 h lowest observed effect concentration (LOEC) for rainbow trout (*Oncorhynchus mykiss*), fathead minnow (*Pimephales promelas*), and zebrafish (*Danio rerio*) exposed to 50 nm CuNPs was 170, 23, and <23 μg/L, respectively (Song et al., 2015). Exposure to CuNPs can lead to detrimental effects including oxidative stress and immune suppression (Wang et al., 2015), reduced Na^+/K^+-ATPase activity (Shaw et al., 2012), and histopathological injuries (Al-Bairuty et al., 2013) in different fish tissues.

Fish chemoreception is crucial for mediating reproductive behaviours, finding food, homing, and avoiding predation (Døving, 2007; Kasumyan, 2004). Olfactory sensory neurons (OSNs) are in direct contact with water and are therefore directly exposed to environmental contaminants (Mirza et al., 2009; Tierney et al., 2010). Previous studies demonstrated environmentally relevant contaminant concentrations might be sufficient to impair fish olfaction (Dew et al., 2016; Kusch et al., 2008; Pyle and Mirza, 2007; Scholz et al., 2000). For instance, a 30 min exposure to 10 and 15 µg/L of copper, impaired the olfactory function of fathead minnows by 72 and 79%, respectively (Green et al., 2010). Although several studies have evaluated various aspects of copper toxicity on fish olfaction (Azizishirazi et al., 2015; Dew et al., 2014; Lari et al., 2019; Lazzari et al., 2017; Sommers et al., 2016), the olfactory toxicity of CuNPs has not been well investigated. Studies on silver nanoparticles (AgNPs) have demonstrated that metal NPs target the sensory system (the olfactory bulb and lateral line neuromasts) and ionocytes in zebrafish (Osborne et al., 2016). Furthermore, exposure to AgNPs has resulted in disruption of fish olfactory function (Bilberg et al., 2011). However, only one study has demonstrated impairment of fish olfactory-mediated behaviour in response to an alarm cue after a 12 h exposure to 50 µg/L of CuNPs (Sovová et al., 2014). Therefore, the effects of CuNPs on fish olfactory acuity and associated olfactory-mediated behaviours require further investigation.

Copper NPs have the potential to dissolve, releasing ions from their surfaces. However, the relative contributions between the particles and ions in CuNPs toxicity is not well described (Al-Bairuty et al., 2016; Griffitt et al., 2007; Shaw et al., 2012; Sovová et al., 2014). Therefore, it is unclear whether the effects of CuNPs on the fish olfactory system are distinct from dissolved copper ions. The primary objective of this study was to

investigate the time-dependent effects of CuNPs and copper ions (Cu^{2+}) on olfactory sensitivity and olfactory-mediated behaviours in rainbow trout. The copper salt ($CuSO_4$) was used as a source of Cu^{2+} to test any possible differences between fish olfactory toxicity caused by CuNPs and Cu^{2+}.

2.3. Materials and Methods

2.3.1. Preparation of copper stock suspensions

A fresh stock solution of copper as $CuSO_4.5H_2O$ (98.5–100.5% purity; BHD, USA) was prepared at a concentration of 100 mg/L $CuSO_4$ in 18.2 MΩ/cm water (ddH_2O, Millipore, USA) and acidified to 0.4% HNO_3 (concentrated, TraceSelect grade; Sigma Aldrich, Canada). Copper NP powder (35 nm, 99.8% purity; partially passivated) was purchased from Nanostructured & Amorphous Materials, Inc (Houston, USA) and stored at room temperature in a dark bottle. The stock suspension of CuNPs at the nominal concentration of 250 mg/L was prepared by suspending the powder in ddH_2O followed by dispersion for 30 min in a water bath sonicator (UD 150SH 6LQ; 150 W; Eumax; USA) at room temperature. The CuNPs stock suspension was always prepared immediately before use.

2.3.2 Characterization of CuNPs

The behaviour, toxicity, and fate of metal NPs in the aquatic environment are dependent on the characteristics of metal NPs and conditions of the receiving waters. Therefore, characterization of CuNPs in the environmental media itself is crucial for evaluation of nano-toxicology studies (Cross et al., 2015; Klaine et al., 2008). The size and shape of CuNPs were confirmed using transmission electron microscopy (TEM, FEI Tecnai-20) in 10 mg/L suspensions in ddH_2O (Zhang et al., 2018). The corresponding size

distribution of CuNPs (10 mg/L) was measured using image analysis and processing software (ImageJ) based on TEM images (Dorobantu et al., 2015). To determine the aggregation of CuNPs in the experimental suspension, dynamic light scattering (DLS; Zetasizer Nano Series, Malvern) was used in 173° backscatter mode (n=3) (Zhang et al., 2018). In order to evaluate CuNPs aggregation behaviour in the exposure tanks, suspensions were prepared at nominal experimental concentrations using fish tank water. The average hydrodynamic diameter, polydispersity index (PDI), and zeta potential of CuNPs were measured at 0, 2, 4, 8, 16, 24 h. Between the DLS measurements, samples were covered by parafilm and remained static.

2.3.3. Test animals and experimental design

Juvenile rainbow trout (n=210, total length of 13.3 ± 0.7 cm, and mass of 24.5± 3.6 g (mean ± SE)) were obtained from Sam Livingston Fish Hatchery in Calgary, Alberta, Canada and transferred to holding tanks at a stocking density of 5 g/L in the Aquatic Research Facility (ARF) of the University of Lethbridge (16 h light: 8 h dark photoperiod, 12°C). Fish were allowed to acclimate to ARF water for two weeks. During this time, fish were treated with parasiticide (PraziPro, Hikari, USA) to ensure they were free of any *Gyrodactylus salmonis,* an olfactory-related parasite of rainbow trout and other potential ectoparasites, prior to beginning research (Lari and Pyle, 2017a). All associated experiments in this study were reviewed and approved by the University of Lethbridge Animal Welfare Committee (protocol #1612).

To establish CuNP- or Cu^{2+}-induced olfactory-impairment thresholds, fish were exposed to a geometric dilution series of CuNPs or Cu^{2+} for 24 h, and olfactory sensitivity was measured using electro-olfactography (EOG), following the procedure described by

Lari and Pyle (Lari and Pyle, 2017b). Previous studies have demonstrated that copper has different effects on OSN sub-populations, as it causes a greater impairment in ciliated OSNs than microvillous OSNs (Dew et al., 2014; Lazzari et al., 2017). To determine if CuNPs cause a greater impairment in specific OSNs, rainbow trout olfactory sensitivity was measured in response to 10^{-5} mol/L L-alanine (Fisher Scientific, Canada) or taurocholic acid (TCA; Sigma-Aldrich, USA) that are known to activate microvillous or ciliated OSNs, respectively (Dew et al., 2014; Zielinski and Hara, 2006). Based on these EOG responses, equi-toxic concentrations of CuNPs or Cu^{2+} that impair olfaction by 50% (i.e., 24-h median inhibitory concentration; 24-h IC50), were determined. Both copper contaminants were more toxic to ciliated OSNs relative to microvillous OSNs (Fig. 2.4); therefore, the 24 h-IC50 of the contaminants to ciliated OSNs were selected as a functional unit of toxicity for the following neurophysiological and behavioural studies. To determine the time-dependent effects, fish were exposed to 24-h IC50 concentrations of CuNPs and Cu^{2+}, as calculated at 320 ± 13 and 7 ± 1 µg/L (mean ± SD), respectively, for 24 h or 96 h and their olfactory sensitivity or olfactory-mediated behaviour in response to TCA were studied.

During the 96 h exposure period, 100% of the solution in each tank was replaced with the same solution every day. The water quality was monitored as follows (mean ± SD; n=5): temperature, 12.3 ± 0.4 °C; dissolved oxygen, 9.5 ± 0.4 mg/L; conductivity, 331.8 ± 0.9 µS/cm; hardness, 148 ± 2.4 mg/L as $CaCO_3$; alkalinity: 120.8 ± 2.1 mg/L as $CaCO_3$; median pH, 7.91 (range 7.7-8.12), and dissolved organic carbon, 2.35 ± 0.66 mg/L. Fish were not fed during the exposure periods.

2.3.4. Copper analysis and dissolution of CuNPs

To ascertain the actual concentration of copper in fish tanks, water samples were collected and acidified to 1% HNO_3 at the beginning and end of the 24-h exposure period, or before and after each water change in the 96-h exposure. Copper samples were analyzed by graphite furnace atomic absorption spectrometry (GFAAS) equipped with a graphite tube atomizer (240FS GFAAS, Agilent Technologies, USA). For all copper analyses, pyrolytically coated graphite tubes were used (Agilent Technologies, USA). In order to reduce carryover of high concentration solutions to below the analytical detection limit, the pre-installed instrument analytical method (SpectrAA) was modified to extend the atomization step to 4 s. For QA/QC of copper measurements, a certified reference material (SLRS-6: River Water, National Research Council Canada, Ottawa, ON, Canada) was run every 10 samples (mean percent recovery was 95% and within the accepted ± 10% error), the calibration curve was resloped every 10 samples, and duplicate samples were run every 20 samples (<2% different from each other). The method detection limit (MDL) for Cu was approximately 2 µg/L.

In order to better understand CuNP toxicity, the contribution of dissolved copper in olfactory toxicity must be determined.(Shaw et al., 2016). To determine the concentration of dissolved copper released from CuNPs in exposure tanks, a time-dependent ultrafiltration experiment was conducted using Amicon Ultra-4 Centrifugal Filter Units with the pore size of 1-2 nm (3K regenerated cellulose membrane, Merck Millipore Ltd., USA) (Furtado et al., 2014). The term "dissolved copper" refers to Cu^{2+} and its soluble complexes that can pass through the 3K (~ 1.4 nm diameter pore size) filter membrane. Water samples were collected from CuNPs exposed fish tanks and control tanks (at 0, 4, 8,

12, 16, 20, and 24 h) and filtered through ultrafiltration units that were centrifuged at 2750 g at 12°C for 90 min (n=3). The filtrates were acidified to 1% HNO_3 and stored in the fridge before analyzing. The recovery percentage of the filtration membrane was 78% which was determined as the ratio of filtrate copper to the total concentration of copper (before filtration) for 10 µg/L Cu as $CuSO_4$.

2.3.5. Neurophysiological and behavioural assays

Following exposure to contaminants or clean water for 24 h or 96 h, fish (6 individuals per treatment) were anesthetized using 120 mg/L TMS (tricaine methanesulfonate, AquaLife, Canada) and buffered to pH 7.4 using 360 mg/L $NaHCO_3$ (Fisher Scientific, USA). The intranarial septum that separates the anterior and posterior nares was removed to facilitate access to the underlying olfactory rosette. The olfactory response to 10^{-5} mol/L TCA was determined using EOG (Lari and Pyle, 2017b). The recording probe (glass microelectrode) was placed immediately over the third lamella, approximately at the top 1/3 of the lamellar length and 1/2 of lamellar width. The reference probe was positioned on the skin close to the naris where the recording electrode was placed. During the recording period, a stimulus was delivered to the olfactory chamber every 90 s using a six-channel valve controller (Warners Instrument Co., USA). The resulting EOG signals were amplified approximately 10 times by a differential amplifier (EX1, Cornerstone series, Dagan corporation, USA) and filtered using a 0.3 Hz low-cut pass, a 100 kHz high-cut pass, with a gain of 10. Following signal amplification, EOG output was recorded by a digital data acquisition system (PowerLab 4SP, AD-Instruments, USA). To prevent any possible olfactory recovery during the recordings in the CuNPs or Cu^{2+} treatments, all solutions including the anaesthetizing solution, olfactory perfusion,

blank water and olfactory stimulus solution were made of culture water spiked with contaminants. The solutions for the control treatment were made of clean culture water. All EOG responses to TCA were blank corrected.

Olfactory-mediated behaviour in response to TCA was studied using a flow-through choice maze, which has been previously described (Lari and Pyle, 2017b). In short, the maze had two identical arms (50 cm long and 20 cm wide) which were separated from the acclimation zone (20 cm length and 40 cm width) by removable gates. Two peristaltic pumps (Fischer Scientific, Canada) delivered either clean culture water or water spiked with contaminants to both arms of the maze at a rate of 1.6 L/min during an 18-minute acclimation period. Flow rates of the peristaltic pumps remained constant throughout the experiment, and the water depth was held constant at 10 cm for each trial. A preliminary arm-bias test was conducted to ensure that there was no bias for one maze arm over the other when no behavioural stimuli were present. A dye test was also performed to confirm a laminar flow through both arms and that no mixing of water from arms of the maze was occurring in the acclimation zone.

After a 24 h or 96 h exposure to either contaminants or clean water, a single rainbow trout was placed directly into the acclimation area of the maze. At the end of the acclimation period, a chemosensory stimulus (i.e., either TCA or distilled water) was randomly delivered to the distal end of each arm of the maze. Video recording began as soon as the stimuli entered the maze. The gates to both arms of the maze were gently lifted simultaneously to avoid disturbing the fish. The fish was then able to swim freely throughout the entire flow-through choice maze and was recorded for four minutes. The

olfactory-mediated behavioural response was calculated according to the following equation (Olsén and Höglund, 1985):

$$Rv = \left[\frac{Ic - Iw}{Ic + Iw}\right] \times 100$$

where *Rv* = response variable, *Ic* = time spent on the side of the maze receiving cue, *Iw* = time spent on the side of the maze receiving non-cue water.

2.3.6. Statistical analyses

Statistical analyses were performed in R version 3.4.3 (Team, 2018). Experimental data were examined for normality and homogeneity of variance using a Shapiro-Wilks and a Bartlett test, respectively. To ascertain the effect of time on CuNPs zeta potential a one-way analysis of variance (ANOVA) was used. To determine the effect of time on polydispersity index or hydrodynamic diameter, where the assumption of normality was violated, a non-parametric Kruskal–Wallis test was used together with a Dunn's multiple comparisons test.

To compare the EOG responses to different stimuli (TCA and L-alanine) at various concentration of CuNPs or Cu^{2+}, two-way ANOVA was used. To specify the comparisons (the relative EOG response of OSNs to TCA or L-alanine at a certain concentration) and prevent the experiment-wise error, a custom contrast matrix was defined to adjust the reported p-value using lsmeans (Lenth, 2016) and multcomp (Westfall, 2008) packages. The 24 h-IC50 for CuNPs or Cu^{2+} were calculated based on the EOG measurements using the drc package (Gerhard, 2015). To compare the EOG and olfactory-mediated behavioural responses to TCA in different treatments (control, Cu^{2+}, and CuNPs) over time (24 h and 96 h), two-way ANOVA was performed followed by a Tukey's post hoc test.

2.4. Results and discussion

2.4.1. Physicochemical characteristics of CuNPs

The behaviour and fate of metal NPs in the aquatic environment are strongly affected by the physicochemical transformations such as aggregation (Peijnenburg et al., 2015). Nanoparticle aggregation can alter bioavailability, distribution, and toxicity of NPs. The TEM images illustrate the primary size and semi-spherical nature of CuNPs used in this study (Fig. 2.1). Based on the TEM images, the average diameter of CuNPs was 32 ± 1 nm (mean ± SEM, n = 349; Fig. 2.1C). The time-dependent DLS measurements of CuNPs also suggest that particles aggregated over the 24 h exposure period (Fig. 2.2). The polydispersity index, an indicator of particles' relative distribution, demonstrated that CuNPs were highly polydispersed (PDI = 1) after 16 h in the experimental tanks (χ^2 (5) = 13.89, p = 0.02; Fig. 2.2A). The hydrodynamic diameter of CuNPs was significantly increased at 16 h (p = 0.006) and 24 h (p = 0.016) which indicated that particles were not stable in the water suspension over time (χ^2 (5) = 13, p = 0.02; Fig. 2.2B). Likewise, the zeta potential, which is a measurement of the particles' surface charge, was significantly reduced over time and supported CuNPs aggregation (F (5, 12) = 8.68, p = 0.001; Fig. 2.2C). The particles' zeta potential indicated a noticeable decrease at 16 h and 24 h in the fish tanks (p = 0.009 and 0.024, respectively; Fig. 2.2C). Decreasing the particles surface potential can reduce the electrostatic or steric repulsion forces between particles that prevent CuNPs aggregation.(Cross et al., 2015) Subsequently, over the last few hours of exposure, particles tended to settle out from the water, and were less bioavailable for the fish. All reported DLS measurements for CuNPs might be slightly different if we were able to correct for the background DLS values associated with the fish tank water itself.

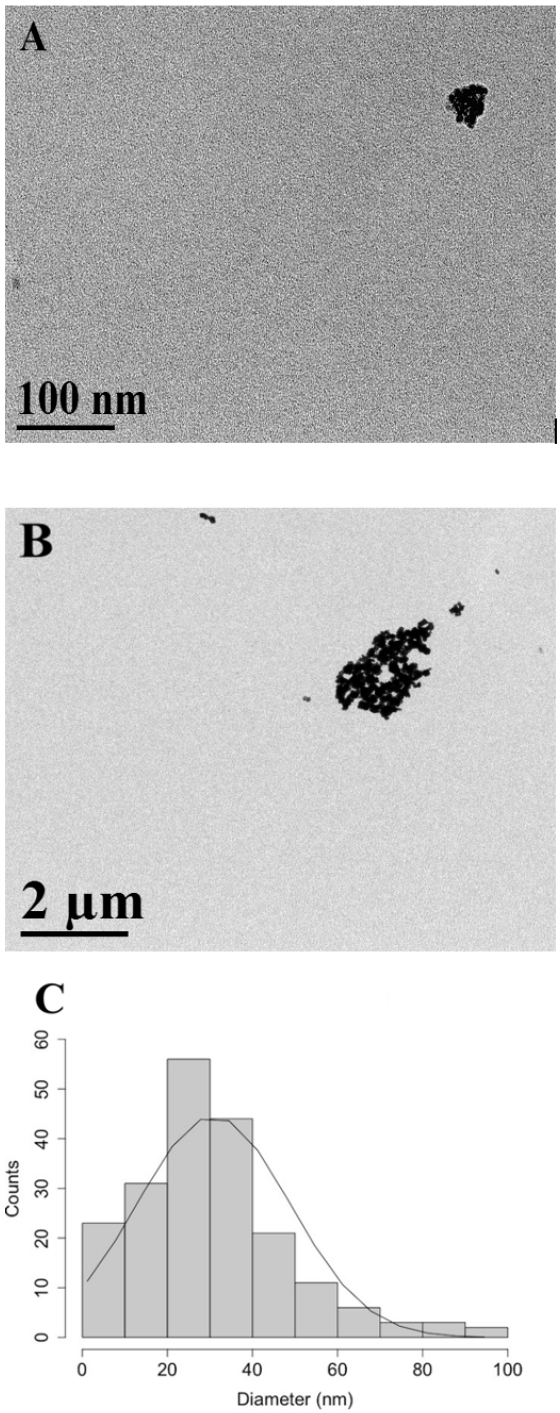

Figure 2.1. The primary size of CuNPs at 10 mg/L in ddH_2O at different scale using TEM, (A) scale bar = 100 nm, (B) scale bar = 2000 nm, (C) Size distribution of CuNPs.

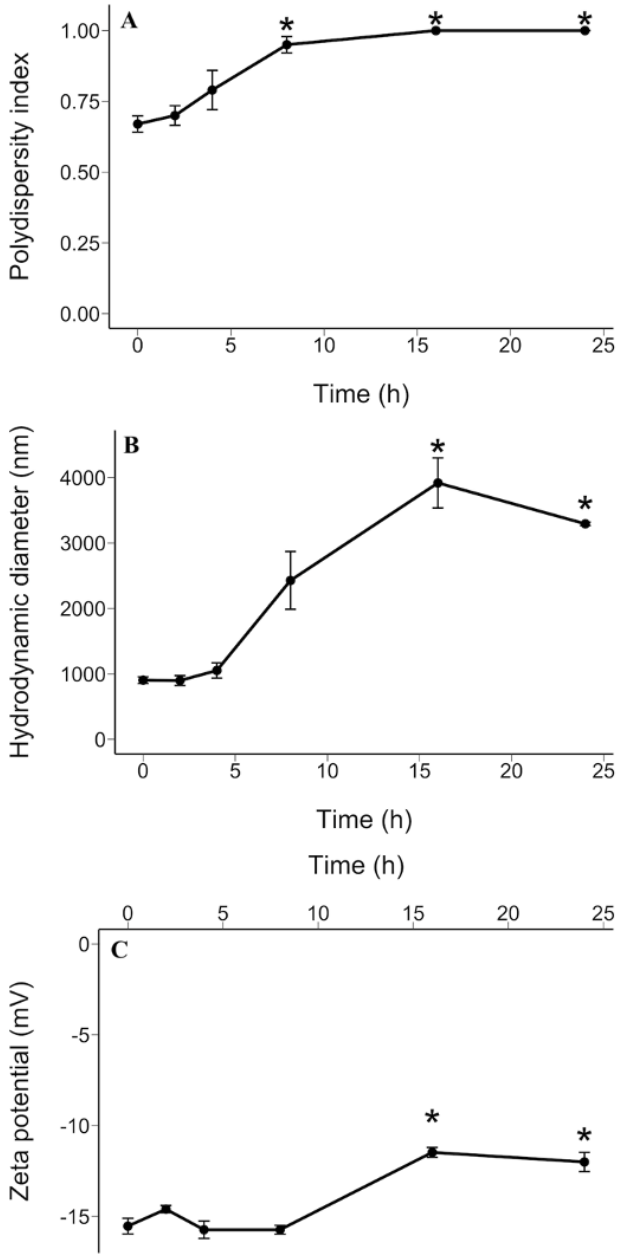

Figure 2.2. Measurements of CuNPs aggregation behaviour in the exposure tanks at 0, 2, 4, 8, 16, and 24 h using DLS. (A) Average of CuNPs polydispersity index; (B) Average of CuNPs hydrodynamic diameter; (C) Average of CuNPs zeta potential. Asterisks denote significant changes in the measured parameters over time ($p \leq 0.05$, n = 3, error bars: ± 1 SEM).

2.4.2. Copper analysis and dissolution of CuNPs

Total concentration of copper and the time-dependent dissolution behaviour of CuNPs were determined using GFAAS (Fig. 2.5). Immediately after spiking the test tanks (0 h), the total concentration of copper in the CuNPs treatment was 259 ± 2 µg/L (mean ± SD; 80.5% of the nominal concentration) which decreased to 202 ± 12 µg/L over 24 h (62.7% of the nominal concentration). These measurements reflect that CuNPs tend to bind to the fish tank walls and lids or settle out on the bottom of the tanks. The total concentration of copper in the Cu^{2+} treatment was 7 ± 1 and 8 ± 1 µg/L immediately after exposing fish (0 h) and 24 h post-exposure, respectively.

Dissolution of metal NPs is another type of transformation that can influence the fate and toxicity of NPs in aquatic ecosystems. Dissolved free ions are highly bioavailable to organisms and can lead to toxicity in living cells (Peijnenburg et al., 2015). There was a time-dependent release of dissolved copper from CuNPs over 24 h in the fish tanks (Fig. 2.5). This gradual release of dissolved copper by CuNPs resulted in dissolved Cu concentrations in the CuNP treatment up to 14 µg/L, whereas the Cu concentration in the Cu^{2+} treatment remained steady at 7 µg/L over 24 h. The mean dissolved Cu concentration in the CuNP treatment over 24 h was 8 µg/L, which was very close to the 24-h IC50 for Cu^{2+} of 7 µg/L used in the Cu^{2+} treatment. At time 0 h and 24 h, the concentration of dissolved copper was below the MDL of GFAAS and 14 ± 0 µg/L, respectively (Fig. 2.5).

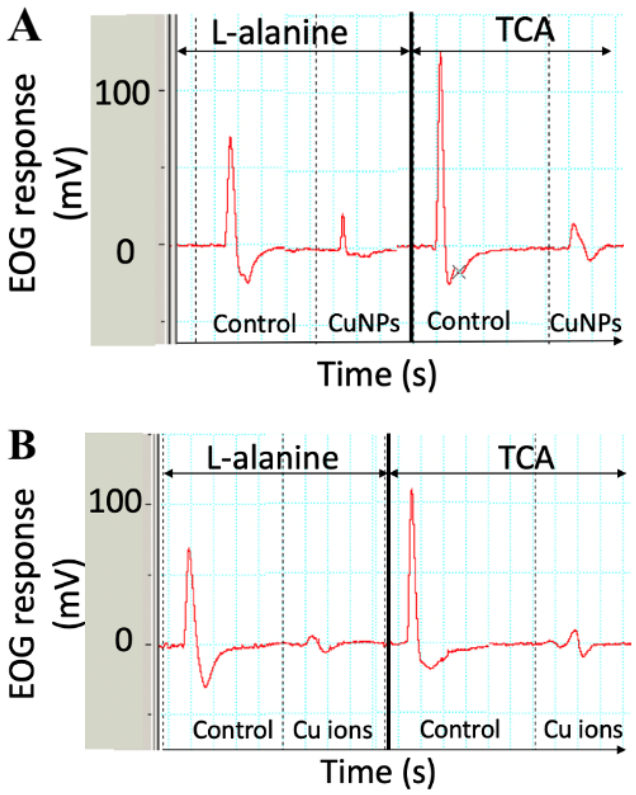

Figure 2.3. Representative EOG traces of rainbow trout in response to L-alanine or TCA after 24 h exposures to 500 µg/L CuNPs (A), or 40.5 µg/L Cu^{2+} (B).

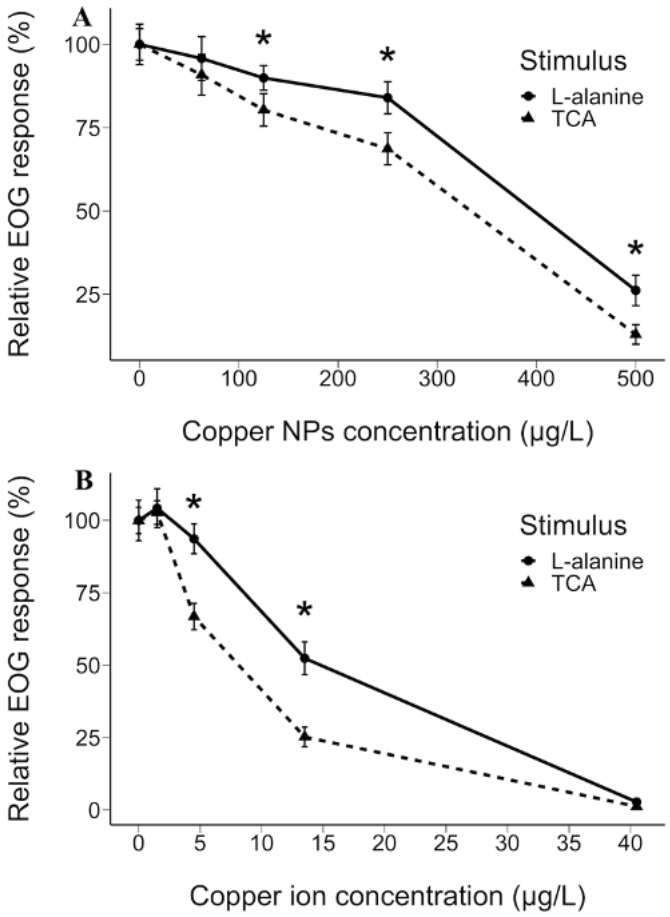

Figure 2.4. The control corrected electro-olfactography response of rainbow trout in response to L-alanine (stimulates microvillous cells) or TCA (stimulates ciliated cells). (A) The average EOG responses after exposing fish to CuNPs; (B) The average EOG responses after exposing fish to Cu^{2+}. Asterisks denote significant differences in the relative EOG responses to TCA vs. L-alanine at each contaminant concentration ($p \leq 0.05$, n = 6, error bars: ± 1 SEM).

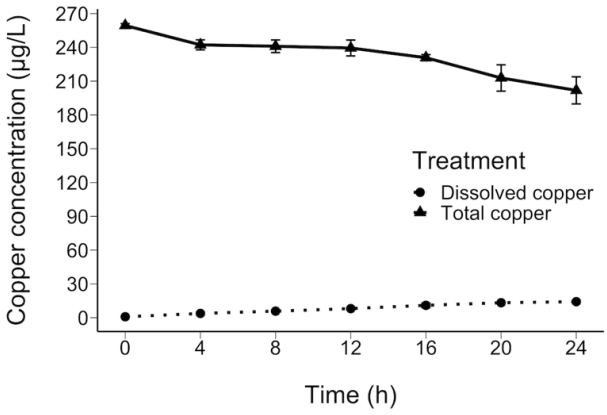

Figure 2.5. The measured concentration of total copper and dissolved copper in the CuNPs exposure tanks over 24 h (n = 3, error bars: ± 1 SEM).

As 100% of the solutions in fish tanks were changed every day, the dissolution of CuNPs was only measured over 24 h. These data demonstrate dissolved copper may be contributing to olfactory toxicity in the CuNP treatment.

2.4.3. Differential response of rainbow trout OSN sub-populations to copper

Following the 24 h exposure to different concentrations of CuNPs, Cu^{2+}, or clean water, the olfactory responses of rainbow trout to TCA and L-alanine were recorded using EOG (Fig. 2.3 and 2.4). The representative magnitude of the EOG voltages in response to different stimuli—control, Cu^{2+}, and CuNPs—are shown in Fig. 2.3. The relative EOG response of fish to TCA and L-alanine were significantly different after exposure to CuNPs ($F(4, 50) = 4.80$, $p = 0.002$; Fig. 2.4A) or Cu^{2+} ($F(4, 50) = 27.02$, $p < 0.001$; Fig. 2.4B). Rainbow trout that were exposed to ≥125 µg/L of CuNPs for 24 h showed significant differences between the relative EOG responses to TCA and L-alanine ($p = 0.005$ at 125 µg/L of CuNPs and $p < 0.001$ for 250 and 500 µg/L of CuNPs; Fig. 2.4A). Similar to the CuNP treatment, exposure to 4.5 and 13.5 µg/L Cu^{2+} caused a differential relative EOG response between TCA and L-alanine ($p < 0.001$; Fig. 2.4B). Exposure to the high concentration of Cu^{2+} (40.5 µg/L) led to the impairment in both ciliated and microvillous

OSNs (1.2% and 2.7% EOG response relative to the control, respectively). Therefore, there was no significant difference between relative EOG responses to TCA and L-alanine at 40.5 µg/L of Cu^{2+} ($p = 0.92$; Fig. 2.4B).

Given that TCA is an olfactory stimulus for ciliated OSNs, and L-alanine stimulates microvillous OSNs, EOG results showed that CuNPs and Cu^{2+} were more toxic to ciliated cells than microvillous cells (Fig. 2.4). Previous work has shown that ciliated cells are more sensitive to Cu^{2+} exposure than microvillous cells (Dew et al., 2014; Lazzari et al., 2017). However, to the best of our knowledge, no study has been conducted previously to test whether exposure to CuNPs causes differential responses between OSN classes. Although ciliated OSNs are more sensitive to copper than microvillous cells, they also recover better than microvillous cells after fish are transferred to clean water (Lazzari et al., 2017).

2.4.4. Neurophysiological and behavioural assays

As predicted, a 24-h exposure to the equi-toxic concentrations of CuNPs or Cu^{2+} caused an approximately 50% reduction in the EOG response to TCA ($p < 0.001$, Fig. 2.6 and 2.7). A 96-h exposure to CuNPs caused a drastic reduction in EOG response to 6% of the control response, whereas a 24 h exposure reduced olfactory sensitivity to 48% of the control ($p < 0.001$, Fig. 2.7). However, a partial recovery in olfactory response was observed at 96 h relative to 24 h when fish were exposed to Cu^{2+} ($p = 0.016$, Fig. 2.7). There were no significant differences between control fish over the 24 h and 96 h exposure periods ($p > 0.99$).

Behavioural responses of rainbow trout to TCA confirmed the EOG results reported above (Fig. 2.8). Both the copper treatments as well as the exposure periods resulted in significantly different behavioural responses ($F(2, 106) = 16.07$, $p < 0.001$; Fig. 2.8). A

24-h exposure to both contaminants significantly decreased the olfactory-mediated aversion to TCA as compared to control fish. Following a 96-h exposure to Cu^{2+}, the avoidance response of fish to TCA had significantly increased relative to the 24-h exposure period, indicating a recovery in fish olfactory function ($p < 0.001$). However, a longer exposure period (96 h) to CuNPs resulted in progressive disruption of the behavioural response to TCA compared to the 24 h exposure period ($p = 0.033$). In other words, CuNPs impaired fish olfaction in a time-dependent manner.

Findings of both neurophysiological and behavioural studies demonstrated that despite exposing fish to equi-toxic concentrations of contaminants, extending the exposure period from 24 h to 96 h caused progressive deterioration in CuNP-exposed rainbow trout olfactory function; however, at least a partial olfactory recovery was observed for continuous Cu^{2+} exposure. Sovova et al. (2014) demonstrated that CuNPs and Cu^{2+} have different patterns of toxicity in rainbow trout. In fact, a 12 h exposure to an equivalent concentration of CuNPs or Cu^{2+} (50 µg/L) caused significantly greater impairment of anti-predatory behaviour in the CuNPs treatment. Studying an oxidative stress marker (the ratio of oxidized to reduced glutathione), revealed CuNP, but not Cu^{2+}, elevated oxidative stress in the fish brain. Nevertheless, exposure to CuNPs did not result in any structural alteration in the rosette, while exposure to Cu^{2+} resulted in significant depletion of both OSNs and nonsensory cells (Sovová et al., 2014). In contrast to the toxicity of CuNPs and Cu^{2+}, treating fish with 45 µg/L AgNPs or 35 µg/L Ag^{+} for 15 min caused similar impairment in the olfactory acuity (Bilberg et al., 2011). The observed differences between fish olfactory responses to AgNPs or CuNPs compared to their respective metal ions might be related to differential metal NPs' inherent properties.

Considering that CuNPs induced a different time-dependent toxicity pattern on the fish olfactory system than Cu^{2+}, they may have a different mechanism of effect on fish olfactory systems relative to Cu^{2+}. However, there are several considerable gaps in our understanding of the mechanistic basis of NPs effects on fish olfactory systems. Given that Cu^{2+} is a potent olfactory disrupter and CuNPs release dissolved copper in a time-dependent manner (Fig. 2.5), we hypothesized that the olfactory toxicity caused by CuNPs was a function of both dissolved copper and nanoparticulate Cu. The continuous olfactory impairment in the CuNP treatment versus the observed olfactory recovery in the Cu^{2+} treatment over 96 h of continuous exposure suggested that the dissolved Cu^{2+} ions are not the only contributors to the CuNP-induced olfactory toxicity. In fact, nanoparticulate Cu might aggregate on the olfactory epithelium and block olfactory receptors and/or ion channels that are involved in olfactory signal transduction (OST). Consequently, action potentials may not be generated, and fish may not perceive the olfactory stimulus. Furthermore, NPs might increase mucus production on the surface of the epithelium and reduce or prevent odour molecules from crossing the mucus layer toward the olfactory epithelium and binding to receptors (Bilberg et al., 2011; Sovová et al., 2014). Alternately, CuNPs might be taken up by OSNs and distributed throughout the olfactory system, thereby leading to malfunctioning of OSNs, the olfactory nerve, and/or the olfactory bulb (Handy et al., 2008). To our knowledge, there is no study assessing potential uptake routes of NPs by OSNs. Still, vesicular processes such as endocytosis are the most probable uptake routes for NPs (Pulido-Reyes et al., 2017).

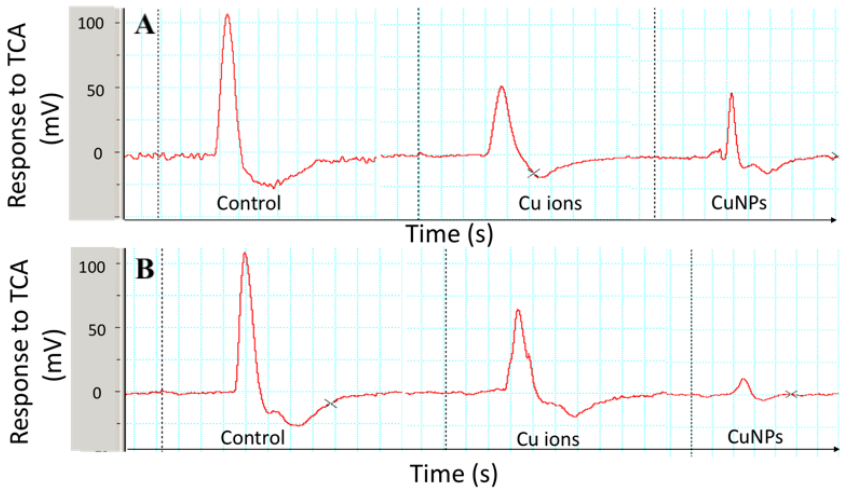

Figure 2.6. Representative EOG traces of rainbow trout after exposures to CuNPs, Cu^{2+}, or clean water for 24 h (A), or 96 h (B).

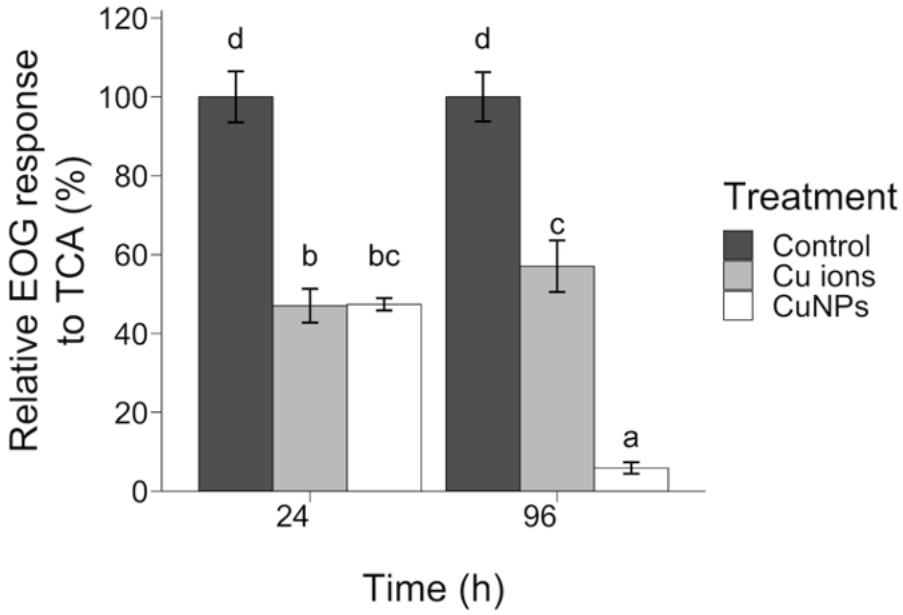

Figure 2.7. The relative electro-olfactography responses of rainbow trout to TCA after exposure to clean water, Cu^{2+}, or CuNPs over 24 h or 96 h. Lower-case letters indicate significant differences ($p \leq 0.05$, n = 6, error bars: ± 1 SEM).

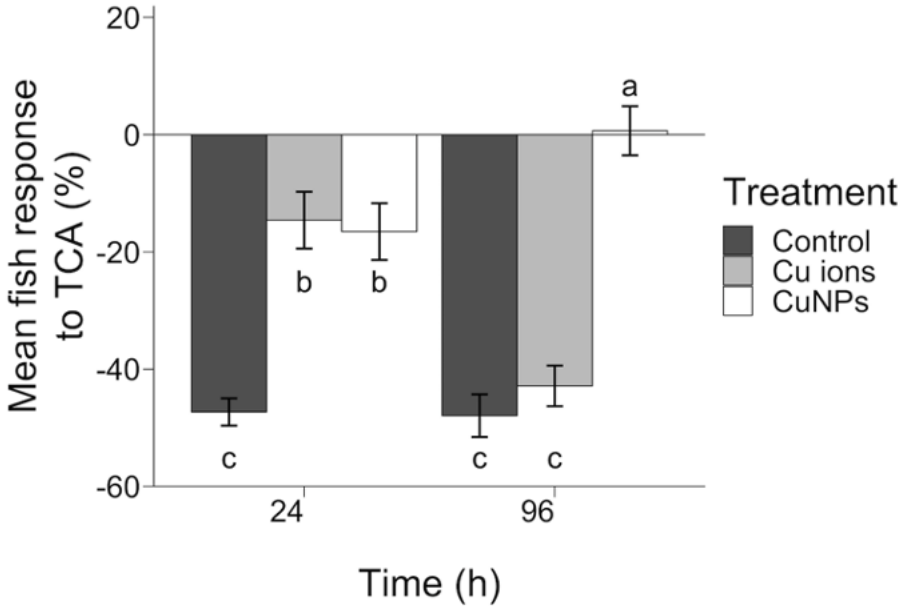

Figure 2.8. Rainbow trout behavioural responses to TCA following exposure to clean water, Cu^{2+}, or CuNPs over 24 h or 96 h. Lower-case letters indicate significant differences ($p \leq 0.05$, n = 19, error bars: ± 1 SEM).

Although further investigations are required to explore the mechanisms of fish olfactory toxicity caused by CuNPs, the Cu-induced mechanisms of effects have been investigated. A short-term Cu exposure (i.e. 4 h exposure to 5-50 µg/L of Cu^{2+}) in coho salmon (*Oncorhynchus kisutch*) resulted in alteration of mediators involved in OST pathway. A significant loss of type 3 adenylate cyclase (ACIII) and reduced level of intracellular cyclic guanosine monophosphate (cGMP) were observed in the Cu-exposed coho salmon (Wang et al., 2013b). Another study showed that a 24 h exposure to environmentally relevant concentrations of Cu (i.e., 6.3 to 40 µg/L of Cu^{2+}) caused a reduction in the transcription of genes involved in the OST pathway in zebrafish (including the olfactory rosette, nerve and bulb) (Tilton et al., 2008). Furthermore, exposing zebrafish to Cu altered the expression of miRNAs that regulate the expression of genes involved in

OST or other neurological processes in a concentration-response manner through epigenetic post-transcriptional regulatory mechanisms (Wang et al., 2013a). Similar epigenetic and transcriptional mechanisms in the OST pathway might have resulted in the observed olfactory impairment in rainbow trout after a 24 h exposure to Cu^{2+}. In contrast to the Cu-exposed zebrafish, Azizishirazi et al. (2015) reported a different gene transcription profile in wild yellow perch (*Perca flavescens*) olfactory rosettes that were exposed to Cu (i.e., 10 µg/L of Cu^{2+} for the EOG experiment, and 20 µg/L of Cu^{2+} for the microarray experiment). The transcription profile in the olfactory epithelium of wild yellow perch was not fully associated with olfactory dysfunction in the Cu-exposed fish (Azizishirazi et al., 2015). Species-specific differences or different protocols of microarray expression profiling (i.e. a novel 1000 candidate-gene microarray for wild yellow perch and 14,900-transcript microarray for zebrafish) might explain why there was no differential transcription in the wild yellow perch, while gene expression patterns in Cu-exposed zebrafish support functional olfactory impairment. However, in both zebrafish and wild yellow perch studies, the expression of the Na^+/K^+-ATPase gene in the olfactory epithelium was down-regulated in response to Cu exposure (Azizishirazi et al., 2015; Tilton et al., 2008). This enzyme is responsible for the active extrusion of Na^+ from the OSN cytoplasm to the extracellular environment across the apical surface of the OSN into the olfactory chamber (Azizishirazi et al., 2015). Exposure to CuNPs can also inhibit the function of Na^+/K^+-ATPase in the fish brain (Shaw et al., 2012). This potential mechanism might apply to the fish olfactory epithelium exposed to Cu^{2+} or CuNPs.

Although Cu exposure causes fish olfactory impairment, OSNs have the potential to recover their function (Azizishirazi et al., 2013; Green et al., 2010; Sandahl et al., 2006).

Recovery might occur at low, ecologically relevant Cu concentrations despite the continued presence of Cu. Dew et al. (2012) reported a partial recovery in olfaction of fathead minnows despite continual exposure to 6.7 μg/L of Cu^{2+} over 96 h, which was consistent with our study. Nevertheless, the mechanism by which recovery occurred in the fish olfactory system is not clear (Dew et al., 2012). Cellular defense mechanisms might play key roles against copper-induced olfactory impairment that led to the observed olfactory recovery. Upregulation of genes involved in the antioxidant pathway such as metallothionein (MT) and glutathione reductase (GR) has been documented in fish tissues following Cu exposure (Minghetti et al., 2008; Wu et al., 2007). Similar to other fish tissues, defense strategies against metal exposures have been applied in the olfactory system. For instance, glutathione S-transferases (GSTs) and MT were expressed in the olfactory system of different fishes following short-term exposure to cadmium, another olfactory inhibitor (Espinoza et al., 2012; Wang and Gallagher, 2013). Short-term exposure to environmentally relevant concentrations of Cu also resulted in dysregulation of miRNAs which silence the genes that transcribe proteins with anti-oxidative stress functions such as quinone 1 in the zebrafish olfactory system (Wang et al., 2013a). Therefore, the fish olfactory system may employ antioxidant mechanisms to maintain olfactory function even under metal-induced oxidative stress. Although these potential mechanisms were not directly assessed in the present study, our results suggest that these mechanisms were not involved or are insufficient to compensate for the impairments caused by CuNPs in the fish olfactory system.

The partial recovery of olfaction as measured by EOG and full recovery of olfactory-mediated behaviours were observed in fish continuously exposed to Cu^{2+} for 96

h (Fig. 2.7 and 2.8). These differences between neurophysiological and behavioural responses might be due to the higher sensitivity of the behavioural assay to chemical cues as compared to the EOG technique. In fact, it is likely that even partial recovery in neurophysiological function of OSNs was enough for fish to detect and avoid TCA in the behavioural trials. The limitation of the EOG technique is supported by previous studies (Scott and Scott-Johnson, 2002). For instance, a recent study demonstrated that rainbow trout can detect and avoid very low concentrations of hydrocarbon-contaminated water (i.e. 0.1 %) in a choice maze whereas this same concentration did not produce an EOG response (Lari and Pyle, 2017b).

2.5. Conclusion

Copper has long been known as a powerful olfactory toxicant. However, most studies have only focused on dissolved Cu, and very little work has been done on examining the effects of CuNP on fish olfaction and olfactory-mediated behaviours. This study demonstrated that rainbow trout exposed to equi-toxic concentrations of Cu^{2+} or CuNPs showed olfactory impairment after 24 h. After 96 h of exposure, fish exposed to Cu^{2+} showed a partial recovery of olfactory function, whereas those exposed to CuNP showed a time-dependent deterioration of olfactory function. This observation suggests that Cu^{2+} and CuNP probably act through two distinct mechanisms to exert their toxic effects on fish olfaction. Further investigations are in progress to study the mechanism of toxicity caused by CuNPs relative to Cu^{2+}-induced toxicity in the fish olfactory system. Although both neurophysiological and behavioural endpoints corroborated this pattern of chemosensory impairment, behavioural endpoints were more sensitive. As has been demonstrated previously for Cu^{2+}, CuNP appears to target ciliated OSNs over microvillous

OSNs. Taken together, our results suggest that fish inhabiting waters contaminated by CuNP may be unable to detect and respond to important social cues, such as TCA, and their olfactory acuity will continue to deteriorate over time. Consequently, development of water quality criteria designed to protect fish against CuNP-induced olfactory dysfunction is warranted.

2.6. References

Al-Bairuty GA, Boyle D, Henry TB, Handy RD. Sublethal effects of copper sulphate compared to copper nanoparticles in rainbow trout (*Oncorhynchus mykiss*) at low pH: physiology and metal accumulation. Aquatic Toxicology 2016; 174: 188-198.

Al-Bairuty GA, Shaw BJ, Handy RD, Henry TB. Histopathological effects of waterborne copper nanoparticles and copper sulphate on the organs of rainbow trout (*Oncorhynchus mykiss*). Aquatic Toxicology 2013; 126: 104-115.

Azizishirazi A, Dew WA, Bougas B, Bernatchez L, Pyle GG. Dietary sodium protects fish against copper-induced olfactory impairment. Aquatic Toxicology 2015; 161: 1-9.

Azizishirazi A, Dew WA, Forsyth HL, Pyle GG. Olfactory recovery of wild yellow perch from metal contaminated lakes. Ecotoxicology and Environmental Safety 2013; 88: 42-47.

Bilberg K, Døving KB, Beedholm K, Baatrup E. Silver nanoparticles disrupt olfaction in Crucian carp (*Carassius carassius*) and Eurasian perch (Perca fluviatilis). Aquatic Toxicology 2011; 104: 145-152.

Chio C-P, Chen W-Y, Chou W-C, Hsieh N-H, Ling M-P, Liao C-M. Assessing the potential risks to zebrafish posed by environmentally relevant copper and silver nanoparticles. Science of The Total Environment 2012; 420: 111-118.

Cross RK, Tyler C, Galloway TS. Transformations that affect fate, form and bioavailability of inorganic nanoparticles in aquatic sediments. Environmental Chemistry 2015; 12: 627-642.

Dew WA, Azizishirazi A, Pyle GG. Contaminant-specific targeting of olfactory sensory neuron classes: Connecting neuron class impairment with behavioural deficits. Chemosphere 2014; 112: 519-525.

Dew WA, Veldhoen N, Carew AC, Helbing CC, Pyle GG. Cadmium-induced olfactory dysfunction in rainbow trout: Effects of binary and quaternary metal mixtures. Aquatic Toxicology 2016; 172: 86-94.

Dew WA, Wood CM, Pyle GG. Effects of continuous copper exposure and calcium on the olfactory response of *fathead minnows*. Environmental Science & Technology 2012; 46: 9019-9026.

Dorobantu LS, Fallone C, Noble AJ, Veinot J, Ma G, Goss GG, et al. Toxicity of silver nanoparticles against bacteria, yeast, and algae. Journal of Nanoparticle Research 2015; 17: 172.

Døving KB. The functional organization of the fish olfactory system. Progress in Neurobiology 2007; 82: 80-86.

Espinoza HM, Williams CR, Gallagher EP. Effect of cadmium on glutathione S-transferase and metallothionein gene expression in *coho salmon* liver, gill and olfactory tissues. Aquatic Toxicology 2012; 110: 37-44.

Furtado LM, Hoque ME, Mitrano DM, Ranville JF, Cheever B, Frost PC, et al. The persistence and transformation of silver nanoparticles in littoral lake mesocosms monitored using various analytical techniques. Environmental Chemistry 2014; 11: 419-430.

Gerhard CRaFBaJCSaD. Dose-Response Analysis Using R. PLOS ONE 2015; 10: 1-13.

Green WW, Mirza RS, Wood CM, Pyle GG. Copper binding dynamics and olfactory impairment in fathead minnows (*Pimephales promelas*). Environmental Science & Technology 2010; 44: 1431-1437.

Griffitt RJ, Weil R, Hyndman KA, Denslow ND, Powers K, Taylor D, et al. Exposure to copper nanoparticles causes gill injury and acute lethality in zebrafish (*Danio rerio*). Environmental Science & Technology 2007; 41: 8178-8186.

Handy RD, Henry TB, Scown TM, Johnston BD, Tyler CR. Manufactured nanoparticles: their uptake and effects on fish—a mechanistic analysis. Ecotoxicology 2008; 17: 396-409.

Joo SH, Zhao D. Environmental dynamics of metal oxide nanoparticles in heterogeneous systems: A review. Journal of Hazardous Materials 2017; 322: 29-47.

Kasumyan A. The olfactory system in fish: structure, function, and role in behavior. Journal of Ichthyology 2004; 44: S180.

Klaine SJ, Alvarez PJ, Batley GE, Fernandes TF, Handy RD, Lyon DY, et al. Nanomaterials in the environment: behavior, fate, bioavailability, and effects. Environmental Toxicology and Chemistry 2008; 27: 1825-1851.

Kusch RC, Krone PH, Chivers DP. Chronic exposure to low concentrations of waterborne cadmium during embryonic and larval development results in the long-term hindrance of antipredator behavior in zebrafish. Environmental Toxicology and Chemistry 2008; 27: 705-710.

Lari E, Pyle G. Gyrodactylus salmonis infection impairs the olfactory system of rainbow trout. Journal of Fish Diseases 2017a; 40: 1279-1284.

Lari E, Pyle GG. Rainbow trout (*Oncorhynchus mykiss*) detection, avoidance, and chemosensory effects of oil sands process-affected water. Environmental Pollution 2017b; 225: 40-46.

Lari E, Razmara P, Bogart SJ, Azizishirazi A, Pyle GG. An epithelium is not just an epithelium: Effects of Na, Cl, and pH on olfaction and/or copper-induced olfactory deficits. Chemosphere 2019; 216: 117-123.

Lazzari M, Bettini S, Milani L, Maurizii MG, Franceschini V. Differential response of olfactory sensory neuron populations to copper ion exposure in zebrafish. Aquatic Toxicology 2017; 183: 54-62.

Lenth RV. Least-Squares Means: The R Package lsmeans. Journal of Statistical Software 2016; 69: 1-33.

Li Y, Fu J, Chen R, Huang M, Gao B, Huo K, et al. Core–shell TiC/C nanofiber arrays decorated with copper nanoparticles for high performance non-enzymatic glucose sensing. Sensors and Actuators B: Chemical 2014; 192: 474-479.

Minghetti M, Leaver MJ, Carpene E, George SG. Copper transporter 1, metallothionein and glutathione reductase genes are differentially expressed in tissues of sea bream (*Sparus aurata*) after exposure to dietary or waterborne copper. Comparative Biochemistry and Physiology Part C: Toxicology & Pharmacology 2008; 147: 450-459.

Mirza R, Green W, Connor S, Weeks A, Wood C, Pyle G. Do you smell what I smell? Olfactory impairment in wild yellow perch from metal-contaminated waters. Ecotoxicology and Environmental Safety 2009; 72: 677-683.

Olsén KH, Höglund LB. Reduction by a surfactant of olfactory mediated attraction between juveniles of *Arctic charr*, *Salvelinus alpinus* (L.). Aquatic Toxicology 1985; 6: 57-69.

Peijnenburg WJ, Baalousha M, Chen J, Chaudry Q, Von der kammer F, Kuhlbusch TA, et al. A review of the properties and processes determining the fate of engineered nanomaterials in the aquatic environment. Critical Reviews in Environmental Science and Technology 2015; 45: 2084-2134.

Perelshtein I, Applerot G, Perkas N, Wehrschuetz-Sigl E, Hasmann A, Guebitz G, et al. CuO–cotton nanocomposite: Formation, morphology, and antibacterial activity. Surface and Coatings Technology 2009; 204: 54-57.

Pulido-Reyes G, Leganes F, Fernández-Piñas F, Rosal R. Bio-nano interface and environment: A critical review. Environmental Toxicology and Chemistry 2017; 36: 3181-3193.

Pyle GG, Mirza RS. Copper-impaired chemosensory function and behavior in aquatic animals. Human and Ecological Risk Assessment 2007; 13: 492-505.

Rai M, Ingle A. Role of nanotechnology in agriculture with special reference to management of insect pests. Applied Microbiology and Biotechnology 2012; 94: 287-293.

Ramyadevi J, Jeyasubramanian K, Marikani A, Rajakumar G, Rahuman AA. Synthesis and antimicrobial activity of copper nanoparticles. Materials letters 2012; 71: 114-116.

Sandahl JF, Miyasaka G, Koide N, Ueda H. Olfactory inhibition and recovery in chum salmon (*Oncorhynchus keta*) following copper exposure. Canadian Journal of Fisheries and Aquatic Sciences 2006; 63: 1840-1847.

Scholz NL, Truelove NK, French BL, Berejikian BA, Quinn TP, Casillas E, et al. Diazinon disrupts antipredator and homing behaviors in chinook salmon (*Oncorhynchus tshawytscha*). Canadian Journal of Fisheries and Aquatic Sciences 2000; 57: 1911-1918.

Schrand AM, Rahman MF, Hussain SM, Schlager JJ, Smith DA, Syed AF. Metal-based nanoparticles and their toxicity assessment. Wiley Interdisciplinary Reviews: Nanomedicine and Nanobiotechnology 2010; 2: 544-568.

Scott JW, Scott-Johnson PE. The electroolfactogram: a review of its history and uses. Microscopy Research and Technique 2002; 58: 152-160.

Shaw BJ, Al-Bairuty G, Handy RD. Effects of waterborne copper nanoparticles and copper sulphate on rainbow trout,(*Oncorhynchus mykiss*): physiology and accumulation. Aquatic Toxicology 2012; 116: 90-101.

Shaw BJ, Liddle CC, Windeatt KM, Handy RD. A critical evaluation of the fish early-life stage toxicity test for engineered nanomaterials: experimental modifications and recommendations. Archives of Toxicology 2016; 90: 2077-2107.

Shende S, Gaikwad N, Bansod S. Synthesis and evaluation of antimicrobial potential of copper nanoparticle against agriculturally important Phytopathogens. International Journal of Biology Research 2016; 1: 41-47.

Sommers F, Mudrock E, Labenia J, Baldwin D. Effects of salinity on olfactory toxicity and behavioral responses of juvenile salmonids from copper. Aquatic Toxicology 2016; 175: 260-268.

Song L, Vijver MG, Peijnenburg WJ, Galloway TS, Tyler CR. A comparative analysis on the in vivo toxicity of copper nanoparticles in three species of freshwater fish. Chemosphere 2015; 139: 181-189.

Sovová T, Boyle D, Sloman KA, Pérez CV, Handy RD. Impaired behavioural response to alarm substance in rainbow trout exposed to copper nanoparticles. Aquatic Toxicology 2014; 152: 195-204.

Tang X-F, Yang Z-G, Wang W-J. A simple way of preparing high-concentration and high-purity nano copper colloid for conductive ink in inkjet printing technology. Colloids and Surfaces A: Physicochemical and Engineering Aspects 2010; 360: 99-104.

Team RDC. R: a Language and Environment for Statistical Computing. R Foundation for Statistical Computing,, Vienna, Austria, 2018.

Teli MD, Sheikh J. Modified bamboo rayon–copper nanoparticle composites as antibacterial textiles. International Journal of Biological Macromolecules 2013; 61: 302-307.

Tierney KB, Baldwin DH, Hara TJ, Ross PS, Scholz NL, Kennedy CJ. Olfactory toxicity in fishes. Aquatic Toxicology 2010; 96: 2-26.

Tilton F, Tilton SC, Bammler TK, Beyer R, Farin F, Stapleton PL, et al. Transcriptional biomarkers and mechanisms of copper-induced olfactory injury in zebrafish. Environmental Science & Technology 2008; 42: 9404-9411.

Wang L, Bammler TK, Beyer RP, Gallagher EP. Copper-induced deregulation of microRNA expression in the zebrafish olfactory system. Environmental Science & Technology 2013a; 47: 7466-7474.

Wang L, Espinoza HM, Gallagher EP. Brief exposure to copper induces apoptosis and alters mediators of olfactory signal transduction in *coho salmon*. Chemosphere 2013b; 93: 2639-2643.

Wang L, Gallagher EP. Role of Nrf2 antioxidant defense in mitigating cadmium-induced oxidative stress in the olfactory system of zebrafish. Toxicology and Applied Pharmacology 2013; 266: 177-186.

Wang T, Long X, Liu Z, Cheng Y, Yan S. Effect of copper nanoparticles and copper sulphate on oxidation stress, cell apoptosis and immune responses in the intestines of juvenile *Epinephelus coioides*. Fish & Shellfish immunology 2015; 44: 674-682.

Westfall THaFBaP. Simultaneous Inference in General Parametric Models. Biometrical Journal 2008; 50: 346-363.

Wu S, Ho Y-C, Shih M. Effects of Ca^{2+} or Na^{+} on metallothionein expression in tilapia larvae (*Oreochromis mossambicus*) exposed to cadmium or copper. Archives of Environmental Contamination and Toxicology 2007; 52: 229-234.

Zhang Y, Blewett TA, Val AL, Goss GG. UV-induced toxicity of cerium oxide nanoparticles (CeO 2 NPs) and the protective properties of natural organic matter (NOM) from the Rio Negro Amazon River. Environmental Science: Nano 2018; 5: 476-486.

Zielinski BS, Hara TJ. Olfaction. Fish Physiology. 25. Academic Press, 2006, pp. 1-43.

CHAPTER 3: Rainbow trout (*Oncorhynchus mykiss*) chemosensory detection of and reactions to copper nanoparticles and copper ions

In this research chapter, we investigated if the equitoxic concentrations (i.e., 20% olfactory inhibitory concentrations (24 h IC20s)) of CuNPs and Cu^{2+} are detectable and perceivable for rainbow trout. The IC20 of soluble Cu was suggested as a benchmark index to determine if the Cu water quality criteria is protective for fish.

A version of this chapter has been published in *Environmental Pollution*:

Razmara, P., Sharpe, J., Pyle, G. (2020). Rainbow trout (*Oncorhynchus mykiss*) chemosensory detection of and reactions to copper nanoparticles and copper ions. Environmental Pollution, 260, 113925.

https://www.sciencedirect.com/science/article/abs/pii/S0269749119360099

Contribution of authors: I designed and performed research, collected and analysed data, and wrote the manuscript. Justin Sharpe performed a part of the behavioural assay and collected data. Dr. Pyle provided guidance, scientific input, supervision, and funding for this research. All authors edited and approved the final manuscript.

3.1. Abstract

Copper is known to interfere with fish olfaction. Although the chemosensory detection and olfactory toxicity of copper ions (Cu^{2+}) has been heavily studied in fish, the olfactory-driven detection of copper nanoparticles (CuNPs)—a rapidly emerging contaminant to aquatic systems—remains largely unknown. This study aimed to investigate the olfactory response of rainbow trout to equitoxic concentrations of CuNPs or Cu^{2+} using electro-olfactography (EOG, a neurophysiological technique) and olfactory-mediated behavioural assay. In the first experiment, the concentration of contaminants known to impair olfaction by 20% over 24 h (EOG-based 24-h IC20s of 220 and 3.5 µg/L for CuNPs and Cu^{2+}, respectively) were tested as olfactory stimuli using both neurophysiological and behavioural assays. In the second experiment, to determine whether the presence of CuNPs or Cu^{2+} can affect the ability of fish to perceive a social cue (taurocholic acid (TCA)), fish were acutely exposed to one form of Cu-contaminants (approximately 15 min). Following exposure, olfactory sensitivity was measured by EOG and olfactory-mediated behaviour within a choice maze was recorded in the presence of TCA. Results of neurophysiological and behavioural experiments demonstrate that rainbow trout can detect and avoid the IC20 of CuNPs. The IC20 of Cu^{2+} was below the olfactory detection threshold of rainbow trout, as such, fish did not avoid Cu^{2+}. The high sensitivity of behavioural endpoints revealed a lack of aversion response to TCA in CuNP-exposed fish, despite this change not being present utilizing EOG. The reduced response to TCA during the brief exposure to CuNPs may be a result of either olfactory fatigue or blockage of olfactory sensory neurons (OSNs) by CuNPs. The observed behavioural interference caused by CuNP exposure may indicate that CuNPs have the ability to

interfere with other behaviours potentially affecting fitness and survival. Our findings also revealed the differential response of OSNs to CuNPs and Cu^{2+}.

3.2. Introduction

Owing to their distinctive antimicrobial, electrical, optical, and catalytic properties, engineered copper nanoparticles (CuNPs) have become increasingly attractive in many different fields including agriculture (Kanhed et al., 2014; Kasana et al., 2016), healthcare and medicine (Abbasi et al., 2015; Prabhu et al., 2011; Woźniak-Budych et al., 2016), and electronics (Abhinav K et al., 2015; Hwang et al., 2016). Inevitably, a portion of CuNPs will escape to the environment during production, utilization, and disposal of CuNP-containing products (Keller et al., 2017). The introduction of CuNPs to water bodies through soil leaching, water treatment plant effluent, and atmospheric deposition results in a high likelihood of aquatic ecosystems being a prominent sink for CuNPs. The environmental concentration of CuNPs has been estimated to be 60 μg/L (with a 95% confidence interval (CI) of 10 – 910 μg/L CuNPs) in some receiving waters (Chio et al., 2012).

Emission and accumulation of CuNPs in aquatic ecosystems and their potential toxicity has raised concerns regarding the health of aquatic organisms. Aquatic animals living in nano-copper contaminated waters are highly vulnerable to the adverse effects of CuNPs. Induction of oxidative stress, cytotoxicity, apoptosis, immunotoxicity (Torrealba et al., 2019; Wang et al., 2016; Wang et al., 2015; Wang et al., 2019), ionoregulatory toxicity (Shaw et al., 2012), Cu distribution and accumulation in fish tissues (Lindh et al., 2019; Shaw et al., 2012), tissues structural alteration and damage (Forouhar Vajargah et al., 2018; Gupta et al., 2016), and neurotoxicity (Hua et al., 2014; Zhao et al., 2011) are

evident following exposure to CuNPs in many species of fish. Recent work has demonstrated olfactory-mediated behavioural abnormalities in fish exposed to CuNPs (Razmara et al., 2019; Sovová et al., 2014). Behavioural alterations are usually due to the disruption of sensory system(s) (e.g., olfactory system) and/or the central nervous system.

Fish olfaction is a chemosensory system receiving vital information from surroundings. The received and perceived olfactory inputs are employed in fundamental activities including foraging, mating, homing, and avoiding predation which are crucial for fish growth, reproduction, and survival. Furthermore, the olfactory system enables fish to detect numerous types of contaminants including trace metals (i.e. nickel, copper, and cadmium) (Lari et al., 2018), calcium (Dew and Pyle, 2014), and oil sands process-affected water (Lari and Pyle, 2017), allowing them to escape from high-risk areas to safe and clean environments. Contaminant avoidance responses of fish are usually driven by chemo-sensation. Nevertheless, chemosensory avoidance of contaminants is highly chemical-specific. Zebrafish (*Danio rerio*) can actively avoid glyphosate-based herbicides but not atrazine-based herbicides or tebuconazole-based fungicides (da Rosa et al., 2016). Olfactory-mediated attraction to some psychotropic medicines including diazepam, fluoxetine, risperidone and buspirone are also observed in zebrafish (Abreu et al., 2016).

Olfactory-mediated avoidance of contaminants may aid in, but will not ensure, fish survival. In general, there is an avoidance threshold for chemicals that can evoke aversion reactions in fish (Tierney, 2016). For some chemicals the olfactory avoidance threshold is different from the olfactory impairment threshold. If the concentration of a contaminant in water is higher than or equal to the olfactory aversion threshold, but lower than or equal to

the olfactory impairment threshold (olfactory avoidance threshold ≤ water contaminant concentration ≤ olfactory impairment threshold), fish can avoid the polluted area and protect themselves from potential contaminant-induced toxicity (Tierney, 2016). For instance, the avoidance threshold of the water soluble fraction (WSF) of oil in European seabass (*Dicentrarchus labrax*) is 1:20 diluted WSF-contaminated water which has 8.54 µg/L of total polycyclic aromatic hydrocarbon (PAH) (Claireaux et al., 2018). The reported PAH concentration (µg/L) is below the toxic threshold of petroleum hydrocarbons (mg/L) for the European seabass. Therefore, the seabass avoidance of WSF can protect fish against contamination and subsequent toxicity (Claireaux et al., 2018).

Research investigating olfactory-mediated aversion/attraction responses of fish to CuNPs are limited; however, soluble forms of copper have been well-studied and it has been demonstrated that soluble copper (particularly Cu^{2+}) triggers avoidance responses in different fish, especially salmonids (Giattina et al., 1982; Hansen et al., 1999; Meyer and Adams, 2010; Morris et al., 2019; Van Genderen et al., 2016). The Cu-induced olfactory toxicity can be influenced by some water quality characteristics including dissolved organic carbon (DOC) and salinity (Kennedy et al., 2012; Sommers et al., 2016). The olfactory avoidance threshold of Cu may also be dependent on water chemistry (Morris et al., 2019). Rainbow trout living in soft water with low DOC (hardness of 25-27 mg/L as $CaCO_3$, 0.98 mg/L DOC) can avoid Cu^{2+} at concentrations as low as 1.6 µg/L, while the Cu^{2+} olfactory-inhibition concentration is 2.4-2.7 µg/L (Hansen et al., 1999; Morris et al., 2019). Therefore, depending on the specific water chemistry of the exposure medium, trout are able to avoid elevated Cu^{2+} concentrations. Our previous study demonstrated that CuNPs and Cu^{2+} exert different effects on the fish olfactory system over time (Razmara et

al., 2019). Accordingly, the olfactory detection and avoidance/attraction of fish facing CuNPs and their differences with Cu^{2+} needs to be studied.

In 2010, the 20% impairment concentration of soluble Cu (IC20) was suggested as a benchmark index to determine whether the Cu water quality criteria (WQC) is protective for fish (i.e. IC20 of Cu ≥ WQC of Cu) (Meyer and Adams, 2010). If fish are able to avoid the IC20 of Cu, they will be protected against Cu-induced toxicity. This study investigated whether the 24-h IC20 of CuNPs or Cu^{2+} induce avoidance or attraction responses in rainbow trout. Given that the presence of copper contaminants may interfere with the ability for fish to respond to stimuli (Araújo et al., 2016; Lari and Pyle, 2017), the present work also studied how the presence of CuNPs or Cu^{2+} may affect the olfactory detection and perception of a chemical social cue.

3.3. Materials and Methods

3.3.1. Experimental animals

Juvenile rainbow trout (n=148, total length 13.4 ± 1.3 cm; weight, 25.3 ± 3.8 g (mean ± SD)) were obtained from the Lethbridge College Aquaculture Centre fish hatchery (Alberta, Canada), and transferred to the Aquatic Research Facility (ARF) of the University of Lethbridge. Fish were kept in holding tanks at a stocking density of 5 g/L (16 h light: 8 h dark photoperiod, 12°C). During two weeks of acclimation to ARF water, fish were treated with parasiticide (PraziPro, Hikari, USA) to ensure removal of any olfactory parasites. The University of Lethbridge Animal Welfare Committee reviewed and approved all experiments conducted in this study (protocol #1612). The quality of ARF culture water was measured as follows (mean ± SD; n=3): temperature, 12.1 ± 0.5 °C; dissolved oxygen, 8.9 ± 0.6 mg/L; conductivity, 331.3 ± 0.8 µS/cm; hardness, 156 ± 2.8

mg/L as $CaCO_3$; alkalinity, 129.1 ± 1.9 mg/L as $CaCO_3$; median pH, 8.2 (range 8.0-8.4); and dissolved organic carbon, 2.52 ± 0.52 mg/L. The ARF culture water was used for both neurophysiological and behavioral experiments in this study.

3.3.2. Preparation of stimuli

To make the Cu^{2+} stimulus, a fresh stock solution of 10 mg/L $CuSO_4$ (98.5–100.5% purity; BHD, USA) in 18.2 MΩ/cm water (ddH_2O, Millipore, USA) was prepared and used as the source of Cu^{2+}. A fresh stock suspension of CuNPs at the nominal concentration of 250 mg/L was prepared by suspending the nanocopper powder (35 nm; 99.8% purity; partially passivated, Nanostructured & Amorphous Materials Inc, USA) in ddH_2O followed by a 30 min dispersion in a water bath sonicator (UD 150SH6LQ; 150 W; Eumax; USA) at room temperature. To make the social stimulus, a stock solution of taurocholic acid (TCA; Sigma-Aldrich, USA) was prepared at a concentration of 10^{-3} mol/L utilizing clean culture water.

To determine the 20% impairment concentration of CuNPs or Cu^{2+} (IC20) for rainbow trout, we used the electro-olfactography (EOG)-based inhibitory concentration curve which was established in our previous study. In the previous experiment, fish were exposed to a geometric dilution series of CuNPs or Cu^{2+} for 24 h, and their olfactory sensitivity was measured by EOG in response to the 10^{-5} mol/L TCA (nominal concentration) (Razmara et al., 2019). The 24 h IC20 of CuNPs and Cu^{2+} were 223 ± 16 and 3.5 ± 0.2 µg/L (mean ± SE; n=6), respectively. The 24 h equitoxic IC20 concentration of CuNPs and Cu^{2+} were selected as stimuli concentrations in the current study to test if fish can detect and avoid the Cu contaminants. Although the 24 h IC20s of CuNPs and Cu^{2+} were equitoxic in the fish olfactory system (both inhibit the fish olfaction by 20%),

the IC20 for CuNPs was not environmentally relevant relative to the IC20 of Cu^{2+}. The TCA concentration of 10^{-5} mol/L was used to investigate how the presence of each Cu contaminant (IC20) affects the olfactory perception of TCA.

3.3.3. Characterization of CuNPs and Cu analyses

Characterization of CuNPs was conducted following the same protocol reported in our previous study (we utilized the same batch of CuNPs in both the past and present study). In short, transmission electron microscopy (TEM; FEI Tecnai-20) indicated that CuNPs were semi-spherical with an average diameter of 32 ± 1 nm (mean ± SEM; n=349) (Razmara et al., 2019). Parameters indicating aggregation behaviour of CuNPs, including polydispersity index (PDI), hydrodynamic diameter (HDD), and zeta potential were measured using dynamic light scattering (DSL; Zetasizer Nano Series, Malvern) in 173° backscatter mode over 2 h (n=3).

As waterborne CuNPs can potentially release Cu ions from their surfaces, the concentration of dissolved Cu must be characterized after CuNPs are introduced to the fish culture water. To measure the dissolution of CuNPs, dissolved Cu was separated from CuNPs using Amicon Ultra-4 Centrifugal Filter Units with a pore size of 1-2 nm (3K regenerated cellulose membrane, Merck Millipore Ltd., USA) (Razmara et al., 2019). The term "dissolved Cu" refers to all filtrate Cu complexes (particularly Cu^{2+}) in the CuNPs suspension that could pass through the 3K membrane after 90 min centrifugation at 2750 g. The dissolution behaviour of CuNPs was determined at 0 h and 2 h after the experimental concentration of CuNPs was introduced to the culture water (n=3). The filtrates (acidified to 1% HNO_3) were analyzed by graphite furnace atomic absorption spectrometry (GFAAS) (240FS GFAAS, Agilent Technologies, USA). Following our previous protocol, the

QA/QC of Cu measurements were conducted (Razmara et al., 2019). A certified reference material (SLRS-6: River Water, National Research Council Canada, Ottawa, ON, Canada) was measured every 10 samples (mean percent recovery was 94%, which was within the accepted ± 10% error), a standards calibration curve was resloped every 10 samples and recalibrated every 20 samples. Duplicate samples were run after each standards recalibration (<2% different from each other). The Cu detection limit (MDL) by GFAAS was approximately 2 μg/L. The actual concentrations of Cu were also measured in both Cu stimuli (CuNPs or $CuSO_4$) and control (no added Cu) by GFAAS.

3.3.4. Electro-olfactography assay

The olfactory detection of CuNPs or Cu^{2+} (as olfactory stimuli) were measured using EOG in rainbow trout (n=10). Fish were anesthetized in 120 mg/L tricaine methanesulfonate (AquaLife, Canada) which was buffered to pH 7.4 by 360 mg/L $NaHCO_3$ (Fisher Scientific, USA). Once anesthetized, the intranarial olfactory chamber septum was removed to allow better access to the olfactory rosette. To keep the fish anesthetized during the recording period, gills were constantly perfused with a half dose of anaesthetizing solution (60 mg/L). The olfactory response of each fish to one of four stimuli (CuNPs, Cu^{2+}, blank (clean culture water) or TCA (as a positive control)) was measured following the EOG procedure described by Razmara et al. (2019). Every 90 s, a stimulus was randomly delivered to the olfactory chamber, and the response to each stimulus was recorded three times. The olfactory rosette was constantly irrigated with clean culture water between stimulus deliveries. All stimuli, gill perfusion, and olfactory irrigation solutions were kept at 12°C.

To study our second objective, the olfactory detection of TCA (as a social stimulus), was measured in the presence of CuNPs, Cu^{2+}, or control (clean culture water) using EOG. In this experiment, the EOG recordings in response to TCA had 3 phases: 1) a 7.5 min pre-exposure period during which the olfactory response of all fish (6 individuals per treatment) to TCA were measured while the olfactory chamber was perfused with clean culture water (no Cu added to the irrigation water or TCA solution). 2) for 15 min, during which the olfactory chamber was continuously exposed to either the IC20 of Cu^{2+}, CuNPs, or clean culture water (as control) (both olfactory irrigation stream and TCA solution were switched to the ones that were spiked with CuNPs or Cu^{2+}). 3) a 7.5 min post-exposure period, identical to the first (pre-exposure) phase in which no Cu was present.

3.3.5. Olfactory-mediated behavioural assay

To investigate the avoidance/attraction behaviour of fish to the IC20s of CuNPs or Cu^{2+}, we used a flow-through choice maze which has been described previously (Lari and Pyle, 2017; Razmara et al., 2019). The QA/QC experiments including arm-bias and dye tests were conducted to ensure fish showed no preference for a particular arm of the maze and to confirm uniform water flow, respectively. Fish were introduced to the acclimation zone of the maze while the gates of the maze were lowered, preventing the fish from entering either arm of the maze. During the 15 min acclimation period, the water flow rate was held at 1.6 L/min using two peristaltic pumps (Fisher Scientific, Canada). After acclimation, a 4-min trial ensued which was video recorded as the gates were gently lifted and a stimulus (i.e., CuNPs, Cu^{2+}, or clean culture water) was randomly delivered to one of the maze arms. All video footage was analysed using video-tracking software (20 individuals per stimulus) (EthoVision XT, Version 14.0 by Noldus Information

Technology) to quantify the attraction/avoidance responses of fish based on the time spent in each arm, described in Razmara et al. (2019).

In the second behavioral experiment, to test the olfactory-driven behavioural responses of fish to TCA in the presence of CuNPs or Cu^{2+}, either clean culture water (in control treatment) or water spiked with Cu contaminants (in the Cu treatments) was delivered to the entire maze. At the end of the acclimation period, a solution of TCA (made of clean culture water in control and spiked with CuNPs or Cu^{2+} in Cu treatments) was randomly delivered to one of the maze arms. The 4-minute trial was run in the same manner described previously and the resulting data were analyzed by the same equation (20 individuals per treatment).

3.3.6. Statistical analyses

Statistical analyses were performed by R version 3.6.2 (R Core Team, 2019). Normality and homogeneity of variance were examined for all experimental data using Shapiro-Wilks and a Bartlett test, respectively. To determine whether polydispersity index, hydrodynamic diameter, and zeta potential of CuNPs were changed over 2 h, a paired t-test was used. The olfactory responses of fish to different stimuli (i.e., the EOG responses to clean water, CuNPs, Cu^{2+}, or TCA) were analyzed using repeated measures one-way ANOVA. To analyze the EOG responses to TCA in the presence of CuNPs, Cu^{2+}, or clean water, a repeated measure two-way ANOVA was used. The olfactory-driven behavioural responses of fish to different stimuli (i.e. clean water, CuNPs, or Cu^{2+}) were analyzed by one-way ANOVA followed by a Tukey's post hoc test. Any possible alteration in the perception of TCA after brief exposure to CuNPs or Cu^{2+} was also analysed by one-way ANOVA and Tukey's post hoc test.

3.4. Results and discussion

3.4.1. Characterization of CuNPs and Cu analyses

Copper NPs may undergo physicochemical transformations (e.g. aggregation and dissolution) in the aquatic environment over time. In general, aggregated NPs are less bioavailable for pelagic organisms as they are removed from the water column by flocculation, whereas dissolved NPs (e.g. metal ions) are more bioavailable for the organisms (Peijnenburg et al., 2015). The bioavailability of a chemical to the olfactory sensory neurons (OSNs) determines an organism's ability to detect it by olfaction. Table 3.1 demonstrates the aggregation and dissolution behaviour of CuNPs over 2 h after being introduced to clean culture water. The DLS measurements suggest the aggregation state of CuNPs did not change over 2 h (Table 3.1) and the IC20 of CuNPs was partially bioavailable to OSNs. The PDI indicates the NPs relative distribution (PDI=0 indicates NPs are monodispersed and less aggregated, and PDI=1 indicates NPs are highly polydispersed and aggregated). The PDI measurements showed CuNPs were partially polydispersed (PDI= 0.57-0.59), but did not increase over 2 h ($t(2) = -1.31$, $p = 0.32$; Table 3.1). The HDD, an indicator of NPs stability in the water, showed the stability of CuNPs as HDD remained unchanged over 2 h ($t(2) = -1.17$, $p = 0.36$; Table 1). The measure of surface charge of CuNPs, shown as zeta potential also did not change over 2 h ($t(2) = -1.86$, $p = 0.2$; Table 3.1), indicating CuNPs were not becoming increasingly aggregated over 2 h. The concentration of dissolved Cu was below the MDL of GFAAS, indicating extremely low (if any) dissolution of CuNPs over the 2 h period (Table 3.1). The lack of physicochemical transformations observed over 2 h indicate that during this time fish are mostly encountering unchanged CuNPs.

Table 3.1. Copper NPs characterization: aggregation (polydispersity index, hydrodynamic diameter, and zeta potential measured by DLS), and dissolution (measured by GFAAS) over 2 h (mean ± SD, n = 3). *: Below the MDL of GFAAS

Nominal Cu concentration (µg/L)	Actual Cu concentration (µg/L)	Time (h)	Dissolved Cu concentration (µg/L)	PDI	HDD (nm)	Zeta potential (mV)
223	189 ± 9	0	< 2*	0.570 ± 0.026	704 ± 28	-16.2 ± 0.5
		2	< 2*	0.591 ± 0.018	724 ± 30	-15.4 ± 0.3

The actual total concentration of Cu was also measured during both EOG and behavioural assays. In the CuNPs treatment, the average of measured Cu concentration was 85% of CuNPs nominal concentration (Table 3.1). The measured Cu concentration in the Cu^{2+} and control treatment was 3 ± 0 µg/L (mean ± SD, n = 6; 86% of nominal concentration) and below MDL, respectively.

3.4.2. Olfactory-mediated responses of fish to Cu stimuli

The results of EOG indicated fish displayed differential responses to the 24-h IC20s of Cu stimuli ($F(3, 27) = 80.47$, $p < 0.001$; Fig. 3.1). While the IC20 of CuNPs and TCA (positive control) significantly stimulated the fish olfactory system relative to the blank ($p = 0.01$ and $p < 0.001$, respectively), the IC20 of Cu^{2+} was not detectable by the fish olfactory system ($p > 0.05$; Fig. 3.1). The Cu-induced neurophysiological responses were corroborated by olfactory-mediated behavioural responses which demonstrated the distinct olfactory perception of CuNPs and Cu^{2+} in rainbow trout ($F(2, 57) = 4.22$, $p = 0.02$; Fig. 3.2). The IC20 of CuNPs was the only stimulus that resulted in behavioural avoidance relative to the control ($p = 0.04$; Fig. 3.2). The low concentration of dissolved Cu in the CuNPs treatment (Table 3.1) indicated that they were mostly CuNPs, not dissolved Cu such as Cu^{2+}, that were detectable by OSNs.

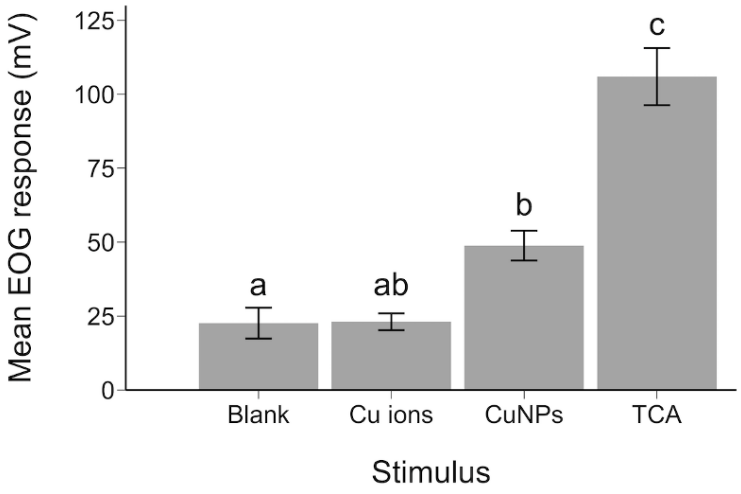

Figure 3.1. The electro-olfactography responses of rainbow trout to the blank (clean culture water as a negative control), TCA (as a positive control), and IC20s of CuNPs and Cu^{2+}. Lower-case letters indicate significant differences ($p \leq 0.05$, n=10, error bars: ± 1 SEM).

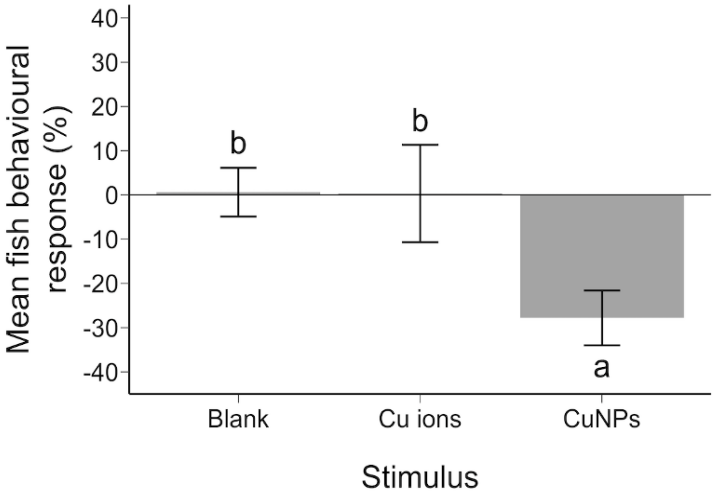

Figure 3.2. The olfactory-driven behavioural responses of rainbow trout to different stimuli (blank and IC20s of CuNPs and Cu^{2+}). Lower-case letters indicate significant differences ($p \leq 0.05$, n=10, error bars: ± 1 SEM).

As synthetic chemicals that are structurally similar to a natural analog can evoke aversion responses (Tierney, 2016), CuNPs can either serve as a unique stimulus, or mimic a natural stimulus and be perceived by fish. To the best of our knowledge, this is the first study to aversive responses triggered by the IC20 of CuNPs in rainbow trout. Previous

work investigating the olfactory detection of NPs in fish is scarce. A previous study indicated zebrafish have a differential response to silver nanoparticles (AgNPs) relative to silver ions (Ag^{+}) (Bilberg et al., 2012). In this study, zebrafish displayed an avoidance reaction (i.e. increased swimming activity and escape behaviour by thigmotaxis) to Ag^{+}, but not AgNPs. Therefore, the olfactory detection of NPs can be both species-specific and NP-specific. In contrast to CuNPs, the olfactory-mediated detection of Cu^{2+} has received more attention. Our neurophysiological and behavioural results suggest that the IC20 of Cu^{2+} (3.5 µg/L) is not detectable by rainbow trout ($p > 0.05$; Fig. 3.1 and 3.2); however, previous studies reported that the avoidance behaviour of rainbow trout can be triggered in the range of 1.6 - 9.2 µg/L of Cu^{2+} (Giattina et al., 1982; Hansen et al., 1999; Van Genderen et al., 2016). Different experimental water qualities (e.g., DOC) between our studies and others may explain the differences in olfactory-driven behaviours. A study from our lab, with similar water quality, showed that a higher concentration of Cu^{2+} (i.e. 20 µg/L of Cu^{2+}) is detectable by rainbow trout (Lari et al., 2018).

In our study, despite using the same water for all exposures and equitoxic concentrations of CuNPs and Cu^{2+}, different olfactory responses were observed in rainbow trout (Fig. 3.1 and 3.2). Copper NPs and Cu^{2+} have many disparate physicochemical characteristics that lead to unique olfactory responses in fish. For instance, the currently used CuNPs were 32 nm and semi-spherical with a negative surface potential (Table 1) as opposed to Cu^{2+} which is smaller than CuNPs and has a spherical shape with a positive charge. In contrast to CuNPs, Cu^{2+} is completely water soluble and shows a greater stability in water over a long period of time (Razmara et al., 2019). The distinct characteristics of CuNPs and Cu^{2+}, their reactions to other contaminants or natural suspensions, and

consequently their behaviour and bioavailability to the OSNs might also be different (Klaine et al., 2008). To our knowledge, despite the evident differences between CuNPs and Cu^{2+}, there is no particular water quality guideline for CuNPs which is of potential concern.

The influence of environmental conditions to Cu toxicity, including water chemistry, species-specific sensitivity, and ligand-receptor specificity (e.g. olfactory vs. gill epithelium) raises concern about the ability of the established WQC to protect against olfactory toxicity (Meyer and Adams, 2010). The current hardness-adjusted copper criterion published by Alberta Environment and Parks (AEP) is 25 µg/L in water with a hardness of 156 mg/L as $CaCO_3$. The results of our previous and current work indicate that the EOG-based 24-h IC20 and IC50 of Cu^{2+} are 3.5 and 7 µg/L, respectively for rainbow trout (Razmara et al., 2019). As the current AEP water quality criterion for Cu exceeded both IC20 and IC50 values for chemosensory responses, this WQC is considerably underprotective against rainbow trout Cu-induced chemosensory dysfunction. In contrast, the hardness-based Cu criterion in Canadian Council of Ministers of the Environment (CCME) is 3.46 µg/L which is comparable to the IC20 of Cu^{2+}; therefore, the CCME Cu criterion is approximately 80% protective for the rainbow trout chemosensory function. Results of a recent meta-analysis conducted on the reported Cu-induced chemosensory responses in aquatic animals (i.e. fish, amphibians, and invertebrates) indicated the biotic ligand model based (BLM-based) WQC of the gill epithelium has increased protectivity against the Cu-induced olfactory impairments compared to the hardness-based WQC (Meyer and DeForest, 2018). While the BLM-based WQC for Cu does provide increased protection to olfactory impairment compared to hardness-based WQC, organizations

utilizing the BLM-based approach, such as the United States Environmental Protection Agency (U.S. EPA) continue to set restrictions that are not protective for olfactory impairment. The U.S. EPA acute (criterion maximum concentration (CMC)) and chronic (criterion continuous concentration (CCC) WQC for Cu was calculated using the Windward Environmental Cu BLM Ver 3.41.2.45 (Windward Environmental, 2019); based on our water chemistry, the CMC and CCC values are 21.43 and 13.31 µg/L of Cu, respectively. Chronic Cu exposures showed the EOG-based 10-day IC20 of Cu^{2+} to be 6 µg/L in rainbow trout (Lari et al., 2019), well below both U.S. EPA's acute and chronic values. These results indicate that the gill BLM-based WQC may be underprotective for the olfactory epithelium in some water chemistries.

Previous studies have shown that exposure to CuNPs and Cu^{2+} impair fish neurophysiological and behavioural functions, which may consequently threaten fish survival (Green et al., 2010; Razmara et al., 2019; Sovová et al., 2014; Tilton et al., 2008). Contaminant-induced alteration of animal behaviour, especially the avoidance reaction, is an early indicator of a potentially contaminated environment and can serve as an early warning sign to an organism's ability to avoid potentially dangerous environments (Hellou, 2011). Considering the high sensitivity of olfactory function to the low concentration of Cu and the importance of chemosensory function to fish survival, it is highly recommended to include the Cu-induced chemosensory responses in the estimation of WQC and develop a specific BLM-based WQC for the olfactory epithelium.

3.4.3. Impacts of CuNPs and Cu^{2+} on the olfactory responses to TCA

To ensure that the developed WQC are protective, it is crucial to assess toxicity of highly sensitive tissues. As olfactory tissue shows a greater sensitivity to copper than gill

tissue, the olfactory response to various stimuli should be analyzed. In this study, the EOG responses of fish to TCA (a social stimulus) was measured in the presence and absence of CuNPs or Cu^{2+} ($F(4, 30) = 3.22$, $p = 0.03$; Fig. 3.3). The response to TCA was not significantly affected by the presence of CuNPs or Cu^{2+} relative to the control ($p > 0.05$; Fig. 3.1). During exposure, the olfactory-mediated responses to TCA in the CuNP-exposed fish were significantly lower than the olfactory response in the Cu^{2+}-exposed ones ($p = 0.01$; Fig. 3.3), which is related to the inherent differences between CuNPs and Cu^{2+}. The sudden increase in the olfactory response to TCA during the brief exposure to Cu^{2+}, may be associated with the potential Cu-induced disruption of ion homeostasis (e.g. calcium (Ca^{2+})) in the OSNs. We hypothesize that exposure to Cu^{2+} has the potential to increase the intracellular concentration of cations (such as Ca^{2+}) leading to neuronal excitation. Disturbed Ca^{2+} homeostasis following exposure to Cu^{2+} has been previously observed in fish hepatocytes (Manzl et al., 2004; Song et al., 2016). Nevertheless, further investigation is required to test the Cu^{2+}-induced Ca^{2+} homeostasis impairment in the OSNs. There were no significant differences in the EOG responses to TCA among the treatments in the post-exposure period ($p > 0.05$; Fig. 3.3). Therefore, the impacts of Cu contaminants on TCA detection appear restricted to the period in which contaminants are present.

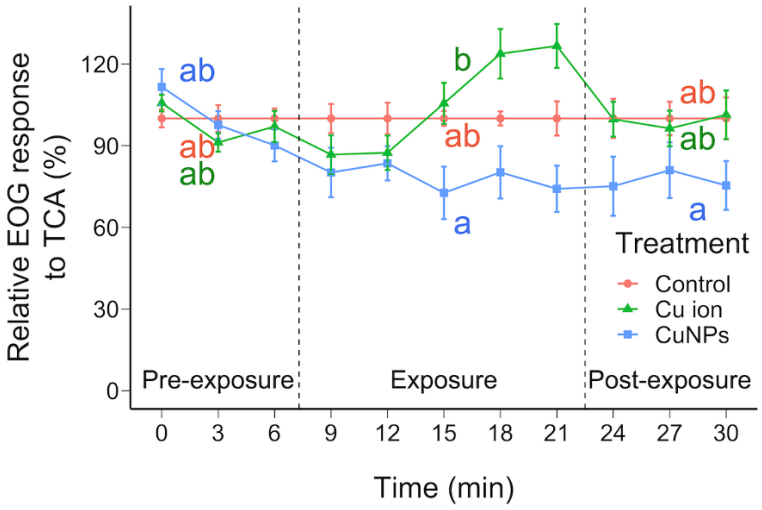

Figure 3.3. The relative electro-olfactography responses of rainbow trout to TCA measured in 3 phases: pre-exposure (clean water), exposure (to the IC20 of CuNPs, Cu^{2+}, or clean water), and post-exposure (clean water). Lower-case letters indicate significant differences among treatments and exposure phases measured by a repeated measure two-way ANOVA ($p \leq 0.05$, n=10, error bars: ± 1 SEM).

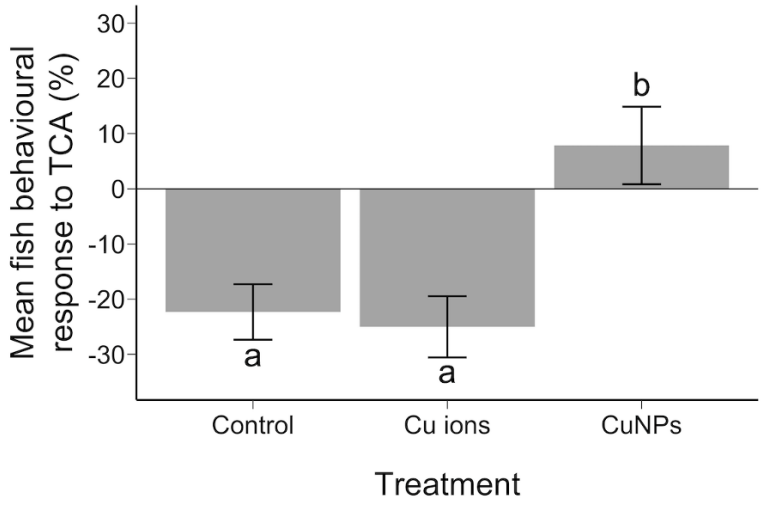

Figure 3.4. The olfactory-driven behavioural responses of rainbow trout to TCA in the presence of IC20 of CuNPs, Cu^{2+}, or clean water. Lower-case letters indicate significant differences ($p \leq 0.05$, n=10, error bars: ± 1 SEM).

To corroborate the neurophysiological results, the impact of CuNPs and Cu^{2+} on fish TCA perception was studied ($F(2, 57) = 12.28$, $p < 0.001$; Fig. 3.4). The behavioural test confirmed the interference of CuNPs in TCA perception which led to an inability to

avoid TCA relative to the control or Cu^{2+} ($p < 0.001$; Fig. 3.4). The sensitivity of behavioural responses is much higher than other sub-lethal endpoints such as neurophysiological responses (Gerhardt, 2007; Razmara et al., 2019); hence, our suspicion about the reduced, but statistically insignificant, EOG response to TCA elicited in the CuNP-exposed fish is supported by the observed behavioural avoidance of TCA (Fig. 3.3 and 3.4). It is likely that the brief exposure to CuNPs resulted in a blockage of OSNs, eliminating the ability for fish to smell TCA. Furthermore, the simultaneous presence of different odorants and their potential interactions may lead to olfactory fatigue, reduce the sensitivity of OSNs to a specific stimulus, and induce the behavioural confusion. For instance, the sensitivity of rainbow trout OSNs to a food cue was remarkably reduced in the presence of another stimulus, 1% oil sands process-affected water (Lari and Pyle, 2017). In addition, if fish remain trapped in a contaminated zone for an extended duration, it is possible that the IC20 of both CuNPs and Cu^{2+} will affect other vital behaviours, including predator avoidance or food attraction. It has also been reported that the behavioural avoidance pattern of tilapia fry (*Oreochromis* spp.) from tuna fish processing plant effluents — which serves as a chemosensory stimulus — was significantly altered in the presence of food cue, and fish moved toward effluents where they could feed (Araújo et al., 2016). Thus, the presence of various stimuli in natural habitats might compete with or disguise contaminant avoidance and risk the fish's health. To implement the IC20s of Cu contaminant as a protective regulatory benchmark index, further investigations on the interactions of IC20 of CuNPs or Cu^{2+} with other stimuli are warranted.

3.5 Conclusions

Fish are vulnerable to both CuNPs and Cu^{2+} contamination. To minimize the level of harm induced by these toxicants, the Cu IC20 has been proposed as a protective index in water quality regulatory guideline. This study demonstrated that rainbow trout could detect and avoid the IC20 concentration of CuNPs, but not Cu^{2+}. The differential olfactory responses between CuNPs and Cu^{2+} emphasize the need for developing a water quality guideline for CuNPs. Our findings also suggest that some current Cu WQC including the hardness-based AEP and BLM-based U.S. EPA are not protective against Cu-induced chemosensory dysfunction in rainbow trout. The brief exposure to CuNPs altered the perception and interpretation of the social cue, TCA. Accordingly, the interference of CuNPs to the avoidance of TCA may be indicative of CuNPs' ability to alter additional, vital behaviours and, in turn, impact individual fitness. Our findings also revealed the higher sensitivity of behavioural endpoints relative to neurophysiological endpoints; thus, behavioural ecotoxicological endpoints have the potential to be implemented as a regulatory tool. Taken together, considering no avoidance from IC20 of Cu^{2+} and eliminated avoidance of TCA in the presence of CuNPs IC20, setting the WQC based on the IC20s of Cu contaminants may not be 100% protective for rainbow trout. Further studies on the effects of IC20 of Cu contaminants in different organisms' life stages (e.g., non-motile larval stage) and other species are warranted.

3.6. References

Abbasi F, Hayat T, Alsaedi A. Peristaltic transport of magneto-nanoparticles submerged in water: model for drug delivery system. Physica E: Low-dimensional Systems and Nanostructures 2015; 68: 123-132.

Abhinav K V, Rao R VK, Karthik PS, Singh SP. Copper conductive inks: synthesis and utilization in flexible electronics. RSC Advances 2015; 5: 63985-64030.

Abreu MS, Giacomini ACV, Gusso D, Rosa JG, Koakoski G, Kalichak F, et al. Acute exposure to waterborne psychoactive drugs attract zebrafish. Comparative Biochemistry and Physiology Part C: Toxicology & Pharmacology 2016; 179: 37-43.

Araújo CV, Rodríguez EN, Salvatierra D, Cedeño-Macias LA, Vera-Vera VC, Moreira-Santos M, et al. Attractiveness of food and avoidance from contamination as conflicting stimuli to habitat selection by fish. Chemosphere 2016; 163: 177-183.

Bilberg K, Hovgaard MB, Besenbacher F, Baatrup E. In vivo toxicity of silver nanoparticles and silver ions in zebrafish (*Danio rerio*). Journal of Toxicology 2012; 2012: 1-9.

Chio C-P, Chen W-Y, Chou W-C, Hsieh N-H, Ling M-P, Liao C-M. Assessing the potential risks to zebrafish posed by environmentally relevant copper and silver nanoparticles. Science of the Total Environment 2012; 420: 111-118.

Claireaux G, Quéau P, Marras S, Le Floch S, Farrell AP, Nicolas-Kopec A, et al. Avoidance threshold to oil water-soluble fraction by a juvenile marine teleost fish. Environmental Toxicology and Chemistry 2018; 37: 854-859.

da Rosa JGS, de Abreu MS, Giacomini ACV, Koakoski G, Kalichak F, Oliveira TA, et al. Fish aversion and attraction to selected agrichemicals. Archives of Environmental Contamination and Toxicology 2016; 71: 415-422.

Dew WA, Pyle GG. Smelling salt: Calcium as an odourant for fathead minnows. Comparative Biochemistry and Physiology Part A: Molecular & Integrative Physiology 2014; 169: 1-6.

Forouhar Vajargah M, Mohamadi Yalsuyi A, Hedayati A, Faggio C. Histopathological lesions and toxicity in common carp (*Cyprinus carpio* L. 1758) induced by copper nanoparticles. Microscopy Research and Technique 2018; 81: 724-729.

Gerhardt A. Aquatic behavioral ecotoxicology—prospects and limitations. Human and Ecological Risk Assessment 2007; 13: 481-491.

Giattina JD, Garton RR, Stevens DG. Avoidance of copper and nickel by rainbow trout as monitored by a computer-based data acquisition system. Transactions of the American Fisheries Society 1982; 111: 491-504.

Green WW, Mirza RS, Wood CM, Pyle GG. Copper binding dynamics and olfactory impairment in fathead minnows (*Pimephales promelas*). Environmental Science & Technology 2010; 44: 1431-1437.

Gupta YR, Sellegounder D, Kannan M, Deepa S, Senthilkumaran B, Basavaraju Y. Effect of copper nanoparticles exposure in the physiology of the common carp (Cyprinus carpio): Biochemical, histological and proteomic approaches. Aquaculture and Fisheries 2016; 1: 15-23.

Hansen JA, Marr JC, Lipton J, Cacela D, Bergman HL. Differences in neurobehavioral responses of chinook salmon (*Oncorhynchus tshawytscha*) and rainbow trout (*Oncorhynchus mykiss*) exposed to copper and cobalt: behavioral avoidance. Environmental Toxicology and Chemistry: An International Journal 1999; 18: 1972-1978.

Hellou J. Behavioural ecotoxicology, an "early warning" signal to assess environmental quality. Environmental Science and Pollution Research 2011; 18: 1-11.

Hua J, Vijver MG, Ahmad F, Richardson MK, Peijnenburg WJ. Toxicity of different-sized copper nano-and submicron particles and their shed copper ions to zebrafish embryos. Environmental Toxicology and Chemistry 2014; 33: 1774-1782.

Hwang Y-T, Chung W-H, Jang Y-R, Kim H-S. Intensive Plasmonic Flash Light Sintering of Copper Nanoinks Using a Band-Pass Light Filter for Highly Electrically Conductive Electrodes in Printed Electronics. ACS Applied Materials & Interfaces 2016; 8: 8591-8599.

Kanhed P, Birla S, Gaikwad S, Gade A, Seabra AB, Rubilar O, et al. In vitro antifungal efficacy of copper nanoparticles against selected crop pathogenic fungi. Materials Letters 2014; 115: 13-17.

Kasana RC, Panwar NR, Kaul RK, Kumar P. Copper Nanoparticles in Agriculture: Biological Synthesis and Antimicrobial Activity. In: Ranjan S, Dasgupta N, Lichtfouse E, editors. Nanoscience in Food and Agriculture 3. Springer International Publishing, Cham, 2016, pp. 129-143.

Keller AA, Adeleye AS, Conway JR, Garner KL, Zhao L, Cherr GN, et al. Comparative environmental fate and toxicity of copper nanomaterials. NanoImpact 2017; 7: 28-40.

Kennedy CJ, Stecko P, Truelson B, Petkovich D. Dissolved organic carbon modulates the effects of copper on olfactory-mediated behaviors of chinook salmon. Environmental Toxicology and Chemistry 2012; 31: 2281-2288.

Klaine SJ, Alvarez PJ, Batley GE, Fernandes TF, Handy RD, Lyon DY, et al. Nanomaterials in the environment: behavior, fate, bioavailability, and effects. Environmental Toxicology and Chemistry 2008; 27: 1825-1851.

Lari E, Bogart SJ, Pyle GG. Fish can smell trace metals at environmentally relevant concentrations in freshwater. Chemosphere 2018; 203: 104-108.

Lari E, Pyle GG. Rainbow trout (*Oncorhynchus mykiss*) detection, avoidance, and chemosensory effects of oil sands process-affected water. Environmental Pollution 2017; 225: 40-46.

Lari E, Razmara P, Bogart SJ, Azizishirazi A, Pyle GG. An epithelium is not just an epithelium: Effects of Na, Cl, and pH on olfaction and/or copper-induced olfactory deficits. Chemosphere 2019; 216: 117-123.

Lindh S, Razmara P, Bogart S, Pyle G. Comparative tissue distribution and depuration characteristics of copper nanoparticles and soluble copper in rainbow trout (*Oncorhynchus mykiss*). Environmental Toxicology and Chemistry 2019; 38: 80-89.

Manzl C, Enrich J, Ebner H, Dallinger R, Krumschnabel G. Copper-induced formation of reactive oxygen species causes cell death and disruption of calcium homeostasis in trout hepatocytes. Toxicology 2004; 196: 57-64.

Meyer JS, Adams WJ. Relationship between biotic ligand model-based water quality criteria and avoidance and olfactory responses to copper by fish. Environmental Toxicology and Chemistry 2010; 29: 2096-2103.

Meyer JS, DeForest DK. Protectiveness of Cu water quality criteria against impairment of behavior and chemo/mechanosensory responses: An update. Environmental Toxicology and Chemistry 2018; 37: 1260-1279.

Morris JM, Brinkman SF, Takeshita R, McFadden AK, Carney MW, Lipton J. Copper toxicity in Bristol Bay headwaters: Part 2—Olfactory inhibition in low-hardness water. Environmental Toxicology and Chemistry 2019; 38: 198-209.

Peijnenburg WJ, Baalousha M, Chen J, Chaudry Q, Von der kammer F, Kuhlbusch TA, et al. A review of the properties and processes determining the fate of engineered nanomaterials in the aquatic environment. Critical Reviews in Environmental Science and Technology 2015; 45: 2084-2134.

Prabhu V, Uzzaman S, Grace VMB, Guruvayoorappan C. Nanoparticles in drug delivery and cancer therapy: the giant rats tail. J Cancer Ther 2011; 2: 325-334.

R Core Team. A language and environment for statistical computing. R Foundation for Statistical Computing, Vienna, Austria2014. In: Team RC, editor, 2019.

Razmara P, Lari E, Mohaddes E, Zhang Y, Goss GG, Pyle GG. The effect of copper nanoparticles on olfaction in rainbow trout (*Oncorhynchus mykiss*). Environmental Science: Nano 2019; 6: 2094–2104.

Shaw BJ, Al-Bairuty G, Handy RD. Effects of waterborne copper nanoparticles and copper sulphate on rainbow trout,(*Oncorhynchus mykiss*): physiology and accumulation. Aquatic Toxicology 2012; 116: 90-101.

Sommers F, Mudrock E, Labenia J, Baldwin D. Effects of salinity on olfactory toxicity and behavioral responses of juvenile salmonids from copper. Aquatic Toxicology 2016; 175: 260-268.

Song Y-F, Luo Z, Zhang L-H, Hogstrand C, Pan Y-X. Endoplasmic reticulum stress and disturbed calcium homeostasis are involved in copper-induced alteration in hepatic lipid metabolism in yellow catfish *Pelteobagrus fulvidraco*. Chemosphere 2016; 144: 2443-2453.

Sovová T, Boyle D, Sloman KA, Pérez CV, Handy RD. Impaired behavioural response to alarm substance in rainbow trout exposed to copper nanoparticles. Aquatic Toxicology 2014; 152: 195-204.

Tierney KB. Chemical avoidance responses of fishes. Aquatic Toxicology 2016; 174: 228-241.

Tilton F, Tilton SC, Bammler TK, Beyer R, Farin F, Stapleton PL, et al. Transcriptional biomarkers and mechanisms of copper-induced olfactory injury in zebrafish. Environmental Science & Technology 2008; 42: 9404-9411.

Torrealba D, More-Bayona JA, Wakaruk J, Barreda DR. Innate Immunity Provides Biomarkers of Health for Teleosts Exposed to Nanoparticles. Frontiers in Immunology 2019; 9.

Van Genderen EL, Dishman DL, Arnold WR, Gorsuch JW, Call DJ. Sub-lethal effects of copper on salmonids: an avoidance evaluation using a direct test method. Bulletin of Environmental Contamination and Toxicology 2016; 97: 11-17.

Wang T, Chen X, Long X, Liu Z, Yan S. Copper nanoparticles and copper sulphate induced cytotoxicity in hepatocyte primary cultures of *Epinephelus coioides*. PloS One 2016; 11: e0149484.

Wang T, Long X, Liu Z, Cheng Y, Yan S. Effect of copper nanoparticles and copper sulphate on oxidation stress, cell apoptosis and immune responses in the intestines of juvenile *Epinephelus coioides*. Fish & Shellfish Immunology 2015; 44: 674-682.

Wang T, Wen X, Hu Y, Zhang X, Wang D, Yin S. Copper nanoparticles induced oxidation stress, cell apoptosis and immune response in the liver of juvenile *Takifugu fasciatus*. Fish & Shellfish Immunology 2019; 84: 648-655.

Windward Environmental. Biotic Ligand Model Windows Interface, Research Ver 3.41.2.45: User's Guide and Reference Manual, Seattle, WA, USA, 2019.

Woźniak-Budych MJ, Langer K, Peplińska B, Przysiecka Ł, Jarek M, Jarzębski M, et al. Copper-gold nanoparticles: Fabrication, characteristic and application as drug carriers. Materials Chemistry and Physics 2016; 179: 242-253.

Zhao J, Wang Z, Liu X, Xie X, Zhang K, Xing B. Distribution of CuO nanoparticles in juvenile carp (*Cyprinus carpio*) and their potential toxicity. Journal of Hazardous Materials 2011; 197: 304-310.

CHAPTER 4: Mechanism of copper nanoparticle toxicity in rainbow trout olfactory mucosa

In the first chapter we demonstrated that equitoxic concentrations of CuNPs and Cu^{2+} induce different olfactory toxicity over time. In this research chapter we aimed to investigate the molecular mechanisms underlying the CuNP- and Cu^{2+}- induced olfactory toxicity. This chapter describes the overarching results RNA-sequencing analyses in the Cu-exposed olfactory mucosa. This chapter has a supplementary material which is presented in the appendix section (at the end of the dissertation). It also has three datasets (excel sheets) which are available in separate files:

Dataset S1. Enriched GO terms in the rainbow trout olfactory mucosa following the 96 h Cu^{2+} exposure. Sheet 1: List of enriched GO terms of downregulated gene transcripts ($p < 0.05$). Sheet 2: Highly enriched GO terms of downregulated gene transcripts, as indicated in Fig. 4.3C ($p < 0.01$). Sheet 3: List of enriched GO terms upregulated gene transcripts ($p < 0.05$). Sheet 4: Highly enriched GO terms of upregulated gene transcripts, as indicated in Fig.3C ($p < 0.01$).

Dataset S2. Enriched GO terms in the rainbow trout olfactory mucosa following the 96 h CuNPs exposure. Sheet 1: List of enriched GO terms of downregulated gene transcripts ($p < 0.05$). Sheet 2: Highly enriched GO terms of downregulated gene transcripts, as indicated in Fig.3B ($p < 0.01$). Sheet 3: List of enriched GO terms of upregulated gene transcripts ($p < 0.05$). Sheet 4: Highly enriched GO terms of upregulated gene transcripts, as indicated in Fig. 4.3B ($p < 0.01$).

Dataset S3. Gene set enrichment analysis (GSEA) in the rainbow trout olfactory mucosa that was treated with CuNPs and Cu^{2+}. Sheet 1: GSEA in CuNPs treatment. Sheet 2: GSEA in Cu^{2+} treatment.

The work presented here will form the basis of next 3 chapters. A version of this chapter has been submitted to *Environmental Pollution* (under review):

Razmara, P., Imbery, J., Koide, E., Helbing, C., Wiseman, S., Gauthier, P., Bray, D., Needham, M., Haight, T., Zovoilis, A., Pyle G. (2021), Mechanism of copper nanoparticle toxicity in rainbow trout olfactory mucosa, Environmental Pollution.

Contribution of authors: I designed and performed research, collected and analysed data, and wrote the manuscript. Jacob Imbery and Emily Koide provided scientific input and analysed a part of RNA-seq data. Dr. Helbing provided scientific input and guidance in experimental design and research performance. Dr. Wiseman provided scientific input, guidance, and access to his laboratory. Dr. Gauthier analysed a part of RNA-seq data and provided scientific input. Douglas Bray and Dr. Needham provided training and assistance with transmission electron microscopy. Travis Haight provided training to analyse a part of RNA-seq data. Dr. Zovoilis provided access to his supercomputer. Dr. Pyle provided guidance, scientific input, supervision, and funding for this research. All authors edited and approved the final manuscript.

4.1 Abstract

Chemosensory perception is crucial for fish reproduction and survival. Direct contact of olfactory neuroepithelium to the surrounding environment makes it vulnerable to contaminants in aquatic ecosystems. Copper nanoparticles (CuNPs), which are increasingly used in commercial and domestic applications due their exceptional properties, can impair fish olfactory function. However, the molecular events underlying olfactory toxicity of CuNPs are largely unexplored. Here, we demonstrate that CuNPs were bioavailable to olfactory mucosal cells and bioaccumulated in intracellular organelles. Using RNA-seq, we compared the effect of CuNPs and copper ions (Cu^{2+}) on gene transcript profiles of rainbow trout (*Oncorhynchus mykiss*) olfactory mucosa. The narrow overlap in differential gene expression between the CuNP- and Cu^{2+}-exposed fish revealed that these two contaminants exert their effects through distinct mechanisms. We propose a transcript-based conceptual model that shows that olfactory signal transduction, calcium homeostasis, and synaptic vesicular signaling were affected by CuNPs in the olfactory sensory neurons (OSNs). Neuroregenerative pathways were also impaired by CuNPs. In contrast, Cu^{2+} did not induce toxicity pathways and rather upregulated regeneration pathways. Both Cu treatments reduced immune system pathway transcripts. However, suppression of transcripts that were associated with inflammatory signaling was only observed with CuNPs. Neither oxidative stress or apoptosis were triggered by Cu^{2+} or CuNPs in mucosal cells. Dysregulation of transcripts that regulate function, maintenance, and reestablishment of damaged olfactory mucosa represents critical mechanisms of toxicity of CuNPs. The loss of olfaction by CuNPs may impact survival of rainbow trout and impose an ecological risk to fish populations in contaminated environments.

4.2. Introduction

Having efficient sensory and cognitive systems that can detect and translate peripheral signals into intelligible codes for fish is essential for their survival. Fish obtain important environmental information from their sensory systems that drive a broad range of survival-related activities including foraging, evaluating the risk of predation, homing, mating, and avoiding contaminants (Hamdani and Døving, 2007; Kermen et al., 2013). Odorant perception is a multistep process that begins with odorants interacting with neural circuits in the olfactory rosette of the nasal cavity. Once an odorant molecule is bound to an olfactory receptor (OR) on an olfactory sensory neuron (OSN), an olfactory signal transduction pathway (OST) transduces the chemical signal into an electrical receptor potential, which results in the generation of an action potential. The generated action potential is transmitted first to the olfactory bulb (OB) before being propagated to other processing centres in the central nervous system (CNS). The signal is ultimately processed and translated to a specific behavioural output (Laberge and Hara, 2001). Because OSNs are in direct contact with the external environment, they are vulnerable to potentially damaging environmental contaminants and pathogens. Exposure to these environmental hazards can impair any or all steps in the process of olfactory signal perception—from odorant reception to olfactory-driven behaviours—which can threaten fish survival (Tierney et al., 2010).

Copper, specifically copper ions (Cu^{2+}) and copper nanoparticles (CuNPs), are two anthropogenic neurotoxicants which are both capable of impairing fish olfaction (Green et al., 2010; Ma et al., 2018; Razmara et al., 2019; Sovová et al., 2014). Storm water runoff (mostly from motor vehicle brakes, engine, and tires) (Hwang et al., 2016), industrial and

mining effluents (Abraham and Susan, 2017; Balci and Demirel, 2018; Bilal et al., 2013), and agriculture runoff (Bereswill et al., 2012) are major sources of Cu^{2+} to waterbodies. The unique antimicrobial properties of engineered CuNPs makes them useful in many domestic and commercial applications including biomedical (Sun et al., 2019), wastewater treatment (Luan et al., 2019), food and agriculture (He et al., 2019), and textiles (Sharma et al., 2019; Turakhia et al., 2020). Owing to the widespread production and utilization of CuNPs, their incidental release to aquatic environments is expected. Given that CuNPs may dissolve and release copper ions (e.g., Cu^{2+}), CuNP-induced olfactory toxicity is a function of both dissolved copper and nanoparticulate Cu. Yet the olfactory impairment induced by CuNPs is different than Cu^{2+}-induced olfactory toxicity (Razmara et al., 2019; Sovová et al., 2014).

We previously reported that the rainbow trout (*Oncorhynchus mykiss*) olfactory system exhibits distinct neurophysiological and behavioral responses to equitoxic concentrations of CuNPs and Cu^{2+}. A 24 h exposure to the 50% olfactory inhibitory concentration (24 h IC50) of Cu^{2+} resulted in olfactory inhibition in rainbow trout; however, as the exposure period was extended to 96 h, partial recovery was observed. On the other hand, exposure to the 24 h IC50 of CuNPs led to a steady reduction in olfactory function over time (Razmara et al., 2019). A study that focused on gene expression in the zebrafish olfactory system demonstrated that the OST pathway was downregulated in fish exposed to Cu^{2+} for 24 h (Tilton et al., 2008). Moreover, miRNAs that post-transcriptionally regulate the expression of OST-related transcripts were significantly affected after a 24 h Cu^{2+} exposure of zebrafish (Wang et al., 2013). These results suggest that the disruption of receptor-potential generation through the OST pathway is the

underlying mechanism for Cu^{2+}-induced olfactory dysfunction. Nonetheless, the induced olfactory toxicity by the 24 h IC50 of Cu^{2+} in rainbow trout was sufficiently minor that OSNs could restore their functionality over the 96 h Cu^{2+} exposure. The continuous decline of olfactory function, that we observed over 96 h of CuNP exposure revealed a more severe effect of CuNPs on the fish olfaction relative to the effect induced by an equitoxic exposure to Cu^{2+} (Razmara et al., 2019). Despite the importance of the olfactory system in fish survival, molecular mechanisms underlying CuNP-induced olfactory toxicity remain elusive.

The toxicity of Cu contaminants on the olfactory system are not restricted to their adverse effects on OSN functionality. Olfactory stem cells residing in the olfactory mucosa have an innate regenerative capability to replace damaged or dead OSNs, and consequently maintain olfactory function. Nonetheless, neurotoxicant-induced adverse outcomes, such as chronic inflammation and injuries in the lamina propria, may alter the competency of stem cell neuroregeneration (Bergman et al., 2002; Chen et al., 2019). Our current knowledge of possible effects of Cu contaminants on olfactory neuron replacement is scarce, and its underlying molecular mechanism is largely unknown.

To investigate the molecular mechanisms underlying CuNP-induced olfactory toxicity, we compared the transcriptomic profiles of rainbow trout olfactory mucosa following a 96 h exposure to IC50 concentrations of CuNPs and Cu^{2+} (320 and 7 μg/L,

respectively). Our findings suggest that exposure to CuNPs have not only disrupted odorant perception, but also impaired the maintenance and reestablishment of olfactory mucosa.

4.3. Materials and Methods

4.3.1. Test animals and experimental design

Juvenile diploid rainbow trout (n = 129, total length 14.8 ± 1.8 cm; weight, 27.4 ± 4.2 g (mean ± SD)) were obtained from Sam Livingston Fish Hatchery (Alberta, Canada) and transferred to the Aquatic Research Facility (ARF) of the University of Lethbridge. In our previous study, the 24 h CuNP- or Cu^{2+}-induced olfactory-impairment thresholds were established using electro-olfactography (EOG). The EOG recordings were conducted in response to 10^{-5} mol/L taurocholic acid (TCA). According to the results of EOG, the 50% inhibitory concentration of CuNPs and Cu^{2+} (EOG-based 24 h-IC50) were calculated and used as a functional unit of toxicity. The 24 h IC50s of CuNPs and Cu^{2+} were 320 ± 13 and 7 ± 1 μg/L (mean ± SD), respectively (Razmara et al., 2019). In the current study, to investigate the mechanism(s) of CuNPs and Cu^{2+} olfactory toxicity, fish were exposed to the 24 h IC50s of Cu contaminant for 24 h and/or 96 h. All the conducted experiments in this study were approved by the University of Lethbridge Animal Welfare committee (protocol #1612).

4.3.2. Copper analyses

To investigate whether fish olfactory mucosal cells were able to take up and accumulate CuNPs and Cu^{2+}, we initially analyzed the Cu concentration in the olfactory rosette following the 24 and 96 h exposure periods. The olfactory rosettes were dissected, dried, digested in HNO_3 (concentrated, TraceSelect grade; Sigma Aldrich, Canada) following the protocol described in supplementary material. The total Cu concentration

was analyzed by graphite furnace atomic absorption spectrometry (GFAAS) (240FS GFAAS, Agilent Technologies, USA).

4.3.3. Transmission electron microscopy

For transmission electron microscopy (TEM) analyses, following the 24 and 96 h exposure to CuNPs and Cu^{2+}, olfactory rosettes (n = 2 per treatment) were dissected and preserved in modified Karnovsky's solution (4% paraformaldehyde, 2.5% glutaraldehye, 0.1 sodium cacodylate buffer, pH 7.2) for 24 h. Following fixation, the rosette tissue pieces were rinsed in 0.1 M sodium cacodylate buffer (pH 7.2), post-fixed in 1% osmium tetroxide (OsO_4) for 1 h, dehydrated in ascending ethanol concentrations (70-100%), embedded in Epon resin, and polymerized at 60˚C for 24 h (Matisz et al., 2010). The resulting blocks were sectioned with LKB ultramicrotome at a thickness of 100 nm, mounted onto 200 mesh Cu grids, and stained with 4% uranyl acetate for 20 min followed by 5 min in Reynolds lead citrate. Digital micrographs were taken with a Hitachi H-7500 TEM operation at 100keV.

4.3.4. RNA isolation and Illumina sequencing

RNA-sequencing (RNA-seq) was used to determine transcript profiles in olfactory rosettes of trout exposed to CuNPs and Cu^{2+}. Following the 96 h exposure to CuNPs and Cu^{2+}, fish were euthanized to dissect their olfactory rosettes. Olfactory rosettes were flash-frozen in liquid nitrogen and stored in -80°C. Total RNA of olfactory rosettes was isolated using RNeasy Mini Kit (catalogue # 74106; Qiagen) according to the manufacturer's protocol. The RNA quality and quantity were verified by a Nanodrop spectrophotometer (Thermo Scientific NanoDrop One spectrophotometer, Thermo Scientific). The integrity of isolated RNA was analyzed using a Bioanalyzer 2100 (Agilent Technologies), and

samples with RNA integrity number (RIN) of > 7 were used for RNA-Seq analyses (5 biological replicates per treatment). RNA samples were shipped on dry ice to Canada's Michael Smith Genome Sciences Centre (Vancouver, British Columbia, Canada), where strand-specific mRNA libraries were constructed and sequenced using Illumina HiSeq 2500 (paired-end platform generating 2 x 75 base pair reads).

4.3.5. RNA-seq analyses

Read quality was assessed using FastQC (Andrews, 2020) to ensure high read quality in all samples. Reads were aligned to *O. mykiss* genome assembly, Omyk_1.0 (GCF_002163495.1) using STAR two-pass alignment (version 2.6.1) (Dobin et al., 2013). Mapped reads were assembled and counted using StringTie (version 1.3.4) with a minimum read coverage of 1 for most transcripts, and 4.75 for single-exon transcripts (Pertea et al., 2015). Transcript counts were exported as transcript count tables comparing individual transcript counts from the treated animals to transcript counts from the control animals. Transcripts were annotated using BLASTX against National Center for Biotechnology Information (NCBI) non-redundant (nr) protein database. Differential transcript abundance analysis was performed using DESeq2 (version 1.28.1) (Love et al., 2014) as described previously (Jackman et al., 2018) with a $p_{adj} \leq 0.05$ cut-off used to deem statistical significance. Non-metric multidimensional scaling (NMDS) was applied to ordinate similarities among treatments and their transcript profiles based. Subsequently, we carried out PERMANOVA analysis on the Euclidean distance matrix to determine the effect of Cu treatments on transcript profile of mucosal cells. A post hoc test was performed on the PERMANOVA to determine differences among treatments. To identify the function of the differentially expressed transcripts and to investigate the corresponding enriched

pathways with which these transcripts were involved, we performed gene annotation enrichment analysis. To perform functional annotation analysis, query sequences were imported to Blast2Go Pro (OmicsBox version 1.3.11) (Götz et al., 2008) and mapped to retrieve Gene Ontology (GO) terms to the blast hits. Statistical analysis to identify the enriched GO terms in the CuNPs and Cu^{2+} treatments were conducted using the Fisher's exact test in Blast2GO. Moreover, gene set enrichment analysis was conducted on the differentially expressed sequences of both Cu treatments (500 permutations, $p < 0.05$). Additional details about this section are given in supplementary material.

4.3.6. Quantitative real-time PCR (qPCR) analyses

In order to validate the results of RNA-seq analyses (at the 96 h exposure) and to compare the Cu-induced transcript abundance changes at 24 h and 96 h exposures, we used qPCR. Total RNA of olfactory rosettes (n = 5 per treatment) was isolated using the same protocol used in RNA-seq analyses. Following verification of RNA purity and quantity by Nanodrop, 1 µg of the total RNA was used to synthesize cDNA (QuantiTec Reverse Transcription Kit, catalogue # 205311, Qiagen). To quantify target gene transcripts, PCR reaction mixtures, containing RT² SYBR Green qPCR master mix (catalogue # 330503, Qiagen), primers (0.25 µM), cDNA, and UltraPure water, were amplified and quantified using a Bio-Rad thermocycler (C1000 Touch thermocycler, CFX96 Real-Time System, Bio-Rad). Target gene transcripts were normalized to the geometric means of reference gene transcripts, *ACTB* (Aegerter et al., 2005) and *EF1a* (Polakof et al., 2010), which were not differentially expressed in response to Cu^{2+} or CuNP, according to RNA-seq results. Quantification of the target transcripts relative to that of the reference genes was analyzed

according the Pfaffl method (Pfaffl, 2001). Additional details about qPCR analyses are given in supplementary material.

4.3.7. Lipid peroxidation assay

Following the 24 h and 96 h exposure to Cu contaminants, lipid peroxidation (LPO), a biomarker of oxidative stress, was analyzed in the fish olfactory rosettes (n = 4 per treatment). The LPO was measured by quantifying the malondialdehyde (MDA) content, using thiobarbituric acid reactive substances (TBARS) Parameter assay kit (catalogue # KGE013; R&D Systems). The MD contents were normalized to concentration of proteins. The protein concentration was quantified using Bicinchoninic Acid Kit (catalogue # BCA1, Sigma-Aldrich) according to the protocol provided by manufacturer.

4.3.8. DNA laddering assay

DNA laddering, an index of apoptosis, was determined using olfactory rosettes at 24 and 96 h exposure. DNA was extracted from olfactory rosettes (n = 3 per treatments) using a QIAamp DNA Micro Kit (catalogue # 56304; Qiagen). To investigate any endonuclease cleavage products induced by apoptosis, the extracted DNA was separated on a 3% agarose gel electrophoresis and visualized using SYBR® Safe DNA Gel Stain (catalogue # S33102, Invitrogen) on a ChemiDoc imaging system (Bio-Rad).

4.4. Results and Discussion

4.4.1. Copper content was increased in the CuNP-exposed olfactory mucosal cells

Despite the fact that Cu is an essential element for all aerobic organisms through its involvement in a number of enzymatic processes, excessive intracellular Cu induces toxicity (Balamurugan and Schaffner, 2006). To investigate whether fish olfactory mucosal

cells were able to take up and accumulate CuNPs and Cu^{2+}, we initially analyzed the Cu concentration in the olfactory rosette following the 24 and 96 h exposure to IC50 concentrations. Total Cu increased in the CuNP-treated mucosal cells over both exposure periods ($p < 0.001$; Fig. 4.1A). In contrast, no Cu bioaccumulation was observed in the Cu^{2+}-exposed olfactory mucosa ($p = 0.98$; Fig. 4.1A). It is possible that Cu^{2+} was taken up by mucosal cells. However, the insignificant Cu accumulation in the Cu^{2+}-treated olfactory rosette can be attributed to the similar Cu uptake and elimination rate in the olfactory tissue, which needs further investigation.

A growing body of evidence suggests that metal NPs can be translocated from the olfactory epithelium to the brain through transcellular or paracellular pathways to induce neural dysfunction (Lin et al., 2020; Zhang et al., 2012). To explore if CuNPs can accumulate in fish brain, we measured Cu concentration in the brain following exposure to CuNPs. Despite a slight elevation of Cu content in the brain of CuNP-exposed fish, the effect was not significant ($F(2, 24) = 0.431$, $p = 0.66$; Fig. 4.1B). These results suggest that the olfactory mucosal cells were at a higher risk of CuNP toxicity relative to the brain (Fig. 4.1A and B).

Transmission electron microscopy demonstrated CuNPs were bioaccumulated in the mucosal cells. Endocytosed CuNPs were entrapped within endosomes and lysosomes of the mucosal cells (Fig. 4.1C and D). During intracellular trafficking of CuNPs, mature endosomes (i.e., late endosomes) fuse with lysosomes to digest their cargo (Lojk et al., 2015; Zhang et al., 2018). Further investigation is needed to determine if complete lysosomal degradation of CuNPs was accomplished. The bioaccumulation of CuNPs indicated that mucosal cells were internally exposed to CuNPs.

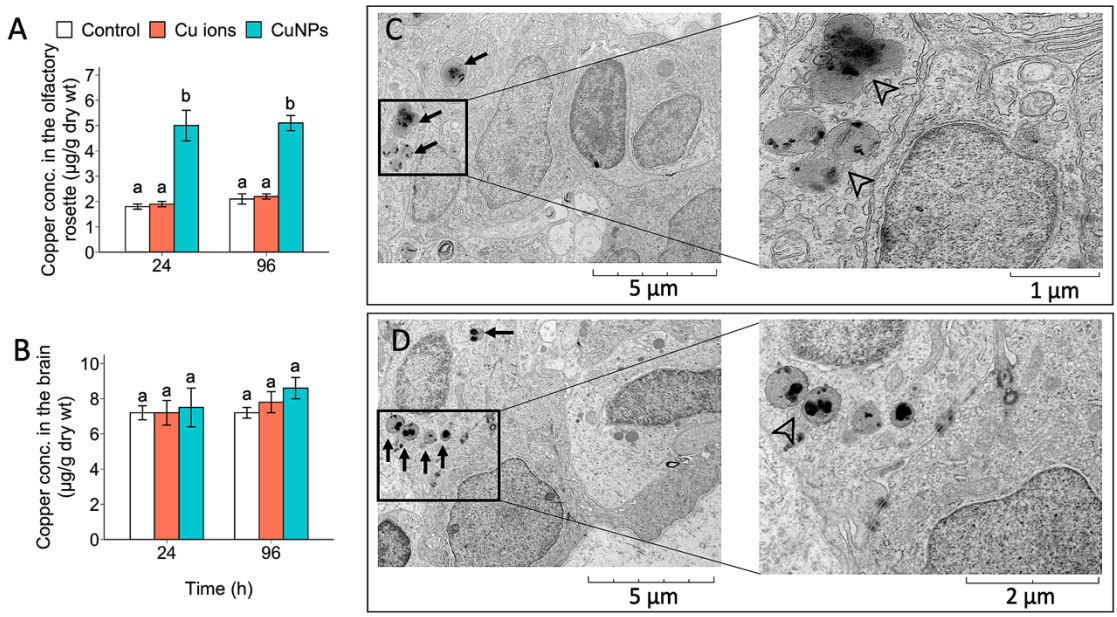

Figure 4.1. Copper bioaccumulation in the olfactory rosette and brain of rainbow trout following 24 or 96 h exposure to CuNPs or Cu ions. Measured concentrations of total Cu in the olfactory rosette (A) and brain (B) using graphite furnace atomic absorption spectrometry (conc., concentration). Different lower-case letters indicate significant differences ($p \leq 0.05$, error bars ± 1 SEM). Transmission electron micrographs of olfactory rosette following the 24 (C) and 96 h (D) exposure to CuNPs, demonstrating nanocopper bioaccumulation. Arrows indicate endosomes/lysosomes containing CuNPs. Arrow heads indicate endosome-lysosome fusion.

4.4.2. Olfactory mucosal cells exhibited differential transcriptomic responses to CuNPs and Cu^{2+} exposure

In the olfactory mucosa, 2.1% of the transcripts was differentially expressed in each of the CuNPs and Cu^{2+} treatment (SI appendix, Table S2). Results of the PERMANOVA analysis on the Euclidean distance matrix derived for non-metric multidimensional scaling (NMDS) revealed that exposure to CuNPs and Cu^{2+} resulted in differential transcript profiles of olfactory mucosa ($F(2, 19) = 8.48$, $p = 0.0009$; Fig. 4.2A). The transcript profiles of CuNP- and Cu^{2+}-exposed fish were significantly different from one another ($p = 0.027$) as well as the control ($p = 0.006$ and 0.003, respectively). Only a small proportion (approximately 14%) of differentially expressed transcripts were common between the two

copper treatments (Fig. 4.2B). Not surprisingly, the over-represented gene ontology (GO) terms in CuNPs and Cu^{2+} treatments displayed a small number of shared terms (i.e., approximately 20% of the total GO terms were shared between the two Cu treatments) (Fig. 4.2C and D, Dataset S3). Contaminant-induced adverse outcomes occurring at high levels of biological organization (e.g., organ and organism) are generally associated with transcript effects that occur at the cellular level (Ankley et al., 2010). The distinctive transcript profile of olfactory mucosa in the CuNPs and Cu^{2+} treatments help explain the differential responses reported at the tissue and organism levels in each Cu treatment in rainbow trout (Razmara et al., 2019; Sovová et al., 2014).

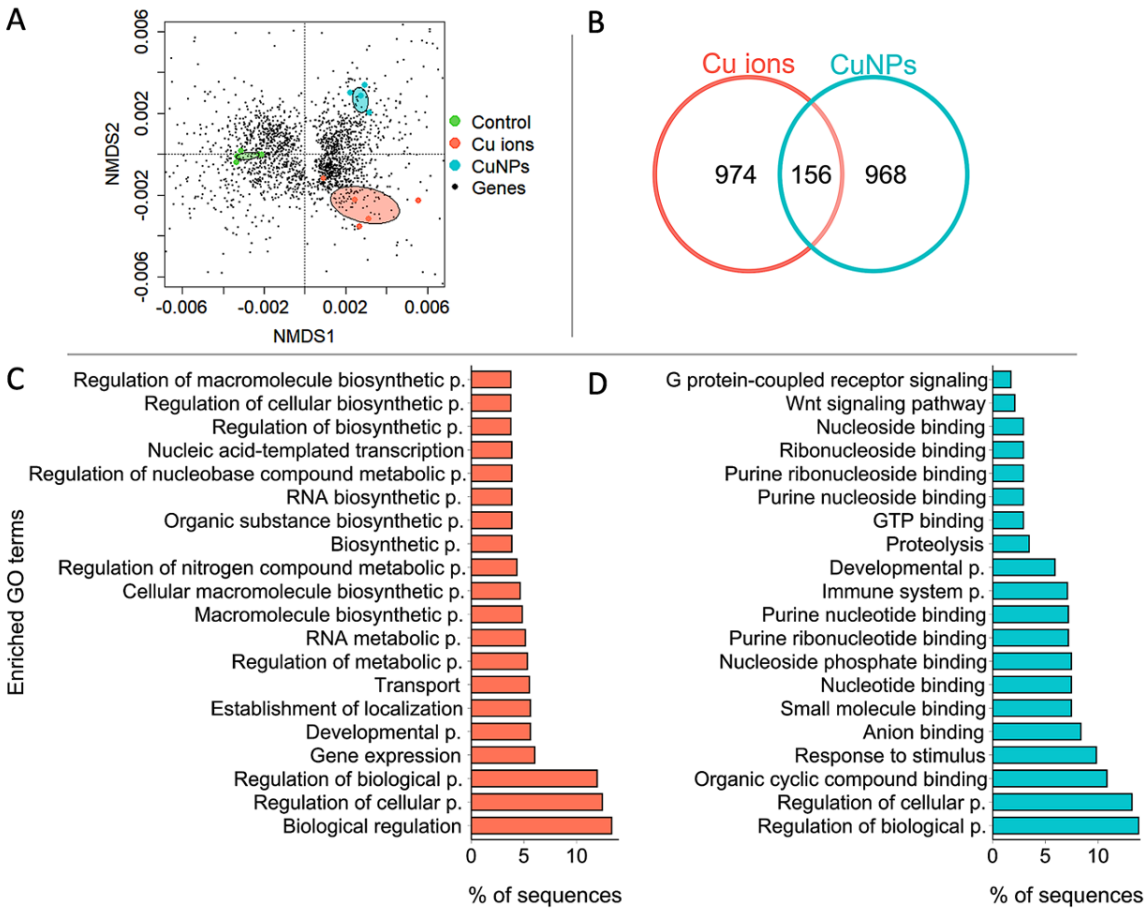

Figure 4.2. Impact of CuNPs and Cu^{2+} on the transcript profile of rainbow trout olfactory mucosa. (A) Non-metric multidimensional scaling of olfactory mucosal gene transcripts under different treatments. Ellipses represent standard deviations of ordination scores for each treatment group. (B) Venn diagram of olfactory mucosal differentially expressed transcripts demonstrating the number of specific and shared transcripts between the CuNPs and Cu^{2+} treatment. (C and D) Enrichment analysis of GO terms following the 96 h exposure to Cu^{2+} (C) and CuNPs (D) ($p < 0.05$). Bar graphs demonstrate top 20 GO terms enriched in each Cu treatment (p., process).

4.4.3. The CuNP-induced transcript profile in OSNs reflect mechanisms of dysfunction

Pathway enrichment analysis in the CuNP treatment demonstrated that many of the transcripts were involved in enriched GO terms associated with olfactory function, including G protein-coupled receptor signaling, transmembrane signaling receptor activity,

and response to stimulus (Fig. 4.2C, Dataset S3). To better understand the mechanism of CuNPs olfactory toxicity, we also determined the enriched pathways that comprise downregulated or upregulated transcripts. Experimental samples in different treatments were clustered based on their mRNA abundances (Fig. 4.3A). Downregulation of transcripts that associated with olfactory-related enriched GO terms, including sensory perception of smell, G protein-coupled receptor activity, signaling receptor binding, nervous system process, and synapse, was a further indication of olfactory dysfunction in the CuNP treatment (Fig. 4.3B and Dataset S2).

We previously observed a continuous decline in both olfactory-driven neurophysiological and behavioural responses after we increased the duration of exposure to CuNPs from 24 to 96 h (Razmara et al., 2019).These observations suggest that odorant reception and possibly olfactory signal transmission to the brain was disrupted. Adopting the CuNP-affected functionally annotated transcript set, we extracted transcripts that play a role in odorant reception and signal transmission in OSNs. According to the transcript pattern of CuNP-affected genes in OSNs, we proposed a conceptual model that displays the underlying transcript alterations leading to OSN dysfunction. The model shows that all key processes of OSN function including receptor potential generation (i.e., OST cascade), action potential generation, and synaptic transmission were affected following the 96 h exposure to CuNPs (Fig. 4.4).

In the OST cascade, the association of G protein-coupled receptors (i.e., ORs) with odorant ligands leads to the dissociation of the G protein (G_{olf}) alpha subunit from the Gβγ subunit complex in the G protein. The dissociated G_{olf} subsequently activates adenylate cyclase (AC III) to generate cyclic AMP (cAMP). The cAMP, in turn, activates cyclic

nucleotide gated channel (CNG), resulting in the influx of Ca^{2+} and Na^{+} into the cilium resulting in membrane depolarization (Pifferi et al., 2006). The increased intracellular $[Ca^{2+}]_i$ activates calcium-gated chloride channels (CaCC), which extrude Cl^{-} from the olfactory cilia thereby deepening the depolarization (Dibattista et al., 2017). The mRNA abundance of several ORs, including *OR10G4*, *OR2AT4*, *OR2M3*, *OR52A1, OR4C5*, and *OLFR472*, along with *GNB1* (encoding β subunit of the G protein) and *CNG1*, which all serve in depolarization of olfactory receptor potential, was reduced in the CuNP treatment (Fig. 4.4; SI appendix, Table S3). During the repolarization phase of the receptor potential, the elevated $[Ca^{2+}]_i$ is restored to a resting state. Calcium also complexes with calmodulin (Ca^{2+}-CAM) which eventually reduces the affinity of CNG to cAMP and causes sensory adaptation. Regulated $[Ca^{2+}]_i$ in cilia is essential for both depolarization and repolarization phases of the receptor potential generation. Our transcript results revealed that the main cytosolic calcium clearance strategies that are essential for OSN repolarization (Fluegge et al., 2012; Pyrski et al., 2007; Weeraratne et al., 2006) may be influenced by CuNPs. While calcium extrusion from cilia may reduce due to the low mRNA abundance of calcium transporters, including *NCX1*, *PMCA2*, *NCKX3*, intercellular calcium storage organelles in both lysosome and mitochondria may increase their calcium discharge through their upregulation of calcium extruders (*TPCN2* and *NCLX*, respectively) (Fig. 4.4; SI appendix, Table S3). In corroboration with our results, previous studies also demonstrated that exposure to NPs can disrupt neural $[Ca^{2+}]_i$ balance through targeting calcium channels and transporters and intracellular calcium stores (Lovisolo et al., 2018; Tang et al., 2008; Yin et al., 2019). Olfactory marker protein (OMP), a marker of mature OSNs (Lee et al., 2011), also operates in the OST cascade by regulating cAMP activity (Dibattista and Reisert,

2016) and facilitating NCX activity (Kwon et al., 2009). The mRNA abundance of *OMP* was also reduced in the CuNP treatment (Fig. 4.4; SI appendix, Table S3). The dysregulations of transcripts regulating calcium homeostasis along with the impairment of the OST cascade can explain the previously observed neurophysiological dysfunction in the CuNP-exposed fish.

Following the stimulation of the OST cascade by an odorant molecule in OSN cilia, the depolarized receptor potential activates voltage-gated calcium channels (VGCCs) to amplify the generated potential and facilitate signal propagation to the dendritic knob, cell body, and ultimately axon hillock, where the action potential is generated (Solís-Chagoyán et al., 2016; Solís-Chagoyán et al., 2019). The mRNA abundance for the β subunit of the VGCC (*CaCNB1*), which can accelerate the activation and inactivation of the VGCCs and the subsequent Ca^{2+} influx (Shiraiwa et al., 2007), was elevated in the CuNP treatment. The abundances of key transcripts involved in action potential generation including *SCN8A* (encoding voltage-gated sodium channel), *KCNB1* (encoding voltage-gated potassium channel), and *ATP1A1* (encoding sodium/potassium ATPase pump, subunit alpha 1) were also increased (Fig. 4.4; SI appendix, Table S3). Moreover, GO term enrichment analysis indicated the level of transcripts involved in ion transmembrane transporter activity were upregulated (Dataset S2). The influence of nano-copper oxide (CuO) on neural sodium and potassium currents was studied using whole cell patch-clamp (Liu et al., 2011; Xu et al., 2009). Exposure to nano-CuO not only inhibited the peak amplitude of the sodium current, but also impaired the potassium current in the delayed rectifier potassium channel. These data revealed that the generation of the action potential was strongly influenced by nano-CuO. The strengthened receptor potential propagation and action potential generation

through increasing the mRNA abundance of genes encoding related ion channels, may compensate for the weakened receptor potential and the possible inhibited action potential by CuNPs.

Despite the upregulation of transcripts associated with the production of action potentials in CuNP-exposed OSNs, the molecular process that mediates the action potential transmission to mitral cells was disrupted. In fact, mRNA abundances of transcripts required for synaptic vesicle cycling, which regulates neurotransmitter release from the OSN axon terminal, was dysregulated by CuNPs (Fig. 4.4). During synaptic vesicle cycling, synaptic vesicles (SVs) are continuously loaded with neurotransmitter. The filling of SVs with neurotransmitter is highly dependent on the SV's acidification; there will be no neurotransmitter loading when the SVs acidification is insufficient. The SVs acidification is regulated by proton pumps (vATPases) and vesicular neurotransmitter transporters (Gowrisankaran and Milosevic, 2020). Following the 96 h exposure to CuNPs, mRNA abundance of an accessory subunit of vATPase, *ATP6AP1*, was reduced (SI appendix, Table S3). Besides the role of ATP6AP1 in vATPase-mediated acidification, it also participates in vATPase trafficking and exocytosis (Jansen et al., 2012). Vesicular neurotransmitter transporters extrude protons from the SV's lumen while importing neurotransmitters (e.g., ATP) to the lumen (Gowrisankaran and Milosevic, 2020). The mRNA abundance of *SLC17A9*, a vesicular ATP transporter, was upregulated in response to the CuNPs exposure (SI appendix, Table S3).

Together, these data indicated SV lumens may receive fewer protons through vATPases while losing more protons through the upregulation of the vesicular ATP transporter. Therefore, the SV's acidification and the neurotransmitter reloading may be

disrupted in the CuNP-exposed OSNs. Furthermore, mRNA abundance of *DOC2B*, encoding a cytosolic protein involved in the calcium-dependent SV exocytosis (Houy et al., 2017; Yu et al., 2013), was dramatically reduced in response to the CuNPs (Fig. 4.4; SI appendix, Table S3). The downregulation of *DOC2B* may reduce the fusion SVs to the axon membrane and reduce subsequent synaptic transmission of the OSNs. Transcript level of *DNM1*, on the other hand, was elevated in the CuNP-exposed cells (SI appendix, Table S3). The DNM1 is one of the primary components of the endocytosis machinery during synaptic vesicle cycling (Koopmans et al., 2018). This upregulation of *DNM1* could be a compensatory response to the reduced neurotransmitter release, by which OSNs attempt to accelerate the SV cycling process in the axon terminal. Given the low odorant reception and reduced synaptic neurotransmission from the OSNs to the OB (Fig. 4.4), odorant perception by the brain and the consequent olfactory-driven behaviour were impaired in the CuNP-exposed fish (Razmara et al., 2019). We previously showed that rainbow trout can detect and avoid the 24 h 20% inhibitory concentration (24 h IC20) of CuNPs (Razmara et al., 2020). Nonetheless, when fish are unable to avoid CuNP-contaminated areas, their olfactory function can be disrupted.

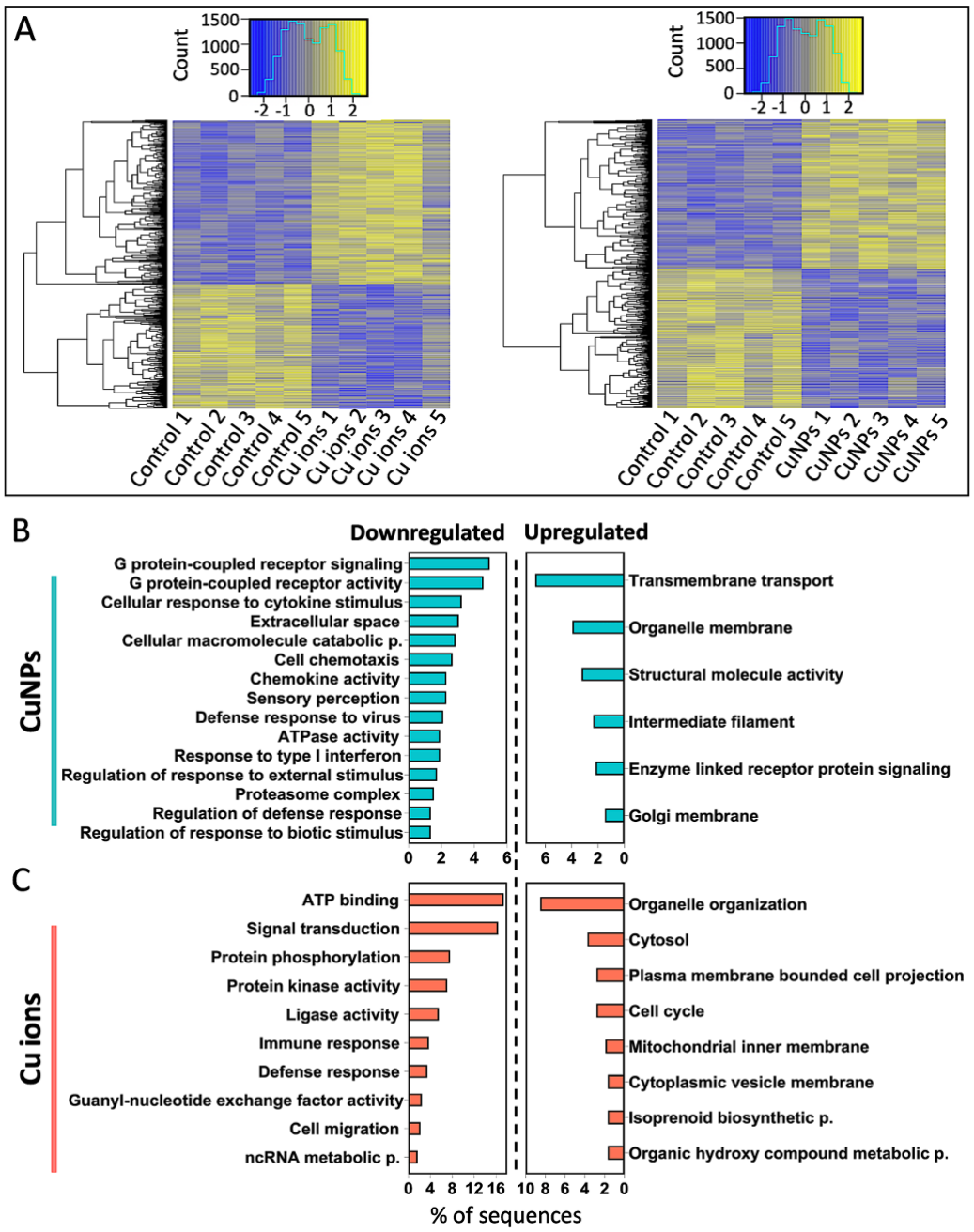

Figure 4.3. The gene transcript pattern in rainbow trout olfactory mucosa affected by CuNPs and Cu^{2+}. (A) Heat maps of differentially expressed transcripts under Cu^{2+} (left) and CuNPs (right) treatments relative to the control ($p < 0.05$). The rows represent individual transcripts and the columns represent biological replicates. Colour scale represents the relative abundance z-score of statistically significant differentially expressed transcripts, as depicted in the colour scale above each heat map. The distribution of transcripts by abundance from each treatment group is overlayed on the colour scale. (B and C) Enriched functional GO terms of transcripts that were significantly upregulated or downregulated in CuNPs (B) and Cu^{2+} (C) treatments (p., process). Bar graphs show the over-represented functional GO terms of all categories (i.e., biological processes,

molecular functions, and cellular components) which ordered by percentage of sequences related to each function (Fisher's exact test, $p < 0.01$).

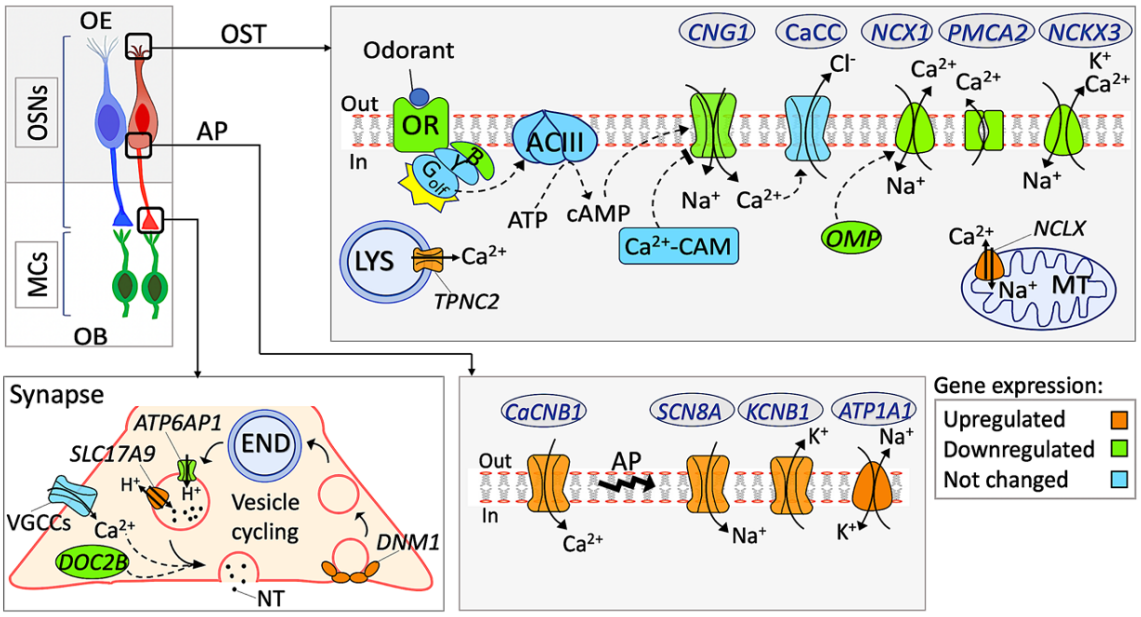

Figure 4.4. Proposed conceptual model displaying how exposure to CuNPs can impair OSN function at the transcript level in rainbow trout. The model shows molecular events that were affected by CuNPs in the cilia (OST pathway), axon hillock (AP generation), and axon terminal (synaptic vesicle cycling). The colour-coded legend represents the transcript abundance pattern of the differentially expressed transcripts. Most constituents of the OST pathway were downregulated by CuNPs, suggesting that the receptor potential may not be generated. In the OST pathway, the activated OR stimulates the dissociation of G_{olf} from the Gβγ subunit complex. The dissociated G_{olf} activates ACIII, which results in cAMP generation and CNG stimulation. When the CNG is open, Na^+ and Ca^{2+} enter the cytosol, which consequently depolarizes the OSN. The ensuing Ca^{2+} influx, stimulates CaCC to extrude Cl^- and cause further depolarization. Following that, the CNG is closed by Ca^{2+}-CAM, and Ca^{2+} is cleared from the cytosol to ultimately repolarize the OSN. Our model shows that intracellular Ca^{2+} clearance by membrane transporters or internal organelles was disrupted by CuNPs at the transcript level. However, the mRNA abundance of genes involved in receptor potential propagation and AP generation were increased. Following the membrane depolarization, a calcium channel will be stimulated to propagate the receptor potential to the axon hillock. In the axon hillock, the transmitted receptor potential activates Na^+ channel and initiates AP generation. Following that, K^+ is extruded from the cytosol, which returns the membrane potential to the resting potential. Ultimately, The Na^+/K^+ pump restores the ion gradients and prepares the membrane for the next AP. The AP propagates to axon terminal and stimulates a synapse between an OSN and a MC. The model suggests that the synaptic transmission was impaired by CuNP exposure. During synaptic vesicle cycling, fusion of vesicles containing NT with the terminal membrane is regulated by Ca^{2+} and presynaptic proteins (e.g., DOC2B). Following the vesicle fusion and release of NT into the synaptic cleft, with the help of specific proteins (e.g., DNM1),

the empty vesicle is endocytosed and recycled to be reloaded with NT. Acidic pH, which is essential for vesicles refilling, is regulated by ion transporters/exchangers in vesicle membrane (e.g., VATPase). Due to the downregulation of transcripts regulating acidity in the CuNP exposure, the vesicle lumen can be less acidic, and consequently, synaptic vesicles may not be reloaded properly.

4.4.4. Cu^{2+}-induced transcript alterations in OSNs were small

The GO enrichment analysis of transcripts that were significantly altered in response to Cu^{2+} treatment showed that signal transduction and response to stimulus, both of which may be related to olfactory function, were downregulated (Fig. 4.3B and Dataset S1). Nonetheless, the GO terms attributed to sensory perception were not represented in the 96 h Cu^{2+}-exposed fish. The aforementioned olfactory-related gene transcripts that were altered in the CuNP treatment remained unchanged in the Cu^{2+} treatment. We previously observed a significant functional improvement in the Cu^{2+}-exposed OSNs over the 96 h exposure (Razmara et al., 2019). Considering that Cu^{2+} did not significantly accumulate in the olfactory mucosa (Fig. 4.1A), restoring OSN functionality was more feasible in the Cu^{2+} treatment than the CuNP treatment.

4.4.5. Cu impacts on OSN transcripts hinge on exposure time

Figure 4.5 shows the mRNA abundance of a subset of genes involved in the OSNs function (e.g., ORs and ion channels described in the proposed model) over different exposure periods using qPCR (Fig. 4.5A-G). The mRNA abundance of all candidate genes was significantly affected by CuNPs (shown by RNA-seq analysis). Results of the qPCR analysis was consistent with results of RNA-Seq analyses (Fig. 4.5). Regardless of the exposure time, OST-related gene transcripts, including *OR10G4*, *OLF472*, and *OMP*, was suppressed by CuNPs (Fig. 4.5A-C). These findings can account for the continuous olfactory impairment that we previously observed in the CuNP-exposed fish (Razmara et al., 2019). Compared to the CuNP treatment, the OST-related candidate genes were less-

responsive to Cu^{2+}. The *OR10G4* was the only gene that showed a significant reduction of mRNA abundance over the 24 h exposure (Fig. 4.5 A). This effect may be sufficient to induce the 50% inhibition in the olfactory response to taurocholic acid (the odorant that was used to study the olfactory function) that we observed in the Cu^{2+} treatment (Razmara et al., 2019). It is also possible that Cu^{2+} exerts its effects on a different set of ORs that were not studied over the 24 h exposure period.

Distinct transcript impacts of Cu^{2+} on zebrafish and sea lamprey olfaction suggested that Cu^{2+}-induced olfactory toxicity can be species-specific (Jones et al., 2019; Tilton et al., 2008). A 24 h exposure of zebrafish to 6 µg/L of Cu^{2+} reduced the levels of transcripts involved in the OST cascade (Tilton et al., 2008). However, a 24 h exposure to 5 and 10 µg/L of Cu^{2+} had no effect on OST-related transcripts including ORs in sea lamprey (Jones et al., 2019). These differential effects of Cu^{2+} on the OST cascade in zebrafish and sea lamprey can be associated to the differences in the olfactory system of these two fishes. Compare to teleostean such as zebrafish, sea lamprey poses a rudimentary olfactory system with limited types of ORs (Jones et al., 2019). Phylogenetically close species probably display more similar transcript responses to Cu^{2+} exposure. From an evolutionary perspective, rainbow trout and zebrafish are more related to one another than to the sea lamprey, which is more primitive. Therefore, the abundance of OST-related transcripts in rainbow trout was possibly declined over the 24 h Cu^{2+} exposure and revived over the 96 h exposure.

In the 24-exposure period, *CaCNB1* was the only transcript, which its abundance was elevated in both Cu treatments (Fig. 4.5D). Over the 96 h exposure, the qPCR mRNA abundances of all candidate ion-related genes, including *SCN8A*, *ATP1A1*, *CaCNB1*, and

TPCN2, were increased in the CuNPs treatment, which confirms the results of RNA-Seq (Fig. 4.5D-G). These data suggest the 96 h CuNP exposure may alter ion homeostasis in the OSNs. Given that the function of OSNs is completely reliant on ion currents, the disruption of ion balance can impair olfactory function. Collectively, the duration of Cu exposure can dramatically change the effect of CuNPs and Cu^{2+} on the abundances of transcripts that are related to OSNs function. The abundances of transcripts in OSNs were progressively altered in response to CuNPs, while less transcripts were affected by Cu^{2+} over time (Fig. 4.5A-G).

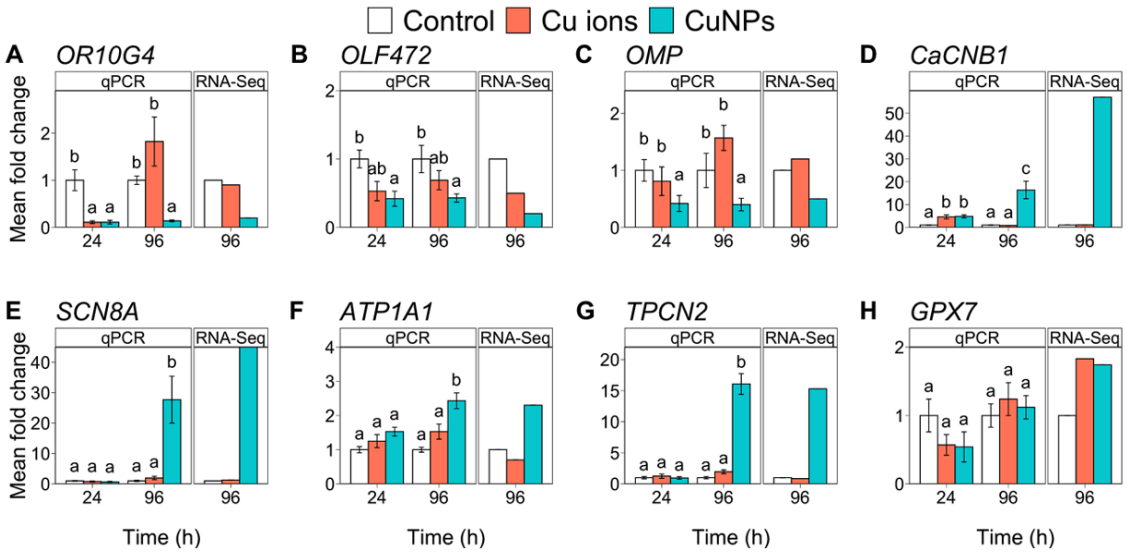

Figure 4.5. Gene transcript levels in response to CuNPs and Cu^{2+} exposure over different exposure periods (24 and 96 h) in the rainbow trout olfactory mucosa. qPCR data also validated the RNA-seq results over the 96 h exposure. (A) Olfactory receptor 10G4 (*OR10G4*). (B) Olfactory receptor 472 (*OLF472*). (C) Olfactory marker protein (*OMP*). (D) Voltage-dependent L-type calcium channel subunit beta1(*CaCNB1*). (E) Sodium channel protein type 8 subunit alpha (*SCN8A*). (F) Na^+/K^+ ATPase alpha-1 subunit (*ATP1A1*). (G) Two pore calcium channel protein 2 (*TPCN2*). (H) Glutathione peroxidase 7 (*GPX7*). Different lower-case letters indicate significant differences ($p \leq 0.05$, error bars ± 1 SEM).

4.4.6. Olfactory neuroregeneration showed unique transcript responses to CuNPs and Cu^{2+}

Olfactory mucosa is well-known for its unique lifelong neuroregenerative ability. Basal stem cells undergo proliferation and differentiation to replace dysfunctional OSNs with new ones (Klimenkov et al., 2020; Yu and Wu, 2017). Development-related GO terms were over-represented in both CuNPs and Cu^{2+} treatment (Fig. 4.2C and D). Nonetheless, CuNPs and Cu^{2+} had different effects on the neurogenesis-related pathways in the olfactory mucosa. In the Cu^{2+} treatment, GO enrichment analyses highlighted that the cell cycle and its regulators, developmental processes, and epithelium development were among the pathways that were upregulated (Fig. 4.3C and Dataset S1). Upregulation of gene transcripts involved in neuroregeneration and their associated miRNAs revealed that the neuroregeneration process was activated under Cu^{2+} treatment in zebrafish olfactory system (Tilton et al., 2008; Wang et al., 2011). A recent study demonstrated different OSN sub-populations had differential regeneration competency following a Cu^{2+} exposure (Ma et al., 2018). While a rapid regeneration of microvillous OSNs was evident following a 24 h exposure to Cu^{2+} in zebrafish larvae, ciliated OSNs were not regenerated. Interestingly, despite no regeneration in ciliated OSNs following the 24 h Cu^{2+} exposure in zebrafish larvae, their function recovered. These findings suggest that in response to Cu^{2+}-induced olfactory toxicity, OSNs may be reconstituted or repaired. In the CuNP treatment, neurogenesis was one of the enriched neuroregeneration-related GO terms that consisted of downregulated genes (Dataset S2). Gene transcripts involved in regulation of Wnt signaling pathway, another neuroregeneration-related functional term, were reduced in the CuNP-treated fish (Dataset S2). Wnt signaling pathway is a major pathway regulating stem

cell proliferation, differentiation, polarity, and migration (Wang et al., 2011; Yue et al., 2020). Our current knowledge of CuNP impacts on olfactory neuroregeneration is minimal. A previous study indicated that CuNPs can disrupt neurite growth in primary culture of rat dorsal root ganglion neurons (Prabhu et al., 2010).

Olfactory neurogenesis is modulated by immune cells and their derived signaling proteins, including pro-inflammatory cytokines and chemokines (Berger et al., 2020). The level of inflammation in the olfactory epithelium can shift the role of olfactory stem cells from neuroregeneration to immune defense. Chronic inflammation can halt stem cell neuroregeneration, whereas acute inflammation is essential to initiate olfactory stem cell proliferation and promote neuroregeneration (Chen et al., 2017; Chen et al., 2019). Inflammatory-related GO terms including inflammatory response, chemokine and cytokine activity, chemokine and cytokine receptor binding, and cytokine mediated signaling pathway were among the enriched functional terms that comprised downregulated transcripts in the CuNP treatment (Fig. 4.3B and dataset S2). Given that anti-inflammatory treatments can reduce stem cell proliferation and impair neuroregeneration in the olfactory mucosa (Chang and Glezer, 2018; Chen et al., 2017; Crisafulli et al., 2018), downregulation of inflammatory pathways in the CuNP-exposed olfactory mucosa may further indicate the interruption of neurogenesis

4.4.7. Copper exposure can lead to immunodeficiency in the olfactory mucosa

The olfactory mucosa is a potential site for pathogens to invade the CNS (Butowt and Bilinska, 2020). Fish olfactory mucosa, like the olfactory mucosa from many other vertebrates, is equipped with an efficient immune system that battles against nasal pathogenic invaders (Tacchi et al., 2014). Our findings indicated that exposure to both Cu

contaminants resulted in a massive suppression of the immune system in rainbow trout olfactory mucosa. The CuNP and Cu^{2+} exposures repressed transcripts encoding proteins required for immune system process, immune system response, defense response, innate immune response, response to virus, and antigen processing and representation (Fig. 4.3 B and C; Dataset S1 and 2). The Cu-induced dysfunction of immune system in the olfactory mucosa may facilitate the translocation of pathogens to the brain, which can consequently trigger neurodegeneration. Enrichment of the inflammatory response, response to interferons (gamma and type I), and the aforementioned cytokine and chemokine-related GO terms in the CuNP treatment, revealed that the innate immune system in the olfactory mucosa was more affected by CuNPs than Cu^{2+} (Fig. 4.3B and Dataset S2). Previous studies also reported that nanoparticles, including CuNPs, can induce immune suppression (Dwivedi et al., 2009; Lee et al., 2018).

4.4.8. Oxidative stress and apoptosis were not the primary mechanisms of Cu-induced olfactory toxicity

Exposure to excessive concentrations of Cu may induce intracellular oxidative stress. Copper-induced oxidants (e.g., reactive oxygen species (ROS)) may attack biomolecules such as lipids and consequently, induce lipid peroxidation (Yonar et al., 2016). Malondialdehyde (MDA) is a mutagenic aldehyde formed as a by-product of lipid peroxidation (Ayala et al., 2014). Despite a slight MDA elevation in the 96 h Cu^{2+}-exposed olfactory mucosa, MDA was not affected in Cu-exposed fish (Fig. 4.6A).

In the Cu^{2+} treatment, detoxification was among the top 20 GO terms (SI appendix, Fig. S1). Nonetheless, GO term enrichment analysis indicated that detoxification was not significantly enriched. Although there was no evidence of Cu^{2+}-induced oxidative stress,

mRNA abundances of a few antioxidant genes were significantly upregulated. Increased transcripts encoding antioxidant enzymes in the Cu^{2+} treatment was probably a defensive strategy to amend any Cu^{2+}-induced changes in the cell's redox status and prevent ROS-generated injuries. The transcription of a number of antioxidant proteins is regulated by the NRF1 transcription factor (Song et al., 2014). NRF1 can bind to antioxidant response elements (AREs) and enhance the expression of target genes including GCLC, GSH, and MT1, which are involved in the oxidative stress response pathway (Biswas and Chan, 2010). While the mRNA abundance of *NRF1* in Cu^{2+}-exposed cells was significantly increased, there was a slight but significant *NFR1* mRNA reduction in the CuNP treatment (SI appendix, Table S3).

Furthermore, the mRNA abundance of other oxidative stress response genes, including *CAT*, *GPX7*, *MSRA*, and *GSTA*, was increased following the Cu^{2+}-exposure (SI appendix, Table S3). Of these antioxidant enzymes, the transcript encoding GPX7 was elevated in the CuNP-exposed fish. Despite the slight elevation in the mRNA abundance of *GPX7* in both Cu treatments over the 96 h exposure, there were no significant differences among the treatments (Fig. 4.5H). This discrepancy between the qPCR and RNA-Seq analyses can be attributed to the methodological differences between the two technologies in quantifying transcript abundance (Everaert et al., 2017).

Complex I is a multi-subunit structure involved in the mitochondrial electron transport chain. Deficiency of complex I stimulates the generation of ROS in mitochondria, which ultimately triggers apoptosis (Ott et al., 2007; Perier et al., 2005). Exposure of neuroblastoma cells to high concentrations of Cu^{2+} (3.2-19.1 mg/L for 24 h) resulted in reduced complex I protein expression and increased mitochondrial ROS formation, which

consequently triggered cell death (Arciello et al., 2005). Nevertheless, mRNA abundance of two subunits of complex I, *NDUFS1* and *NDUFS8*, was elevated in the Cu^{2+}-treated olfactory mucosa (SI appendix, Table S3). Under high Cu^{2+} concentrations and the corresponding high oxidative stress rate in neuroblastoma, the extent of induced cellular damage is higher than cellular repair competency (Arciello et al., 2005). In our study, however, the results suggest olfactory mucosal cells were capable of compensating for Cu^{2+}-induced damage. Accordingly, mRNA abundances of complex I subunits and antioxidant enzymes were increased to offset any Cu^{2+} interference. Given that mRNA abundances of oxidative stress genes mostly remained unchanged in the CuNP treatment, there was no oxidative stress in the CuNP-exposed olfactory mucosa.

We observed no apoptosis-induced DNA fragmentation in the Cu-exposed olfactory mucosa (Fig. 4.6B). In this study, exposure to Cu^{2+} resulted in a downregulation of transcripts associated with apoptosis and apoptosis regulation, but no apoptosis-related GO term was over-represented in the CuNPs treatment (Dataset S1). The mRNA abundance of two caspases, *CASP6* and *CASP8*, was significantly reduced in the Cu^{2+} treatment (SI appendix, Table S3). CASP6 is a downstream effector of CASP8, and both caspases are involved in apoptosis (Cowling and Downward, 2002; Monnier et al., 2011). Inhibition of CASP8 activation can impede OSN apoptosis following acute axonal lesion (Carson et al., 2005). Furthermore, the inhibition of both CASP6 and CASP8 in the mammalian CNS promoted axonal regeneration (Monnier et al., 2011). Therefore, apoptosis was inhibited in the Cu^{2+}-exposed olfactory mucosal cells. In the CuNP-exposed olfactory mucosa, mRNA abundance of *BAX* was significantly reduced (SI appendix, Table S3). In the intrinsic apoptosis pathway, BAX acts as an apoptotic activator that promotes

the release of cytochrome C from the mitochondria (Robinson et al., 2003). The downregulation of *BAX* mRNA along with no DNA fragmentation revealed that the apoptotic pathway was not stimulated by CuNPs in the olfactory mucosa.

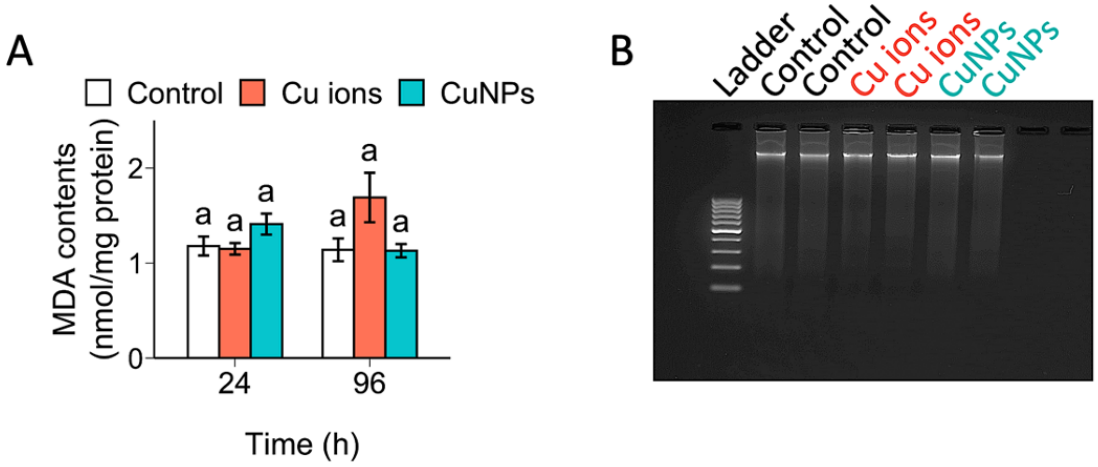

Figure 4.6. Effect of CuNPs and Cu^{2+} on oxidative stress and apoptosis in rainbow trout olfactory mucosa. (A) Level of malondialdehyde (MDA) in the olfactory mucosa measured as an indicator of lipid peroxidation in the Cu-treated olfactory mucosa over different exposure periods. Different lower-case letters indicate significant differences ($p \leq 0.05$, error bars ± 1 SEM). (B) DNA fragmentation analysis (DNA laddering) of olfactory mucosa following the 96 h exposure to Cu contaminants.

4.5. Conclusions

Our findings provide novel insight into the molecular mechanisms underlying the toxicity of CuNPs and Cu^{2+} to rainbow trout olfactory mucosa. By establishing a conceptual model, we illustrated that the CuNP-exposed OSNs were impaired in their ability to generate receptor potential and transmit the AP to the brain. Moreover, our results revealed that accumulated CuNPs in mucosal cells disrupted the neuroregenerative pathways in the olfactory mucosa. In contrast to the CuNP olfactory toxicity, the effect of Cu^{2+} on OSNs was comparatively small, and regenerative pathways were activated at the transcript level. The immune system transcripts were supressed in both Cu treatments; however, the inflammatory signaling pathways were only affected by CuNPs. Our findings

also demonstrated that oxidative stress and apoptosis did not significantly contribute to the olfactory toxicity of Cu. Collectively, our results suggest that the key pathways regulating olfactory function and maintenance were impaired by CuNPs. These CuNP-induced olfactory impairments may consequently pose a risk to fish survival. Elucidating the molecular mechanisms that are linked to adverse outcomes (i.e., olfactory-driven behavioral dysfunction) in the CuNP olfactory toxicity provides valuable information for ecological risk assessment of systems contaminated by CuNPs.

4.6. References

Abraham MR, Susan TB. Water contamination with heavy metals and trace elements from Kilembe copper mine and tailing sites in Western Uganda; implications for domestic water quality. Chemosphere 2017; 169: 281-287.

Aegerter S, Jalabert B, Bobe J. Large scale real-time PCR analysis of mRNA abundance in rainbow trout eggs in relationship with egg quality and post-ovulatory ageing. Molecular Reproduction and Development: Incorporating Gamete Research 2005; 72: 377-385.

Andrews S. FastQC: a quality control tool for high throughput sequence data. 2010, 2020.

Ankley GT, Bennett RS, Erickson RJ, Hoff DJ, Hornung MW, Johnson RD, et al. Adverse outcome pathways: a conceptual framework to support ecotoxicology research and risk assessment. Environmental Toxicology and Chemistry: An International Journal 2010; 29: 730-741.

Arciello M, Rotilio G, Rossi L. Copper-dependent toxicity in SH-SY5Y neuroblastoma cells involves mitochondrial damage. Biochemical and Biophysical Research Communications 2005; 327: 454-459.

Ayala A, Muñoz MF, Argüelles S. Lipid peroxidation: production, metabolism, and signaling mechanisms of malondialdehyde and 4-hydroxy-2-nonenal. Oxidative Medicine and Cellular Longevity 2014; 2014.

Balamurugan K, Schaffner W. Copper homeostasis in eukaryotes: teetering on a tightrope. Biochimica et Biophysica Acta (BBA)-Molecular Cell Research 2006; 1763: 737-746.

Balci N, Demirel C. Prediction of acid mine drainage (AMD) and metal release sources at the Küre Copper Mine Site, Kastamonu, NW Turkey. Mine Water and the Environment 2018; 37: 56-74.

Bereswill R, Golla B, Streloke M, Schulz R. Entry and toxicity of organic pesticides and copper in vineyard streams: erosion rills jeopardise the efficiency of riparian buffer strips. Agriculture, Ecosystems & Environment 2012; 146: 81-92.

Berger T, Lee H, Thuret S. Neurogenesis right under your nose. Nature Neuroscience 2020; 23: 297-298.

Bergman U, Östergren A, Gustafson A-L, Brittebo E. Differential effects of olfactory toxicants on olfactory regeneration. Archives of Toxicology 2002; 76: 104-112.

Bilal M, Shah JA, Ashfaq T, Gardazi SMH, Tahir AA, Pervez A, et al. Waste biomass adsorbents for copper removal from industrial wastewater—a review. Journal of Hazardous Materials 2013; 263: 322-333.

Biswas M, Chan JY. Role of Nrf1 in antioxidant response element-mediated gene expression and beyond. Toxicology and Applied Pharmacology 2010; 244: 16-20.

Butowt R, Bilinska K. SARS-CoV-2: olfaction, brain infection, and the urgent need for clinical samples allowing earlier virus detection. ACS Chemical Neuroscience 2020; 11: 1200-1203.

Carson C, Saleh M, Fung FW, Nicholson DW, Roskams AJ. Axonal dynactin p150Glued transports caspase-8 to drive retrograde olfactory receptor neuron apoptosis. Journal of Neuroscience 2005; 25: 6092-6104.

Chang SY, Glezer I. The balance between efficient anti-inflammatory treatment and neuronal regeneration in the olfactory epithelium. Neural Regeneration Research 2018; 13: 1711.

Chen M, Reed RR, Lane AP. Acute inflammation regulates neuroregeneration through the NF-κB pathway in olfactory epithelium. Proceedings of the National Academy of Sciences 2017; 114: 8089-8094.

Chen M, Reed RR, Lane AP. Chronic inflammation directs an olfactory stem cell functional switch from neuroregeneration to immune defense. Cell Stem Cell 2019; 25: 501-513. e5.

Cowling V, Downward J. Caspase-6 is the direct activator of caspase-8 in the cytochrome c-induced apoptosis pathway: absolute requirement for removal of caspase-6 prodomain. Cell Death & Differentiation 2002; 9: 1046-1056.

Crisafulli U, Xavier AM, dos Santos FB, Cambiaghi TD, Chang SY, Porcionatto M, et al. Topical dexamethasone administration impairs protein synthesis and neuronal regeneration in the olfactory epithelium. Frontiers in Molecular Neuroscience 2018; 11: 50.

Dibattista M, Pifferi S, Boccaccio A, Menini A, Reisert J. The long tale of the calcium activated Cl− channels in olfactory transduction. Channels 2017; 11: 399-414.

Dibattista M, Reisert J. The odorant receptor-dependent role of olfactory marker protein in olfactory receptor neurons. Journal of Neuroscience 2016; 36: 2995-3006.

Dobin A, Davis CA, Schlesinger F, Drenkow J, Zaleski C, Jha S, et al. STAR: ultrafast universal RNA-seq aligner. Bioinformatics 2013; 29: 15-21.

Dwivedi PD, Misra A, Shanker R, Das M. Are nanomaterials a threat to the immune system? Nanotoxicology 2009; 3: 19-26.

Everaert C, Luypaert M, Maag JL, Cheng QX, Dinger ME, Hellemans J, et al. Benchmarking of RNA-sequencing analysis workflows using whole-transcriptome RT-qPCR expression data. Scientific Reports 2017; 7: 1-11.

Fluegge D, Moeller LM, Cichy A, Gorin M, Weth A, Veitinger S, et al. Mitochondrial Ca 2+ mobilization is a key element in olfactory signaling. Nature Neuroscience 2012; 15: 754-762.

Götz S, García-Gómez JM, Terol J, Williams TD, Nagaraj SH, Nueda MJ, et al. High-throughput functional annotation and data mining with the Blast2GO suite. Nucleic Acids Research 2008; 36: 3420-3435.

Gowrisankaran S, Milosevic I. Regulation of synaptic vesicle acidification at the neuronal synapse. IUBMB Life 2020; 72: 568-576.

Green WW, Mirza RS, Wood CM, Pyle GG. Copper binding dynamics and olfactory impairment in fathead minnows (*Pimephales promelas*). Environmental Science & Technology 2010; 44: 1431-1437.

Hamdani EH, Døving KB. The functional organization of the fish olfactory system. Progress in Neurobiology 2007; 82: 80-86.

He X, Deng H, Hwang H-m. The current application of nanotechnology in food and agriculture. Journal of Food and Drug Analysis 2019; 27: 1-21.

Houy S, Groffen AJ, Ziomkiewicz I, Verhage M, Pinheiro PS, Sørensen JB. Doc2B acts as a calcium sensor for vesicle priming requiring synaptotagmin-1, Munc13-2 and SNAREs. Elife 2017; 6: e27000.

Hwang H-M, Fiala MJ, Park D, Wade TL. Review of pollutants in urban road dust and stormwater runoff: part 1. Heavy metals released from vehicles. International Journal of Urban Sciences 2016; 20: 334-360.

Jackman KW, Veldhoen N, Miliano RC, Robert BJ, Li L, Khojasteh A, et al. Transcriptomics investigation of thyroid hormone disruption in the olfactory system of the *Rana [Lithobates] catesbeiana* tadpole. Aquatic Toxicology 2018; 202: 46-56.

Jansen EJ, van Bakel NH, Loohuis NFO, Hafmans TG, Arentsen T, Coenen AJ, et al. Identification of domains within the V-ATPase accessory subunit Ac45 involved in V-ATPase transport and Ca2+-dependent exocytosis. Journal of Biological Chemistry 2012; 287: 27537-27546.

Jones J, Wellband K, Zielinski B, Heath DD. Transcriptional basis of copper-induced olfactory impairment in the sea lamprey, a primitive invasive fish. G3: Genes, Genomes, Genetics 2019; 9: 933-941.

Kermen F, Franco LM, Wyatt C, Yaksi E. Neural circuits mediating olfactory-driven behavior in fish. Frontiers in Neural Circuits 2013; 7: 62.

Klimenkov IV, Sudakov NP, Pastukhov MV, Kositsyn NS. the phenomenon of compensatory cell proliferation in olfactory epithelium in fish caused by prolonged exposure to natural odorants. Scientific Reports 2020; 10: 1-11.

Koopmans F, Pandya NJ, Franke SK, Phillippens IH, Paliukhovich I, Li KW, et al. Comparative hippocampal synaptic proteomes of rodents and primates: differences in neuroplasticity-related proteins. Frontiers in Molecular Neuroscience 2018; 11: 364.

Kwon HJ, Koo JH, Zufall F, Leinders-Zufall T, Margolis FL. Ca 2+ extrusion by NCX is compromised in olfactory sensory neurons of OMP−/− mice. PLoS One 2009; 4: e4260.

Laberge F, Hara TJ. Neurobiology of fish olfaction: a review. Brain Research Reviews 2001; 36: 46-59.

Lee AC, He J, Ma M. Olfactory marker protein is critical for functional maturation of olfactory sensory neurons and development of mother preference. Journal of Neuroscience 2011; 31: 2974-2982.

Lee I-C, Ko J-W, Park S-H, Shin N-R, Shin I-S, Moon C, et al. Copper nanoparticles induce early fibrotic changes in the liver via TGF-β/Smad signaling and cause immunosuppressive effects in rats. Nanotoxicology 2018; 12: 637-651.

Lin Y, Hu C, Chen A, Feng X, Liang H, Yin S, et al. Neurotoxicity of nanoparticles entering the brain via sensory nerve-to-brain pathways: injuries and mechanisms. Archives of Toxicology 2020: 1-17.

Liu Z, Liu S, Ren G, Zhang T, Yang Z. Nano-CuO inhibited voltage-gated sodium current of hippocampal CA1 neurons via reactive oxygen species but independent from G-proteins pathway. Journal of Applied Toxicology 2011; 31: 439-445.

Lojk J, Bregar VB, Rajh M, Miš K, Kreft ME, Pirkmajer S, et al. Cell type-specific response to high intracellular loading of polyacrylic acid-coated magnetic nanoparticles. International Journal of Nanomedicine 2015; 10: 1449.

Love MI, Huber W, Anders S. Moderated estimation of fold change and dispersion for RNA-seq data with DESeq2. Genome Biology 2014; 15: 550.

Lovisolo D, Dionisi M, Ruffinatti FA, Distasi C. Nanoparticles and potential neurotoxicity: focus on molecular mechanisms. AIMS Mol. Sci 2018; 5: 1-13.

Luan H, Teychene B, Huang H. Efficient removal of As (III) by Cu nanoparticles intercalated in carbon nanotube membranes for drinking water treatment. Chemical Engineering Journal 2019; 355: 341-350.

Ma EY, Heffern K, Cheresh J, Gallagher EP. Differential copper-induced death and regeneration of olfactory sensory neuron populations and neurobehavioral function in larval zebrafish. Neurotoxicology 2018; 69: 141-151.

Matisz CE, Goater CP, Bray D. Migration and site selection of Ornithodiplostomum ptychocheilus (Trematoda: Digenea) metacercariae in the brain of fathead minnows (Pimephales promelas). Parasitology 2010; 137: 719.

Monnier PP, D'Onofrio PM, Magharious M, Hollander AC, Tassew N, Szydlowska K, et al. Involvement of caspase-6 and caspase-8 in neuronal apoptosis and the regenerative failure of injured retinal ganglion cells. Journal of Neuroscience 2011; 31: 10494-10505.

Ott M, Gogvadze V, Orrenius S, Zhivotovsky B. Mitochondria, oxidative stress and cell death. Apoptosis 2007; 12: 913-922.

Perier C, Tieu K, Guégan C, Caspersen C, Jackson-Lewis V, Carelli V, et al. Complex I deficiency primes Bax-dependent neuronal apoptosis through mitochondrial oxidative damage. Proceedings of the National Academy of Sciences 2005; 102: 19126-19131.

Pertea M, Pertea GM, Antonescu CM, Chang T-C, Mendell JT, Salzberg SL. StringTie enables improved reconstruction of a transcriptome from RNA-seq reads. Nature Biotechnology 2015; 33: 290-295.

Pfaffl MW. A new mathematical model for relative quantification in real-time RT–PCR. Nucleic Acids Research 2001; 29: e45-e45.

Pifferi S, Boccaccio A, Menini A. Cyclic nucleotide-gated ion channels in sensory transduction. FEBS Letters 2006; 580: 2853-2859.

Polakof S, Médale F, Skiba-Cassy S, Corraze G, Panserat S. Molecular regulation of lipid metabolism in liver and muscle of rainbow trout subjected to acute and chronic insulin treatments. Domestic Animal Endocrinology 2010; 39: 26-33.

Prabhu BM, Ali SF, Murdock RC, Hussain SM, Srivatsan M. Copper nanoparticles exert size and concentration dependent toxicity on somatosensory neurons of rat. Nanotoxicology 2010; 4: 150-160.

Pyrski M, Koo JH, Polumuri SK, Ruknudin AM, Margolis JW, Schulze DH, et al. Sodium/calcium exchanger expression in the mouse and rat olfactory systems. Journal of Comparative Neurology 2007; 501: 944-958.

Razmara P, Lari E, Mohaddes E, Zhang Y, Goss GG, Pyle GG. The effect of copper nanoparticles on olfaction in rainbow trout (*Oncorhynchus mykiss*). Environmental Science: Nano 2019; 6: 2094-2104.

Razmara P, Sharpe J, Pyle GG. Rainbow trout (*Oncorhynchus mykiss*) chemosensory detection of and reactions to copper nanoparticles and copper ions. Environmental Pollution 2020: 113925.

Robinson AM, Conley DB, Kern RC. Olfactory neurons in bax knockout mice are protected from bulbectomy-induced apoptosis. Neuroreport 2003; 14: 1891-1894.

Sharma P, Pant S, Dave V, Tak K, Sadhu V, Reddy KR. Green synthesis and characterization of copper nanoparticles by Tinospora cardifolia to produce nature-friendly copper nano-coated fabric and their antimicrobial evaluation. Journal of Microbiological Methods 2019; 160: 107-116.

Shiraiwa T, Kashiwayanagi M, Iijima T, Murakami M. Involvement of the calcium channel β3 subunit in olfactory signal transduction. Biochemical and Biophysical Research Communications 2007; 355: 1019-1024.

Solís-Chagoyán H, Flores-Soto E, Reyes-García J, Valdés-Tovar M, Calixto E, Montaño LM, et al. Voltage-activated calcium channels as functional markers of mature neurons in human olfactory neuroepithelial cells: implications for the study of neurodevelopment in neuropsychiatric disorders. International Journal of Molecular Sciences 2016; 17: 941.

Solís-Chagoyán H, Flores-Soto E, Valdés-Tovar M, Cercós MG, Calixto E, Montaño LM, et al. Purinergic signaling pathway in human olfactory neuronal precursor cells. Stem Cells International 2019; 2019.

Song MO, Mattie MD, Lee C-H, Freedman JH. The role of Nrf1 and Nrf2 in the regulation of copper-responsive transcription. Experimental Cell Research 2014; 322: 39-50.

Sovová T, Boyle D, Sloman KA, Pérez CV, Handy RD. Impaired behavioural response to alarm substance in rainbow trout exposed to copper nanoparticles. Aquatic Toxicology 2014; 152: 195-204.

Sun L, Li A, Hu Y, Li Y, Shang L, Zhang L. Self-Assembled Fluorescent and Antibacterial GHK-Cu Nanoparticles for Wound Healing Applications. Particle & Particle Systems Characterization 2019; 36: 1800420.

Tacchi L, Musharrafieh R, Larragoite ET, Crossey K, Erhardt EB, Martin SA, et al. Nasal immunity is an ancient arm of the mucosal immune system of vertebrates. Nature Communications 2014; 5: 1-11.

Tang M, Wang M, Xing T, Zeng J, Wang H, Ruan D-Y. Mechanisms of unmodified CdSe quantum dot-induced elevation of cytoplasmic calcium levels in primary cultures of rat hippocampal neurons. Biomaterials 2008; 29: 4383-4391.

Tierney KB, Baldwin DH, Hara TJ, Ross PS, Scholz NL, Kennedy CJ. Olfactory toxicity in fishes. Aquatic Toxicology 2010; 96: 2-26.

Tilton F, Tilton SC, Bammler TK, Beyer R, Farin F, Stapleton PL, et al. Transcriptional biomarkers and mechanisms of copper-induced olfactory injury in zebrafish. Environmental science & technology 2008; 42: 9404-9411.

Turakhia B, Divakara MB, Santosh MS, Shah S. Green synthesis of copper oxide nanoparticles: a promising approach in the development of antibacterial textiles. Journal of Coatings Technology and Research 2020: 1-10.

Wang L, Bammler TK, Beyer RP, Gallagher EP. Copper-induced deregulation of microRNA expression in the zebrafish olfactory system. Environmental Science & Technology 2013; 47: 7466-7474.

Wang Y-Z, Yamagami T, Gan Q, Wang Y, Zhao T, Hamad S, et al. Canonical Wnt signaling promotes the proliferation and neurogenesis of peripheral olfactory stem cells during postnatal development and adult regeneration. Journal of Cell Science 2011; 124: 1553-1563.

Weeraratne SD, Valentine M, Cusick M, Delay R, Van Houten JL. Plasma membrane calcium pumps in mouse olfactory sensory neurons. Chemical Senses 2006; 31: 725-730.

Xu LJ, Zhao JX, Zhang T, Ren GG, Yang Z. In vitro study on influence of nano particles of CuO on CA1 pyramidal neurons of rat hippocampus potassium currents. Environmental Toxicology: An International Journal 2009; 24: 211-217.

Yin S, Liu J, Kang Y, Lin Y, Li D, Shao L. Interactions of nanomaterials with ion channels and related mechanisms. British Journal of Pharmacology 2019; 176: 3754-3774.

Yonar M, Ispir U, Yonar SM, Kirici M. Effect of copper sulphate on the antioxidant parameters in the rainbow trout fry, Oncorhynchus mykiss. Cellular and Molecular Biology 2016; 62: 55-58.

Yu CR, Wu Y. Regeneration and rewiring of rodent olfactory sensory neurons. Experimental Neurology 2017; 287: 395-408.

Yu H, Rathore SS, Davis EM, Ouyang Y, Shen J. Doc2b promotes GLUT4 exocytosis by activating the SNARE-mediated fusion reaction in a calcium-and membrane bending–dependent manner. Molecular Biology of the Cell 2013; 24: 1176-1184.

Yue Y, Xue Q, Yang J, Li X, Mi Z, Zhao G, et al. Wnt-activated olfactory ensheathing cells stimulate neural stem cell proliferation and neuronal differentiation. Brain Research 2020; 1735: 146726.

Zhang J, Zou Z, Wang B, Xu G, Wu Q, Zhang Y, et al. Lysosomal deposition of copper oxide nanoparticles triggers HUVEC cells death. Biomaterials 2018; 161: 228-239.

Zhang L, Bai R, Liu Y, Meng L, Li B, Wang L, et al. The dose-dependent toxicological effects and potential perturbation on the neurotransmitter secretion in brain following intranasal instillation of copper nanoparticles. Nanotoxicology 2012; 6: 562-575.

CHAPTER 5: Effect of copper nanoparticles on the architecture of rainbow trout olfactory mucosa

We previously reported that CuNPs can impair the function of fish olfactory mucosa. In this chapter, we compared the effect of CuNPs and Cu^{2+} on the structure of olfactory mucosa. We applied the transcript profiles of Cu-exposed olfactory mucosa to investigate how molecular composition of cell junctions was affected by CuNPs or Cu^{2+}. We also evaluated the effect of Cu contaminants on the transcripts and density of goblet cells.

As this chapter flows from the results reported in chapter 4, we are not able to submit this work before chapter 4's paper gets accepted. A version of this chapter is going to be submitted to *Chemosphere*.

Contribution of authors: I designed and performed research, analysed data, and wrote the manuscript. Dr. Pyle provided guidance, scientific input, supervision, funding, and comments on the manuscript.

5.1. Abstract

Olfactory epithelial cells are in direct contact with myriad environmental contaminants which may consequently disrupt their structure and function. Copper ions (Cu^{2+}) and copper nanoparticles (CuNPs) are two types of olfactory neurotoxicants. However, their effects on the structure of olfactory epithelium are largely uninvestigated. Here, using light microscopy, we measured changes in the density of olfactory goblet cells in CuNP- and Cu^{2+}-exposed rainbow trout over time. The density of goblet cells displayed an initial increase over the 24 h exposure and returned to the normal level over the 96 h exposure in both copper (Cu) treatments. These data suggested the 96-h exposure to Cu contaminants interfered with the protection barrier provided by goblet cells. The gene transcript profile of olfactory mucosa studied by RNA-seq indicated Cu^{2+} and CuNPs were differentially targeted the molecular composition of cell junctions. In the Cu^{2+} treatment, reduced mRNA abundance of tight junctions, adherens junction, desmosomes and hemidesmosomes, suggest that Cu^{2+}-exposed mucosal cells had weak junctional complexes. In the CuNP treatment, on the other hand, the transcript abundances of cell junction compositions, except adherens junction, were upregulated. Transcripts associated with gap junctional channels were increased in both Cu treatments. The elevated transcripts level of gap junctions in both Cu treatments suggested that the demand for intercellular communication was increased in the Cu-exposed olfactory mucosa. Overall, our findings suggested that Cu^{2+} induced greater adverse effects on the molecular composition of olfactory cell junctions relative to CuNPs. Impairment of junctional complexes may disrupt the structural integrity of olfactory mucosa.

5.2. Introduction

Fish reproduction and survival rely on a functional olfactory system that receives odorant signals and transmits them to the brain to be processed (Tierney et al., 2010). Olfactory epithelium (OE) is a polarized (i.e., asymmetrical) structure that is composed of different types of cells including olfactory sensory neurons (OSNs), sustentacular cells (a.k.a., supporting cells), goblet cells (a.k.a., mucosa cells), and basal stem cells (Steinke et al., 2008). The direct exposure of olfactory epithelial cells to anthropogenic contaminants can lead to structural and functional impairment. In response to contaminants, the density of olfactory epithelial cells may change. Goblet cells, the mucus-secreting cells residing in the apical domain of OE, provide the first line of defense against pathogens and contaminants (Bols et al., 2001). Previous studies reported that metal exposure increases the number of goblet cells and elevates mucus production in the OE (Kolmakov et al., 2009; Williams and Gallagher, 2013). However, it is unclear if increased mucus production can entirely protect the epithelium against the adverse effects of contaminants.

The organization, stabilization, and interaction of olfactory epithelial cells, is reliant on junctional complexes (Beaudoin III, 2016; Vasileva and Citi, 2018). Moreover, junctional complexes are responsible for establishing selective barriers that allow the epithelium to control the transport of ions and solutes (Steinke et al., 2008; Sarkar and De, 2014; Van Itallie and Anderson, 2014). In the lateral domain of OE, different types of cellular junctions, comprising tight junctions, zonula adherens, desmosomes, and gap junctions, facilitate cell-to-cell connections. In the basal domain, olfactory stem cells (specifically horizontal basal stem cells) are attached to the basal lamina through

hemidesmosomes — specialized cell adhesion complexes that are associated with extracellular matrix (Sarkar and De, 2014; Ferreira et al., 2015). Impairment of olfactory junctional barriers may not only disrupt the structure and function of OE, but also facilitate the direct passage of small toxicants to the brain. For instance, reducing the protein expression of occludin, which is a structural component of the tight junction, increased the permeability of OE and enhanced drug delivery from nose to brain (Krishan et al., 2014). Chitosan nanoparticles also interact with olfactory tight junctions and increase the paracellular permeability of OE for drug delivery (Casettari and Illum, 2014). Despite the importance of junctional complexes in maintaining the OE, impacts of contaminants on the olfactory intercellular junctions remain elusive. In other epithelia, contaminants such as metals, had significant adverse effects on junctional complexes (Ferruzza et al., 2002; Vinken et al., 2010).

Copper nanoparticles (CuNPs) are emerging environmental contaminants. The intentional or natural production of CuNPs has increased the risk of their entrance to the aquatic environment (Rajput et al., 2019). A recent study reported that atmospheric particulate matter (PM, 10 – 425 μm), collected from an area near a steel manufacturing facility, contained considerable amounts of metal nanoparticles including CuNPs (Souza et al., 2020). The formation of metal nanoparticles from the PM in water suggested that industrial PM can be a source of CuNP contamination in aquatic ecosystems (Souza et al., 2020). Nanocopper is used in herbicides, pesticides and fertilizers. Therefore, agricultural waste-waters are another source of CuNP contamination in aquatic ecosystems (Pradhan and Mailapalli, 2017). In addition to anthropogenic sources of CuNP contamination, deep concealed metal deposits have been reported as natural sources of CuNPs in the aquatic

environments (Hu and Cao, 2019). The entry of CuNPs to water bodies has raised concerns about their potential toxicity in aquatic organisms (Malhotra et al., 2020). Our previous studies indicated that CuNPs have many adverse effects on the rainbow trout olfactory mucosa. Exposure to CuNPs impaired the olfactory function, disrupted neural repair mechanisms, and suppressed immune responses at the transcript level (Razmara et al., 2019) (chapter 4). Considering that CuNPs release dissolved copper (Cu^{2+}) in the aqueous environment, we compared the toxicity of CuNPs and Cu^{2+} in the rainbow trout olfactory mucosa. Our results revealed that CuNPs and Cu^{2+} exert their toxicity through different mechanisms. These findings suggest that the toxicity of CuNPs was more attributed to particulate copper rather than released ions (Razmara et al., 2019) (Chapter 4).

In this study, we investigated the comparative effect of CuNPs and Cu^{2+} on the structure of rainbow trout olfactory mucosa. We investigated how the density of olfactory goblet cells was altered in response to copper (Cu) treatments over time. Using gene transcript profiles of olfactory mucosa, we also studied molecular alterations of junctional complexes in the CuNP- and Cu^{2+}-exposed fish.

5.3. Materials and methods

5.3.1. Preparation of Cu stock mixtures

A fresh stock mixture of CuNPs was prepared as described by Razmara et al. (2019). To make a stock suspension of 250 mg/L CuNPs, nanocopper powder (35 nm; 99.8% purity; partially passivated, Nanostructured & Amorphous Materials Inc, USA) were suspended in in ddH_2O (18.2 MΩ/cm water, Millipore, USA) using a 30 min water bath sonicator (UD 150SH6LQ; 150 W; Eumax; USA). To make a stock solution of Cu^{2+},

we used $CuSO_4.5H_2O$ (>98% purity; BHD, USA). A fresh stock solution of Cu^{2+} was prepared at the nominal concentration of 100 mg/L $CuSO_4$ in ddH_2O.

5.3.2. Fish housing and experimental design

Rainbow trout with an average weight of 27.3 ± 4.6 g (mean ± SD; n = 69) were obtained from Sam Livingston fish hatchery (Alberta, Canada) and transferred into a holding tank (16 h light: 8 h dark photoperiod) at the University of Lethbridge Aquatic Research Facility (ARF). Fish were acclimated to ARF water for two weeks. The culture water quality was measured as follows (mean ± SD; n = 3): temperature, 12.3 ± 0.2 °C; dissolved oxygen, 8.9 ± 0.5 mg/L; conductivity, 331.1 ± 0.1 µS/cm; hardness, 154 ± 5.1 mg/L as $CaCO_3$; alkalinity: 127.1 ± 3.0 mg/L as $CaCO_3$; median pH 8.1 (range 7.8 – 8.4), and dissolved organic carbon, 2.4 ± 0.8 mg/L.

In our previous study using electro-olfactography, we determined the 50% olfactory inhibitory concentrations of CuNPs and Cu^{2+} (24 h IC50) as the functional units of toxicity that induce equal impairments in the olfactory mucosa (Razmara et al., 2019). The 24 h IC50s of CuNPs and Cu^{2+} were 320 ± 13 and 7 ± 1 µg/L (mean ± SD), respectively. In the current study, to be able to compare the effects of CuNPs and Cu^{2+} on the structure of olfactory mucosa, fish were exposed to the 24 h IC50s of Cu contaminant for 24 h or 96 h. The total Cu solutions were changed every day by transferring fish to new sets of tanks containing fresh water and Cu solutions. During the exposure period fish were not fed.

5.3.3. Copper analysis and CuNPs characterization

We measured the total concentration of Cu in the fish tanks using graphite furnace atomic absorption spectrometry (240FS GFAAS, Agilent Technologies, USA). In the

CuNPs tanks, the Cu concentration at the beginning (1 h after CuNPs spikes) and end of the exposures (24 h after CuNPs spikes) were 265 ± 26 and 209 ± 11 μg/L, respectively. In the Cu^{2+} tanks, the actual Cu concentration was 7 ± 1 μg/L and remained unchanged during the 24-h. In the control tanks, the concentration of Cu was below the GFAAS detection limit. The QA/QC of Cu measurements were examined according to the protocol described in Razmara et al. (2019).

The physicochemical properties of CuNPs were previously characterized (Razmara et al., 2019), and the same source of characterized nanocopper was used in this study. In short, the CuNPs had an average diameter of 32 ± 1 nm (mean ± SEM). The indicators of CuNPs aggregation, including polydispersity index (PDI), hydrodynamic diameter (HDD), and zeta potential, indicated the CuNPs stability were reduced during the 24-h. There were significant elevations in the PDI and HDD after 16 h in the CuNPs tanks. Zeta potential was also reduced over after 16 h exposure. These measurements revealed that CuNPs were less bioavailable over the last few h of exposure (Razmara et al., 2019). To measure the dissolution of CuNPs, the particulate Cu was separated from the dissolved fraction using Amicon Ultra-4 centrifugal filter units (3K regenerated cellulose membrane, Merck Millipore Ltd., USA). The concentration of Cu in the dissolved fraction was measured using GFAAS over 24 h (Razmara et al., 2019). There was a time-dependent release of dissolved Cu during the 24-h exposure, and the highest dissolution was 14 μg/L at 24 h (Razmara et al., 2019).

5.3.4. Analysis of goblet cell density using light microscopy

To analyze the density of the olfactory goblet cells, following the 24-h and 96-h exposures, olfactory rosettes (n = 4 per treatment) were dissected and preserved in in

Bouin's solution (Sigma-Aldrich) for 12 h. The fixed rosettes were rinsed with 70% ethanol three times and dehydrated by ethanol series (70-100%). The dehydrated samples were clarified by xylene substitute, Hemo-De (Electron Microscopy Sciences), perfused with paraffin wax (Sigma-Aldrich), and embedded in paraffin blocks. The paraffin blocks were cut into 6 μm sections using a rotary microtome (Leica RM2235) and placed in a warm water bath (45 ˚C). The sections were then mounted and dried on one-end frosted glass slides (Sigma-Aldrich). The tissue sections were stained according to Alcian Blue/ Periodic Acid–Schiff (PAS) staining kit protocol which detects goblet cells mucosubstances (part # 91022A; Newcomer Supply). Images from the rosette sections were captured by an Axiocam camera (Zeiss, Germany) that was mounted on a compound light microscope (Axioskop 40, Zeiss, Germany). The density of goblet cells in the olfactory rosettes were analyzed using an image analysis and processing software (ImageJ, National Institutes of Health, Bethesda, Maryland, USA).

5.3.5. RNA extraction and RNA-seq analyses

Following the 96-h exposure to CuNPs and Cu^{2+}, fish (5 biological replicates per treatment) were euthanized, olfactory rosettes were dissected, flash-frozen in liquid nitrogen, and stored in -80°C (chapter 4). Total RNA was extracted using RNeasy Mini Kit (catalogue # 74106; Qiagen). Quality and quantity of RNA were assessed using a Nanodrop spectrophotometer (Thermo Scientific NanoDrop One spectrophotometer, Thermo Scientific). The RNA integrity number (RIN) was measured by a Bioanalyzer 2100 (Agilent Technologies). All samples had high RIN (>7) (chapter 4).

Strand-specific mRNA libraries were constructed in Canada's Michael Smith Genome Sciences Centre (GSC, BC cancer research, Canada). Libraries were sequenced

using HiSeq 2500 (Illuina, San Diego, California, USA) as paired-end platforms (2 * 75 base pair (bp) reads per sample) (chapter 4). RNA-seq analyses were carried out using a pipeline described in chapter 4. In short, the quality of reads were evaluated using FastQC (Andrews, 2020). Using STAR two-pass alignment version 2.6.1 (Dobin et al., 2013), the reads were aligned to rainbow trout reference transcriptome (Omyk_1.0, GCF_002163495.1). The aligned reads were assembled and counted using StringTie version 1.3.4 (Pertea et al., 2015). The query transcripts were annotated against National Center for Biotechnology Information (NCBI) non-redundant protein database by BLASTx. Differentially expressed genes were determined using DESeq2 version 1.28.1 ($p_{adj} \leq 0.05$ cut-off used for statistical significance). In the CuNPs and Cu^{2+} treatments, 1124 and 1130 genes were differentially expressed, respectively. Of the total number of the differentially expressed genes, 156 were shared between the two Cu treatments (chapter 4). The differentially expressed genes were imported to Blast2Go Pro (OmicsBox version 1.3.11) to conduct the functional annotation analysis (Götz et al., 2008). The enrichment of gene ontology (GO) terms was determined using Fisher's exact test in Blast2GO ($p < 0.05$).

5.3.6. Gene expression analysis by qPCR

The expression a gene encoding mucin protein (*MUC2L*) and transcription factor *SP3* which regulates the expression of *MUC2L* were studied in different Cu treatments over the 24-h and 96-h exposure periods using qPCR (n = 5 per treatment). The cDNA was synthesized from 1 µg of the total RNA using QuantiTec Reverse Transcription Kit (catalogue # 205311, Qiagen). The *MUC2L* and *SP3* primer sets were designed by NCBI Primer-Blast online software (Ye et al., 2012). The *ACTB* (Aegerter et al., 2005) and *EF1a*

(Polakof et al., 2010) were used as the reference genes. Table 5.1 shows the primers sequences used in qPCR gene expression analysis. The transcription of reference genes remained unchanged in the gene expression analysis. The results of melt curve analysis indicated the primers amplify a single product. The specificity of primers to amplify the target genes (i.e., *MUC2L* and *SP3*) was confirmed by sequencing the PCR products and blasting the sequences in NCBI. The gene expression was quantified using RT² SYBR Green qPCR master mix (catalogue # 330503, Qiagen) on a on a Bio-Rad thermocycler (C1000 Touch thermocycler, CFX96 Real-Time System, Bio-Rad). Quantification of *MUC2L* and *SP3* was relative to that of reference genes was analyzed according the Pfaffl method (Pfaffl, 2001).

Table 5.1. Primer characteristics for qPCR gene expression analysis

Gene name	Sequence of primer (5'- 3')	Efficiency
Mucin 2 like (*MUC2L*)	F: CCATTGAACCTCCGACCACA R: GGTTTGCTGCGTTGTACTCC	1.98
Transcription factor Sp3 (*SP3*)	F: TCAACTCCACACCGCAAATGT R: GCTGAGTGTCCTGATCTCCTGT	2.1
Elongation factor 1 alpha (*EF1a)*	F: TCCTCTTGGTCGTTTCGCTG R: ACCCGAGGGACATCCTGTG	1.99
Beta-actin (*ACTB*)	F: TCCTTCCTCGGTATGGAGTCTT R: ACAGCACCGTGTTGGCGTACAG	1.90

5.3.7. Statistical analyses

Statistical analyses were carried out in R, version 3.6 (R Core Team, 2019). The normality and homogeneity of variances of all data were tested using a Shapiro-Wilks and

a Bartlett test, respectively. To ascertain the effect of Cu treatments and exposure time on the density of goblet cells in the olfactory mucosa, a two-way analysis of variance (ANOVA) with a Tukey's post hoc test were used. To determine the differences in the expression of target genes under different Cu treatments and exposure periods, the two-way ANOVA was performed followed by a Tukey's post hoc test. All graphs were plotted in R using the ggplot2 package (Wickham, 2016).

5.4. Results and discussion

5.4.1. Effect of Cu treatments on olfactory epithelial goblet cells

In the olfactory mucosa, mucus-secreting goblet cells provide protection against pathogens and contaminants. Our results indicated that density of goblet cells was altered in response to the duration of Cu exposures ($F(2, 18) = 5.099$; $p = 0.02$). The density of goblet cells was significantly increased upon exposure to both forms of Cu over the 24 h exposure ($p = 0.02$ and 0.002 in Cu^{2+} and CuNPs, respectively, Fig. 5.1A and B). As a defensive strategy, the number of goblet cells increased to elevate mucus production and provide more protection against the adverse effect of Cu on epithelial cells. A previous study reported that short exposure (10 min) to different concentrations of Cu^{2+} (3-380 µg/L Cu^{2+}) in goldfish increased mucus secretion in the OE. At high Cu^{2+} concentrations (> 63 µg/L Cu^{2+}) the olfactory chambers were filled with mucus, and goldfish did not survive (Kolmakov et al., 2009).

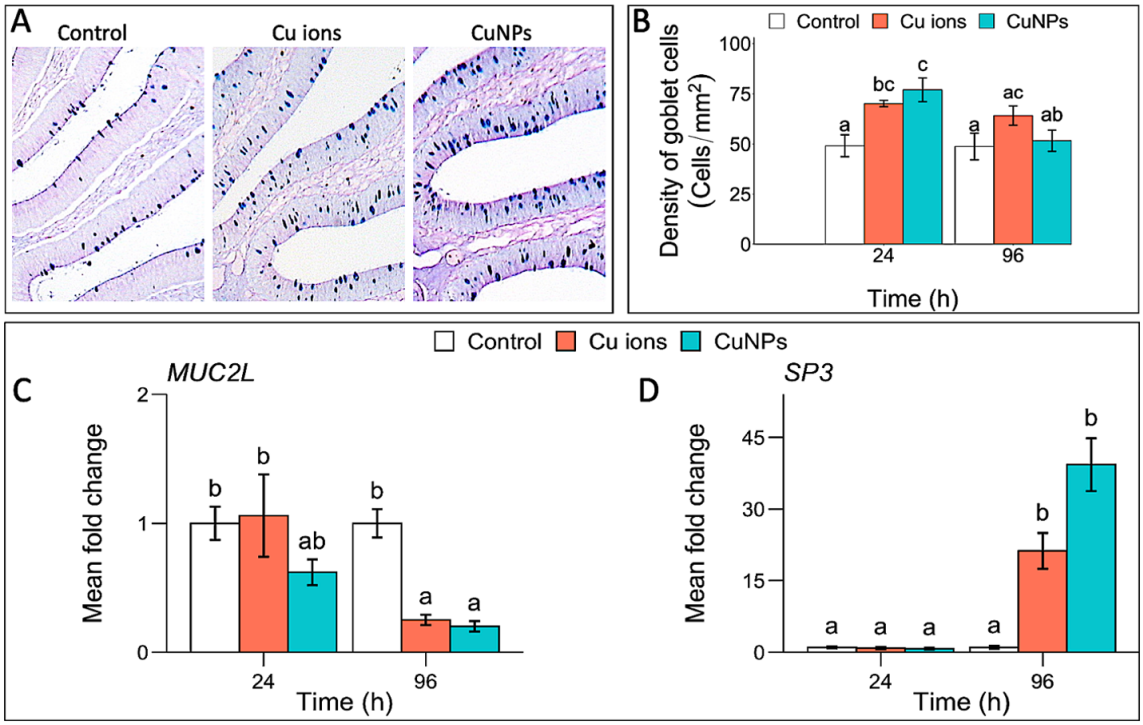

Figure 5.1. Effect of CuNPs and Cu^{2+} on goblet cells in the rainbow trout olfactory epithelium. (A) Light micrographs of olfactory rosettes in cross-section (100X magnification) following the 24-h exposure to copper contaminants. Dark blue spots indicate goblet cells stained by alcian blue. (B) Density of goblet cells in the olfactory rosette following the 24-h and 96-h exposure to CuNPs and Cu^{2+}. (C and D) Relative expression of *MUC2L* and *SP3* in response to CuNPs and Cu^{2+} exposures over time. Lower-case letters indicate significant differences ($p \leq 0.05$, error bars ± 1 SEM).

After the initial increase in the goblet cells observed at 24 h, goblet cell density was restored by 96 h to control levels in Cu treatments (Fig. 5.1B). This shift in the density of Cu-treated goblet cells from 24 h to 96 h can be related to a deficit in the production of mucosubstances. Mucin is a family of glycoproteins, which comprises one of the key components of mucosubstances in the goblet cells (Ma et al., 2018). Adopting the gene transcript profile of Cu-exposed olfactory mucosa, we extracted transcripts encoding mucin. Our RNA-seq data showed abundances of two mucin transcripts, *MUC2L* and *MUC5AC*, were significantly reduced following the 96 h exposure to CuNPs and Cu^{2+} (Table 5.2). These data suggest Cu contaminants may interfere with goblet cell mucin

production. The transcription of these mucin genes is regulated by two members of the SP transcription family, SP1 and SP3 (Andrianifahanana et al., 2006). While the SP1 serves as a promoter for the transcription of these mucin genes, SP3 has a transcriptional inhibitory function (Perrais et al., 2002). The mRNA abundance of *SP1* remained unchanged in both Cu treatments, whereas *SP3* underwent a significant upregulation after 96 h of exposure (Table 5.2).

To investigate if the density of goblet cell alteration was associated with mucin production, we assessed mRNA abundances of *MUC2L* and *SP3* over the 24 h and 96 h exposures using qPCR. At the 96 h exposure, the mRNA abundance of *MUC2L* was reduced in both Cu treatments ($p = 0.03$ and 0.02 in in Cu^{2+} and CuNPs, respectively, Fig. 5.1C). In the 24 h exposure, the mRNA abundance of *MUC2L* did not change in both Cu treatments (Fig. 5.1C). The mRNA abundance of *SP3* also remained unchanged over 24 h in both Cu treatments (Fig. 5.1D). Although the mRNA abundances of *MUC2L* was not upregulated at 24 h in the Cu-treated fish, it is possible that its protein expression was increased. Further investigations are needed to study the expression of MUC2La and other mucin proteins over the 24 h Cu exposures. In the 96 h exposure, in agreement with the RNA-seq results, the level of *SP3* transcript was elevated in response to Cu contaminants (Fig. 5.1D). Collectively, these data revealed the 96 h exposure to Cu can alter the *SP3* transcript abundance, and may consequently, interfere with the olfactory mucin production.

Table 5.2. List of gene transcripts that are associated with structural composition of rainbow trout olfactory mucosa following exposure to CuNPs or Cu^{2+}. Gene expression was analysed by RNA-seq (* indicates significant gene expression relative to the control)

Activity	Transcript name	Fold change in CuNPs	Fold change in Cu^{2+}
Mucus production	Mucin 2 like (*MUC2L*)	0.4 *	0.6 *
	Mucin 5AC (*MUC5AC*)	0.3 *	0.6 *
	Transcription factor SP3 (*SP3*)	34 *	25 *
Tight junctional component	Claudin 1 (*CLD1*)	0.8	0.6 *
	Claudin 4 (*CLD4*)	0.8	0.7 *
	Claudin 8 (*CLD8*)	1.1	0.5 *
	Claudin 12 (*CLD12*)	1.4 *	1.2
	Claudin domain containing 1 (*CLDND*)	1.5 *	1
	Protein shroom 2 (*SHROOM2*)	1.5	0.04 *
Adherens junctional component	Pleckstrin homology domain containing A7 (*PLEKHA7*)	0.06 *	0.04 *
	Catenin alpha-1 (*αE-CAT*)	1	0.5 *
	Neural-cadherin (*N-CAD* or *CDH2*)	0.6 *	0.8
Desmosomal component	Junction plakoglobin (*PG or JUP*)	1	0.7 *
	Desmoplakin (*DSP*)	0.9	0.7 *
	Plakophilin 3 (*PKP3*)	1.3 *	0.7 *
	Plakophilin 1 (*PKP1*)	1.4 *	0.9
	Envoplakin (*EVPL*)	1.7 *	1.1
	Keratin type II cytoskeletal 8 (*KRT8*)	1.5 *	1.1
	Keratin type I cytoskeletal 13 (*KRT13*)	3	1.1
Gap junctional component	Gap junction gamma-1 (*CX45*)	1.7 *	1.4 *
	Gap junction beta 4 (*CX30.3*)	1.4 *	1.1
	Pemphigoid antigen 1 (*BP230*)	1.7	0.01 *

Hemidesmosomal component	Plectin (*PLEC*)	1.2	0 *
	Laminin subunit beta 3 (*LAMB3*)	8.3 *	0.6

5.4.2. Effect of Cu treatments on the transcripts associated with mucosal cell structure

In OE, like other epithelia, the essential mechanical support and the required cell-to-cell and cell-to-extracellular matrix (ECM) communications are facilitated by cell junctions. Results of GO term enrichment analysis indicated structural related transcripts were significantly affected by the 96 h exposure to CuNPs and Cu^{2+}. In both Cu treatments, cell communication and cell-cell junction were among the enriched GO terms that consisted of downregulated transcripts (Table 5.3). However, the bicellular tight junction was only enriched in the Cu^{2+}-treated fish (Table 5.3). In the CuNP treatment, the upregulation of transcripts that are associated with ECM and cytoskeletal structure indicates that mucosal cells attempt to repair the CuNP-induced structural injury (Table 5.3). Functional ECMs are essential for the development and maintenance of olfactory mucosa (Crandall et al., 2000; Ueha et al., 2018).

Table 5.3. Enriched cell-junction GO terms that were significantly upregulated or downregulated in the rainbow trout olfactory mucosa following 96 h exposure of Cu^{2+} and CuNPs (Fisher's exact test, $P < 0.05$)

Treatment	Regulation status of transcripts	Go term	*p* value
Cu^{2+}	Downregulated	Cell communication	< 0.001
		Cell-cell junction	0.027
		Bicellular tight junction	0.036
CuNPs	Downregulated	Cell communication	0.004
		Cell-cell junction	0.029
	Upregulated	Polymeric cytoskeletal fiber	< 0.001
		Intermediate filament	0.001
		Extracellular matrix	0.018
		Actin cytoskeleton	0.036

5.4.3. Effect of Cu treatments on transcripts associated with tight junctions in olfactory mucosa

Tight junctions act as a paracellular barrier which is only permeable to very small molecules (4 - 8 Å) (Mistry et al., 2009). In the tight junctions, transmembrane barrier proteins (e.g., occludin, claudin (CLD) and JAM), are attached to the peripheral scaffolding proteins (e.g., ZO) which are in turn associated with cytoskeletal filaments (e.g., actins) (Van Itallie and Anderson, 2014). The mRNA abundances of *CLD 1*, *4*, and *8* was significantly reduced in the olfactory epithelium of Cu^{2+}-exposed fish (Table 5.2 and Fig. 5.2A). These data suggest that Cu^{2+} may increase tight junction permeability through downregulation of claudin coding genes in the olfactory epithelium. This notion was

supported by reduced transcript abundance of claudin D in the olfactory system of zebrafish which were exposed to Cu^{2+} (Tilton et al., 2008). The mRNA abundances of claudin family proteins were also reduced in Cu^{2+}-exposed gill epithelium (Wang et al., 2015). Assembly and maintenance of tight junctions rely on their connections to cytoskeletal proteins (Van Itallie and Anderson, 2014). An actin regulatory protein, SHROOM2, controls apical positioning of cytoskeletal proteins and regulates the tight junction organization and epithelial cell shape (Hildebrand, 2005). The abundance of *SHROOM2* transcript was significantly reduced following exposure to Cu^{2+}. Therefore, olfactory tight junctions' structure and maintenance may be vulnerable to Cu^{2+} exposure.

In the CuNP treatment, however, the abundances of *CLD12* and *CLDND* transcripts were increased (Table 5.2 and Fig. 5.2B). Modulation and disruption of paracellular tight junctions by nanoparticles was previously reported in different types of epithelial and endothelial cells (Zhang et al., 2011; Casettari and Illum, 2014; Li et al., 2015). In the present study, upregulation of claudin transcripts can be a defensive response against the CuNP exposure in the olfactory mucosa. These data revealed differential effects of CuNPs and Cu^{2+} on the transcripts involved in olfactory tight junction.

5.4.4. Effect of Cu treatments on transcripts associated with adherens junctions in olfactory mucosa

Adherens junctions (a.k.a., zonula adherens) initiate cell-to-cell adhesion and regulate intracellular processes such as transcription and cytoskeleton rearrangement (Hartsock and Nelson, 2008). Disruption of adherens junctions can weaken the intercellular connections and disorganize tissue architecture (Meng and Takeichi, 2009). In adherens junctions, cadherin transmembrane proteins (e.g., N-CAD and E-CAD) are linked to a protein

complex which bridges cadherins to actin and microtubule filaments in cytoplasm (Meng et al., 2008; Zhang et al., 2011). The protein complex in the adherens junction comprises catenin family (P120, α-CAT, β-CAT), NEZHA, and PLEKHA7. The mRNA abundance of *PLEKHA7* was severely reduced following exposure to both Cu contaminants (Table 5.2 and Fig. 5.2). The association of PLEKH7 with NEZHA and microtubules is required to maintain the integrity and stability of adherens junctions (Meng et al., 2008). Exposure to Cu^{2+}caused a significant reduction in the transcription of *αE-CAT*, an isoform of α-CAT expressed predominantly in sustentacular cells (Beaudoin III, 2016). In the CuNP-exposed fish, the mRNA abundance of *N-CAD* was reduced (Table 5.2 and Fig. 5.2B). Our data suggested that the structural stability and functionality of olfactory adherens junctions may be attenuated by CuNPs and Cu^{2+}.

5.4.5. Effect of Cu treatments on transcripts associated with desmosomes in olfactory mucosa

Like tight junctions and the adherens junction, desmosomes are multiprotein complexes connecting to the cytoskeleton and providing mechanical support for epithelial cells. The core composition of desmosomes comprises transmembrane desmosomal cadherins (DSC and DSG), Armadillo family proteins (PG and PKP), and plakin family proteins (DSP and EVPL) which are linked to keratin filaments (Huber, 2003). Disruption of desmosomal components can not only reduce the intercellular adhesion but also impair their intracellular functions such as regulating cell migration (Rübsam et al., 2018). Exposure to Cu^{2+} resulted in a significant reduction in the transcript level of *PG, PKP3*, and *DSP* in desmosomes (Table 5.2 and Fig. 5.2A). In contrast to the Cu^{2+} treatment, the mRNA abundances of *PKP1* and *PKP3*, *EVPL*, and two keratin transcripts (*KRT8* and

KRT13) were elevated in the CuNP-exposed fish (Table 5.2 and Fig. 5.2B). The olfactory desmosomal responses to the Cu^{2+} and CuNPs exposures were similar to the tight junction responses; through upregulating the expression of genes involved in these complexes and reinforcing the cell junctions, epithelial cells exhibited a better response to CuNPs than Cu^{2+}.

5.4.6. Effect of Cu treatments on transcripts associated with gap junctions in olfactory mucosa

Olfactory mucosal cells, including supporting cells, OECs, and OSNs communicate through gap junctions which are specialized transmembrane channels. The exchange of small signalling particles such as Ca^{2+}, and cAMP through gap junctions facilitates adjacent cell communication (Zhang and Restrepo, 2002). Gap junctions have two hemichannels that are made of a hexameric protein complex named connexins (Vinken et al., 2010). A previous study suggested coupling of OSNs trough gap junctions synchronizes threshold activity of adjacent neurons by mediating a low frequency current through hemichannels and consequently, increases olfactory sensitivity (Zhang, 2010). Moreover, the inhibition of gap junctions resulted in a significant reduction in the odor-evoked intracellular calcium concentration in OSNs. These results suggested that gap junctions can regulate olfactory responses (Yu and Zhang, 2015).

Mature OSNs express different connexin proteins including CX43 and CX45. The CX43 and CX45 make a heterotypic gap junctional channels which may play a role in olfaction (Zhang and Restrepo, 2002). Another connexin protein, CX30.3, may also play a role in olfactory function, as CX30.3 deficient mice showed reduced olfactory-driven behavioural responses to a vanilla odorant. In our study, the mRNA abundance of *CX45*

was significantly increased in response to both Cu treatments (Table 5.2 and Fig. 5.2). In the CuNP treatment, the transcript level of *CX30.3* was also elevated. The increased mRNA abundances of connexin genes may be a compensatory mechanism to the Cu-induced olfactory deficits that we previously observed in rainbow trout (Razmara et al., 2019).

5.4.7. Effect of Cu treatments on transcripts associated with hemidesmosomes in olfactory mucosa

In the olfactory mucosa, hemidesmosomal structures facilitate adhesion of basal cells to the underlying basal lamina through the connection of cytoplasmic keratins to laminin 322 in ECM. Hemidesmosomal complex is composed of two members of the plakin family (plectin and BP230 (a.k.a., dystonin)), integrin α6β4, BP180 (a.k.a., type XVII collagen), and tetraspanin (CD151) (Litjens et al., 2006). Together, plectin and BP230 build the hemidesmosomal inner plaque which is connected to the keratin filaments. Exposure to Cu^{2+} led to a severe mRNA depletion of both plectin (*PLEC*) and *BP230* in the olfactory mucosa (Table 5.2 and Fig. 5.2A). These data suggest the inner plaque of olfactory hemidesmosomes was compromised in the Cu^{2+}-exposed fish. The absence of an inner plaque may detach the horizontal basal stem cells from the basal lamina.

The mRNA abundances of hemidesmosomal components remained unchanged in the CuNP treatment. Nevertheless, the transcript level of a laminin 322 subunit (*LAMB3*) showed a significant upregulation in the CuNP-exposed fish (Table 5.2 and Fig. 5.2B). Laminin 322 is the main component of the basal lamina, and its association with integrin regulates assembly and stabilization of hemidesmosomes. These data suggest that the CuNP-exposed fish had more stabilized hemidesmosomes relative to the Cu^{2+}-exposed ones.

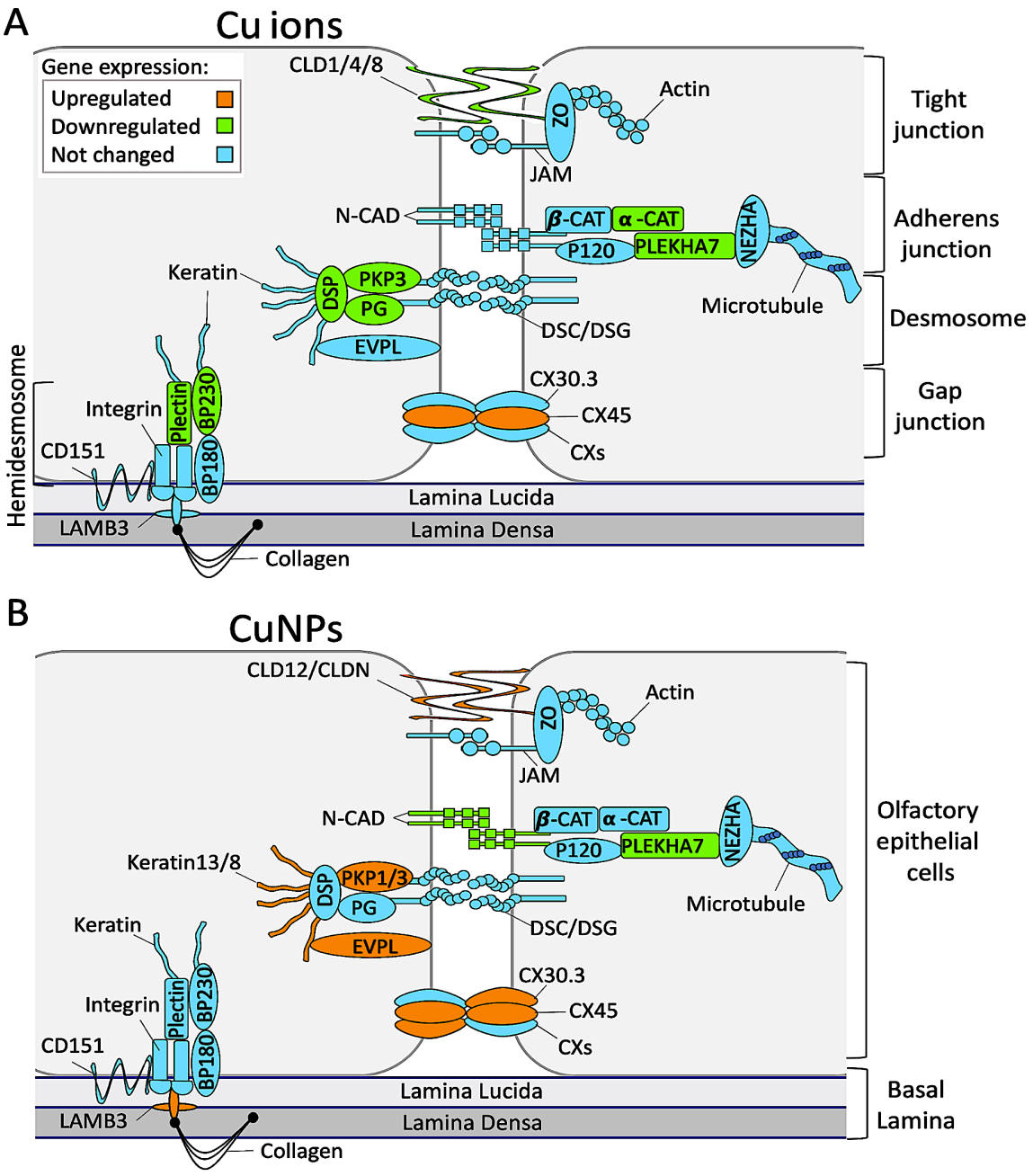

Figure 5.2. Schematic representation of transcript alterations in junctional complexes of rainbow trout olfactory mucosa following the 96 h exposure to Cu2+ (A) and CuNPs (B). The colour-coded legend represents the transcript pattern of the differentially expressed genes. CLD: Claudin, ZO: Zonula occludens, JAM: Junctional adhesion molecule, N-CAD: Neural cadherin, α-CAT: α-catenin, β-CAT: β-catenin, P120: P120 catenin, PLEKHA7: Pleckstrin homology domain containing A7, DSP: Desmoplakin, PKP: Plakophilin, PG: Plakoglobin, DSC: Desmocollin, DSG: Desmoglein, EVPL: Envoplakin, CX: Connexin, BP180: Bullous Pemphigoid antigen 2, BP230: Pemphigoid antigen 1, CD151: CD151 antigen, LAMB3: Laminin subunit beta 3.

5.5. Conclusions

Our results demonstrate that Cu^{2+} and CuNPs altered the structure of rainbow trout olfactory mucosa. We reported an initial increase in the density of goblet cells over the first 24 h of Cu exposures. Nonetheless, the density of goblet cells and the mRNA abundances of transcripts encoding mucin proteins were reduced following the 96 h exposure period. These results indicated duration of exposure to Cu contaminants may affect the mucus barrier by altering the density of goblet cells and dysregulating the genes associated to mucus production. Moreover, our findings have shed light on the molecular dysregulations of olfactory cell junctions following the 96 h exposure to Cu^{2+} and CuNPs. The transcript profile of rainbow trout olfactory mucosa suggested junctional complexes providing paracellular adhesions were less stable in the Cu^{2+} treatment relative to the CuNP treatment. Transcripts of gap junctional channels were upregulated in both Cu treatments, which could be a compensatory response to the Cu-induced olfactory dysfunction. Collectively, Cu contaminants can transform the structure of olfactory mucosa and consequently alter the stability, permeability, and functionality of OE.

5.6. References

Aegerter, S., Jalabert, B., Bobe, J., 2005. Large scale real-time PCR analysis of mRNA abundance in rainbow trout eggs in relationship with egg quality and post-ovulatory ageing. Molecular Reproduction and Development: Incorporating Gamete Research 72, 377-385.

Andrews, S., 2020. FastQC: a quality control tool for high throughput sequence data. 2010.

Andrianifahanana, M., Moniaux, N., Batra, S.K., 2006. Regulation of mucin expression: mechanistic aspects and implications for cancer and inflammatory diseases. Biochimica et Biophysica Acta (BBA)-Reviews on Cancer 1765, 189-222.

Beaudoin III, G.M., 2016. Mosaic cellular patterning in the nose: Adhesion molecules give their two scents. The Journal of Cell Biology 212, 495.

Bols, N.C., Brubacher, J.L., Ganassin, R.C., Lee, L.E., 2001. Ecotoxicology and innate immunity in fish. Developmental & Comparative Immunology 25, 853-873.

Casettari, L., Illum, L., 2014. Chitosan in nasal delivery systems for therapeutic drugs. Journal of Controlled Release 190, 189-200.

Crandall, J., Dibble, C., Butler, D., Pays, L., Ahmad, N., Kostek, C., Püschel, A., Schwarting, G., 2000. Patterning of olfactory sensory connections is mediated by extracellular matrix proteins in the nerve layer of the olfactory bulb. Journal of neurobiology 45, 195-206.

Dobin, A., Davis, C.A., Schlesinger, F., Drenkow, J., Zaleski, C., Jha, S., Batut, P., Chaisson, M., Gingeras, T.R., 2013. STAR: ultrafast universal RNA-seq aligner. Bioinformatics 29, 15-21.

Ferreira, A.R., Felgueiras, J., Fardilha, M., 2015. Signaling pathways in anchoring junctions of epithelial cells: cell-to-cell and cell-to-extracellular matrix interactions. Journal of Receptors and Signal Transduction 35, 67-75.

Ferruzza, S., Scacchi, M., Scarino, M., Sambuy, Y., 2002. Iron and copper alter tight junction permeability in human intestinal Caco-2 cells by distinct mechanisms. Toxicology in vitro 16, 399-404.

Götz, S., García-Gómez, J.M., Terol, J., Williams, T.D., Nagaraj, S.H., Nueda, M.J., Robles, M., Talón, M., Dopazo, J., Conesa, A., 2008. High-throughput functional annotation and data mining with the Blast2GO suite. Nucleic acids research 36, 3420-3435.

Hartsock, A., Nelson, W.J., 2008. Adherens and tight junctions: structure, function and connections to the actin cytoskeleton. Biochimica et Biophysica Acta (BBA)-Biomembranes 1778, 660-669.

Hildebrand, J.D., 2005. Shroom regulates epithelial cell shape via the apical positioning of an actomyosin network. Journal of cell science 118, 5191-5203.

Hu, G., Cao, J., 2019. Metal-containing nanoparticles derived from concealed metal deposits: An important source of toxic nanoparticles in aquatic environments. Chemosphere 224, 726-733.

Huber, O., 2003. Structure and function of desmosomal proteins and their role in development and disease. Cellular and Molecular Life Sciences CMLS 60, 1872-1890.

Kolmakov, N.N., Hubbard, P.C., Lopes, O., Canario, A.V., 2009. Effect of acute copper sulfate exposure on olfactory responses to amino acids and pheromones in goldfish (Carassius auratus). Environmental science & technology 43, 8393-8399.

Krishan, M., Gudelsky, G.A., Desai, P.B., Genter, M.B., 2014. Manipulation of olfactory tight junctions using papaverine to enhance intranasal delivery of gemcitabine to the brain. Drug delivery 21, 8-16.

Li, C.-H., Shyu, M.-K., Jhan, C., Cheng, Y.-W., Tsai, C.-H., Liu, C.-W., Lee, C.-C., Chen, R.-M., Kang, J.-J., 2015. Gold nanoparticles increase endothelial paracellular permeability by altering components of endothelial tight junctions, and increase blood-brain barrier permeability in mice. Toxicological Sciences 148, 192-203.

Litjens, S.H., de Pereda, J.M., Sonnenberg, A., 2006. Current insights into the formation and breakdown of hemidesmosomes. Trends in cell biology 16, 376-383.

Ma, J., Rubin, B.K., Voynow, J.A., 2018. Mucins, mucus, and goblet cells. Chest 154, 169-176.

Malhotra, N., Ger, T.-R., Uapipatanakul, B., Huang, J.-C., Chen, K.H.-C., Hsiao, C.-D., 2020. Review of Copper and Copper Nanoparticle Toxicity in Fish. Nanomaterials 10, 1126.

Meng, W., Mushika, Y., Ichii, T., Takeichi, M., 2008. Anchorage of microtubule minus ends to adherens junctions regulates epithelial cell-cell contacts. Cell 135, 948-959.

Meng, W., Takeichi, M., 2009. Adherens junction: molecular architecture and regulation. Cold Spring Harbor perspectives in biology 1, a002899.

Mistry, A., Stolnik, S., Illum, L., 2009. Nanoparticles for direct nose-to-brain delivery of drugs. International journal of pharmaceutics 379, 146-157.

Perrais, M., Pigny, P., Copin, M.-C., Aubert, J.-P., Van Seuningen, I., 2002. Induction of MUC2 and MUC5AC mucins by factors of the epidermal growth factor (EGF) family is mediated by EGF receptor/Ras/Raf/extracellular signal-regulated kinase cascade and Sp1. Journal of Biological Chemistry 277, 32258-32267.

Pertea, M., Pertea, G.M., Antonescu, C.M., Chang, T.-C., Mendell, J.T., Salzberg, S.L., 2015. StringTie enables improved reconstruction of a transcriptome from RNA-seq reads. Nature biotechnology 33, 290-295.

Pfaffl, M.W., 2001. A new mathematical model for relative quantification in real-time RT–PCR. Nucleic acids research 29, e45-e45.

Polakof, S., Médale, F., Skiba-Cassy, S., Corraze, G., Panserat, S., 2010. Molecular regulation of lipid metabolism in liver and muscle of rainbow trout subjected to acute and chronic insulin treatments. Domestic animal endocrinology 39, 26-33.

Pradhan, S., Mailapalli, D.R., 2017. Interaction of engineered nanoparticles with the agri-environment. Journal of agricultural and food chemistry 65, 8279-8294.

R Core Team, 2019. A language and environment for statistical computing. R Foundation for Statistical Computing, Vienna, Austria2014. in: Team, R.C. (Ed.).

Rajput, V., Minkina, T., Ahmed, B., Sushkova, S., Singh, R., Soldatov, M., Laratte, B., Fedorenko, A., Mandzhieva, S., Blicharska, E., 2019. Interaction of copper-based nanoparticles to soil, terrestrial, and aquatic systems: critical review of the state of the

science and future perspectives. Reviews of Environmental Contamination and Toxicology Volume 252, 51-96.

Razmara, P., Lari, E., Mohaddes, E., Zhang, Y., Goss, G.G., Pyle, G.G., 2019. The effect of copper nanoparticles on olfaction in rainbow trout (*Oncorhynchus mykiss*). Environmental Science: Nano 6, 2094-2104.

Rübsam, M., Broussard, J.A., Wickström, S.A., Nekrasova, O., Green, K.J., Niessen, C.M., 2018. Adherens junctions and desmosomes coordinate mechanics and signaling to orchestrate tissue morphogenesis and function: an evolutionary perspective. Cold Spring Harbor perspectives in biology 10, a029207.

Sarkar, S.K., De, S.K., 2014. Functional anatomy of cellular junctions in olfactory neuroepithelium of *Pseudapocryptes lanceolatus* (Bloch and Schneider).

Souza, I.d.C., Morozesk, M., Mansano, A.S., Mendes, V.A., Azevedo, V.C., Matsumoto, S.T., Elliott, M., Monferrán, M.V., Wunderlin, D.A., Fernandes, M.N., 2020. Atmospheric particulate matter from an industrial area as a source of metal nanoparticle contamination in aquatic ecosystems. Science of The Total Environment 753, 141976.

Steinke, A., Meier-Stiegen, S., Drenckhahn, D., Asan, E., 2008. Molecular composition of tight and adherens junctions in the rat olfactory epithelium and fila. Histochemistry and cell biology 130, 339.

Tierney, K.B., Baldwin, D.H., Hara, T.J., Ross, P.S., Scholz, N.L., Kennedy, C.J., 2010. Olfactory toxicity in fishes. Aquatic toxicology 96, 2-26.

Tilton, F., Tilton, S.C., Bammler, T.K., Beyer, R., Farin, F., Stapleton, P.L., Gallagher, E.P., 2008. Transcriptional biomarkers and mechanisms of copper-induced olfactory injury in zebrafish. Environmental science & technology 42, 9404-9411.

Ueha, R., Shichino, S., Ueha, S., Kondo, K., Kikuta, S., Nishijima, H., Matsushima, K., Yamasoba, T., 2018. Reduction of proliferating olfactory cells and low expression of extracellular matrix genes are hallmarks of the aged olfactory mucosa. Frontiers in aging neuroscience 10, 86.

Van Itallie, C.M., Anderson, J.M., 2014. Architecture of tight junctions and principles of molecular composition. Seminars in cell & developmental biology. Elsevier, pp. 157-165.

Vasileva, E., Citi, S., 2018. The role of microtubules in the regulation of epithelial junctions. Tissue barriers 6, 1539596.

Vinken, M., Ceelen, L., Vanhaecke, T., Rogiers, V., 2010. Inhibition of gap junctional intercellular communication by toxic metals. Chemical research in toxicology 23, 1862-1867.

Wang, B., Feng, L., Jiang, W.-D., Wu, P., Kuang, S.-Y., Jiang, J., Tang, L., Tang, W.-N., Zhang, Y.-A., Liu, Y., 2015. Copper-induced tight junction mRNA expression changes, apoptosis and antioxidant responses via NF-κB, TOR and Nrf2 signaling molecules in the gills of fish: preventive role of arginine. Aquatic toxicology 158, 125-137.

Wickham, H., 2016. ggplot2: elegant graphics for data analysis. springer.

Williams, C.R., Gallagher, E.P., 2013. Effects of cadmium on olfactory mediated behaviors and molecular biomarkers in coho salmon (Oncorhynchus kisutch). Aquatic toxicology 140, 295-302.

Ye, J., Coulouris, G., Zaretskaya, I., Cutcutache, I., Rozen, S., Madden, T.L., 2012. Primer-BLAST: a tool to design target-specific primers for polymerase chain reaction. BMC bioinformatics 13, 134.

Yu, Y., Zhang, C., 2015. The role of connexin 43 in mediating odor response. European journal of cell biology 94, 267-275.

Zhang, C., 2010. Gap junctions in olfactory neurons modulate olfactory sensitivity. BMC neuroscience 11, 1-16.

Zhang, C., Restrepo, D., 2002. Expression of connexin 45 in the olfactory system. Brain research 929, 37-47.

Zhang, G., Ding, L., Renegar, R., Wang, X., Lu, Q., Huo, S., Chen, Y.H., 2011. Hydroxycamptothecin-loaded Fe3O4 nanoparticles induce human lung cancer cell apoptosis through caspase-8 pathway activation and disrupt tight junctions. Cancer science 102, 1216-1222.

CHAPTER 6: Impact of copper nanoparticles on neural repair mechanisms in rainbow trout olfactory mucosa

In the previous chapters we reported that exposure to CuNPs may disrupt the structure and function of olfactory mucosa. Nonetheless, the olfactory mucosa is capable of regeneration. In the current chapter, using the transcript profiles of Cu-exposed fish, we investigated the molecular alterations of the neural repair mechanisms in the olfactory mucosa.

A version of this chapter is going to be submitted to *Environmental Pollution*.

Contribution of authors: I designed and performed research, analysed data, and wrote the manuscript. Dr. Pyle provided guidance, scientific input, supervision, funding, and comments on the manuscript.

6.1 Abstract

Olfactory mucosa is notorious for its lifelong ability for regeneration. Regeneration of neurons and regrowth of severed axons are the most common neural repair mechanisms in olfactory mucosa. Nonetheless, exposure to neurotoxic contaminants, such as copper nanoparticles (CuNPs) and copper ions (Cu^{2+}), may alter the reparative capacity of olfactory mucosa. Here, using RNA-sequencing, we elucidated the molecular basis of neural repair mechanisms that were affected by CuNPs and Cu^{2+} in rainbow trout olfactory mucosa. The transcript profile of olfactory mucosa suggested that regeneration of neurons was inhibited by CuNPs. Exposure to CuNPs reduced the transcript abundances of pro-inflammatory proteins which are required to initiate neuroregeneration. Moreover, the transcript of genes encoding regeneration promoters, including canonical Wnt/β-catenin signaling proteins and developmental transcription factors, were downregulated in the CuNP-treated fish. The mRNA levels of genes regulating axonal regrowth, including the growth-promoting signals secreted from olfactory ensheathing cells, were mainly increased in the CuNP treatment. However, the reduced transcript abundances of a few cell adhesion molecules and neural polarity genes may restrict axonogenesis in the CuNP-exposed olfactory mucosa. In the Cu^{2+}-treated olfactory mucosa, both of the neural repair strategies were initiated at the transcript level. The stimulation of repair mechanisms can lead to the recovery of Cu^{2+}-induced olfactory dysfunction. These results indicated CuNPs and Cu^{2+} differentially affected the neural repair mechanism in olfactory mucosa. Exposure to CuNP had greater effects on olfactory repair mechanisms relative to Cu^{2+} and dysregulated the transcripts associated with stem cell proliferation and neural reconstitution.

6.2. Introduction

Perception of chemosensory signals conveys information to fish that is essential for survival and reproduction success. Detecting the presence of an appropriate mate, the location of food, the risk of predation, and the presence of potentially toxic contaminants in fish habitat is mediated through olfactory sensory neurons (OSNs). These OSNs receive sensory inputs and transmit them to the brain for processing (Laberge and Hara, 2001; Kermen et al., 2013). Due to direct contact of OSNs with myriad biotic and abiotic environmental stressors, they are susceptible to functional impairment. Vertebrate olfactory neuroepithelium is capable of regeneration in response to damage. Reconstitution of damaged OSNs is a key process to restore olfactory function. Nevertheless, some anthropogenic contaminants can interfere with olfactory neuroepithelial regenerative capability, and consequently inhibit the neuroepithelium reestablishment (Wang et al., 2017a; Szymkowicz et al., 2019).

Copper nanoparticles (CuNPs) are emerging environmental contaminants of concern (Malhotra et al., 2020). Due to unique conductivity, catalytic, and antimicrobial properties of engineered CuNPs, they appear as a promising material to be applied in electronics, biomedical, and agriculture (Tabesh et al., 2018; Zhou et al., 2019; Vanti et al., 2020). The application of CuNPs as an antibiofouling agent in fish-cage netting (Ashraf et al., 2017), an antibiofilm agent against fish pathogens (Chari et al., 2017), and a dietary supplement to boost fish growth and immune system (El Basuini et al., 2017), make them popular in the aquaculture industry. The progressive production and utilization of CuNPs enhances their incidental input to water bodies. We have previously demonstrated that CuNPs can be taken up by rainbow trout olfactory mucosal cells and induce olfactory

toxicity (chapter 4). Exposure to CuNPs can not only disrupt OSN function (Razmara et al., 2019) (chapter 4), but also reduce the transcription of neuroregeneration-related pathways in rainbow trout olfactory mucosa (chapter 4). We also compared the toxicity of CuNP and copper ion (Cu^{2+}) which is a well-known olfactory disrupter. In Cu^{2+}-treated fish, unlike those in the CuNP treatment, neuroregenerative pathways was upregulated (chapter 4). This finding indicates that CuNPs and Cu^{2+} have differential effects on the neuroregeneration process in the olfactory mucosa. Nonetheless, the detailed regenerative molecular events that were affected by each of the Cu contaminants remain unknown.

Two types of neural repair mechanisms have been reported in a damaged olfactory mucosa. First is the genesis of new OSNs from stem cells residing in olfactory mucosa (Graziadei and Graziadei, 1979). Olfactory neural replenishment is a complex multiphase process that entails progenitors forming from olfactory stem cells followed by migration and differentiation, which ultimately gives rise to mature OSNs (Nicolay et al., 2006). The basal layer of olfactory epithelium is composed of two populations of stem cells, horizontal basal cells (HBCs) and globose basal cells (GBCs) (Roy et al., 2013). In general, GBCs are mitotically active, whereas the HBCs are a reserve population which remains mitotically quiescent under conditions of non-extensive injury (Choi and Goldstein, 2018). To maintain the integrity of olfactory neuroepithelium, both classes of stems cells actively interact with extrinsic regulators (e.g., immune cells) in their niche (Chen et al., 2019). These intercellular interactions lead to activation of intrinsic regulators, such as transcription factors, that control stem cell proliferation, differentiation, and neuron maturation. The second type of repair is axonal regrowth in existing OSNs. During axon regeneration a specialized type of glial cell, olfactory ensheathing cell (OEC), secretes

extrinsic growth and guidance cues and subsequently, reactivates the intrinsic developmental process in the growing axon (Roet and Verhaagen, 2014). In this study, using the transcription profile of rainbow trout olfactory mucosa, we investigated how exposure to CuNPs and Cu^{2+} differentially affected intrinsic and extrinsic regeneration regulators. Our findings indicated that the transcripts of neuroregenerative regulatory mechanisms, including inflammatory signaling, Wnt signaling, and neurogenesis transcription factors were downregulated in the CuNP-treated olfactory mucosa. Whereas, in the Cu^{2+}-exposed fish, the increased transcript abundances of neurogenesis regulators suggested that neuroregeneration was initiated in mucosal cells. Transcripts associated with axonogenesis promoters were mostly upregulated in both Cu treatments. However, the reduction of a few transcripts regulating axon guidance may interfere with axonogenesis in the CuNP treatment.

6.3. Materials and Methods

6.3.1. Fish husbandry and experimental design

Juvenile rainbow trout with an average weight of 26.5 ± 5.2 g (mean ± SD; n = 15) were obtained from Sam Livingston Fish Hatchery (Alberta, Canada) and housed in a holding tank (16 h light: 8 h dark photoperiod, 12 ºC) at the University of Lethbridge Aquatic Research Facility (ARF). According to our previous study, the 50% olfactory inhibitory concentrations of CuNPs and Cu^{2+} (24-h IC50 measured by electro-olfactography) were 320 ± 13 and 7 ± 1 µg/L (mean ± SD), respectively (Razmara et al., 2019). These IC50s of Cu contaminants were used as a functional unit of toxicity. Following a two-week acclimation period, to investigate the comparative effect of CuNPs and Cu^{2+} on the transcript profiles of rainbow trout olfactory mucosa, fish were exposed to

24-h IC50s of Cu contaminant for 96 h (chapter 4). Every 24 h, fish were transferred to new sets of tanks containing fresh water and Cu solutions. Quality of culture water was measured as follows (mean ± SD; n = 3): temperature, 12.4 ± 0.3 °C; dissolved oxygen, 8.8 ± 0.7 mg/L; conductivity, 331.3 ± 0.3 µS /cm; hardness, 156 ± 3.1 mg/L as $CaCO_3$; alkalinity: 125.0 ± 4.4 mg/L as $CaCO_3$; median pH, 8.1 (range 7.8 – 8.4), and dissolved organic carbon, 2.5 ± 0.7 mg/L. During the exposure period fish were not fed.

6.3.2. Preparation of Cu stock mixtures, Cu analysis, and CuNPs characterization

Copper solution preparation and analysis were described by Razmara et al. (2019). In short, using a 30 min water bath sonicator (UD 150SH6LQ; 150 W; Eumax; USA), nanocopper powder (35 nm; 99.8% purity; partially passivated, Nanostructured & Amorphous Materials Inc, USA) was suspended in ddH_2O (18.2 MΩ/cm water, Millipore, USA) to make a stock suspension of 250 mg/L CuNPs. A fresh stock solution of 100 mg/L $CuSO_4$ (>98% purity; BHD, USA) in ddH_2O was prepared and used as the source of Cu^{2+}. The actual concentration of Cu in the fish tanks was measured by graphite furnace atomic absorption spectrometry (240FS GFAAS, Agilent Technologies, USA). The actual Cu^{2+} and CuNPs concentrations 24 h after spiking the fish tanks with Cu mixtures, were 7 ± 1 µg/L and 210 ± 13 µg/L (65% of nominal CuNPs concentration), respectively (mean ± SD, n = 6) (chapter 4). The Cu concentration in the control was below the GFAAS detection limit.

We previously characterized the CuNPs (Razmara et al., 2019), and we used the same batch nanocopper powder for this study. The CuNPs were semi-spherical with an average diameter of 32 ± 1 nm (mean ± SEM). Polydispersity index (PDI), hydrodynamic

diameter (HDD), and zeta potential, which are indicators of NP aggregation, were changed over 24 h. Sixteen h after spiking the fish tanks water with CuNPs, we observed a significant increase in polydispersity (PDI = 1) and HDD, along with a noticeable reduction in zeta potential. These measurements indicated CuNPs were less stable and consequently, less bioavailable over the last few hours of exposure (Razmara et al., 2019). Using Amicon Ultra-4 Centrifugal Filter Units (3K regenerated cellulose membrane, Merck Millipore Ltd., USA), dissolved Cu was separated from CuNPs. The concentration of dissolved Cu in the filtrate was measured using GFAAS over 24 h (Razmara et al., 2019). We observed a gradual release of dissolved Cu in the fish tanks over time (the highest dissolution after 24 h was 14 μg/L) (Razmara et al., 2019). Therefore, the effects of CuNPs on olfactory mucosa is associated to both nanocopper and dissolved Cu.

6.3.3. RNA isolation

As described in chapter 4, following the 96-h exposure to CuNPs and Cu^{2+}, fish (n = 5) were euthanized using a pH buffered MS222 solution (240 mg/L tricaine methane sulfonate (AquaLife, Canada) and 720 mg/L $NaHCO_3$ (Fisher Scientific, USA)). Immediately after euthanizing, fish olfactory rosettes were dissected, flash-frozen in liquid nitrogen, and stored in -80°C. Using RNeasy Mini Kit manufacturer's protocol (catalogue # 74106; Qiagen), total RNA was isolated from olfactory rosettes. Quality and quantity of isolated RNA were determined by a Nanodrop spectrophotometer (Thermo Scientific NanoDrop One spectrophotometer, Thermo Scientific). The RNA integrity number (RIN) was determined by Bioanalyzer 2100 (Agilent Technologies). The RIN of all samples were > 7 (chapter 4).

6.3.4. Illumina sequencing and RNA-seq analysis

High quality RNA samples were shipped to Canada's Michael Smith Genome Sciences Centre (GSC, BC cancer research, Canada) to construct strand specific mRNA libraries. Each library was sequenced using the HiSeq 2500 (Illuina, San Diego, California, USA) as paired-end platform generating 2 * 75 base pair (bp) reads for each sample (chapter 4). The RNA-seq analysis pipeline is fully described in chapter 4. In brief, reads were assessed for their quality using FastQC (Andrews, 2020), and high quality reads were aligned to rainbow trout reference transcriptome (Omyk_1.0, GCF_002163495.1) using STAR two-pass alignment version 2.6.1 (Dobin et al., 2013). Using StringTie version 1.3.4, mapped reads were assembled and counted (Pertea et al., 2015). The counted transcripts were annotated against National Center for Biotechnology Information (NCBI) non-redundant (nr) protein database using BLASTx. Differential gene expression analyses was conducted using DESeq2 version 1.28.1 (Love et al., 2014) with a $p_{adj} \leq 0.05$ cut-off for statistical significance. Of the total number of transcripts in Cu^{2+} (53141) and CuNPs (53380) treatments, 2.1% were differentially expressed in each treatment. However, there was a narrow overlap between the CuNP- and Cu^{2+}- affected transcripts (chapter 4). The functional annotations of the differentially expressed transcripts was performed in Blast2Go Pro (OmicsBox version 1.3.11) (Götz et al., 2008). The functional annotation analysis showed 87% and 89% of the differentially expressed transcripts were functionally annotated in CuNPs and Cu^{2+} treatment, respectively (chapter 4). Enrichment analysis of gene ontology (GO) terms was conducted using the Fisher's exact test in Blast2GO ($p \leq 0.05$).

6.3.5. Gene expression quantification by qPCR

The results of RNA-seq were previously validated and confirmed by qPCR gene expression (chapter 4). In this study, the expression *TCF7L2*, a key transcription factor involved in Wnt signaling pathway, was studied in both Cu treatments using qPCR. One µg of the total RNA was used to make cDNA using (QuantiTec Reverse Transcription Kit, catalogue # 205311, Qiagen). The TCF7L2 primer set was designed using Primer-Blast online software provided by NCBI (Ye et al., 2012). To ensure the specificity of the primers' amplification, the PCR products were purified (QIAquick PCR Purification kit, catalogue # 28104; Qiagen), sequenced, and blasted in NCBI. The primer sequences for *TCF7L2* (primer efficiency: 102%) were as follows: F - CGAATCAAAGTCCGAACGCA, R - TTTGGAAACGCCGTCGAGA. The quantification of gene expression analysis was carried out in duplicate on a Bio-Rad thermocycler (C1000 Touch thermocycler, CFX96 Real-Time System, Bio-Rad) using RT² SYBR Green qPCR master mix (catalogue # 330503, Qiagen) as described in chapter 4. Expression of *TCF7L2* was normalized to the expression of reference genes, *ACTB* (Aegerter et al., 2005) and *EF1a* (Polakof et al., 2010), which did not changed in the transcriptome analysis. Quantification of the *TCF7L2* transcripts was analyzed according the Pfaffl method of relative quantification (Pfaffl, 2001). To determine whether *TCF7L2* was differentially expressed in response to (CuNPs and Cu^{2+}, we conducted one-way analysis of variance (ANOVA) with Tukey's post hoc test using R, version 3.6 (R Core Team, 2019).

6.4. Results and discussion

6.4.1. Effect CuNPs and Cu^{2+} on the repair mechanism in the olfactory mucosa

Results of pathway enrichment analysis indicated a number of neuroregeneration-related functional GO terms, including neurogenesis, were composed of downregulated genes in the CuNP treatment (Fig. 6.1A). We previously reported that CuNPs, but not Cu^{2+}, were significantly accumulated in the olfactory mucosal cells (chapter 4). Moreover, in the CuNP-treated fish, there was a progressive impairment in the olfactory responses over time (Razmara et al., 2019). These results indicate CuNPs had adverse effects on the OSNs which may not be simple to repair. Our current knowledge of possible effects of CuNPs on olfactory neuroregeneration is scarce. In the central nervous system of zebrafish embryos, exposure to copper oxide nanoparticles resulted in reduced neural development (Xu et al., 2017).

On the other hand, the upregulation of genes encoding developmental-related pathways in the Cu^{2+} treatment, such as cell cycle and epithelium development (Fig. 6.1B), reflects that regeneration processes were activated in the olfactory mucosa. Despite a continuous exposure to Cu^{2+}, we previously observed a functional recovery in Cu^{2+}-exposed OSNs (Razmara et al., 2019). This functional olfactory recovery was a further indication of active repair mechanisms in the Cu^{2+} treatment. A 24-h exposure of the olfactory system to Cu^{2+} increased the level of neurogenesis-related miRNAs and mRNAs in zebrafish (Tilton et al., 2008; Wang et al., 2013). Consistent with our results, developmental pathways were enriched in the Cu^{2+}-exposed zebrafish olfactory system (Tilton et al., 2008). A recent study indicated that different classes of OSNs (i.e. ciliated and microvillous OSNs) in zebrafish larvae display distinct reparative responses following

a 24-h exposure to 16 – 635 μg/L Cu^{2+} (Ma et al., 2018). Regeneration of microvillous cells occurred following a 72-h recovery period whereas, there was no significant regeneration of ciliated OSNs in the Cu^{2+}- exposed larvae. Nonetheless, ciliated cells showed a partial functional improvement following the recovery period (Ma et al., 2018). These results suggested that in the ciliated OSNs, rather than replacement of the injured OSNs with new neurons, axonal regeneration was activated to repair the Cu^{2+}-induced injuries. Confocal images of Cu^{2+}-exposed zebrafish demonstrated that ciliated OSNs had more axon retractions than microvillous cells (Ma et al., 2018). Axonal retractions can stimulate axonal repair mechanisms in ciliated cells. In our study, the upregulation of genes involved in the cell projection GO term suggests axonogenesis may be activated in both CuNP and Cu^{2+} treatment (Fig. 6.1).

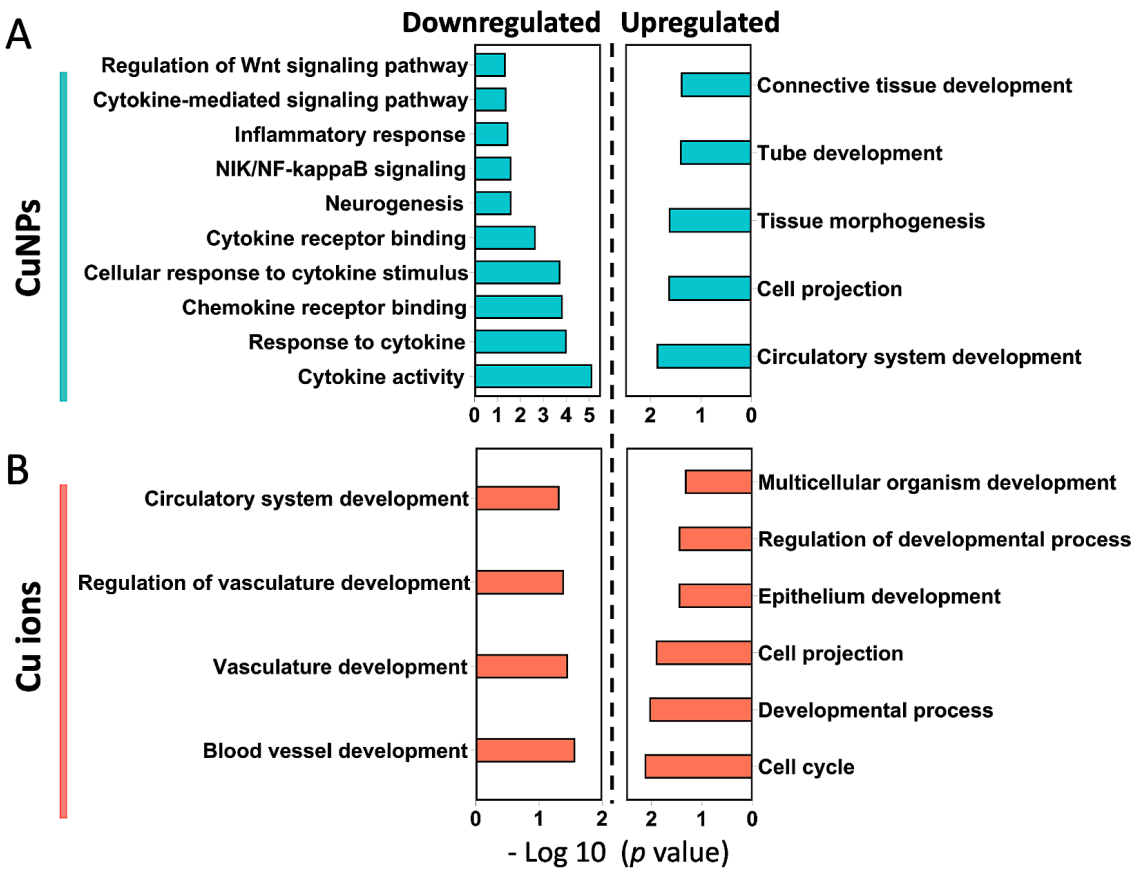

Figure 6.1. Over-represented functional GO terms associated with regeneration in CuNP- and Cu^{2+}-treated rainbow trout olfactory mucosa. Bar graphs show the enriched GO terms of genes that were significantly upregulated or downregulated in CuNPs (A) and Cu^{2+} (B) treatment. The GO terms ordered according to -Log10 (*p* value). The p value for each GO term was calculated through Fisher's exact test ($p \leq 0.05$).

6.4.2. Inflammatory responses in the CuNP- and Cu^{2+}-exposed olfactory mucosa

Various types of innate and adaptive immune cells were present in the olfactory neuroepithelium to defend against invasive pathogens (Tacchi et al., 2014). Inflammatory signaling enables the immune cells to communicate efficiently through secretion of proinflammatory cues. In addition to the defensive role of inflammatory response pathway, inflammation contributed towards the regulation of regeneration (Chen et al., 2017; Chang and Glezer, 2018; Crisafulli et al., 2018; Chen et al., 2019). Proinflammatory proteins are

extrinsic cues that can initiate or block stem cell proliferation depending on inflammation stage and intensity in the niche (Kizil et al., 2015). During chronic inflammation in mouse olfactory mucosa, the reparative activity of stem cells was switched off (Chen et al., 2019). Nevertheless, acute inflammation plays a positive role in neural stem cells function. In the adult zebrafish brain, acute inflammation is required to activate neuroregeneration, and administration of ani-inflammatory dexamethasone (Dex) impeded the regeneration of lesioned brain (Kyritsis et al., 2012). In the mouse olfactory mucosa, repair of lesioned neuroepithelium was also reliant on the induction of acute inflammation (Chen et al., 2017). In Dex-treated mice with low transcript abundances of proinflammatory cytokines, the proliferation and subsequent differentiation of HBCs were significantly impaired (Chen et al., 2017). Moreover, a three-day treatment of lesioned olfactory mucosa with Dex resulted in a marked reduction in the number of regenerated OSNs in mice (Crisafulli et al., 2018). These lines of evidence indicated that inflammation can directly modulate the regeneration process in neural stem cells.

We previously reported that CuNPs may have an immunosuppression effect on rainbow trout mucosal cells (chapter 4). The results of pathway enrichment analysis showed that genes encoding for proinflammatory chemokines and cytokine signaling were significantly downregulated in the CuNP-treated olfactory mucosa (Fig. 6.1A). The reduced transcript abundances of many pro-inflammatory genes including *IL-1β*, *CCL4*, *CCL19*, *CCL20*, and *CCL25* (Table 6.1), in the CuNP treatment suggest CuNPs may act as an anti-inflammatory treatment in the rainbow trout olfactory mucosa. Previous studies demonstrated a number of metal NPs, including CuNPs, can have anti-inflammatory properties (Agarwal et al., 2019; Thiruvengadam et al., 2019). Blocking of cytokine

signaling is reported as the primary mechanism of anti-inflammation induced by metal NPs (Agarwal et al., 2019).

In addition to the low transcript level of *IL-1β* cytokine in the CuNP treatment, activation of its protein may be impaired by CuNPs. The pro IL-1β needs to be activated by a protein complex known as inflammasome (Liu et al., 2017). The transcript abundances of key components of inflammasomes, including *CASP1*, *NLRP3*, and *MEFV* (encoding pyrin) — which are necessary to cleave the pro IL-1β (Liu et al., 2017; Sharma et al., 2019) — was reduced (Table 6.1). Previous studies have demonstrated that transient inflammation mediated by IL-1β promotes regeneration in zebrafish (Hasegawa et al., 2017; Tsarouchas et al., 2018). Inhibiting pro IL-1β activation by blocking CASP1 activity resulted in weak axonal regeneration in zebrafish spinal cord (Tsarouchas et al., 2018). Moreover, IL-1β has been reported to promote the olfactory stem cells migration in a concentration-dependent manner in rat neuroepithelium (Pu et al., 2018). Hence, the downregulation of *IL-1β* and its activators by CuNPs may inhibit olfactory neuroregeneration.

One of the primary cellular inflammatory pathways is nuclear factor-κB (NF- κB) signaling, which regulates expression of a large array of genes implicated in inflammation including *IL-1β* and *NLRP3*. The NF- κB transcription factors mediate two signaling pathways, non-canonical (a.k.a., NIK/NF- κB signaling) and canonical pathways, which both regulate cellular inflammation despite applying different signalling mechanisms (Liu et al., 2017). The NF- κB transcription factor family composed of five members, including NF-κB1 (P50), NF-κB2 (P52), RELA(P65), RELB, and c-REL which are operating as dimeric complexes activating κB enhancer (Pasparakis, 2009). Pathway enrichment

analysis showed the NIK/NF- κB signaling was over-represented in the CuNP treatment (Fig. 6.1). In the NIK/NF- κB signaling pathway, association of specific ligands with tumor necrosis factor superfamily (TNFR), such as CD40, stimulates the production of mature P52 from its precursor p100 (Sun, 2011). Processing of p100 is mediated by NF- κB-inducing kinase (NIK) which activates an inhibitor of NF- κB kinase (IKK) to subsequently induce phosphorylation and ubiquitination of p100 and generate mature p52 (Sun, 2017). The mature p52 forms a heterodimer complex with RELB and, together, translocate to the nucleus to induce the transcription of target genes, such as *CCL19* (Valiño-Rivas et al., 2016). Figure 6.2A displays that exposure to CuNPs reduced the transcript abundances of *CD40*, *P52* in the NIK/NF- κB signaling pathway. The canonical NF- κB pathway was also affected by CuNPs (Fig. 6.2B). In the canonical NF- κB signaling, different stimuli including cytokines and growth factors activate the IKK to phosphorylate the inhibitor of NF- κB (IκBα) and trigger its degradation. The degradation of IκBα results in nuclear translocation of NF- κB transcription factor dimers (P50/RELA or P50/c-REL) and initiation of target gene transcriptions (e.g., *IL-1β*, *NLRP3*, *CCL4*, *CCL20*). In the CuNP-treated olfactory mucosa, while the mRNA level of *c-REL* was reduced, the expression of *IκBα* was slightly increased (Table 6.1 and Fig. 6.2B). The NF-κB signaling pathway plays a critical role in early stages of neurogenesis. Differentiation of neural stem cells is reliant on the activation of NF-κB signaling, and inhibition of canonical NF-κB signaling can block asymmetric cell division which is essential for proper neurogenesis (Zhang et al., 2012). Moreover, impairment of the canonical NF-κB pathway through deletion of RelA inhibited the neuroregeneration in HBCs (Chen et al., 2017). Impairment of NF-κB signaling pathway may comprise the acute inflammatory responses in the CuNP-treated

olfactory mucosa. Given the importance of acute inflammation in neurogenesis initiation, the downregulation of transcripts associated with canonical and non-canonical NF-κB inflammatory pathways suggests neuroregeneration was inhibited in the CuNP treatment.

In contrast to the CuNP treatment, gene expression of pro-inflammatory cytokines and chemokines remained unchanged in the Cu^{2+} treatment. The expression of *NLRP1b*, an important component of inflammasomes involved in CASP1 activation (de Rivero Vaccari et al., 2014), displayed a significant upregulation in Cu^{2+}-treated fish (Table 6.1). The activation of CASP1 can consequently enhance the pro IL-1β cleavage and induce inflammation. Furthermore, the transcript abundances of *NLR12* and *NLRC3*, that both negatively regulate the NF-κB inflammatory signaling (Tuncer et al., 2014; Gharagozloo et al., 2015), were reduced (Table 6.1). These data suggest that olfactory mucosal cells' inflammatory responses were not inhibited as a result of exposure to Cu^{2+}, and consequently, neurogenesis pathways may be activated.

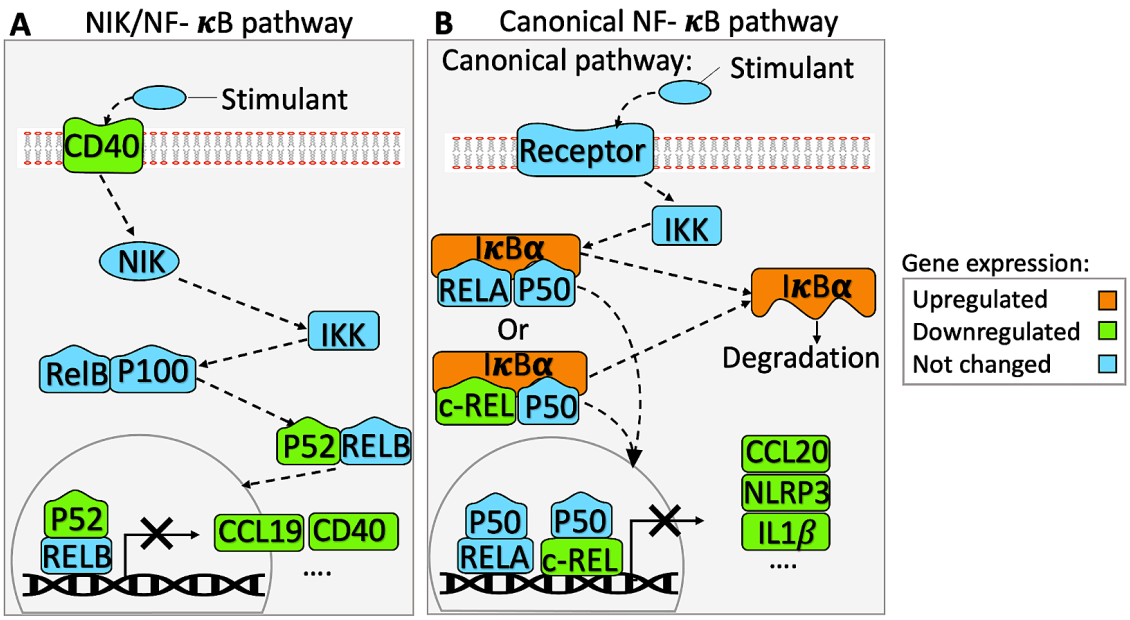

Figure 6.2. Schematic representations of transcriptional alterations in NF-κB signaling pathways following exposure to CuNPs in rainbow trout olfactory mucosa. (A) NIK/NF-κB signaling pathway. (B) canonical NF-κB signaling pathway. The colour-coded legend represents the transcription pattern of the differentially expressed genes.

6.4.3. Effect of Cu contaminants on canonical Wnt/β-catenin signaling pathway

In addition to the suppression of inflammatory signaling, Wnt signaling, one of the major pathways regulating stem cell proliferation and differentiation, was affected by CuNPs (Fig. 6.1). In agreement with our results, a transcript-based study on the lungs of mice exposed to inhalation of copper oxide nanoparticles for two weeks, indicated that the Wnt signaling pathway was significantly enriched (Rossner et al., 2020). Furthermore, copper oxide nanoparticles inhibited the Wnt signaling pathway in prostate cancer cells and attenuated the stemness of cancer cells (Wang et al., 2017b).

Activation of canonical Wnt/β-catenin pathway promotes neurogenesis in the olfactory epithelium (Wang et al., 2011). In GBCs, Wnt/β-catenin pathway plays a key role in maintaining proliferation and promoting neuroregeneration (Chen et al., 2014).

Moreover, the activation of Wnt/β-catenin signaling was both necessary and sufficient to switch the HBCs from a resting state to an activated neurogenic state (Fletcher et al., 2017). In the Wnt/β-catenin pathway, when the Wnt ligand is present, β-catenin relocates from cytoplasm to the nucleus, where it binds to the TCF/LEF transcription factor to promote the expression of many genes involved in cell proliferation (Bengoa-Vergniory and Kypta, 2015). Inhibition of the Wnt/β-catenin signaling through disruption of β-catenin/TCF complex transcriptional activity prevented the regeneration of injured olfactory epithelium (Wang et al., 2011). Following exposure to CuNPs, there was a considerable reduction in the expression of *TCF7L2*, which is a downstream effector of the Wnt pathway (Table 6.1 and Fig. 6.3A). The *TCF7L2* gene expression analysis by qPCR confirmed the result of RNA-seq (Fig. 6.3B). Of the 4 members of the TCF/LEF transcription factor family, TCF7L2 was the most expressed transcription factor in the mouse's entire olfactory epithelium, which had a dense expression in basal stem cells (Wang et al., 2011). In zebrafish, TCF7L2 positively regulated the Wnt/β-catenin pathway in midbrain, and TCF/LEF transcription factors contributed in the homeostasis of olfactory epithelium (Shimizu et al., 2012). As a result of the *TCF7L2* downregulation, the neuroregeneration might be reduced in the CuNP-treated fish.

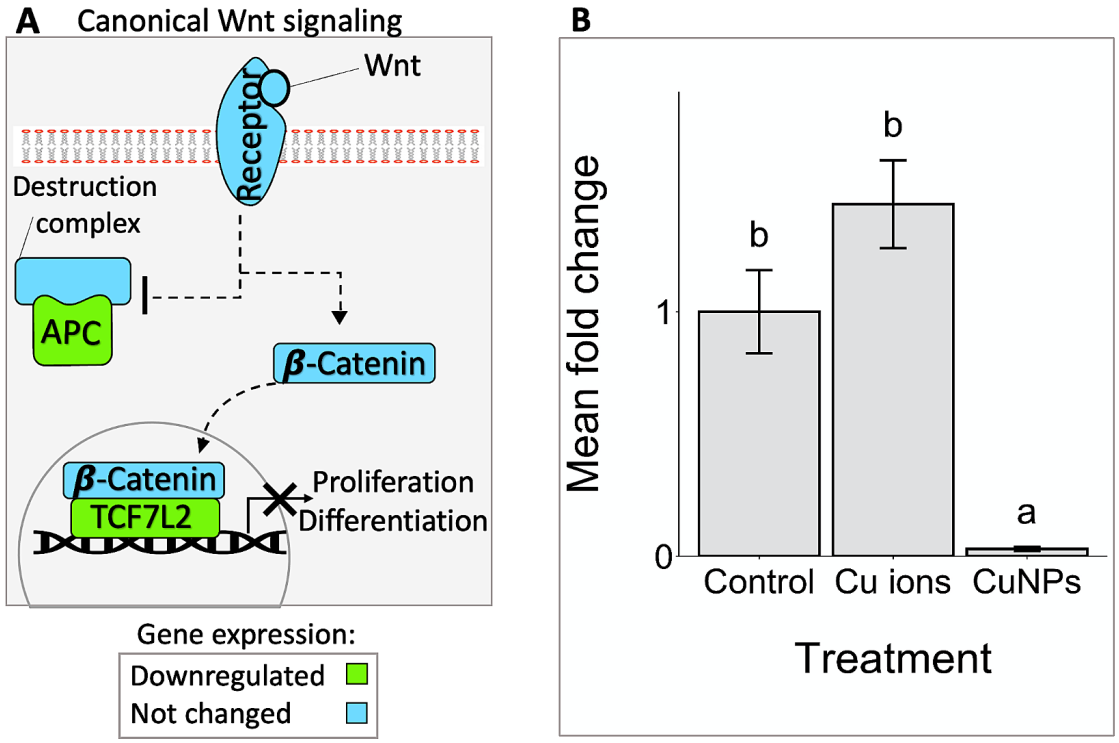

Figure 6.3. Effect of CuNPs on the transcription of genes involved in canonical Wnt signaling pathway in the rainbow trout olfactory mucosa. (A) Schematic representation of canonical Wnt signaling pathway in the CuNP treatment. The colour-coded legend represents the transcription pattern of the differentially expressed genes. (B) The relative expression of *TCF7L2* in response to different Cu treatments in the olfactory mucosa. The gene expression was measured by qPCR. Lower-case letters indicate significant differences ($p \leq 0.05$, error bars ± 1 SEM).

In the absence of Wnt, β-catenin is actively degraded by a destruction complex in the cytoplasm, which consequently diminishes the expression of target genes. One of the components of the β-catenin destruction complex is APC (a tumor suppression factor) (Fig. 6.3A). The APC is a multifunctional protein that not only mediates stem cell maintenance through the regulation of cytoplasm β-catenin, but also promotes neuronal differentiation. Deletion of APC in adult neural stem cells can exhaust the germinal zone and disturb differentiation and migration of neuroblasts in the olfactory bulb (Imura et al., 2010). Our results indicated a serious depletion of *APC* transcript level in the CuNP treatment (Table

6.1 and Fig. 6.3A). The reduced transcript abundances of *TCF7L2* and *APC*, which are involved in the positive and negative regulation of Wnt/β-catenin pathway, respectively, suggests that neurogenesis was disrupted in the CuNP-treated olfactory mucosa. In contrast to the CuNP treatment, there was a significant increase in the mRNA of *APC* in the Cu^{2+} treatment (Table 6.1). These data suggest that CuNPs and Cu^{2+} distinctly influenced neurogenesis-related processes in olfactory mucosa.

Table 6.1. List of differentially expressed genes that regulate repair mechanisms in the rainbow trout olfactory mucosa following exposure to CuNPs or Cu^{2+}. Gene expression was analysed by RNA-seq. * indicates significant expression relative to the control and "Inf" indicates > 150-fold change

Biological process	Gene name	Fold change in CuNPs	Fold change in Cu^{2+}
Inflammatory response	Interleukin-1 beta (*IL-1β*)	0.3 *	0.9
	C-C motif chemokine 4 (*CCL4*)	0.3 *	0.5
	C-C motif chemokine 19 (*CCL19*)	0.4 *	0.8
	C-C motif chemokine 20 (*CCL20*)	0.2 *	0.7
	C-C motif chemokine 25 (*CCL25*)	0.6 *	1
	Caspase-1 (*CASP1*)	0.7 *	0.9
	NACHT, LRR and PYD domains-containing protein 3 (*NLRP3*)	0.8 *	1
	Pyrin (*MEFV*)	0.2 *	1
	Proto-oncogene c-Rel; (*c-REL*)	0.6 *	1
	NF-kappa-B inhibitor alpha (*IκBα*)	1.2 *	0.9

	NF-kappa-B p100 subunit (*NF-κB2* or *P52*)	0.8 *	1.1
	Tumor necrosis factor receptor superfamily member 5 (*TNR5* or *CD40*)	0.7 *	1
	NACHT, LRR and PYD domains-containing protein 1b (*NLRP1b*)	0.9	5 *
	NACHT, LRR and PYD domains-containing protein 12 (*NLRP12*)	1.2	0.5 *
	NLR family CARD domain containing 3 (*NLRC3*)	0.8	0.5 *
Wnt/β-catenin signaling	Transcription factor 7-like 2 (*TCF7L2*)	0 *	2
	Adenomatous polyposis coli protein (*APC*)	0 *	10.2 *
Neurogenesis	Paired box protein Pax-6 (*PAX6*)	0.2 *	1.6 *
	LIM/homeobox protein Lhx2 (*LHX2*)	0.7 *	1.7 *
	GATA-binding factor 3 (*GATA3*)	0.6 *	0.9
	Pre-B-cell leukemia transcription factor 1 (*PBX1*)	1.4	4.1 *
	Homeobox protein OTX1 (*OTX1*)	0.7	1.4 *
	Transcription factor SOX-2 (*SOX2*)	0.9	1.3 *
	Transcription factor SP8 (*SP8*)	1	1.4 *
Axonogenesis	Serpin family E member 1 (*SERPINE1*)	14.5 *	1.4
	Secreted protein acidic and cysteine rich (*SPARC*)	1.5 *	1
	A disintegrin and metalloproteinase with thrombospondin motifs 1 (*ADAMTS1*)	2.8 *	1

Fibroblast growth factor receptor 2 (*FGFR2*)	Inf *	0.7
Mesothelin-like protein (*MSLN*)	9.2 *	9.7 *
Fibronectin (*FINC*)	1.9 *	1.4
Neural-cadherin (*N-CAD* or *CDH2*)	0.6 *	0.8
Neural cell adhesion molecule 1 (*NCAM1*)	0.2 *	0.8
Netrin-1 (*NTN1*)	1.7 *	1.4
Ephrin type-A receptor 4 (*EPHA4*)	2.1 *	0.8
N-acetyllactosaminide beta-1,3-N-acetylglucosaminyltransferase (*β3GNT1*)	2.5 *	1.3
Transcription factor AP-1 (*JUN*)	0.2 *	0.7
Partitioning defective 3 homolog (*PAR3*)	0 *	2.7 *
Biogenesis of lysosome-related organelles complex 1 subunit 1 (*BLOC1S1*)	1.1	1.5 *
Epidermal growth factor receptor substrate 15 (*EPS15L1*)	0.9	Inf *
Phosphatidylinositol-binding clathrin assembly protein (CALM)	2.2	33.3 *
Ras-related protein Rab-3A (*RAB3*)	1	1.5 *
Ras-related protein Rab-10 (*RAB10*)	1	1.4 *
Roundabout Homolog 2 (*ROBO2*)	0.9	1.5 *
T-lymphoma invasion and metastasis-inducing protein 1 (*TIAM1*)	1.2	1.6 *

Microtubule-associated protein 1A (*MAP1A*)	1.2	1.7 *
Microtubule-associated protein 1B (*MAP1B*)	1	1.7 *
Tripartite motif-containing protein 46 (*TRIM46*)	1	2.1 *

6.4.4. Effect of CuNPs and Cu^{2+} on transcription factors associated with olfactory neurogenesis

Transcription factors (TFs) play critical roles in olfactory neuroregeneration (Shetty et al., 2005; Nicolay et al., 2006). In each stage of neurogenesis, specific TFs are activated to mediate and regulate differentiation in the olfactory mucosa. One of the key transcription factors involved in olfactory epithelium development and neuroregeneration is PAX6 (Davis and Reed, 1996; Collinson et al., 2003; Suzuki et al., 2015). The expression of PAX6 was reported in proliferating GBCs in normal and lesioned olfactory epithelium of adult rat (Guo et al., 2010). Deletion of PAX6 in HBCs has resulted in a thinner olfactory epithelial layer with reduced numbers of OSNs in mice (Suzuki et al., 2015). In our study, we observed a 6-fold reduction in the expression of *PAX6* following exposure to CuNPs (Table 6.1). A previous study also demonstrated that the PAX6 protein expression was reduced in the brain of zebrafish embryos that were exposed to copper oxide nanoparticles (Xu et al., 2017). PAX6 has been shown as a downstream target of the β-catenin-TCF transcriptional complex in the Wnt/β-catenin pathway; the β-catenin-TCF complex binds

to the PAX6 promoter and induces its expression (Gan et al., 2014). Given that the expression of *TCF7L2* was severely repressed in the CuNP treatment, and the reduced expression of *PAX6,* the observed reduction of neurogenesis is plausible in CuNP-exposed olfactory mucosa. Additionally, the expression of *LhX2* — a transcription factor engaged in the formation of mature OSNs (Kolterud et al., 2004; Berghard et al., 2012) — was also downregulated following exposure to CuNPs (Table 6.1). Another downregulated TF in the CuNP treatment is *GATA3*, which is an essential TF to initiate stem cells proliferation in adult zebrafish brain (Kizil et al., 2012). The downregulated expression of neurogenesis-related TFs suggested neuroregeneration was impaired in the CuNP treatment.

In contrast to the CuNP-exposed fish, a number of TFs that regulate neurogenesis were significantly upregulated following the exposure to Cu^{2+}. For instance, the expression of both *PAX6* and *LhX2* transcription factors were increased in the olfactory mucosa of the Cu^{2+}-exposed fish (Table 6.1). Besides the *PAX6* and *LhX2*, which belong to the homeobox genes, the expression of two other genes from this group, *PBX1* and *OTX1*, were also upregulated (Table 6.1). The transcriptional activity of both PBX1 (Grebbin and Schulte, 2017) and OTX1 (Heron et al., 2013; Pirrone et al., 2017) regulate neuroregeneration in the olfactory mucosa. Another neurogenesis master TF is *SOX2* (Sokpor et al., 2018), which was significantly induced by Cu^{2+} (Table 6.1). In the absence of SOX2 in HBCs, while the formation of a neuronal lineage was inhibited, the production of non-neural (i.e., sustentacular) cells was not affected. Hence, the regeneration of OSNs relies on SOX2 activity in an injured olfactory epithelium (Gadye et al., 2017). Zinc finger transcription factor *SP8*, which is involved with the development of olfactory epithelium and the olfactory bulb (Waclaw et al., 2006; Kasberg et al., 2013), was also upregulated in the Cu^{2+}

treatment (Table 6.1). The induced gene expression of these neurogenesis-related TFs suggested that neuroregeneration could be initiated in Cu^{2+}-treated olfactory mucosa.

6.4.5. Effect of CuNPs on axonogenesis in the olfactory mucosa

Axonogenesis is an important stage of neural development that ultimately builds a functional connection between new neurons and target cells. In the peripheral nervous system, axonal regeneration mediates functional recovery after injury (He and Jin, 2016). When axon regeneration is initiated, the axon outgrowth will be guided to the olfactory bulb. Following the axons' exit from the olfactory epithelium to the lamina propria, OECs wrap the axons, promote axonal projection, and guide the growth cone to the olfactory bulb (Su and He, 2010). The OECs produce many signaling cues, including growth factors and cell adhesion molecules which facilitate axon regeneration (Roet and Verhaagen, 2014). Following exposure to CuNPs, the OECs altered the olfactory lamina propria microenvironment mostly in favour of axon regeneration. In fact, the expression of neurite outgrowth promoters, which are secreted from OECs, including *SERPINE1*, *SPARC*, *ADAMTS1*, *FGFR2*, *MSLN*, and *FINC* (Roet et al., 2013; Lin et al., 2019), were upregulated (Table 6.1). However, the expression of two cell adhesion molecules (i.e., *NCAM1* and *CDH2* (a.k.a., *N-CAD*)), which can be produced by OEC to promote the axon outgrowth (Rigby et al., 2020), were significantly decreased in the CuNP-exposed fish (Table 6.1). These cell adhesion molecules, which are expressed at the surface of OECs, facilitate the attachment of axon growth cones to the migrating OECs moving toward olfactory bulb (Rigby et al., 2020). In addition to the OEC-derived signaling molecules, axon development is also regulated by intrinsic signals (He and Jin, 2016; Mahar and Cavalli, 2018). For instance, the expression of *NTN1* (Astic et al., 2002; Lakhina et al.,

2012), *EPHA4* (John et al., 2002), *β3GNT1* (Henion et al., 2005), which are all involved in axonal pathfinding, was upregulated following exposure to CuNPs (Table 6.1). These data revealed that axonogenesis regulators endeavor to repair the axonal impairment that may have been induced by CuNPs.

Neurons are highly polarized (i.e., asymmetric) cells which usually have a single long axon. Polarity signaling pathways in the axon establish asymmetry in growth cones and control the direction of axon growth (Zou, 2012, 2020). Axon polarity during development and regeneration is regulated by signaling molecules and intracellular mechanisms which are actively interacting to mediate polarity (Arimura and Kaibuchi, 2007; Stone et al., 2010). The non-canonical Wnt/planar cell polarity (PCP) pathway plays a crucial role in regulating epithelial cells' polarity and axonal growth cone guidance (Zou, 2020). In the PCP pathway, the Wnt ligand will bind to its receptor and induce a cascade of events that ultimately activates the JNK pathway (Winter et al., 2001; Zhang et al., 2012). The JNK signaling pathway regulates the expression of axonal regeneration and polarity related genes (Stone et al., 2010; Hirai et al., 2011; Kawasaki et al., 2018). The expression of *JUN*, which is a TF involved in JNK pathway, was significantly downregulated in the CuNP treatment (Table 6.1). Moreover, there is molecular crosstalk between PCP and other pathways driving axonal polarity, including the PAR complex (aPKC-PAR6-Par3) (Zou, 2012; Chuykin et al., 2018). The interaction of PCP and PAR will increase axonal polarity. The transcript abundance of *PAR3*, which serves as one key mediator of the PAR complex, was diminished following exposure to CuNPs (Table 6.1). These data indicated that polarity mechanisms involved in axonogenesis may be impaired by CuNPs.

Regulating the expression of axonal sprouting and guidance genes is a key step in axon regeneration (McIntyre et al., 2010; He and Jin, 2016). In this study, the upregulated extrinsic and intrinsic axon regrowth and guidance genes may prime the olfactory neuronal axons to regenerate following exposure to CuNPs. Nevertheless, the reduction of cell adhesion molecules (i.e., *NCAM1* and *CDH2*) and polarity regulating genes (i.e., *JUN* and *PAR3*) transcript levels may limit the axonal outgrowth competency in the CuNP treatment. Further investigations are required to determine if axon regeneration is initiated in the CuNP treatment.

6.4.6. Effect of Cu^{2+} on axonogenesis in the olfactory mucosa

In the Cu^{2+} treatment, *MSLN* was the only altered OEC-derived gene that was significantly upregulated. The MSLN is a glycoprotein that is produced by OECs to make the extracellular matrix suitable for axon growth (Roet et al., 2013). Although the OEC-driven axonogenesis was induced more by CuNPs than Cu^{2+}, the transcript abundances of a number of intrinsic regulators of axonogenesis were increased in the Cu^{2+}-exposed olfactory mucosa. Axonal outgrowth is highly dependent on intact intracellular trafficking to deliver essential cargo to the growing axon (McCormick and Gupton, 2020). A multi-subunit protein, BLOC1, is an important component of the cell membrane and of vesicular trafficking in the developing axon (McCormick and Gupton, 2020). Neurons deficient in BLOC1 demonstrated insufficient neurite outgrowth in the hippocampus (Ghiani et al., 2010). The expression of BLOC1 subunit 1 (*BLOC1S1*) was significantly increased in the Cu^{2+} treatment (Table 6.1). Additionally, two endocytic accessory proteins, *EPS15L1* (a.k.a., EPS*15R*) and *CALM*, which participate in intracellular trafficking (Moore and Baleja, 2012), were highly transcribed in the Cu^{2+} treatment. The expression of vesicular

trafficking genes, including *RAB3A* and *RAB10* which regulate synaptic vesicle cycling (Pavlos et al., 2010), were also increased in the Cu^{2+}-exposed fish.

In order to have functional neural wiring in the olfactory system, the polarity and pathfinding mediators must accurately guide the neurons' axons to the olfactory bulb. One of the axonal pathfinding genes is *ROBO2*, which was upregulated in the Cu^{2+} treatment (Table 6.1). Previous studies have suggested that the knockout of ROBO2 in the OSNs can lead to axonal mistargeting in the OB (Miyasaka et al., 2005; Cho et al., 2007). Moreover, the expression of *PAR3* was significantly increased in Cu^{2+}-exposed mucosal cells (Table 6.1). Another important polarity regulation protein in the axonal growth cone is a guanine nucleotide exchange factor named TIAM1 (Montenegro-Venegas et al., 2010). The expression of *TIAM1* was also upregulated following the Cu^{2+} exposure (Table 6.1). The PAR complex (specifically PAR3) has been reported to form a complex with TIAM1 and regulates neural polarization (Zhang and Macara, 2006). The gene expression of two microtubule-associated proteins involved in axon formation and polarization, MAP1A and MAP1B (Halpain and Dehmelt, 2006), were increased in the Cu^{2+} treatment (Table 6.1). The MAP1B plays a role in axonal elongation and neural migration (Takei et al., 2000). In addition, the interaction of MAP1B and TIAM1 is fundamental to regulating polarity in axonogenesis (Montenegro-Venegas et al., 2010). Furthermore, *TRIM46*, which organizes microtubules trafficking and orientation and, consequently, regulates polarity in axons, was upregulated in the Cu^{2+} treatment (Rao et al., 2017). This upregulation of of axonogenesis-related gene transcripts in the Cu^{2+}-exposed olfactory mucosa revealed that the intrinsic neural mechanisms were in play to fulfill the axonal outgrowth requirements in the Cu^{2+}-treated fish.

6.5. Conclusions

This study provides insight into impacts of CuNPs and Cu^{2+} on the neural repair mechanisms in rainbow trout olfactory mucosa. The transcript profile of olfactory mucosa indicated that CuNPs had more inhibitory influences on neuroregeneration mechanisms relative to axonal repair mechanisms. The transcripts of many extrinsic and intrinsic neurogenesis regulators were reduced by CuNPs. The inhibition of neuroregeneration reduces the likelihood of olfactory recovery in CuNP-exposed fish. Nonetheless, exposure to CuNPs induced molecular responses that mostly promote axon regeneration in olfactory mucosa. The functionality of axonal repair in the CuNP treatment needs to be investigated further. In the Cu^{2+} treatment, the upregulated transcripts of many genes directing neurogenesis and axonogenesis reflects that both reparative mechanisms were activated. These results can explain the previously observed functional recovery of Cu^{2+}-exposed OSNs over the 96-h exposure period in rainbow trout. Given that CuNPs may impair the OSN function and reconstitution, development of a water quality criterion to protect fish against CuNPs is warranted.

6.6. References

Aegerter, S., Jalabert, B., Bobe, J., 2005. Large scale real-time PCR analysis of mRNA abundance in rainbow trout eggs in relationship with egg quality and post-ovulatory ageing. Molecular Reproduction and Development: Incorporating Gamete Research 72, 377-385.

Agarwal, H., Nakara, A., Shanmugam, V.K., 2019. Anti-inflammatory mechanism of various metal and metal oxide nanoparticles synthesized using plant extracts: A review. Biomedicine & Pharmacotherapy 109, 2561-2572.

Andrews, S., 2020. FastQC: a quality control tool for high throughput sequence data. 2010.

Arimura, N., Kaibuchi, K., 2007. Neuronal polarity: from extracellular signals to intracellular mechanisms. Nature Reviews Neuroscience 8, 194-205.

Ashraf, P.M., Sasikala, K., Thomas, S.N., Edwin, L., 2017. Biofouling resistant polyethylene cage aquaculture nettings: A new approach using polyaniline and nano copper oxide. Arabian Journal of Chemistry 13, 875-882.

Astic, L., Pellier-Monnin, V., Saucier, D., Charrier, C., Mehlen, P., 2002. Expression of netrin-1 and netrin-1 receptor, DCC, in the rat olfactory nerve pathway during development and axonal regeneration. Neuroscience 109, 643-656.

Bengoa-Vergniory, N., Kypta, R.M., 2015. Canonical and noncanonical Wnt signaling in neural stem/progenitor cells. Cellular and Molecular Life Sciences 72, 4157-4172.

Berghard, A., Hägglund, A.C., Bohm, S., Carlsson, L., 2012. Lhx2-dependent specification of olfactory sensory neurons is required for successful integration of olfactory, vomeronasal, and GnRH neurons. The FASEB Journal 26, 3464-3472.

Chang, S.Y., Glezer, I., 2018. The balance between efficient anti-inflammatory treatment and neuronal regeneration in the olfactory epithelium. Neural Regeneration Research 13, 1711.

Chari, N., Felix, L., Davoodbasha, M., Ali, A.S., Nooruddin, T., 2017. In vitro and in vivo antibiofilm effect of copper nanoparticles against aquaculture pathogens. Biocatalysis and Agricultural Biotechnology 10, 336-341.

Chen, M., Reed, R.R., Lane, A.P., 2017. Acute inflammation regulates neuroregeneration through the NF-κB pathway in olfactory epithelium. Proceedings of the National Academy of Sciences 114, 8089-8094.

Chen, M., Reed, R.R., Lane, A.P., 2019. Chronic inflammation directs an olfactory stem cell functional switch from neuroregeneration to immune defense. Cell Stem Cell 25, 501-513. e505.

Chen, M., Tian, S., Yang, X., Lane, A.P., Reed, R.R., Liu, H., 2014. Wnt-responsive Lgr5+ globose basal cells function as multipotent olfactory epithelium progenitor cells. Journal of Neuroscience 34, 8268-8276.

Cho, J.H., Lépine, M., Andrews, W., Parnavelas, J., Cloutier, J.-F., 2007. Requirement for Slit-1 and Robo-2 in zonal segregation of olfactory sensory neuron axons in the main olfactory bulb. Journal of Neuroscience 27, 9094-9104.

Choi, R., Goldstein, B.J., 2018. Olfactory epithelium: cells, clinical disorders, and insights from an adult stem cell niche. Laryngoscope Investigative Otolaryngology 3, 35-42.

Chuykin, I., Ossipova, O., Sokol, S.Y., 2018. Par3 interacts with Prickle3 to generate apical PCP complexes in the vertebrate neural plate. Elife 7, e37881.

Collinson, J.M., Quinn, J.C., Hill, R.E., West, J.D., 2003. The roles of Pax6 in the cornea, retina, and olfactory epithelium of the developing mouse embryo. Developmental Biology 255, 303-312.

Crisafulli, U., Xavier, A.M., dos Santos, F.B., Cambiaghi, T.D., Chang, S.Y., Porcionatto, M., Castilho, B.A., Malnic, B., Glezer, I., 2018. Topical dexamethasone administration impairs protein synthesis and neuronal regeneration in the olfactory epithelium. Frontiers in Molecular Neuroscience 11, 50.

Davis, J.A., Reed, R.R., 1996. Role of Olf-1 and Pax-6 transcription factors in neurodevelopment. Journal of Neuroscience 16, 5082-5094.

de Rivero Vaccari, J.P., Dietrich, W.D., Keane, R.W., 2014. Activation and regulation of cellular inflammasomes: gaps in our knowledge for central nervous system injury. Journal of Cerebral Blood Flow & Metabolism 34, 369-375.

Dobin, A., Davis, C.A., Schlesinger, F., Drenkow, J., Zaleski, C., Jha, S., Batut, P., Chaisson, M., Gingeras, T.R., 2013. STAR: ultrafast universal RNA-seq aligner. Bioinformatics 29, 15-21.

El Basuini, M., El-Hais, A., Dawood, M., Abou-Zeid, A.S., El-Damrawy, S., Khalafalla, M.S., Koshio, S., Ishikawa, M., Dossou, S., 2017. Effects of dietary copper nanoparticles and vitamin C supplementations on growth performance, immune response and stress resistance of red sea bream, *Pagrus major*. Aquaculture Nutrition 23, 1329-1340.

Fletcher, R.B., Das, D., Gadye, L., Street, K.N., Baudhuin, A., Wagner, A., Cole, M.B., Flores, Q., Choi, Y.G., Yosef, N., 2017. Deconstructing olfactory stem cell trajectories at single-cell resolution. Cell stem cell 20, 817-830. e818.

Gadye, L., Das, D., Sanchez, M.A., Street, K., Baudhuin, A., Wagner, A., Cole, M.B., Choi, Y.G., Yosef, N., Purdom, E., 2017. Injury activates transient olfactory stem cell states with diverse lineage capacities. Cell Stem Cell 21, 775-790. e779.

Gan, Q., Lee, A., Suzuki, R., Yamagami, T., Stokes, A., Nguyen, B.C., Pleasure, D., Wang, J., Chen, H.W., Zhou, C.J., 2014. Pax6 mediates ss-catenin signaling for self-renewal and neurogenesis by neocortical radial glial stem cells. Stem Cells 32, 45-58.

Gharagozloo, M., Mahvelati, T.M., Imbeault, E., Gris, P., Zerif, E., Bobbala, D., Ilangumaran, S., Amrani, A., Gris, D., 2015. The nod-like receptor, Nlrp12, plays an anti-inflammatory role in experimental autoimmune encephalomyelitis. Journal of Neuroinflammation 12, 1-13.

Ghiani, C., Starcevic, M., Rodriguez-Fernandez, I., Nazarian, R., Cheli, V., Chan, L., Malvar, J., De Vellis, J., Sabatti, C., Dell'Angelica, E., 2010. The dysbindin-containing complex (BLOC-1) in brain: developmental regulation, interaction with SNARE proteins and role in neurite outgrowth. Molecular Psychiatry 15, 204-215.

Götz, S., García-Gómez, J.M., Terol, J., Williams, T.D., Nagaraj, S.H., Nueda, M.J., Robles, M., Talón, M., Dopazo, J., Conesa, A., 2008. High-throughput functional annotation and data mining with the Blast2GO suite. Nucleic Acids Research 36, 3420-3435.

Graziadei, G.M., Graziadei, P.P.C., 1979. Neurogenesis and neuron regeneration in the olfactory system of mammals. II. Degeneration and reconstitution of the olfactory sensory neurons after axotomy. Journal of Neurocytology 8, 197-213.

Grebbin, B.M., Schulte, D., 2017. PBX1 as pioneer factor: a case still open. Frontiers in Cell and Developmental Biology 5, 9.

Guo, Z., Packard, A., Krolewski, R.C., Harris, M.T., Manglapus, G.L., Schwob, J.E., 2010. Expression of pax6 and sox2 in adult olfactory epithelium. Journal of Comparative Neurology 518, 4395-4418.

Halpain, S., Dehmelt, L., 2006. The MAP1 family of microtubule-associated proteins. Genome Biology 7, 224.

Hasegawa, T., Hall, C.J., Crosier, P.S., Abe, G., Kawakami, K., Kudo, A., Kawakami, A., 2017. Transient inflammatory response mediated by interleukin-1β is required for proper regeneration in zebrafish fin fold. Elife 6, e22716.

He, Z., Jin, Y., 2016. Intrinsic control of axon regeneration. Neuron 90, 437-451.

Henion, T.R., Raitcheva, D., Grosholz, R., Biellmann, F., Skarnes, W.C., Hennet, T., Schwarting, G.A., 2005. β1, 3-N-acetylglucosaminyltransferase 1 glycosylation is required for axon pathfinding by olfactory sensory neurons. Journal of Neuroscience 25, 1894-1903.

Heron, P.M., Stromberg, A.J., Breheny, P., McClintock, T.S., 2013. Molecular events in the cell types of the olfactory epithelium during adult neurogenesis. Molecular Brain 6, 49.

Hirai, S.-i., Banba, Y., Satake, T., Ohno, S., 2011. Axon Formation in Neocortical Neurons Depends on Stage-Specific Regulation of Microtubule Stability by the Dual Leucine Zipper Kinase–c-Jun N-Terminal Kinase Pathway. Journal of Neuroscience 31, 6468-6480.

Imura, T., Wang, X., Noda, T., Sofroniew, M.V., Fushiki, S., 2010. Adenomatous polyposis coli is essential for both neuronal differentiation and maintenance of adult neural stem cells in subventricular zone and hippocampus. Stem Cells 28, 2053-2064.

John, J.A.S., Pasquale, E.B., Key, B., 2002. EphA receptors and ephrin-A ligands exhibit highly regulated spatial and temporal expression patterns in the developing olfactory system. Developmental Brain Research 138, 1-14.

Kasberg, A.D., Brunskill, E.W., Potter, S.S., 2013. SP8 regulates signaling centers during craniofacial development. Developmental Biology 381, 312-323.

Kawasaki, A., Okada, M., Tamada, A., Okuda, S., Nozumi, M., Ito, Y., Kobayashi, D., Yamasaki, T., Yokoyama, R., Shibata, T., 2018. Growth cone phosphoproteomics reveals that GAP-43 phosphorylated by JNK is a marker of axon growth and regeneration. iScience 4, 190-203.

Kermen, F., Franco, L.M., Wyatt, C., Yaksi, E., 2013. Neural circuits mediating olfactory-driven behavior in fish. Frontiers in Neural Circuits 7, 62.

Kizil, C., Kyritsis, N., Brand, M., 2015. Effects of inflammation on stem cells: together they strive? EMBO Reports 16, 416-426.

Kizil, C., Kyritsis, N., Dudczig, S., Kroehne, V., Freudenreich, D., Kaslin, J., Brand, M., 2012. Regenerative neurogenesis from neural progenitor cells requires injury-induced expression of Gata3. Developmental Cell 23, 1230-1237.

Kolterud, Å., Alenius, M., Carlsson, L., Bohm, S., 2004. The Lim homeobox gene Lhx2 is required for olfactory sensory neuron identity. Development 131, 5319-5326.

Kyritsis, N., Kizil, C., Zocher, S., Kroehne, V., Kaslin, J., Freudenreich, D., Iltzsche, A., Brand, M., 2012. Acute inflammation initiates the regenerative response in the adult zebrafish brain. Science 338, 1353-1356.

Laberge, F., Hara, T.J., 2001. Neurobiology of fish olfaction: a review. Brain Research Reviews 36, 46-59.

Lakhina, V., Marcaccio, C.L., Shao, X., Lush, M.E., Jain, R.A., Fujimoto, E., Bonkowsky, J.L., Granato, M., Raper, J.A., 2012. Netrin/DCC signaling guides olfactory sensory axons to their correct location in the olfactory bulb. Journal of Neuroscience 32, 4440-4456.

Lin, N., Dong, X.J., Wang, T.Y., He, W.J., Wei, J., Wu, H.Y., Wang, T.H., 2019. Characteristics of olfactory ensheathing cells and microarray analysis in Tupaia belangeri (Wagner, 1841). Molecular Medicine Reports 20, 1819-1825.

Liu, T., Zhang, L., Joo, D., Sun, S.-C., 2017. NF-κB signaling in inflammation. Signal Transduction and Targeted Therapy 2, 1-9.

Love, M.I., Huber, W., Anders, S., 2014. Moderated estimation of fold change and dispersion for RNA-seq data with DESeq2. Genome Biology 15, 550.

Ma, E.Y., Heffern, K., Cheresh, J., Gallagher, E.P., 2018. Differential copper-induced death and regeneration of olfactory sensory neuron populations and neurobehavioral function in larval zebrafish. Neurotoxicology 69, 141-151.

Mahar, M., Cavalli, V., 2018. Intrinsic mechanisms of neuronal axon regeneration. Nature Reviews Neuroscience 19, 323-337.

Malhotra, N., Ger, T.-R., Uapipatanakul, B., Huang, J.-C., Chen, K.H.-C., Hsiao, C.-D., 2020. Review of Copper and Copper Nanoparticle Toxicity in Fish. Nanomaterials 10, 1126.

McCormick, L.E., Gupton, S.L., 2020. Mechanistic advances in axon pathfinding. Current Opinion in Cell Biology 63, 11-19.

McIntyre, J.C., Titlow, W.B., McClintock, T.S., 2010. Axon growth and guidance genes identify nascent, immature, and mature olfactory sensory neurons. Journal of Neuroscience Research 88, 3243-3256.

Miyasaka, N., Sato, Y., Yeo, S.-Y., Hutson, L.D., Chien, C.-B., Okamoto, H., Yoshihara, Y., 2005. Robo2 is required for establishment of a precise glomerular map in the zebrafish olfactory system. Development 132, 1283-1293.

Montenegro-Venegas, C., Tortosa, E., Rosso, S., Peretti, D., Bollati, F., Bisbal, M., Jausoro, I., Avila, J., Cáceres, A., Gonzalez-Billault, C., 2010. MAP1B regulates axonal development by modulating Rho-GTPase Rac1 activity. Molecular Biology of the Cell 21, 3518-3528.

Moore, F.B., Baleja, J.D., 2012. Molecular remodeling mechanisms of the neural somatodendritic compartment. Biochimica et Biophysica Acta (BBA)-Molecular Cell Research 1823, 1720-1730.

Nicolay, D.J., Doucette, J.R., Nazarali, A.J., 2006. Transcriptional regulation of neurogenesis in the olfactory epithelium. Cellular and Molecular Neurobiology 26, 801-819.

Pasparakis, M., 2009. Regulation of tissue homeostasis by NF-κB signalling: implications for inflammatory diseases. Nature Reviews Immunology 9, 778-788.

Pavlos, N.J., Grønborg, M., Riedel, D., Chua, J.J., Boyken, J., Kloepper, T.H., Urlaub, H., Rizzoli, S.O., Jahn, R., 2010. Quantitative analysis of synaptic vesicle Rabs uncovers distinct yet overlapping roles for Rab3a and Rab27b in Ca2+-triggered exocytosis. Journal of Neuroscience 30, 13441-13453.

Pertea, M., Pertea, G.M., Antonescu, C.M., Chang, T.-C., Mendell, J.T., Salzberg, S.L., 2015. StringTie enables improved reconstruction of a transcriptome from RNA-seq reads. Nature Biotechnology 33, 290-295.

Pfaffl, M.W., 2001. A new mathematical model for relative quantification in real-time RT–PCR. Nucleic Acids Research 29, e45-e45.

Pirrone, C., Chiaravalli, A.M., Marando, A., Conti, A., Rainero, A., Pistochini, A., Curto, F.L., Pasquali, F., Castelnuovo, P., Capella, C., 2017. OTX1 and OTX2 as possible molecular markers of sinonasal carcinomas and olfactory neuroblastomas. European Journal of Histochemistry: EJH 61.

Polakof, S., Médale, F., Skiba-Cassy, S., Corraze, G., Panserat, S., 2010. Molecular regulation of lipid metabolism in liver and muscle of rainbow trout subjected to acute and chronic insulin treatments. Domestic Animal Endocrinology 39, 26-33.

Pu, Y., Liu, H., Xu, H., Liu, H., Cheng, Y., Chen, X., Xu, W., Xu, Y., Fan, J., 2018. IL-1β promotes the migration of olfactory epithelium neural stem cells through activating matrix metalloproteinase expressions. Pathology-Research and Practice 214, 1210-1217.

R Core Team, 2019. A language and environment for statistical computing. R Foundation for Statistical Computing, Vienna, Austria2014. in: Team, R.C. (Ed.).

Rao, A.N., Patil, A., Black, M.M., Craig, E.M., Myers, K.A., Yeung, H.T., Baas, P.W., 2017. Cytoplasmic dynein transports axonal microtubules in a polarity-sorting manner. Cell reports 19, 2210-2219.

Razmara, P., Lari, E., Mohaddes, E., Zhang, Y., Goss, G.G., Pyle, G.G., 2019. The effect of copper nanoparticles on olfaction in rainbow trout (*Oncorhynchus mykiss*). Environmental Science: Nano 6, 2094-2104.

Rigby, M.J., Gomez, T.M., Puglielli, L., 2020. Glial Cell-Axonal Growth Cone Interactions in Neurodevelopment and Regeneration. Frontiers in Neuroscience 14, 203.

Roet, K.C., Franssen, E.H., de Bree, F.M., Essing, A.H., Zijlstra, S.-J.J., Fagoe, N.D., Eggink, H.M., Eggers, R., Smit, A.B., van Kesteren, R.E., 2013. A multilevel screening strategy defines a molecular fingerprint of proregenerative olfactory ensheathing cells and identifies SCARB2, a protein that improves regenerative sprouting of injured sensory spinal axons. Journal of Neuroscience 33, 11116-11135.

Roet, K.C., Verhaagen, J., 2014. Understanding the neural repair-promoting properties of olfactory ensheathing cells. Experimental Neurology 261, 594-609.

Rossner, P., Vrbova, K., Rossnerova, A., Zavodna, T., Milcova, A., Klema, J., Vecera, Z., Mikuska, P., Coufalik, P., Capka, L., 2020. Gene Expression and Epigenetic Changes in Mice Following Inhalation of Copper (II) Oxide Nanoparticles. Nanomaterials 10, 550.

Roy, D., Ghosh, D., Mandal, D.K., 2013. Cadmium induced histopathology in the olfactory epithelium of a snakehead fish, Channa punctatus (Bloch). International Journal of Aquatic Biology 1, 221-227.

Sharma, D., Malik, A., Guy, C., Vogel, P., Kanneganti, T.-D., 2019. TNF/TNFR axis promotes pyrin inflammasome activation and distinctly modulates pyrin inflammasomopathy. The Journal of Clinical Investigation 129, 150-162.

Shetty, R.S., Bose, S.C., Nickell, M.D., McIntyre, J.C., Hardin, D.H., Harris, A.M., McClintock, T.S., 2005. Transcriptional changes during neuronal death and replacement in the olfactory epithelium. Molecular and Cellular Neuroscience 30, 90-107.

Shimizu, N., Kawakami, K., Ishitani, T., 2012. Visualization and exploration of Tcf/Lef function using a highly responsive Wnt/β-catenin signaling-reporter transgenic zebrafish. Developmental Biology 370, 71-85.

Sokpor, G., Abbas, E., Rosenbusch, J., Staiger, J.F., Tuoc, T., 2018. Transcriptional and epigenetic control of mammalian olfactory epithelium development. Molecular Neurobiology 55, 8306-8327.

Stone, M.C., Nguyen, M.M., Tao, J., Allender, D.L., Rolls, M.M., 2010. Global up-regulation of microtubule dynamics and polarity reversal during regeneration of an axon from a dendrite. Molecular Biology of the Cell 21, 767-777.

Su, Z., He, C., 2010. Olfactory ensheathing cells: biology in neural development and regeneration. Progress in Neurobiology 92, 517-532.

Sun, S.-C., 2011. Non-canonical NF-κB signaling pathway. Cell Research 21, 71-85.

Sun, S.-C., 2017. The non-canonical NF-κB pathway in immunity and inflammation. Nature Reviews Immunology 17, 545.

Suzuki, J., Sakurai, K., Yamazaki, M., Abe, M., Inada, H., Sakimura, K., Katori, Y., Osumi, N., 2015. Horizontal basal cell-specific deletion of Pax6 impedes recovery of the olfactory neuroepithelium following severe injury. Stem Cells and Development 24, 1923-1933.

Szymkowicz, D.B., Sims, K.C., Schwendinger, K.L., Tatnall, C.M., Powell, R.R., Bruce, T.F., Bridges, W.C., Bain, L.J., 2019. Exposure to arsenic during embryogenesis impairs olfactory sensory neuron differentiation and function into adulthood. Toxicology 420, 73-84.

Tabesh, E., Salimijazi, H., Kharaziha, M., Hejazi, M., 2018. Antibacterial chitosan-copper nanocomposite coatings for biomedical applications. Materials Today: Proceedings 5, 15806-15812.

Tacchi, L., Musharrafieh, R., Larragoite, E.T., Crossey, K., Erhardt, E.B., Martin, S.A., LaPatra, S.E., Salinas, I., 2014. Nasal immunity is an ancient arm of the mucosal immune system of vertebrates. Nature Communications 5, 1-11.

Takei, Y., Teng, J., Harada, A., Hirokawa, N., 2000. Defects in axonal elongation and neuronal migration in mice with disrupted tau and map1b genes. The Journal of Cell Biology 150, 989-1000.

Thiruvengadam, M., Chung, I.-M., Gomathi, T., Ansari, M.A., Khanna, V.G., Babu, V., Rajakumar, G., 2019. Synthesis, characterization and pharmacological potential of green synthesized copper nanoparticles. Bioprocess and Biosystems Engineering 42, 1769-1777.

Tilton, F., Tilton, S.C., Bammler, T.K., Beyer, R., Farin, F., Stapleton, P.L., Gallagher, E.P., 2008. Transcriptional biomarkers and mechanisms of copper-induced olfactory injury in zebrafish. Environmental Science & Technology 42, 9404-9411.

Tsarouchas, T.M., Wehner, D., Cavone, L., Munir, T., Keatinge, M., Lambertus, M., Underhill, A., Barrett, T., Kassapis, E., Ogryzko, N., 2018. Dynamic control of proinflammatory cytokines Il-1β and Tnf-α by macrophages in zebrafish spinal cord regeneration. Nature Communications 9, 1-17.

Tuncer, S., Fiorillo, M.T., Sorrentino, R., 2014. The multifaceted nature of NLRP12. Journal of Leukocyte Biology 96, 991-1000.

Valiño-Rivas, L., Gonzalez-Lafuente, L., Sanz, A.B., Ruiz-Ortega, M., Ortiz, A., Sanchez-Niño, M.D., 2016. Non-canonical NFκB activation promotes chemokine expression in podocytes. Scientific Reports 6, 28857.

Vanti, G.L., Masaphy, S., Kurjogi, M., Chakrasali, S., Nargund, V.B., 2020. Synthesis and application of chitosan-copper nanoparticles on damping off causing plant pathogenic fungi. International Journal of Biological Macromolecules 156, 1387-1395.

Waclaw, R.R., Allen II, Z.J., Bell, S.M., Erdélyi, F., Szabó, G., Potter, S.S., Campbell, K., 2006. The zinc finger transcription factor Sp8 regulates the generation and diversity of olfactory bulb interneurons. Neuron 49, 503-516.

Wang, H., Engstrom, A.K., Xia, Z., 2017a. Cadmium impairs the survival and proliferation of cultured adult subventricular neural stem cells through activation of the JNK and p38 MAP kinases. Toxicology 380, 30-37.

Wang, L., Bammler, T.K., Beyer, R.P., Gallagher, E.P., 2013. Copper-induced deregulation of microRNA expression in the zebrafish olfactory system. Environmental Science & Technology 47, 7466-7474.

Wang, Y., Yang, Q.-W., Yang, Q., Zhou, T., Shi, M.-F., Sun, C.-X., Gao, X.-X., Cheng, Y.-Q., Cui, X.-G., Sun, Y.-H., 2017b. Cuprous oxide nanoparticles inhibit prostate cancer by attenuating the stemness of cancer cells via inhibition of the Wnt signaling pathway. International Journal of Nanomedicine 12, 2569.

Wang, Y.-Z., Yamagami, T., Gan, Q., Wang, Y., Zhao, T., Hamad, S., Lott, P., Schnittke, N., Schwob, J.E., Zhou, C.J., 2011. Canonical Wnt signaling promotes the proliferation and neurogenesis of peripheral olfactory stem cells during postnatal development and adult regeneration. Journal of Cell Science 124, 1553-1563.

Winter, C.G., Wang, B., Ballew, A., Royou, A., Karess, R., Axelrod, J.D., Luo, L., 2001. Drosophila Rho-associated kinase (Drok) links Frizzled-mediated planar cell polarity signaling to the actin cytoskeleton. Cell 105, 81-91.

Xu, J., Zhang, Q., Li, X., Zhan, S., Wang, L., Chen, D., 2017. The effects of copper oxide nanoparticles on dorsoventral patterning, convergent extension, and neural and cardiac development of zebrafish. Aquatic Toxicology 188, 130-137.

Ye, J., Coulouris, G., Zaretskaya, I., Cutcutache, I., Rozen, S., Madden, T.L., 2012. Primer-BLAST: a tool to design target-specific primers for polymerase chain reaction. BMC Bioinformatics 13, 134.

Zhang, H., Macara, I.G., 2006. The polarity protein PAR-3 and TIAM1 cooperate in dendritic spine morphogenesis. Nature Cell biology 8, 227-237.

Zhang, Y., Liu, J., Yao, S., Li, F., Xin, L., Lai, M., Bracchi-Ricard, V., Xu, H., Yen, W., Meng, W., 2012. Nuclear factor kappa B signaling initiates early differentiation of neural stem cells. Stem Cells 30, 510-524.

Zhou, Y., Wu, S., Liu, F., 2019. High-performance polyimide nanocomposites with polydopamine-coated copper nanoparticles and nanowires for electronic applications. Materials Letters 237, 19-21.

Zou, Y., 2012. Does planar cell polarity signaling steer growth cones? Current topics in developmental biology. Elsevier, pp. 141-160.

Zou, Y., 2020. Breaking symmetry–cell polarity signaling pathways in growth cone guidance and synapse formation. Current Opinion in Neurobiology 63, 77-86.

CHAPTER 7: Recovery of rainbow trout olfactory function following exposure to copper nanoparticles

In the previous chapter, we reported that neural repair processes show better transcript responses to the Cu^{2+}-induced olfactory injury relative to CuNPs. In this research chapter, we examined the recovery of olfactory function after the removal of Cu. We also explored if the transcripts associated with neural function were dysregulated after the recovery period.

A version of this chapter is going to be submitted to *Science of the Total Environment*.

Contribution of authors: I designed and performed research, analysed data, and wrote the manuscript. Dr. Pyle provided guidance, scientific input, supervision, funding, and comments on the manuscript.

7.1. Abstract

In response to environmental information received by olfactory sensory neurons (OSNs), fish display different behaviours that are crucial for reproduction and survival. Damage to OSNs from direct exposure to environmental contaminants can disrupt fish olfaction. Copper nanoparticles (CuNPs) are neurotoxic contaminants which can impair fish olfactory function. However, it is uncertain if CuNP-induced olfactory dysfunction is reversible. Here, we compared the recovery of rainbow trout olfactory mucosa after being exposed to CuNPs or dissolved copper (Cu^{2+}). Following a 96 h exposure to CuNPs or Cu^{2+}, recovery was tested 14 minutes and 7 days after exposure using electro-olfactography (EOG). Results indicated the 14-minute recovery period was not sufficient to improve the olfactory sensitivity in either Cu treatment. After 7 days of transition to clean water, olfactory mucosa was able to recover from Cu^{2+}-induced dysfunction, while no recovery was observed in the CuNP-exposed OSNs. This olfactory dysfunction in the CuNP treatment was observed when no Cu was significantly accumulated in the olfactory mucosa after the recovery period. The transcript abundances of a subset of genes involved in olfactory signal transduction (OST) were downregulated in the CuNP-exposed fish after the 7-day recovery period. These results revealed that odorant reception through OST cascade remained impaired over the recovery period in the CuNP-treated OSNs. The ion regulation gene transcripts were not dysregulated in either Cu treatment, which suggests that neural ion balance was not affected following the recovery period. Collectively, our findings revealed the CuNP-induced olfactory dysfunction was irreversible after the 7-day recovery period. The CuNP-induced impairment of odorant reception may pose risks to the survival of fish.

7.2. Introduction

Perception of olfactory inputs initiates a broad range of vital activities in fish, including foraging, mating, social interactions, migration, defensive responses, and avoiding hazardous substances (Olivares and Schmachtenberg, 2019). Transduction of olfactory inputs begins in the cilia of olfactory sensory neurons (OSNs), where odorant molecules bind to olfactory receptors (ORs). The association of odorant with OR activates a series of neural events in the olfactory signal transduction pathway (OST), which initially generate receptor potentials and ultimately action potentials. The generated action potential transmits odorant information to neurons in the olfactory bulb (OB), which in turn relay the information to the regions of the central nervous system that control behaviours influenced by olfaction (Hamdani and Døving, 2007).

In the nasal cavities of fish, water is in continuous contact with olfactory cilia ensuring that OSNs have direct access to odorant molecules. A consequence of this direct contact of OSNs to ambient water is that these neurons are exposed to environmental contaminants (Tierney et al., 2010). Copper ions (Cu^{2+}) and copper nanoparticles (CuNPs) are waterborne contaminants that can induce neurotoxicity (Bulcke et al., 2017). Runoff from roofs, roads, carparks, mines, and agricultural activities are among the primary sources of Cu^{2+} to aquatic ecosystems (Charters et al., 2020; Pompermaier et al., 2020). The presence of CuNPs in aquatic environments can be attributed to the incidental release of naturally produced or engineered CuNPs during some stage of their life cycle (e.g., during production and/or application of CuNPs) (Hu and Cao, 2019; Rajput et al., 2019; Souza et al., 2020).

Exposure to Cu^{2+} and CuNPs can impair fish olfactory function. Rainbow trout exposed to CuNP showed greater impairment in their olfactory-mediated behavioural responses relative to the fish that were exposed to an equivalent concentration of Cu^{2+} (Sovová et al., 2014). Moreover, compared to Cu^{2+}, CuNPs exert more severe olfactory dysfunction in rainbow trout over time (Razmara et al., 2019). Following exposure to equitoxic concentration of Cu^{2+} and CuNPs (i.e., 24 h of 50% olfactory inhibitory concentration of the two Cu contaminants), the neurophysiological olfactory response (measured by electro-olfactography; EOG) declined steadily in the CuNP-exposed rainbow trout over time. In contrast, continuous exposure to Cu^{2+} resulted in a significant improvement of the neurophysiological olfactory response in rainbow trout (Razmara et al., 2019). Transcript profiles of rainbow trout olfactory mucosa indicated transcripts associated with the OST pathway and sensory perception of smell were dysregulated by CuNPs, but not Cu^{2+} over a 96 h exposure period (chapter 4). These results suggest that the ions released from CuNPs were not the only contributor to CuNP-induced olfactory toxicity, and particulate copper actively participated in fish olfactory dysfunction.

Vertebrate olfactory mucosa is capable of repairing neural injuries through regeneration of new neurons or regrowth of severed axons (Nicolay et al., 2006; Roet and Verhaagen, 2014). As long as these neural repair mechanisms remain intact, they can recover the functionality of injured olfactory mucosa. Recovery of fish olfactory function has been reported during continuous exposure to low concentration of Cu^{2+} and following the Cu^{2+} removal from culture water (Bettini et al., 2006; Dew et al., 2012). Despite the importance of olfactory function in fish survival, it is not clear if the olfactory impairment induced by CuNPs is reversible. Here, following a 96 h exposure to equitoxic

concentrations of Cu^{2+} and CuNPs, recovery of rainbow trout olfaction was tested 14 minutes and 7 days after Cu exposures using EOG. Moreover, transcript abundances of a few genes associated with the OST pathway and ion regulation in OSNs were investigated following the 7-day recovery period.

7.3. Materials and Methods

7.3.1. Preparation of Cu stock mixtures

A fresh stock suspension of 250 mg/L CuNPs was prepared by suspending nanocopper powder (35 nm; 99.8% purity; partially passivated, Nanostructured & Amorphous Materials Inc, USA) in ddH_2O (18.2 MΩ/cm water, Millipore, USA) using a 30 minute water bath sonicator (UD 150SH6LQ; 150 W; Eumax; USA) (Razmara et al., 2019). A fresh stock solution of Cu^{2+} as $CuSO_4.5H_2O$ (>98% purity; BHD, USA) was prepared at the concentration of 100 mg/L $CuSO_4$ in ddH_2O and acidified to 0.4% HNO_3 (concentrated; TraceSelect grade, Sigma Aldrich, Canada).

7.3.2. Animal housing and experimental set-up

Juvenile diploid rainbow trout (25.2 ± 3.9 g; mean ± SD, n = 72) were obtained from Sam Livingston fish hatchery (Alberta, Canada) and housed in a holding tank at the University of Lethbridge Aquatic Research Facility (ARF). Animals were acclimated to ARF water for a period of two weeks (16 h light: 8 h dark photoperiod). The quality of water was analysed as follows (mean ± SD; n = 3): temperature, 12.4 ± 0.1 °C; conductivity, 330.7 ± 0.1 µS/cm; dissolved oxygen, 8.7 ± 0.6 mg/L; alkalinity: 127.6 ± 2.8 mg/L as $CaCO_3$; hardness, 154 ± 4.9 mg/L as $CaCO_3$; median pH 8.1 (range 7.8 – 8.4), and dissolved organic carbon, 2.4 ± 0.8 mg/L.

In our previous study, to establish the toxicity units of Cu^{2+} and CuNPs that induce equal olfactory impairments in rainbow trout, we determined the 50% olfactory inhibitory concentrations of Cu^{2+} and CuNPs following a 24 h exposure (24 h IC50) using EOG (Razmara et al., 2019). In this study, to investigate the recovery of olfactory function in Cu-exposed fish, they were initially exposed to the 24 h IC50s for Cu^{2+} or CuNPs, as calculated at 7 ± 1 μg/L and 320 ± 13 (mean ± SD), respectively, for 96 h. During the exposure period, fish were not fed, and the Cu solutions were changed every 24 h by transferring fish to new sets of tanks containing fresh Cu solutions or clean water (control). After the 96 h exposure period, to study the immediate recovery of olfactory function, the olfactory rosettes of one group of fish were exposed to clean water (no Cu added) for 14 min (more details are provided in the neurophysiological assay section). The second group of Cu-exposed fish were transferred into tanks containing clean water for 7 days to recover.

7.3.3. Copper nanoparticles characterization

In the current study, we used the same source of CuNPs that was previously characterized (Razmara et al., 2019). In brief, the CuNPs were semi spherical with an average diameter of 32 ± 1 nm (mean ± SEM). During a period of 24 h, indicators of nanoparticles' aggregation, including hydrodynamic diameter, polydispersity index, and zeta potential, showed over the last few h of exposure (after 16 h), CuNPs were less stable and consequently less bioavailable (Razmara et al., 2019).

The dissolution of CuNPs was measured using Amicon Ultra-4 centrifugal filter units (3K regenerated cellulose membrane, Merck Millipore Ltd., USA) which can separate dissolved fraction from particulate Cu. The Cu concentration in the dissolved fraction was measured using graphite furnace atomic absorption spectrometry (240FS GFAAS, Agilent

Technologies, USA) during 24 h. Dissolved Cu was gradually released over time with the average Cu concentration of 8 µg/L (Razmara et al., 2019).

7.3.4. Copper analyses in the water and fish tissues

Total concentration of Cu in the tanks was measured by GFAAS. The QA/QC of Cu measurements was tested according to the protocol described in Razmara et al. (2019). The measured concentration of Cu in the CuNPs tanks at 1 h and 24 h after CuNPs spikes were 273 ± 19 and 214 ± 7 µg/L, respectively. The measured Cu concentration in the Cu^{2+} tanks was 7 ± 1 µg/L during the 24 h. In the control tanks and recovery tanks, the Cu concentration was not detectable by GFAAS.

Following 7 days of recovery, the total concentration of Cu was measured in the olfactory rosette (n = 7 per treatment) and brain (n = 6 per treatment) of rainbow trout. Fish were euthanized using an overdose of buffered MS222 (240 mg/L tricaine methane sulfonate, AquaLife, Canada) and 720 mg/L $NaHCO_3$ (Fisher Scientific, USA)). Olfactory rosettes and brains were harvested, oven-dried (at 60 °C), and weighed. The dried tissues were digested in concentrated HNO_3 using a hot block at 60 °C for 3 h. (chapter 4). The digested samples were reached to room temperature made up to 2 mL volume with ddH_2O. The Cu concentration in the samples were measured by GFAAS. The QA/QC of digestion protocol was tested following the protocol described in Razmara et al. (2021).

7.3.5. Neurophysiological analyses

To examine the quick recovery of EOG responses, following the exposure period, fish (n = 6 per treatment) were anaesthetized (120 mg/L tricaine methane sulfonate and 360 mg/L $NaHCO_3$). The intranarial septum of the olfactory chamber was removed to have a better access to the underlying olfactory rosette. During the EOG recording, gills were

perfused with a half dose of the anaesthetizing solution to keep the animal anaesthetized. Taurocholic acid (TCA; Sigma-Aldrich, USA) was used as an odorant at a concentration of 10^{-5} mol/L (Razmara et al., 2020). The recordings were performed according to the EOG procedures described by Razmara et al. (2019). In 90 s intervals, TCA or blank (culture water) was delivered to the olfactory chamber using a six-channel valve controller (Warners Instrument Co., USA). Between TCA deliveries, the olfactory chamber was continuously irrigated with culture water. In the immediate recovery experiment, the olfactory responses of each fish to TCA were measured in the presence (exposure phase) and absence (recovery phase) of Cu contaminants to test olfactory impairment and recovery, respectively. In the exposure phase of the recording, the olfactory response of fish to TCA was measured while the olfactory chamber was constantly exposed to either Cu^{2+}, CuNPs, or clean water (as control) for 7 minutes. Olfactory irrigation stream, blank, and TCA solution were spiked with Cu^{2+} or CuNPs for the Cu-treated fish in the exposure phase. In the recovery phase, the irrigation stream, blank, and TCA solutions were switched to those that were not spiked with Cu contaminants, and the olfactory chamber was only perfused with clean water for 14 minutes.

In the 7-day recovery experiment (n = 6 per treatment), there was no Cu contaminant in any of the EOG tubing, and the olfactory response to TCA was recorded three times. All EOG responses to TCA were corrected for blank (Razmara et al., 2020).

7.3.6. RNA isolation and quantitative real-time PCR (qPCR) analyses

At the end of the exposure period, fish (n = 5 per treatment) were euthanized, olfactory rosettes were dissected, flash-frozen in liquid nitrogen, and stored at -80°C. Total RNA of rosettes was isolated using RNeasy Mini Kit (catalogue # 74106; Qiagen)

according to the manufacturer's protocol. The isolated RNA quality and purity were determined using a Nanodrop spectrophotometer (Thermo Scientific NanoDrop One spectrophotometer, Thermo Scientific).

Results of our previous study indicated that a 96 h exposure to CuNPs can dysregulate the abundances of gene transcripts encoding olfactory receptors (*OR10G4* and *OLF472*), olfactory marker protein (OMP), and ion channels/transporters (*SCN8A*, *ATP1A1*, *CaCNB1*, and *TPCN2*) which all play a role in OSNs function (chapter 4). In the current study, we measured the mRNA abundances of these transcripts to examine whether the 7 days of recovery period was sufficient to restore the transcripts level in OSNs. cDNA was synthesized from the isolated RNA using QuantiTec Reverse Transcription Kit (catalogue # 205311, Qiagen). Using a Bio-Rad thermocycler (C1000 Touch thermocycler, CFX96 Real-Time System, Bio-Rad) and RT^{2}SYBR Green qPCR master mix (catalogue # 330503, Qiagen), we quantified target gene transcripts following the same protocol that was described previously (chapter 4). According to the Pfaffl method for quantification of transcripts, target gene transcripts were quantified relative to the reference genes, *ACTB* and *EF1a* (Pfaffl, 2001). Reference genes were not differentially expressed in response to Cu treatments (chapter 4).

7.3.7. Statistical analyses

All statistical analyses were performed by R, version 3.6 (R Core Team, 2019). The normality and homogeneity of variances of all data were examined by a Shapiro-Wilks and a Bartlett test, respectively. To investigate the effect of Cu^{2+} and CuNPs on the Cu content of olfactory rosette and brain, a one-way analysis of variance (ANOVA) with a Tukey's post hoc test was used. To analyse the EOG responses to TCA in different treatments

(control, Cu^{2+}, and CuNPs) under different exposure conditions (i.e., in the presence or absence of Cu contaminants), a repeated measures two-way ANOVA was used. The EOG responses to TCA after the 7-day recovery period in different treatment were analysed by the one-way ANOVA followed by a Tukey's post hoc test. Any possible differences in the expression of target genes under different Cu treatments was also analysed by one-way ANOVA and Tukey's post hoc test. Graphs were plotted in R using the ggplot2 package (Wickham, 2016).

7.4. Results and discussion

7.4.1. Copper accumulation in the fish tissue

Our previous results revealed that CuNPs were accumulated in the internal organelles of olfactory mucosal cells, and Cu concentration in the olfactory rosette was elevated over both 24 h and 96 h exposure to CuNPs (chapter 4). Nevertheless, after the 7-day recovery period, total Cu concentration in the Cu^{2+}- and CuNP-treated olfactory rosette did not significantly increase relative to the control ($F(2, 18) = 3.01$, $p = 0.07$; Fig. 7.1A). These results indicated that this recovery period was sufficient to eliminate the excessive accumulated Cu in the CuNP-exposed olfactory mucosa. However, it is not clear if the Cu depuration was a result of Cu excretion (e.g., exocytosed) by the mucosal cells or a consequence of Cu translocation to other tissues.

Redistribution of Cu was previously reported in different tissues of CuNP-injected rainbow trout over time (Lindh et al., 2019). The Cu concentrations in gills, carcass, and intestine of CuNP-injected rainbow trout decreased over 192 h post-injection, whereas the Cu concentration in the liver increased (Lindh et al., 2019). Moreover, nanoparticles, such as CuNPs, can be translocated to the brain via axonal transport of the olfactory nerve (Lin

et al., 2020). Therefore, the reduced Cu concentration of the olfactory mucosa after the 7-day recovery period can be attributed to CuNPs being translocated to the brain. Despite a slight increase of Cu content in the brain of CuNP-exposed fish, Cu was not statistically significantly accumulated in the brain (F (2, 15) = 3.41, p = 0.06; Fig. 7.1B). Further investigation is warranted to determine if the increased level of Cu in the brain is biologically significant and affects motor function. Moreover, the mechanism underlying the CuNPs depuration in the olfactory mucosa has yet to be determined.

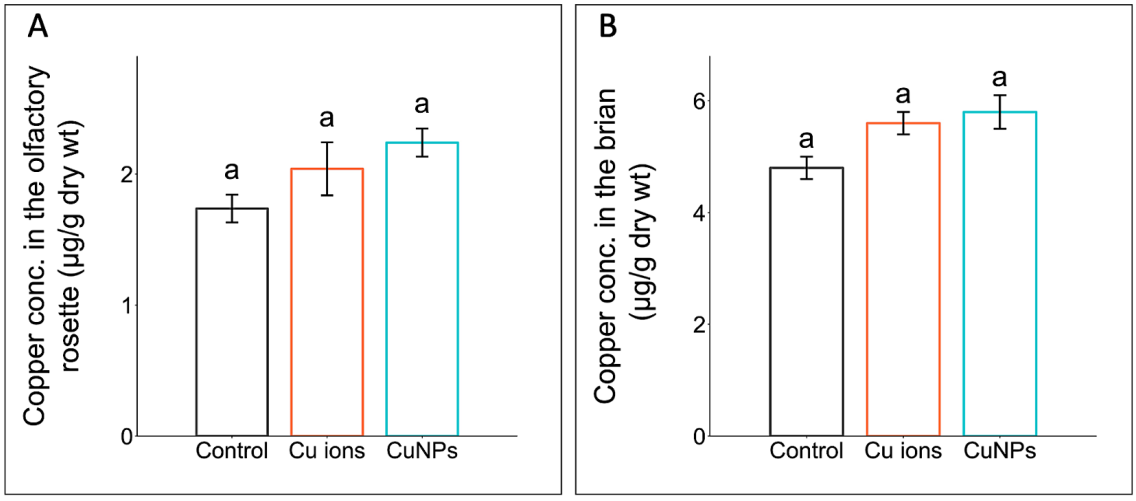

Figure 7.1. Copper bioaccumulation in olfactory rosette (A) and brain (B) of the Cu ion- and CuNP- exposed rainbow trout after 7 days of transition to clean water. Lower-case letters indicate significant differences ($p \leq 0.05$, error bars ± 1 SEM).

7.4.2. Neurophysiological analyses

Results of EOG recordings during the exposure phase and 14-minute recovery phase showed no sign of recovery in the olfactory responses to TCA in any of the Cu treatments (p = 0.71; Fig. 7.2A). These findings suggest that the effect of both Cu contaminants was not restricted to superficial blocking of ORs or ion channels which can be easily washed off of the OE by a clean water flow. In agreement with our results, rainbow trout that were previously exposed to CuNPs for 12 h, displayed a significant

impairment in their olfactory-mediated behavioural responses to skin extract (SE) after being transferred to clean water for 10 minutes (Sovová et al., 2014). The behavioural responses of Cu^{2+}-exposed fish to SE was not affected by transfer to clean water (Sovová et al., 2014).

Despite extending the recovery period to 7 days, the effect of treatment on rainbow trout olfactory sensitivity was significant ($F(2, 15) = 85.59$, $p < 0.001$; Fig. 7.2B). Olfactory function of CuNP-exposed fish showed a significant impairment relative to the control or Cu^{2+} treatment ($p < 0.001$; Fig. 7.2B). These data indicated that the generation of a receptor potential through the OST pathway was still impaired over the duration of the 7-day recovery period. Given that the olfactory sensitivity of CuNP-exposed fish remained low over the recovery period, it is possible that the residue of accumulated Cu in the olfactory mucosa, which was statistically insignificant, was sufficient to induce olfactory impairment. We previously reported that transcripts regulating olfactory neuroregeneration were downregulated in the CuNP-exposed fish (chapter 4). Reduced neural development was also observed in zebrafish embryos following exposure to copper oxide nanoparticles (Xu et al., 2017). It is likely that disruption of neural repair mechanisms by CuNPs continued during the 7-day recovery period, and as a result, olfactory dysfunction did not recover. Further investigations are required to explore the effect of CuNPs on the neural repair mechanisms in the olfactory system.

In the Cu^{2+} treatment, however, there was a full recovery of olfaction after 7 days of exposure to clean water ($p = 0.111$; Fig. 7.2B). A partial improvement of olfactory sensitivity was previously observed in rainbow trout despite continuous exposure to Cu^{2+} (Razmara et al., 2019). Hence, repair mechanisms can operate during both exposure and

recovery periods in the Cu^{2+}-exposed olfactory mucosa. Although recovery of Cu^{2+}-exposed olfactory function has been documented in different fishes (Bettini et al., 2006; Sandahl et al., 2006; Dew et al., 2012), repair of damaged OSNs is highly dependent on the concentration of Cu^{2+}, exposure time, and type of OSN (i.e., ciliated and microvillous OSNs) (Lazzari et al., 2017; Ma et al., 2018). For instance, regeneration of ciliated OSNs, but not microvillous OSNs, was reported in zebrafish larvae following a 72 h recovery from Cu^{2+} exposure (a 3 h exposure to 16 µg/L of Cu^{2+}) (Ma et al., 2018). No significant regeneration was observed when OSNs exposed to high Cu concentrations (64 - 635 µg/L), and only microvillous OSNs were regenerated when the exposure period was extended to 24 h (Ma et al., 2018). In the current study, we only investigated the recovery of ciliated OSNs, as they are more sensitive to Cu toxicity than microvillous ones (Lazzari et al., 2017; Razmara et al., 2019).

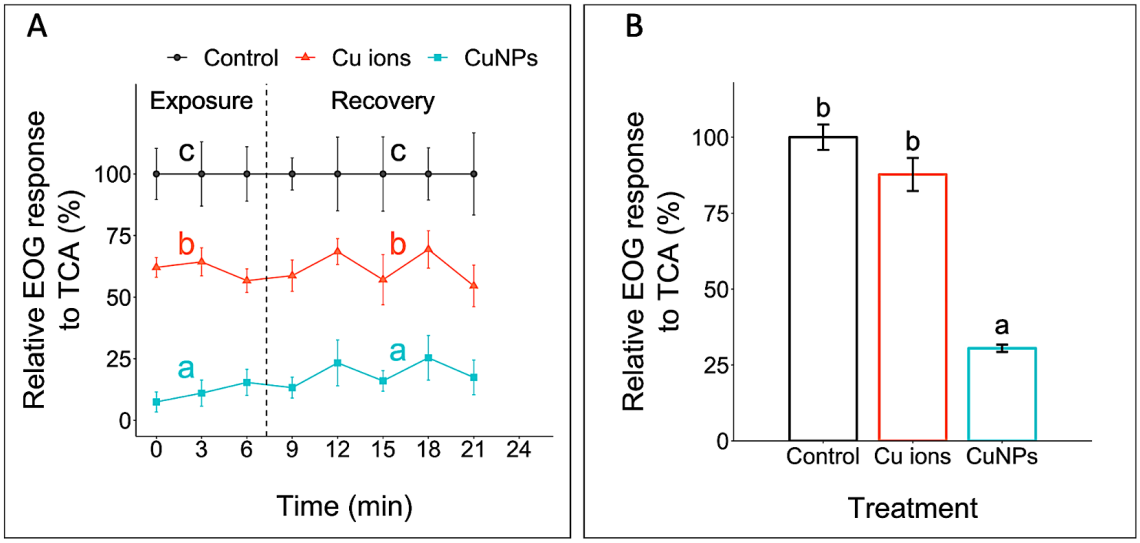

Figure 7.2. Olfactory recovery of Cu ion- and CuNP- exposed rainbow trout after transition to clean water. Fish were initially exposed to Cu contaminants or clean water (control) for 96 h. (A) Relative electro-olfactography responses of fish to TCA during the presence (exposure phase) and absence (recovery phase) of Cu contaminants. (B) Relative electro-olfactography responses of fish to TCA after 7 days of recovery period. Lower-case letters indicate significant differences ($p \leq 0.05$, n = 6, error bars ± 1 SEM).

7.4.3. qPCR analyses

After the 7-day recovery period, the transcript abundances of *OR10G4*, *OLF472*, and *OMP* were significantly low in the CuNP-exposed olfactory mucosa (p = 0.012, 0.006, and 0.011, respectively; Fig. 7.3A-C). OR10G4 and OLF472 belongs to the superfamily of G proteins-coupled receptors which initiate the generation of receptor potential in the presence of their specific odorants in ciliated OSNs (Hansen et al., 2004). The OMP, which expresses in ciliated OSNs (Ma et al., 2018), regulates the activity of cyclic AMP and sodium-calcium exchanger in the OST pathway (Kwon et al., 2009; Dibattista and Reisert, 2016). The dysfunction of CuNP-exposed ciliated OSNs after the recovery period can be attributed to the reduced mRNA level of these three genes which all serve in the OST pathway. The reduced transcript abundances of *OR10G4*, *OLF472*, and *OMP* along with the impaired odorant reception in the CuNP-exposed OSNs after the 7-day recovery period reflect that the OST pathway is highly vulnerable to CuNPs toxicity. It is possible that the functionality of CuNP-exposed OSNs can be restored if the recovery period is extended. Nonetheless, loss of odorant reception during the period of CuNP exposure and recovery may threaten fish survival. The effect of Cu^{2+} on the transcript abundances of OST-related genes was insignificant (Fig. 7.3A-C), which supports the full recovery of olfactory function in the Cu^{2+}-treated fish.

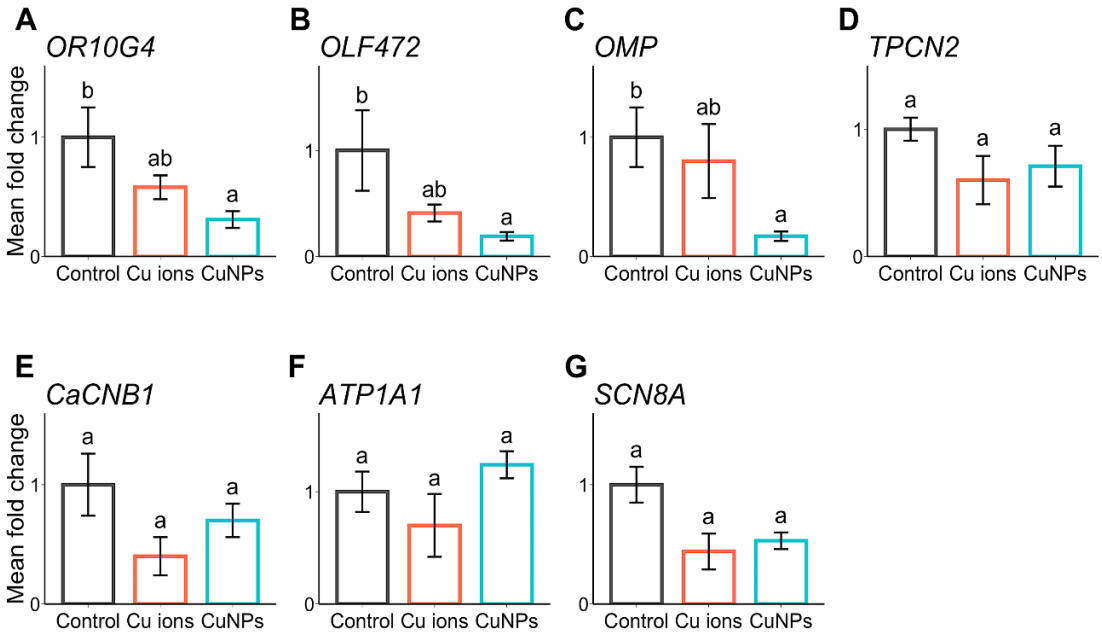

Figure 7.3. Gene transcript levels in the Cu-exposed rainbow trout olfactory mucosa following the 7 day recovery period. (A) Olfactory receptor 10G4 (*OR10G4*). (B) Olfactory receptor 472 (*OLF472*). (C) Olfactory marker protein (OMP). (D) Two pore calcium channel protein 2 (*TPCN2*). (E) Voltage-dependent L-type calcium channel subunit beta1(*CaCNB1*). (F) Na^+/K^+ ATPase alpha-1 subunit (*ATP1A1*). (G) Sodium channel protein type 8 subunit alpha (*SCN8A*). Lower-case letters indicate significant differences ($p \leq 0.05$, n = 5, error bars ± 1 SEM).

Perturbation of cytosolic ion homeostasis, such as calcium, is one of the adverse effects induced by nanoparticles (Huang et al., 2017; Lovisolo et al., 2018). Nanoparticles may alter the expression of neural ion channels or directly interact with channels/transporters and modulate their activities (Lovisolo et al., 2018). We previously reported that the mRNA abundances of ion regulating genes, including *TPCN2*, *CaCNB1*, *ATP1A1,* and *SCN8A*, were upregulated following the 96 h exposure to CuNPs (chapter 4). Nonetheless, the transcript abundances of these genes were not significantly dysregulated in the Cu treatments following the recovery period (Fig. 7.3D-G). The *TPCN2* encodes a calcium extruder on lysosomes which regulates the intracellular cellular calcium

concentration $[Ca^{2+}]_i$ in neurons (Lakpa et al., 2020). The *CaCNB1* encodes the β subunit of the calcium voltage gated channel which amplifies the receptor potential and facilitates odorant signal propagation to the axon hillock where action potential generation is initiated (Solís-Chagoyán et al., 2016). Both *ATP1A1* (encoding sodium/potassium ATPase pump, subunit alpha 1) and *SCN8A* (encoding voltage-gated sodium channel) regulate action potential generation (O'Brien and Meisler, 2013; Azizishirazi et al., 2015). The restored transcript abundances of candidate ion channels/transporters over the recovery period suggested the ion balance in OSNs were not disrupted following the CuNP removal from water.

7.5. Conclusions

Our findings provide insight into the recovery of olfactory function in Cu^{2+}- and CuNP-exposed rainbow trout after being transferred to clean water. Neurophysiological responses of OSNs to TCA showed no sign of quick recovery over the 14 minutes of exposure to clean water in the Cu-treated fish. Following the 7-day recovery period, Cu^{2+}-induced olfactory dysfunction recovered, whereas the olfactory dysfunction induced by CuNPs persisted. The impaired olfactory function of CuNP-exposed fish after the 7-day recovery period can be attributed to the downregulation of genes, such as olfactory receptors, involved in the OST pathway. The unaffected transcript abundances of ion regulating genes, however, suggested ion balance of Cu-exposed OSNs was not perturbed over the recovery period. Taken together, these results demonstrate that rainbow trout olfactory mucosa had a better ability to recover from Cu^{2+}-induced dysfunction relative to impairments induced by CuNPs. The continued olfactory dysfunction after CuNP removal

demonstrated the severity of CuNP-induced olfactory damages which is difficult to repair and can inhibit many survival-related activities.

7.6. References

Azizishirazi, A., Dew, W.A., Bougas, B., Bernatchez, L., Pyle, G.G., 2015. Dietary sodium protects fish against copper-induced olfactory impairment. Aquatic Toxicology 161, 1-9.

Bettini, S., Ciani, F., Franceschini, V., 2006. Recovery of the olfactory receptor neurons in the African Tilapia mariae following exposure to low copper level. Aquatic Toxicology 76, 321-328.

Bulcke, F., Dringen, R., Scheiber, I.F., 2017. Neurotoxicity of copper. Neurotoxicity of Metals. Springer, pp. 313-343.

Charters, F.J., Cochrane, T.A., O'Sullivan, A.D., 2020. The influence of urban surface type and characteristics on runoff water quality. Science of The Total Environment 755, 142470.

Dew, W.A., Wood, C.M., Pyle, G.G., 2012. Effects of continuous copper exposure and calcium on the olfactory response of fathead minnows. Environmental Science & Technology 46, 9019-9026.

Dibattista, M., Reisert, J., 2016. The odorant receptor-dependent role of olfactory marker protein in olfactory receptor neurons. Journal of Neuroscience 36, 2995-3006.

Hamdani, E.H., Døving, K.B., 2007. The functional organization of the fish olfactory system. Progress in Neurobiology 82, 80-86.

Hansen, A., Anderson, K.T., Finger, T.E., 2004. Differential distribution of olfactory receptor neurons in goldfish: structural and molecular correlates. Journal of Comparative Neurology 477, 347-359.

Hu, G., Cao, J., 2019. Metal-containing nanoparticles derived from concealed metal deposits: An important source of toxic nanoparticles in aquatic environments. Chemosphere 224, 726-733.

Huang, Y.-W., Cambre, M., Lee, H.-J., 2017. The toxicity of nanoparticles depends on multiple molecular and physicochemical mechanisms. International Journal of Molecular Sciences 18, 2702.

Kwon, H.J., Koo, J.H., Zufall, F., Leinders-Zufall, T., Margolis, F.L., 2009. Ca 2+ extrusion by NCX is compromised in olfactory sensory neurons of OMP−/− mice. PLoS One 4, e4260.

Lakpa, K.L., Halcrow, P.W., Chen, X., Geiger, J.D., 2020. Readily releasable stores of calcium in neuronal endolysosomes: Physiological and pathophysiological relevance. Calcium Signaling. Springer, pp. 681-697.

Lazzari, M., Bettini, S., Milani, L., Maurizii, M.G., Franceschini, V., 2017. Differential response of olfactory sensory neuron populations to copper ion exposure in zebrafish. Aquatic Toxicology 183, 54-62.

Lin, Y., Hu, C., Chen, A., Feng, X., Liang, H., Yin, S., Zhang, G., Shao, L., 2020. Neurotoxicity of nanoparticles entering the brain via sensory nerve-to-brain pathways: injuries and mechanisms. Archives of Toxicology, 1-17.

Lindh, S., Razmara, P., Bogart, S., Pyle, G., 2019. Comparative tissue distribution and depuration characteristics of copper nanoparticles and soluble copper in rainbow trout (Oncorhynchus mykiss). Environmental Toxicology and Chemistry 38, 80-89.

Lovisolo, D., Dionisi, M., Ruffinatti, F.A., Distasi, C., 2018. Nanoparticles and potential neurotoxicity: focus on molecular mechanisms. AIMS Molecular Sciemces 5, 1-13.

Ma, E.Y., Heffern, K., Cheresh, J., Gallagher, E.P., 2018. Differential copper-induced death and regeneration of olfactory sensory neuron populations and neurobehavioral function in larval zebrafish. Neurotoxicology 69, 141-151.

Nicolay, D.J., Doucette, J.R., Nazarali, A.J., 2006. Transcriptional regulation of neurogenesis in the olfactory epithelium. Cellular and Molecular Neurobiology 26, 801-819.

O'Brien, J.E., Meisler, M.H., 2013. Sodium channel SCN8A (Nav1. 6): properties and de novo mutations in epileptic encephalopathy and intellectual disability. Frontiers in Genetics 4, 213.

Olivares, J., Schmachtenberg, O., 2019. An update on anatomy and function of the teleost olfactory system. PeerJ 7, e7808.

Pfaffl, M.W., 2001. A new mathematical model for relative quantification in real-time RT–PCR. Nucleic Acids Research 29, e45-e45.

Pompermaier, A., Varela, A.C.C., Fortuna, M., Mendonça-Soares, S., Koakoski, G., Aguirre, R., Oliveira, T.A., Sordi, E., Moterle, D.F., Pohl, A.R., 2020. Water and suspended sediment runoff from vineyard watersheds affecting the behavior and physiology of zebrafish. Science of The Total Environment, 143794.

Rajput, V., Minkina, T., Ahmed, B., Sushkova, S., Singh, R., Soldatov, M., Laratte, B., Fedorenko, A., Mandzhieva, S., Blicharska, E., 2019. Interaction of copper-based nanoparticles to soil, terrestrial, and aquatic systems: critical review of the state of the science and future perspectives. Reviews of Environmental Contamination and Toxicology Volume 252, 51-96.

Razmara, P., Lari, E., Mohaddes, E., Zhang, Y., Goss, G.G., Pyle, G.G., 2019. The effect of copper nanoparticles on olfaction in rainbow trout (Oncorhynchus mykiss). Environmental Science: Nano 6, 2094-2104.

Razmara, P., Sharpe, J., Pyle, G.G., 2020. Rainbow trout (Oncorhynchus mykiss) chemosensory detection of and reactions to copper nanoparticles and copper ions. Environmental Pollution, 113925.

Roet, K.C., Verhaagen, J., 2014. Understanding the neural repair-promoting properties of olfactory ensheathing cells. Experimental neurology 261, 594-609.

Sandahl, J.F., Miyasaka, G., Koide, N., Ueda, H., 2006. Olfactory inhibition and recovery in chum salmon (Oncorhynchus keta) following copper exposure. Canadian Journal of Fisheries and Aquatic Sciences 63, 1840-1847.

Solís-Chagoyán, H., Flores-Soto, E., Reyes-García, J., Valdés-Tovar, M., Calixto, E., Montaño, L.M., Benítez-King, G., 2016. Voltage-activated calcium channels as functional markers of mature neurons in human olfactory neuroepithelial cells: implications for the study of neurodevelopment in neuropsychiatric disorders. International journal of molecular sciences 17, 941.

Souza, I.d.C., Morozesk, M., Mansano, A.S., Mendes, V.A., Azevedo, V.C., Matsumoto, S.T., Elliott, M., Monferrán, M.V., Wunderlin, D.A., Fernandes, M.N., 2020. Atmospheric particulate matter from an industrial area as a source of metal nanoparticle contamination in aquatic ecosystems. Science of The Total Environment 753, 141976.

Sovová, T., Boyle, D., Sloman, K.A., Pérez, C.V., Handy, R.D., 2014. Impaired behavioural response to alarm substance in rainbow trout exposed to copper nanoparticles. Aquatic Toxicology 152, 195-204.

Tierney, K.B., Baldwin, D.H., Hara, T.J., Ross, P.S., Scholz, N.L., Kennedy, C.J., 2010. Olfactory toxicity in fishes. Aquatic toxicology 96, 2-26.

Xu, J., Zhang, Q., Li, X., Zhan, S., Wang, L., Chen, D., 2017. The effects of copper oxide nanoparticles on dorsoventral patterning, convergent extension, and neural and cardiac development of zebrafish. Aquatic Toxicology 188, 130-137.

CHAPTER 8: Conclusions

The present dissertation addressed several knowledge gaps regarding the olfactory toxicity of CuNPs in rainbow trout. This study described how exposure to CuNPs affected different levels of biological organization, including whole organism (i.e., olfactory-driven behaviours), tissue effects (i.e., neurophysiological responses of olfactory rosette and density of goblet cells), and cellular and molecular responses (i.e., Cu accumulation, lipid peroxidation, DNA fragmentation, and transcript profile of olfactory mucosa) in rainbow trout. In attempt to explore the contribution of dissolved Cu to the CuNPs toxicity, the effects of CuNPs on the olfactory mucosa were also compared to Cu^{2+}. Olfactory detection and perception of CuNPs and Cu^{2+} were also examined in rainbow trout. Moreover, recovery of fish olfactory function after the removal of Cu from the exposure water was also evaluated in this dissertation. Based on the findings of this study, I come to a number of major conclusions which are presented in the following paragraphs.

First, according to the results of EOG and behavioural studies, CuNPs and Cu^{2+} exert different patterns of olfactory toxicity over time. During continuous exposure to Cu^{2+} (96 h), rainbow trout olfactory function was at least partially recovered. The olfactory function of CuNP-exposed fish, however, showed a steady decline over time with no sign of recovery. Our findings also demonstrated that exposure to CuNPs or Cu^{2+} can impair the generation of receptor potentials in both ciliated and microvillous OSNs in rainbow trout. Nonetheless, the function of ciliated OSNs was more sensitive to Cu contaminants relative to microvillous OSNs. Therefore, as has been previously reported for Cu^{2+}, the cAMP-mediated OST pathway is more vulnerable to Cu contaminants relative to the IP_3-mediated pathway.

Second, rainbow trout exhibited differential olfactory responses to equitoxic concentrations of CuNPs and Cu^{2+} (24 h IC20s CuNPs and Cu^{2+}) which were tested as olfactory stimuli. While rainbow trout detected and avoided the CuNPs, the 24 h IC20 concentration of Cu^{2+} was not perceivable by fish. However, a brief (14 min) exposure to 24 h IC20 concentration of CuNPs reduced the detection and perception of TCA, which is a chemical social cue. Hence, the presence of CuNPs in the surrounding water may eliminate the ability of fish to smell other stimuli, such as TCA.

Third, CuNPs and Cu^{2+} induced differential effects on the transcript profiles of rainbow trout olfactory mucosa. In fact, there was a small (14%) overlap between the transcript profiles of CuNP- and Cu^{2+}-exposed olfactory mucosa. Gene ontology analyses revealed that many pathways associated with olfactory function, including sensory perception of smell and G protein-coupled receptor activity, were only enriched in the CuNP-exposed olfactory mucosa. Based on the results of RNA-seq, we proposed a model that shows transcripts associated with odorant reception (i.e., cAMP-mediated OST) and action potential transmission were downregulated by CuNPs, but not Cu^{2+}. Immune system transcripts were downregulated in both Cu treatments; however, transcription of genes involved in inflammation signaling were only targeted by CuNPs. Our findings also indicated that CuNPs were bioavailable to olfactory epithelial cells. Accumulation of CuNPs in the endo/lysosomes were confirmed by TEM. Moreover, the nonsignificant effect of Cu contaminants on lipid peroxidation and DNA fragmentations in the Cu-exposed olfactory mucosa suggested that oxidative stress and apoptosis were not induced by Cu contaminants. Based on our findings we conclude that CuNPs operate through a

completely different mechanism of toxic action than Cu^{2+} in the fish olfactory system, and their effects are more severe leading to a lower likelihood of recovery.

Fourth, the molecular composition of intercellular junctions was more sensitive to Cu^{2+} than CuNPs. Our results indicated that 96 h exposure to Cu^{2+} can downregulate a number of transcripts associated to tight junctions, adherens junction, desmosomes and hemidesmosomes. In contrast, the majority of cell junction transcripts, except adherens junction, were upregulated in the CuNP treatment. Given that junctional complexes provide intercellular mechanical supports in the olfactory mucosa, the stability and integrity of Cu^{2+}-exposed OE may be reduced. Furthermore, the density of goblet cells in the Cu-exposed OE was initially increased at 24 h and returned to control level at 96 h. The reduced density of goblet cells at 96 h can be related to the repressed transcript abundances of genes regulating the production of mucin, which is a primary component of mucosubstances in goblet cells. These results suggested that mucosal cells were better protected by mucus at 24 h Cu exposure compared to the 96 h exposure time.

Fifth, the molecular basis of neural repair (i.e., neuroregeneration and axon regrowth) in the olfactory mucosa was differentially affected by CuNPs and Cu^{2+}. The 96 h exposure to CuNPs reduced the abundance of transcripts involved in olfactory neuroregeneration. In particular, the mRNA levels of neuroregeneration promoters, including pro-inflammatory proteins, canonical Wnt/β-catenin signaling proteins, and developmental transcription factors were reduced in the CuNP-exposed fish. Nonetheless, the abundances of transcripts associated to axon regrowth were mostly upregulated in the CuNP treatment. In the Cu^{2+}-exposed olfactory mucosa, the transcripts associated with both neuroregeneration and axon regeneration were increased. These results suggest neural

repair mechanisms were more strongly activated in response to Cu^{2+} relative to CuNPs. Hence, the olfactory recovery of Cu^{2+}-exposed fish is more probable than CuNP-exposed ones.

Sixth, rainbow trout olfactory mucosa had a better ability to recover from Cu^{2+}-induced olfactory toxicity relative to CuNPs. The CuNP-exposed rainbow trout were not able to recover their olfactory function after a 7-day recovery period, whereas the Cu^{2+}-exposed fish were fully recovered. After the recovery period, the transcript abundances of a few genes that were involved in the cAMP-mediated OST pathway were downregulated in the CuNP treatment. These results revealed that the receptor potential generation remained impaired in the CuNP-exposed OSNs over the recovery period. Moreover, in either Cu treatment, the 14-minute exposure to clean water did not result in olfactory improvement in rainbow trout. Therefore, Cu-induced olfactory impairment was not a result of simple binding of Cu to the olfactory cilia which can be washed off after Cu removal. The CuNP-induced olfactory impairment, which was not reversible over the 7-day recovery period, may threaten rainbow trout survival in the CuNPs contaminated areas.

Collectively, CuNPs induce severe impairments in the rainbow trout olfactory mucosa, which can persist even after the removal of CuNPs from the ambient water. The toxicity of CuNPs in the olfactory mucosa is a function of both nanocopper and dissolved ions; however, dissolved ions are not the main driver in the CuNP-induced olfactory toxicity. Our findings indicate that molecular sensory processes, including OST and synaptic transmission, were negatively affected by CuNPs. As reflected in olfactory-driven behavioural responses, dysregulation of neural pathways has ultimately impaired odorant perception in CuNP-exposed rainbow trout. Non sensory molecular pathways, such as

neural repair mechanisms and inflammatory signaling, were also dysregulated by exposure to CuNPs. Therefore, CuNPs can not only impair the fish olfactory function, but also disrupt the processes involved in the maintenance of olfactory mucosa.

Following the AOP predictive model, our data created strong linkages among CuNP-induced molecular responses, neurophysiological responses, and behavioural responses in rainbow trout. The outcomes of our study can be used for predicting and extrapolating the CuNP-induced toxicity to the fish individual and improve the ecological risk assessment of CuNPs or similar chemicals. Based on our data, we propose an AOP for fish olfactory injury following exposure to environmental contaminants (Fig. 8.1). Interaction of contaminants (e.g., CuNPs) with DNA of olfactory mucosal cells is the molecular initiating event (MIE) in our proposed AOP framework. The interaction of contaminant with DNA leads to a few key events in different levels of biological organization that ultimately inhibit fish olfactory-driven behaviours (Fig. 8.1). The first key event is the dysregulation of gene transcripts which play crucial role in OST pathway, including olfactory receptors and ion channels and transporters. As a result of dysregulation of these transcripts, generation of receptor potential will be disrupted by the contaminant, and neurophysiological responses of olfactory mucosa will be dramatically reduced. Therefore, contaminant-exposed fish are not able to receive the chemical inputs of odorants. In consequence, vital olfactory-driven behaviours, including finding food, mating, homing, avoiding predation and contaminants, which are essential for fish growth, reproduction, and survival will be inhibited. Given that an AOP is a living document, when more knowledge is generated about the chemical-induced olfactory injury, our proposed AOP for olfactory injury can evolve over time.

The proposed AOP for fish olfactory injury can predict the adverse effect of wide range of aquatic contaminants that trigger the same MIE (i.e., DNA binding) in the olfactory mucosa and improve ecological risk assessment. Moreover, applying the proposed AOP in risk assessment can reduce the number of experimental animals required for toxicity tests.

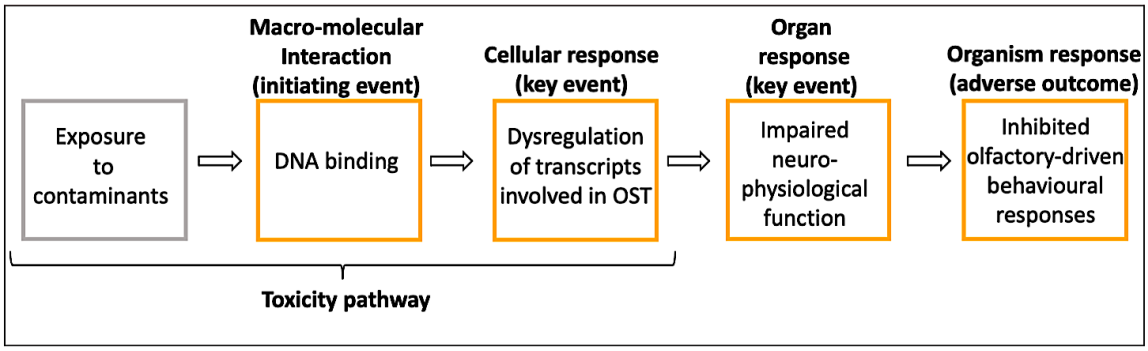

Figure 8.1. Conceptual diagram representing adverse outcome pathway for olfactory injury. The pathway begins with the interaction of contaminant with DNA which leads to sequential key events which subsequently inhibit many essential olfactory-driven behavioral responses.

Other findings of our study, including dysregulated gene transcripts that are involved in the maintenance of olfactory mucosa (e.g., genes associated with neuroregeneration and immune responses), can also be used to develop AOP(s) for non-sensory injuries in contaminant-exposed olfactory mucosa. Impairment of maintenance processes in the olfactory mucosa may lead to chronic or permanent loss of olfaction, and threaten fish growth, reproduction, and survival.

Future investigations should strive to examine our transcript-based olfactory model at higher levels of organization, including measuring of ion channels expression and activity. Moreover, the effect of CuNPs on the functionality of stem cells regeneration, axon regeneration, immune system, and cell junctions must be further studied. Finally,

assessing the effect of CuNPs on the olfactory-associated brain function can be beneficial in our understanding of CuNP-induced olfactory toxicity.

APENDIX

Supplementary material for chapter 4:

Mechanism of copper nanoparticle toxicity in rainbow trout olfactory mucosa

Materials and Methods

Preparation of Copper Stock Mixtures and Characterization of CuNPs

Following the same protocol described in our previous study (Razmara et al., 2019), a fresh stock solution of 100 mg/L $CuSO_4$ (>98% purity; BHD, USA) and a fresh stock suspension of 250 mg/L CuNPs (35 nm; 99.8% purity; partially passivated, Nanostructured & Amorphous Materials Inc, USA) were prepared in 18.2 MΩ/cm water (ddH_2O, Millipore, USA). To disperse the CuNPs in the ddH_2O, the stock suspension was sonicated (water bath sonicator; UD 150SH 6LQ; 150 W; Eumax; USA) for 30 min at room temperature.

A full characterization of CuNPs is described by Razmara et al., 2019 (the same batch of CuNPs was utilized in both the past and present study) (Razmara et al., 2019). In short, the average diameter of CuNPs was 32 ± 1 nm (mean ± SEM; n = 349), and the particles were semi-spherical. The aggregation indicators of NPs, including polydispersity index (PDI), hydrodynamic diameter (HDD), and zeta potential were measured over 24 h in a 2 h intervals. After the 16 h in the CuNPs experimental tanks, the CuNPs displayed a noticeable increase in polydispersity (PDI = 1) and HDD, along with a significant reduction in zeta potential. These aggregation markers indicated over the last few hours of exposure, CuNPs were less stable, and consequently, less bioavailable fort the fish. To measure the dissolution of CuNPs, dissolved Cu was separated from CuNPs using Amicon Ultra-4 Centrifugal Filter Units with a pore size of 1-2 nm (3K regenerated cellulose membrane, Merck Millipore Ltd., USA) over 24 h (Razmara et al., 2019). The filtrates (containing dissolved Cu) were analyzed by graphite furnace atomic absorption spectrometry (GFAAS) (240FS GFAAS, Agilent Technologies, USA). Results demonstrated the CuNPs release dissolved Cu in a time dependent manner (up to 14 μg/L of dissolved Cu released over the 24 h CuNPs exposure period). Therefore, the effects of CuNPs is attributed to both nanocopper and dissolved Cu (Razmara et al., 2019).

Copper Analyses in the Water and Olfactory Rosette

The actual concentration of Cu in the water was measured at the beginning (i.e., 1 h after the Cu spikes) and end of the exposure (i.e., 24 h after the Cu spikes) using GFAAS. Following our previous protocol, we performed QA/QC for Cu analyses (Razmara et al., 2019). In brief, the Cu concentration of a certified reference material (SLRS-6: River Water, National Research Council Canada, Ottawa, ON, Canada) was measured every 10 samples (mean percent recovery was 93%, which was within the accepted ± 10% error). The Cu standards calibration curve was resloped and recalibrated very 10 and 20 sample, respectively. Furthermore, during each standards recalibration, analytical duplicates were

analyzed to ensure the accuracy of measurements (duplicates were < 2% different from each other). The GFAAS detection limit (MDL) for Cu was 2 µg/L. Results of Cu concentration in the experimental tanks are showed in Table S1. The Cu concentration in the control was below MDL.

Following the 24 and 96 h exposure to Cu contaminants, fish (n = 6 per treatment) were euthanized using a buffered MS222 solution (240 mg/L TMS (tricaine methane sulfonate, AquaLife, Canada) and 720 mg/L $NaHCO_3$ (Fisher Scientific, USA)), and their olfactory rosettes were dissected to analyze the Cu accumulation. The rosettes were oven-dried (at 60 °C) to reach a constant mass. The dried rosettes were weighted (average 4-10 mg) and placed into microcentrifuge tubes with locking caps. To digest the rosettes, HNO_3 (concentrated, TraceSelect grade; Sigma Aldrich, Canada) was added to the samples at a ratio of 1:10 (tissue mass [mg]: acid volume [µL]) (Lindh et al., 2019). To complete the digestion process, acidified samples were seated in a hot block at 60 °C for 3 h. To assess the accuracy of the digestion protocol, aliquots of a certified reference material (10 mg of DOLT- 4: dogfish liver; National Research Council Canada, Ottawa, ON, Canada) were digested following the same digestion protocol. To ascertain that the digestion protocol is Cu-free, three acid-only tubes (blanks) were simultaneously digested with the experimental samples. Following the acid digestion, the room temperature samples were made up to 2 mL volume with ddH_2O (Lindh et al., 2019). All digested rosettes along with DOLT-4 and blank were analyzed by GFAAS for Cu concentration. The Cu concentration in the blank was below the MDL, and the mean percentage of recovery of Cu in DOLT- 4 was 94%.

Animal Housing and Water Quality

In order to acclimate the fish to the Aquatic Research Facility water (16 h light: 8 h dark photoperiod, 12 ºC), they were introduced into the holding tanks with the stocking density of 5 g/L for two weeks. To remove any possible olfactory parasites from the nasal chambers, fish were treated with parasiticide (PraziPro, Hikari, USA) during the acclimation period. Same as our previous study (Razmara et al., 2019), during the 96 h exposure, 100% of the Cu spiked water in the fish tanks was replaced with same solution every day. During both exposure periods the quality of culture water was measured as follows (mean ± SD; n = 5): temperature, 12.5 ± 0.3 °C; dissolved oxygen, 9 ± 0.6 mg/L; conductivity, 331.5 ± 0.7 µS/cm; hardness, 154 ± 3.6 mg/L as $CaCO_3$; alkalinity: 124.6 ± 3.2 mg/L as $CaCO_3$; median pH, 8.1 (range 7.8 – 8.4), and dissolved organic carbon, 2.46 ± 0.82 mg/L. Fish were not fed during the exposure to Cu contaminants.

Differentially Expressed Transcripts and Functional Annotations

Transcript level analyses in different Cu treatments indicated that from the approximately 53000 transcripts in rainbow trout olfactory mucosa, 2.1% were affected by each Cu contaminant (Table S2). The volcano graphs also showed both Cu treatments yielded similar number of Cu-responsive genes in the olfactory mucosa (Fig. S1).

To ensure that the NCBI nr database was a proper database for the rainbow trout query set, a top hit species distribution bar chart was generated by the Blast2Go following the BLAST

search. Species distribution charts for both CuNPs and Cu^{2+} indicated *Oncorhynchus mykiss* was the species to which most contigs were aligned (Fig. S2A and B). The blasted sequences were then mapped to retrieve Gene Ontology (GO) terms to the blast hits. The Go terms were classified into biological processes (BP), molecular functions (MF), and cellular components (CC). As the final step of functional annotation, the query sequences were annotated (i.e., proper Go terms from the mapped Go terms pool were assigned to the sequences). InterProScan annotation against protein databases, including PRINTS, PFAM, TIGRFAMs, ProDom, CDD, HMAP, PIR, Gene3D, and PANTHER, was also performed to assign motif and domain information to the sequences. The functional information attained by InterProScan was merged with the pre-existing functional annotation GO terms. The annotation step of the functional enrichment analysis was performed based on the default settings of Blast2Go. The functional annotation analysis shows 87% and 89% of the total sequences were functionally annotated in CuNPs and Cu^{2+} query set, respectively (Table S2). In the Cu^{2+} treatment, BP, MF, and CC constituted 52%, 25%, 23% of transcripts' GO terms, respectively (Fig. S2C). Similar to the Cu^{2+} treatment, in the CuNPs treatment, BP composed of highest percentage (54%) of GO terms, followed by MF (26%), and CC (20%), 26%, and 20% of (Fig. S2D). To identify the GO terms that were significantly over-represented in each Cu treatment, the Fisher's exact test and gene set enrichment analysis (GSEA) was performed on the differentially expressed genes. There were no significant differences in the top enriched GO terms identified by the two enrichment tests.

Gene Expression Analysis

All genes that were described in the main text along with their expression fold change (measured by RNA-seq) are listed in Table S3. All qPCR primers, except ATP1A1 that was from Richards et al., 2003 (Richards et al., 2003), were designed using Primer-Blast online software provided by NCBI (Ye et al., 2012). Primer characteristics are described in Table S4. Specificity of primers to produce a single PCR product was confirmed by melt curve analysis and gel electrophoresis. To ensure that the primers amplify the desired genes, the PCR products were purified (QIAquick PCR Purification kit, catalog # 28104; Qiagen), sequenced, and blasted in NCBI. To analyze the abundances of target genes transcripts, PCR reaction mixtures (total volume of 10 µL, loaded in duplicates), containing 5 µL of RT² SYBR Green qPCR master mix (catalog # 330503, Qiagen), 0.5 µL of each forward and reverse primers (0.25 µM), 1 µL of cDNA, and water, were amplified and quantified using a Bio-Rad thermocycler (C1000 Touch thermocycler, CFX96 Real-Time System, Bio-Rad). The PCR mixtures were denatured at 95°C for 10 min which was followed by 40 cycles of amplification (i.e., denaturation for 15 s at 95°C and extension for 1 min at 62°C).

Statistical Analysis

Statistical analysis was performed in R, version 3.6 (R Core Team, 2019). To determine whether Cu was significantly accumulated, target genes were differentially expressed, and lipid peroxidation was significantly induced in response to different Cu treatments (CuNPs

and Cu^{2+}) over different exposure periods (24 and 96 h), we conducted two-way analysis of variance (ANOVA) with Tukey's post hoc test.

Non-metric multidimensional scaling was carried out using the 'metaMDS' function from the 'vegan' package (Oksanen et al., 2017) in R to ordinate similarities among treatments and genes (Pinheiro et al., 2017). Genes were pooled for each treatment and genes that showed no differential expression were excluded. Gene expression data were square root transformed and Wisconsin double standardization was performed prior to calculating the Euclidean distance matrix for NMDS. Axes were rotated to maximally represent variation in the first dimension and ordination results were centre-scaled. Ellipses were drawn around the three treatment groups using the 'ordiellipse' function of the 'vegan' package to illustrate standard deviations of NMDS ordinations scores based on replicates (i.e., olfactory rosette samples) within each treatment group. The effects of treatments on gene expression data were analyzed with a PERMANOVA using the Euclidean distance matrix from the NMDS. The PERMANOVA was performed with the 'adonis' function of the 'vegan' package (Anderson, 2001). A post hoc test on the PERMANOVA results was carried out with the "calc_pairwise_permanovas" function of the 'mctoolsr' package (Leff, 2017).

Table S1. Copper concentration in the experimental tanks water measured by GFFAS

Concentration (µg/L)	**Cu^{2+} tanks**	**CuNPs tanks**
Nominal	7	322
Actual (1 h after Cu spike)	7 ± 1	262 ± 31
Actual (24 h after Cu spike)	7 ± 1	210 ± 13

Table S2. Summary of RNA-seq analyses performed on the rainbow trout olfactory mucosa following the 96 h exposure to Cu^{2+} and CuNPs

Analyzed parameter	**Cu^{2+}**	**CuNPs**
Total number of transcripts	53141	53380
Number of differentially expressed (DE) transcripts	1130	1124
Number of upregulated DE transcripts	543	566
Number of downregulated DE transcripts	587	558
% of DE transcripts from total transcripts	2.1	2.1
% of functionally annotated transcripts from DE transcripts	87	89

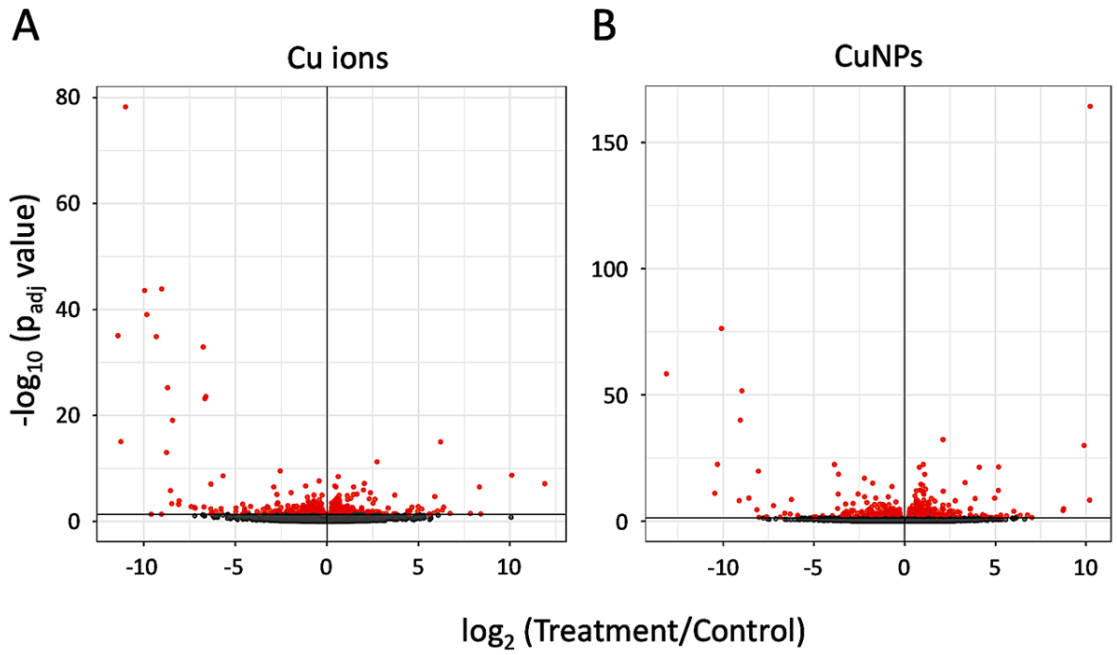

Figure S1. Volcano plots shows similar number of differentially expressed transcripts (red dots; Padj = 0.05) in rainbow trout olfactory mucosa under Cu^{2+} (A) and CuNPs (B) treatments. Grey dots are insignificant transcripts. The relative fold changes (x-axis) are plotted against adjusted p values (y-axis).

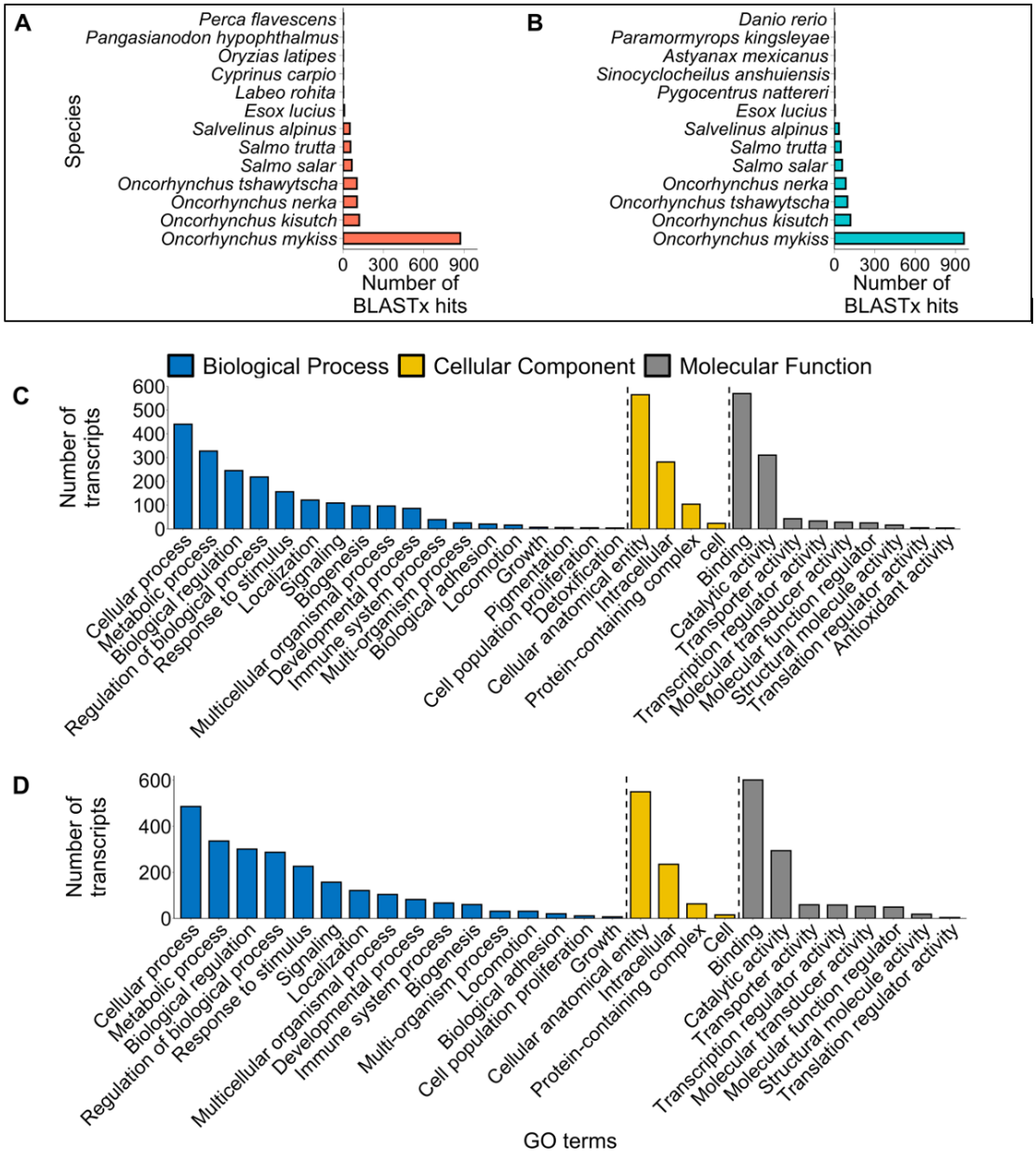

Figure S2. Quality assessment of functional annotations of differentially expressed genes in rainbow trout olfactory mucosa following the 96 h exposure to CuNPs and Cu^{2+}. (A and B) Species distribution based on number of BLASTx hits in Cu^{2+} (A) and CuNPs (B) treatments. The homologous genes were identified by BLASTx algorithm against nr protein database. The E-value cut-off to determine the sequences identity was 1.0 E^{-5}. (C and D) The 2nd level functional annotation of olfactory mucosa in response to Cu^{2+} (C) and CuNPs (D) exposure.

Table S3. List of gene transcripts that are mentioned in the results and discussion. The table shows fold change relative to the control under different Cu treatments in the rainbow trout olfactory mucosa. Gene expression was analyzed by RNA-seq (* indicates significant gene expression relative to the control)

Gene transcript name	Fold change in CuNPs	Fold change in Cu^{2+}
Olfactory receptor 2AT4 (*OR2AT4*)	0.5 *	1.2
Olfactory receptor 2M3 (*OR2M3*)	0.5 *	1.1
Olfactory receptor 52A1 (*OR52A1*)	0.6 *	1.1
olfactory receptor family 4 subfamily C member 5 (*OR4C5*)	0.6 *	0.8
Guanine nucleotide-binding protein G(I)/G(S)/G(T) subunit beta-1 (*GNB1*)	0.04 *	1.1
Cyclic nucleotide gated channel (*CNG1*)	0.4 *	0.9
Sodium-calcium exchanger 1 (*NCX1*)	0.5 *	1.2
Plasma membrane calcium-transporting ATPase 2 (*PMCA2*)	0.3 *	1.1
Sodium/potassium/calcium exchanger 3 (*NCKX3*)	0.5 *	1
Potassium voltage-gated channel subfamily B member 1 (*KCNB1*)	1.5 *	1.3
V-type proton ATPase subunit S1 (*ATP6AP1*)	0.7 *	1
Solute carrier family 17 member 9 (*SLC17A9*)	2.4 *	1
Double C2-like domain-containing protein beta (*DOC2B*)	0 *	1.2
Dynamin 1 isoform X3 (*DNM1*)	4 *	1.2
Nuclear factor erythroid 2-related factor 1 (*NRF1*)	0.8 *	1.9 *
Catalase (*CAT*)	1.2	2 *
Mitochondrial peptide methionine sulfoxide reductase (*MSRA*)	0.7	1.5 *
Glutathione S-transferase A (*GSTA*)	1.3	1.5 *

NADH-ubiquinone oxidoreductase 75 kDa subunit, mitochondrial (*NDUFS1*)	0.7	1.8 *
NADH dehydrogenase [ubiquinone] iron-sulfur protein 8, mitochondrial (*NDUFS8*)	0.9	8.2 *
Caspase 6 (*CASP6*)	1	0.7 *
Caspase 8 (*CASP8*)	0.8	0.7 *
Apoptosis regulator BAX (*BAX*)	0.6 *	0.8

Table S4. Primers list for qPCR gene expression analysis

Gene name	Sequence of primer (5'- 3')	Efficiency
Olfactory receptor 10G4 (*OR10G4*)	F: TGATGCTTGTGTAGGATGTCTTCA R: GCCGTCTGTCCGTCAAAATG	2.07
Olfactory receptor 472 (*OLF472*)	F: GCTGGCTTTTGTAGTCCCCT R: CTTCTCGTCCCTGAAACCGT	1.93
Olfactory marker protein (*OMP*)	F: ACAAGGTCAGCATCTCCGTG R: GCCAATGCTAACTAGTGTTGGTATC	1.92
Sodium channel protein type 8 subunit alpha (*SCN8A*)	F: CTGGGAGTGTTGTCCCATCT R: ACCAGGTTTCCCACAGACAG	2.01
Na^+/K^+ ATPase alpha-1 subunit (*ATP1A1*)	F: CTGCTACATCTCAACCAACAACATT R: CACCATCACAGTGTTCATTGGAT	1.96
Voltage-dependent L-type calcium channel subunit beta1 (*CaCNB1*)	F: CACAGGTGGTCCGGCTAAAC R: CAGTCACCTCGTAGCCCTTC	1.90
Two pore calcium channel protein 2 (*TPCN2*)	F: ACCGGAGTGTCATGTGTTCA R: GTGAGGATGCTGGTGGAGTT	2.06
Glutathione peroxidase 7 (*GPX7*)	F: GCTTTCCGTCCTCACATTGC R: ACCACAAGAGACACCGAACC	2.03
Elongation factor 1 alpha (*EF1a*)	F: TCCTCTTGGTCGTTTCGCTG R: ACCCGAGGGACATCCTGTG	1.99
Beta-actin (*ACTB*)	F: TCCTTCCTCGGTATGGAGTCTT R: ACAGCACCGTGTTGGCGTACAG	1.90

This dissertation has 3 supplementary excel shits (datasets) that are available on separate files:

Dataset S1. Enriched GO terms in the rainbow trout olfactory mucosa following the 96 h Cu^{2+} exposure. Sheet 1: List of enriched GO terms of downregulated gene transcripts ($p < 0.05$). Sheet 2: Highly enriched GO terms of downregulated gene transcripts, as indicated in Fig.3C ($p < 0.01$). Sheet 3: List of enriched GO terms upregulated gene transcripts ($p < 0.05$). Sheet 4: Highly enriched GO terms of upregulated gene transcripts, as indicated in Fig.3C ($p < 0.01$).

Dataset S2. Enriched GO terms in the rainbow trout olfactory mucosa following the 96 h CuNPs exposure. Sheet 1: List of enriched GO terms of downregulated gene transcripts ($p < 0.05$). Sheet 2: Highly enriched GO terms of downregulated gene transcripts, as indicated in Fig.3B ($p < 0.01$). Sheet 3: List of enriched GO terms of upregulated gene transcripts ($p < 0.05$). Sheet 4: Highly enriched GO terms of upregulated gene transcripts, as indicated in Fig.3B ($p < 0.01$).

Dataset S3. Gene set enrichment analysis (GSEA) in the rainbow trout olfactory mucosa that was treated with CuNPs and Cu^{2+}. Sheet 1: GSEA in CuNPs treatment. Sheet 2: GSEA in Cu^{2+} treatment.

References

Anderson, M.J., 2001. A new method for non-parametric multivariate analysis of variance. Austral ecology 26, 32-46.

Leff, J., 2017. Mctoolsr: Microbial Community Data Analysis Tools. R Package Version 0.1. 1.2.

Lindh, S., Razmara, P., Bogart, S., Pyle, G., 2019. Comparative tissue distribution and depuration characteristics of copper nanoparticles and soluble copper in rainbow trout (*Oncorhynchus mykiss*). Environmental toxicology and chemistry 38, 80-89.

Oksanen, J., Blanchet, F.G., Friendly, M., Kindt, R., Legendre, P., McGlinn, D., Minchin, P., O'Hara, R., Simpson, G., Solymos, P., 2017. vegan: Community Ecology Package. R package version 2.4–2. 2017.

Pinheiro, J., Bates, D., DebRoy, S., Sarkar, D., 2017. R Core Team (2017) nlme: linear and nonlinear mixed effects models. R package version 3.1-131.

R Core Team, 2019. A language and environment for statistical computing. R Foundation for Statistical Computing, Vienna, Austria2014, in: Team, R.C. (Ed.).

Razmara, P., Lari, E., Mohaddes, E., Zhang, Y., Goss, G.G., Pyle, G.G., 2019. The effect of copper nanoparticles on olfaction in rainbow trout (*Oncorhynchus mykiss*). Environmental Science: Nano 6, 2094-2104.

Richards, J.G., Semple, J.W., Bystriansky, J.S., Schulte, P.M., 2003. Na+/K+-ATPase α-isoform switching in gills of rainbow trout (*Oncorhynchus mykiss*) during salinity transfer. Journal of Experimental Biology 206, 4475-4486.

Ye, J., Coulouris, G., Zaretskaya, I., Cutcutache, I., Rozen, S., Madden, T.L., 2012. Primer-BLAST: a tool to design target-specific primers for polymerase chain reaction. BMC bioinformatics 13, 134.